INTERPLAY BETWEEN GRAPE SEED PROANTHOCYANIDINS AND CIRCADIAN RHYTHM IN WHITE ADIPOSE TISSUE: NEW FRONTIERS IN OBESITY MANAGEMENT

Marina Colom Pellicer

UNIVERSITAT ROVIRA i VIRGILI

Interplay between grape seed proanthocyanidins and circadian rhythm in white adipose tissue: new frontiers in obesity management

Marina Colom Pellicer

2022

Doctoral Thesis

Department of Biochemistry and Biotechnology

Marina Colom Pellicer

Interplay between grape seed proanthocyanidins and circadian rhythms in white adipose tissue: new frontiers in obesity management

Doctoral Thesis

Directed by Dr. Gerard Aragonès Bargalló

UNIVERSITAT ROVIRA i VIRGILI

Department of Biochemistry and Biotechnology
Nutrigenomics Research Group

2022

UNIVERSITAT ROVIRA i VIRGILI
Dept. de Bioquímica i Biotecnologia

Campus Sescelades, Edifici N4
C/ Marcel·lí Domingo, 1
43007 Tarragona
Tel. +34 977 559 769
Fax +34 977 558 446
http://bioquimica.urv.cat

FAIG CONSTAR que aquest treball, titulat "**Interplay between grape seed proanthocyanidins and circadian rhythms in white adipose tissue: new frontiers in obesity management**", que presenta **Marina Colom Pellicer** per a l'obtenció del títol de Doctor, ha estat realitzat sota la meva direcció al Departament de Bioquímica i Biotecnologia d'aquesta universitat i que compleix els requeriments per poder optar a la Menció Internacional de Doctorat.

HAGO CONSTAR que el presente trabajo, titulado "**Interplay between grape seed proanthocyanidins and circadian rhythms in white adipose tissue: new frontiers in obesity management**", que presenta **Marina Colom Pellicer** para la obtención del título de Doctor, ha sido realizado bajo mi dirección en el Departamento Bioquímica y Biotecnología de esta universidad y que cumple los requisitos para poder optar a la Mención Internacional de Doctorado.

I STATE that the present study, entitled "**Interplay between grape seed proanthocyanidins and circadian rhythms in white adipose tissue: new frontiers in obesity management**", presented by **Marina Colom Pellicer** for the award of the degree of Doctor, has been carried out under my supervision at the Department Biochemistry and Biotechnology of this university and that this thesis is eligible to apply for the International Doctorate Mention.

Tarragona, 7 de juny de 2022
Tarragona, 7 de junio de 2022
Tarragona, 7th June 2022

El director de la tesi doctoral
El director de la tesis doctoral
Doctoral Thesis Supervisor

Dr. Gerard Aragonès Bargalló

♦ Funding

The research work carried out in the present Doctoral Thesis was supported by the grants AGL2013-40707-R and AGL2016-77105-R from the Spanish government. The thesis was performed mainly in the Nutrigenomics Research Group of Universitat Rovira i Virgili with a pre-doctoral fellowship from the Catalan Agència de Gestió d'Ajuts Universitaris i de Recerca (AGAUR; 2019FI_B 00485, 2020FI_B1 00105, 2021FI_B2 00150). An international research stay has been done in the Institute of Neurobiology, Center of Brain, Behavior and Metabolism in the University of Lübeck (Germany) under the supervision of Prof. Dr. Henrik Oster and supported by grants of the German Research Foundation (DFG; CRC/TR296, P13). This phase was also supported by grants from AGAUR, Sociedad Española de la Genética and Erasmus + Programme of the European Union.

♦ Aknowledgments

Gràcies! Gràcies a tots els que heu format part d'aquesta etapa.

Primer de tot agraïr al Grup de Nutrigenòmica per confiar en mi i deixar-me endinsar en el món de la investigació. Gràcies Dr. Lluís Arola per donar-me aquesta oportunitat d'aprenentatge al costat de casa. També vull agraïr a la Begoña per confiar en mi desde que ens vam conèixer, que va ser a l'entrevista per realizar les pràctiques del Màster de Nutrició i Metabolisme en aquest grup. També vull agraïr a la Paqui i a l'Anna Mas pel vostre suport i dedicació durat aquell any de pràctiques. Jo acabava de fer unes pràctiques extracurriculars de la carrera de Biologia a la Universitat de Wageningen, Països Baixos, on vaig aprendre moltíssim durants aquells 6 mesos, i vosaltres em vau seguir transmetent aquesta passió per la ciencia! Gràcies per la vostra constància i ganes d'ensenyar!

També agraeixo tot l'esforç i dedicació del meu director de tesi, Gerard Aragonès. Han estat tres anys i mig, gairebé quatre, de moments bons i altres de no tan bons, però tots han estat necessaris per aprendre i arribar fins aquí!

A tots els investigadors del Departament de Bioquímica i Biotecnologia, que en algún moment o altre m'heu ajudat. Gràcies Anna Arola per aquest consell de final de tesi, realment molt necessari.

Sobretot gràcies Niurka i gràcies Rosa, per tot l'esforç que invertiu en cadascú de nosaltres. Sempre disposades a ensenyar i a resoldre tots els dubtes que ens van sorgint. Us definiría com grans professionals carregades de bon humor!

Gràcies Isabel, Santi i Laia per tota la feina invisible que feu que fa que les classes pràctiques siguin molt més fàcils de preparar per nosaltres. També sempre disposats a transmetre els vostres coneixements.

I would like to thank Prof. Dr. Henrik Oster for the opportunity you gave me to join your group in Lübeck, Germany. I would also like to thank Ankita for the warm welcome and Leo for helping me so much in all the experiments. Gracias Dorothea por tu cálida acogida, fuiste un gran apoyo durante mi estancia en Lübeck, siempre te estaré agradecida. Thanks all of you and all the members of the group, I learnt a lot during these six months, in the lab, corridors and groups meetings, despite the lockdown that did not let us plan many activities.

Sobretot gràcies a cadascú de vosaltres, als companys i amics de despatx i de laboratori. Hem conviscut molts moments al despatx, a l'estabulari, a les safenes, als sacris a les tantes de la nit, també amb els explants a mitjanit… m'enporto molt bon record, i ha estat gràcies al suport que ens hem donat els uns als altres; sempre fent pinya!! També gràcies per aquests congresos a Parma on cada dia buscavem el nostre plaer a la Cremeria Emilia. Per Berna descobirnt la NuGO i la bona vida de Suïssa. I al congrés de Barcelona on ens vam retrobar amb els nostres gelats italians! També gràcies pels cafès, les calçotades, els sopars, les festes, les tardes a la platja i al "xiringuito", els entrenaments, per la mitja marató (impensable fer-la sense el vostre suport), per les esquiades, pel millor carnaval de la meva vida (conus, ja ho sabieu no?!), per les xerrades i pel suport que m'heu donat. Gràcies Èlia, Carme, Fra, Jose, Romi, Jorge,

Raúl, Vero, Alba, Marta, Àlvaro, Nespru (ai, Nestor!), Iván i Pauli per tots aquests moments viscuts! I també a les noves generacions que acabeu d'entrar! Us desitjo el millor!

Gràcies "felices los 4" per aquests sopars esporàdics on parlem de ciència, números, astrología, que porten a parlar d'il·lusions i preocupacions.

Als amics de sempre i als de la uni per seguir fent quedades tot i estar lluny. A la Marina, i a l'Esther per la teva comprensió, suport i carinyo que em dones. M'has ajudat moltíssim en moments d'estrés màxim!

També vull agraïr a les meves cosines, per ser com sou i pel vostre amor incondicional!

Als meus pares, per tota la paciència que heu tingut, per tots els vostres esforços que heu invertit per a què jo pugui arribar on he arribat i sigui la persona que sóc avui. A l'Enric, per estar sempre de bon humor i per la teva meravellosa frase "Si t'agrada, està molt bé!".

Al Jordi per la teva incansable paciència durant aquesta última etapa de la tesi. Gràcies per animar-me en moments durs, per creure en mi des del primer dia i pel teu suport. Amb poc temps hem viscut molts canvis, que ens han fet crèixer com a persones i com a equip per seguir vivint noves experiències!

I a tota la meva família!

A tots vosaltres,

Gràcies!!

A la meva família i amics,

"Tantes llàgrimes de tots i totes
són com pluja pels nostres cors,
que farà créixer la llavor
que Ella a tots ens va implantar"

Tiet

2022

Index

Index

♦ Summary

In obesity, the dysfunction of adipose tissue is associated with the risk to suffer metabolic disorders. Circadian rhythm, governed by light/dark cycle and fasting/feeding cycle, synchronize many metabolic processes, therefore its disruption has been also related to the development of metabolic disorders. The increasing prevalence of obesity remarks the importance of its prevention and treatment. In this context, proanthocyanidins from grape seed (GSPE) have been demonstrated to modulate the biology and molecular clock components of white adipose tissue (WAT). Nevertheless, it has not been studied yet whether GSPE could affect WAT chronobiology depending on time-of-day consumption. Therefore, the aim of this thesis was to determine whether GSPE and a bioactive multi-compound based on these proanthocyanidins have different effects on the metabolism and circadian rhythm of WAT in obese animals depending on time-of-day administration. High calorie intake disrupted molecular clock genes and the metabolism of WAT. Interestingly, the consumption of GSPE restored the metabolism and molecular rhythmicity of WAT in a time-dependent and tissue-specific manner. The combination of different bioactive compounds is also an interesting strategy for the management of obesity depending on the time-of-day administration.

♦ Resum

En l'obesitat, la disfunció del teixit adipós està relacionada amb el risc de patir transtorns metabòlics. El ritme circadià, governat pel cicle de llum/foscor i dejuni/alimentació, sincronitza varis processos metabòlics, per tant, la seva disfunció també està relacionada amb el desenvolupament de malalties metabòliques. L'augment de la prevalença de l'obesitat accentua la importància de la seva prevenció i el seu tractament. En aquest context, s'ha demostrat que les proantocianidines del pinyol del raïm (GSPE) modulen la biología i components del rellotge molecular del teixit adipós blanc (TAB). Malgrat tot, encara no s'ha estudiat si el GSPE pot afectar la cronobiología del TAB depenent del moment del dia en què es consumeix. Per tant, l'objectiu d'aquesta tesi és avaluar si el GSPE i una mescla de compostos bioactius, que també conté aquestes proantocianidines, presenten efectes diferents en el metabolisme i el ritme circadià del TAB en animals obesos depenent del moment del dia en què es consumeixin. Una ingesta alta en calories altera els gens del rellotge molecular i del metabolisme del TAB. Curiosament, el GSPE restaura el metabolisme i la ritmicitat del TAB depenent del moment del dia en què es consumeixen i del dipòsit de teixit adipós. La combinació de diferents compostos bioactius també és una estrategia interessant pel tractament de l'obesitat depenent del moment del dia del seu consum.

♦ Abbreviations

ACACA	Acetyl-CoA carboxylase
ACE	Angiotensin-converting enzyme
AKT	Serine/threonine kinase
AP-1	Activator protein 1
AR	Adrenergic receptor
ATGL	Adipose triglyceride lipase
BAT	Brown adipose tissue
BCAA	Branched chain amino acids
BMAL1	Brain and muscle Arnt-like 1
BMI	Body mass index
C/EBP	CCAAT/enhancer-binding protein
CAF	Cafeteria diet
cAMP	Cyclic adenosine monophosphate
CIDEA	CIDE protein family
CLA	Conjugated linoleic acid
CLOCK	Circadian locomotor output cycles kaput
COX	Cyclooxygenase
CPT1	Carnitine palmitoyltransferase 1
CRY	Cryptochrome
DAG	Diacylglycerol
DNA	Deoxyribonucleic acid
DNL	De novo lipogenesis
eWAT	Epididymal white adipose tissue
FABP	Fatty acid-binding protein
FASN	Fatty acid synthase
FFA	Free fatty acid
FXR	Farnesoid X receptor
G6PD	Glucose-6-phosphate dehydrogenase
GLUT	Glucose transporter
GPAT	Glycerol-3-phosphate acyltransferase
GSPE	Grape seed proanthocyanidin extract
HDAC	Histone deacetylases
HFD	High-fat diet
Hpp11	Hydrolysate from chicken feet
HSL	Hormone-sensitive lipase

Abbreviations

IKK	IκB kinase
IL-6	Interleukin 6
IR	Insulin receptor
IRS	Insulin receptor substrate
iWAT	Inguinal white adipose tissue
JNK	Jun amino-terminal kinase
KLF	Krüppel-like factors
LDL	Low-density lipoproteins
LPL	Lipoprotein lipase
MCP-1	Monocyte chemoattractant protein–1
MGL	Monoglyceride lipase
miRNA	microRNA
MIX	Bioactive multi-compound
mRNA	Messenger RNA
Myf5	Myogenic factor 5
NAD^+	Nicotinamide adenine dinucleotide
NADPH	Nicotinamide adenine dinucleotide phosphate dehydrogenase
NAFLD	Nonalcoholic fatty liver disease
NAMPT	Nicotinamide phosphoribosyltransferase
NEFA	Non-esterified fatty acids
NF-κB	Nuclear factor-κB
NR1D1	Nuclear receptor subfamily 1 group D member 1
Ob-R	Leptin receptor
PER	Period
PI3K	Phosphoinositide 3-kinase
PK	Protein kinase
PLIN1	Perilipin 1
PPAR	Peroxisome proliferatior-activated receptor
PRDM16	PR domain containing 16
PUFA	Polyunsaturated fatty acid
REV-ERBα	Nuclear receptor subfamily 1 group D member 1
RNA	Ribonucleic acid
RORα	RAR-related orphan receptor alpha
RXRα	Retinoid X receptor alpha
SCN	Suprachiasmatic nucleus
SIRT1	Sirtuin 1
SREBP	Sterol response element binding protein

STAT	Signal transducer and activator of transcription
sWAT	Subcutaneous white adipose tissue
TAG	Triacylgliceride
TCA	Tricarboxylic acid cycle
TNF-α	Tumor necrosis factor alpha
TRF	Time-restricted feeding
UCP1	Uncoupling protein 1
VLDL	Very-low density lipoproteins
vWAT	Visceral white adipose tissue
WAT	White adipose tissue
ZT	Zeitgebers

Introduction

Obesity is a global public health issue defined as excessive fat accumulation that presents a risk factor for health. Body mass index (BMI) is the common method used for determining obesity; over 25 is considered overweight, and over 30 is considered obese [1]. Obesity prevalence nearly tripled between 1975 and 2020. In fact, in 2020, 39% of the adult global population were overweight, of these, 11% were obese [2].

Since industrialization, fat and free sugars had increased in our diets and physical activity had decreased due to the new types of work, transportation, and urbanization. Nevertheless, many cases of obesity are preventable and reversable through changing some habits such as diet; reducing the energy consumed from fat and sugars and increasing the portions of proteins, fruits, vegetables, legumes, nuts and whole grains, and engaging in regular physical activity [1].

The fundamental cause of obesity is the imbalance between energy intake and energy expenditure which leads to an increment of white adipose tissue (WAT). WAT plays a critical role in obesity-related comorbidities. The localization of WAT, the size of adipocytes, the alteration of lipid metabolism and immune cells that composed WAT determine the degree of inflammation and the development of insulin resistance, hyperglycemia, dyslipidemia, cardiovascular disease, and specific cancers (**Figure 1**) [3,4]. Indeed, fat increment in obesity is not a passive process, but involves the activation of multiple adverse cellular response to match the surplus energy accumulation. Catabolism increases to oxidize the energy excess, which leads to an increment of reactive oxygen species inducing cellular damage and systemic inflammation. The chronic inflammation could be the link between obesity and metabolic comorbidities [5,6].

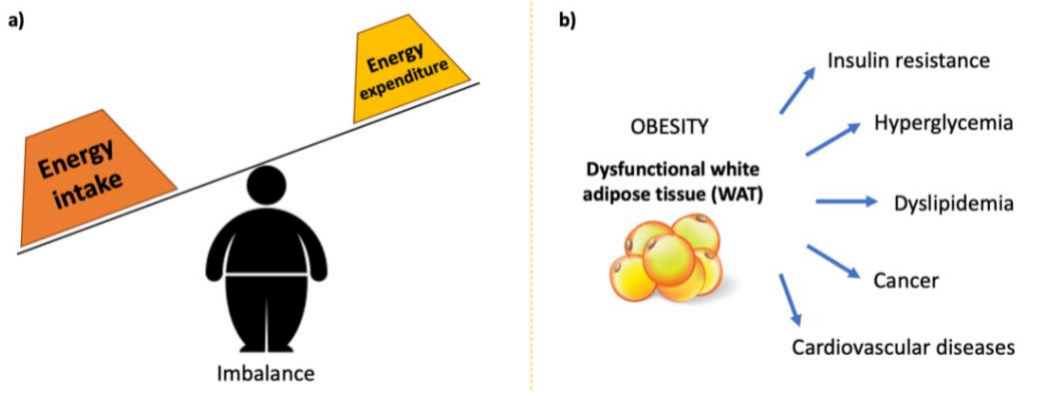

Figure 1. Obesity causes and consequences. a) Imbalance between energy intake and energy expenditure leads to an increment of white adipose tissue and obesity; b) Diseases related to obesity.

Obesity-related comorbidities are not directly associated with BMI. Indeed, some obese people are considered metabolically healthy as they do not display increased risk of any metabolic alteration. In fact, BMI might not adequately reflect adiposity. Many studies which evaluate the association between the risk of metabolic diseases and obesity, they do not discriminate between body fat and lean mass [7].

Nevertheless, it is evident that overweight and obesity increases the risk to suffer metabolic health problems. Therefore, it points the need for further research on new strategies to prevent and treat overweight and obesity, and particularly, the metabolic disorders associated with body weight dysregulation.

1. Adipose tissue

In mammals, adipose tissue is a multi-depot organ; the adipose organ [8]. In the body, adipose organ is distributed in different depots. In adult humans, most of the depots correspond to WAT containing white adipocytes, while some depots correspond to brown adipose tissue (BAT) containing brown adipocytes. Another type of fat cells is beige or brite (brown-in-white) adipocytes, which have both white and brown characteristics.

White adipocytes are characterized to contain a large lipid droplet in the cytoplasm, a peripheral nucleus, and few mitochondria. WAT is mainly responsible for energy storage, but it is also an important endocrine tissue. In contrast, brown adipocytes contain multiple small lipid droplets, multi-locular adipocytes, which contain a high number of mitochondria expressing the thermogenic uncoupling protein 1 (UCP1) in the inner membrane. UCP1 is a transmembrane protein that dissipates heat by uncoupling the respiratory chain maintaining body temperature under cold exposure [9,10]. Beige adipocytes are multi-locular, their density on mitochondria and UCP1 expression is lower compared to brown adipocytes but higher than white adipocytes. Beige adipocytes are also involved in thermogenesis and can also appear in WAT depots to sustain heat production upon certain conditions [10]. Other environmental cues, apart from cold exposure, can promote brown and beige adipocyte activation and/or recruitment in mammals; physical activity, caloric restriction and diet [11,12,13].

WAT functions as a key energy reservoir and plays a fundamental role on regulating whole-body energy homeostasis. This tissue stores energy in form of lipids, and acts as an endocrine organ which produces adipokines that communicate with other organs regulating metabolic pathways. In excess of energy conditions, adipose tissue stores the surplus of nutrients in form of triacylglicerides (TAGs), whereas in energy deficit conditions, adipose tissue induces lipolysis to supply nutrients for other tissues [14]. Lipids are a rich source of energy due to their high-energy bonds, generating twice as many calories per gram than do sugars [15]. The strategy of WAT to store lipids is an essential physiological activity that enhances survival during periods of food scarcity. Besides, WAT has insulation properties which confers protection to organs and tissues.

Under chronic overnutrition, adipose tissue is remodeled through changes in the number and/or size of adipocytes (expansion of adipose tissue) and distribution of WAT [3]. The distribution or localization of WAT would be crucial for the risk to suffer metabolic comorbidities [16].

1.1. Localization of adipose tissue

Metabolic disorders are not only a matter of excessive fat mass but of WAT localization. WAT depots are present in between intra-abdominal regions or visceral tissues (visceral WAT, vWAT) and in subcutaneous compartments or gluteofemoral regions (subcutaneous WAT, sWAT). In humans, android obesity (or apple-shaped) is known when fat is deposited preferentially in vWAT, while gynoid obesity (or pear-shaped) occurs when fat is excessively deposited in sWAT (**Figure 2**) [4,17].

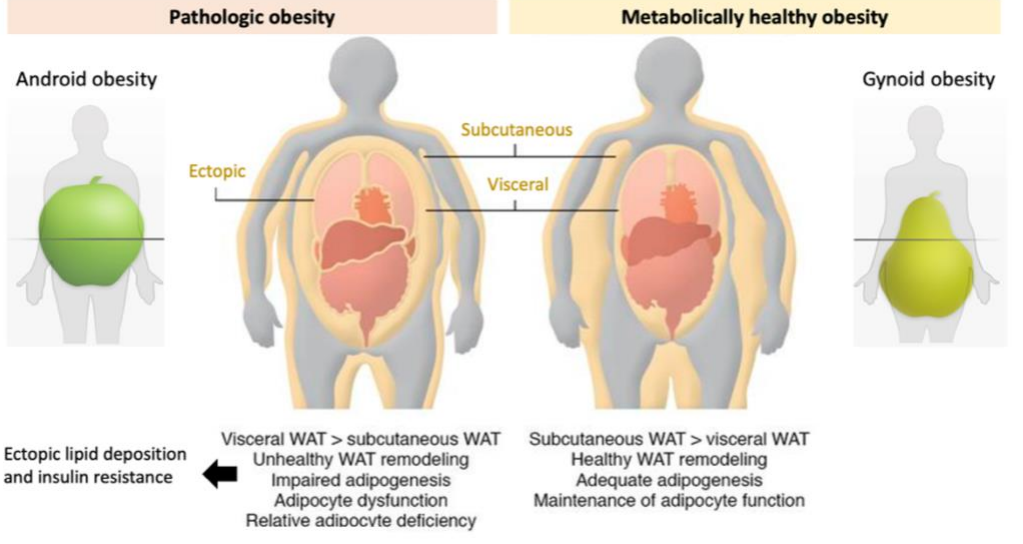

Figure 2. Localization of white adipose tissue in obesity and its association with metabolic complications. Pathologic obesity (or android obesity - apple shape) is characterized by a relative adipocyte deficiency: limited expandability of subcutaneous fat tissue, preferential expansion of visceral adipose tissue depots, and unhealthy adipose tissue remodeling (inflammation, fibrosis, limited adipogenesis). This is associated with ectopic lipid accumulation and insulin resistance. Metabolically healthy obesity (or gynoid obesity - pear shape) is characterized by adequate expansion of protective subcutaneous depots, healthy adipose tissue remodeling (adipocyte hyperplasia), and limited ectopic lipid deposition. Adapted from [17].

WAT depot distribution in humans and rodents is quite similar although with some differences. In humans, vWAT is subdivided in perirenal, retroperitoneal, omental, mesenteric, pericardial and gonadal. Rodents present perirenal, retroperitoneal, mesenteric and gonadal WAT, which in males is located around the testes, epididymal WAT (eWAT). Regarding sWAT, in humans is subdivided in abdominal, gluteal and femoral, while in rodents is classified in anterior and posterior (dorsolumbar, gluteal and inguinal (iWAT)) (**Figure 3**) [3,18,19].

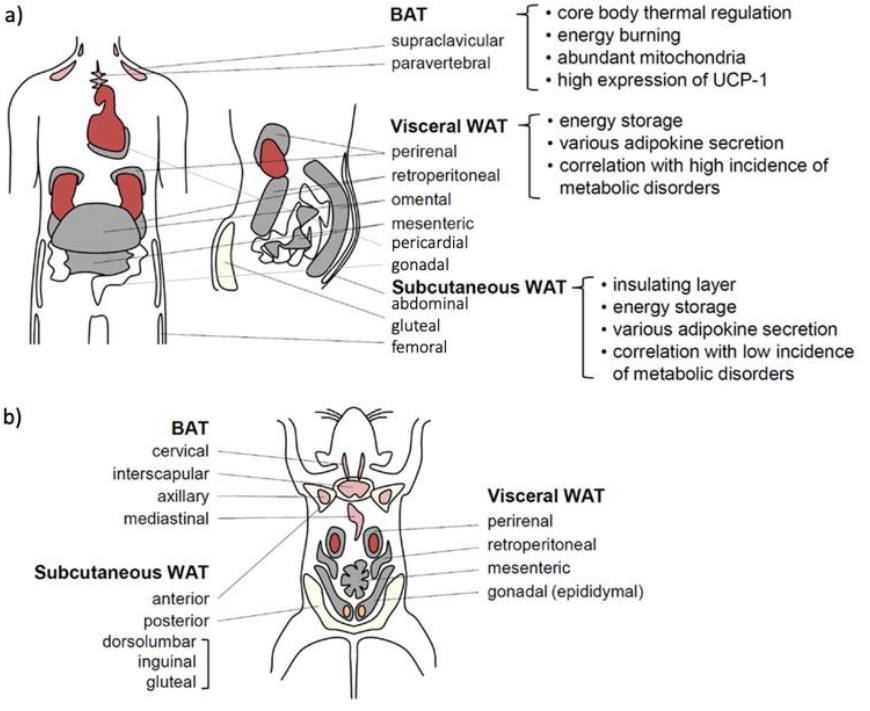

Figure 3. Adipose tissue depots in human (a) and adult mice (b). BAT, brown adipose tissue; WAT white adipose tissue. Adapted from [3].

Body fat distribution is an important metabolic and cardiovascular risk factor, because the proportion of vWAT to sWAT correlates with obesity-associated diseases and mortality. Indeed, the ratio of waist-to-hip was more strongly correlated to metabolic complications and cardiovascular diseases than

BMI [20]. vWAT has been linked to a higher risk of comorbidities such as hypertension, type II diabetes, dyslipidemia, inflammation and low circulating levels of adiponectin [21,22] . While sWAT is associated with neutral or protective effects against metabolic disorders [22].

1.1.1. Visceral white adipose tissue

vWAT syntheses and releases more pro-inflammatory molecules compare to sWAT, which is associated with insulin resistance and type II diabetes [23,24]. Insulin resistance leads to greater lipolytic rate which in turn vWAT liberates large amounts of free fatty acids [25]. Visceral depots have easy access to the liver via the portal circulation, thus free fatty acids and pro-inflammatory molecules liberated by vWAT are associated with hepatic steatosis. Moreover, vWAT expresses angiotensinogen - a precursor of the vasoconstrictor angiotensin II – providing a metabolic link between visceral fat and cardiovascular disease [26,27].

1.1.2. Subcutaneous white adipose tissue

On the other hand, sWAT is associated with a protective lipid and glucose homeostasis and a decreased risk to develop cardiovascular diseases and metabolic disorders. Subcutaneous depots are responsible for long-term fatty acid storage and protects from ectopic fat deposition [24]. sWAT acts as a buffer for daily influx of energy intake, protecting other tissues from lipid overflow and lipotoxicity [25]. It has been shown that sWAT is physiologically more sensitive to insulin protecting against diabetes and cardiovascular diseases [28]. In fact, sWAT has a high lipoprotein lipase activity, facilitating the lipid transport inside the adipocyte. Furthermore, subcutaneous depots present lower rate of lipolysis. Lipolysis is more efficiently inhibited by insulin in sWAT compared to visceral depots contributing to their proper characteristics; sWAT protects from ectopic fat

deposition and insulin sensitivity, and vWAT increases the risk to suffer lipotoxicity, hepatic steatosis and insulin resistance [29]. Indeed, sWAT displays a greater response to insulin compared to vWAT.

Moreover, subcutaneous depots liberate beneficial adipokines, including leptin and adiponectin, and less pro-inflammatory molecules compared to vWAT contributing to a protective adipokine profile. Loss of sWAT is associated with an increased risk in metabolic and cardiovascular diseases.

Furthermore, white adipocytes in subcutaneous depots present the capacity to dedifferentiate into brite adipocyte under certain conditions. During the dedifferentiation, the morphology and gene expression of adipocytes start to change. Specifically, these changes have been observed in iWAT [30]. Therefore, sWAT shows more plastic brown-like characteristics compared to vWAT, and this could be due to the density of nerve fibers which confers higher sympathetic innervation and β-adrenergic signaling necessary for britening of WAT [31]. Furthermore, transplantation of sWAT into the intra-abdominal region of a host mouse exhibited decrease body weight and total fat mass, and increased insulin sensitivity and whole body glucose uptake. Interestingly, these effects are minor when sWAT was transplanted into subcutaneous region, and no effect was observed when vWAT was transplanted into intra-abdominal area. These data suggests that depot differences are due to intrinsic characteristics as well as anatomical localization [32,33].

1.2. Adipose tissue metabolism

1.2.1. Adipogenesis

Adipose tissue comprises a variety of cell types apart from mature adipocytes, including preadipocytes, mesenchymal stem cells, endothelial cells,

fibroblasts, macrophages, and other immune and endothelial cells which together are called stromal vascular fraction [34].

In the recent years it was largely accepted that cell origin of both brown and white adipocytes arose from resident mesenchymal progenitor cells present in adipose tissue. However, the idea that brown and white fat cells arise from similar cellular origin is nowadays outdated. White adipocytes present in WAT are derived from mesenchymal precursor cells, while brown adipocytes present in BAT are derived from Myf5-expressed myogenic precursor cells [35]. Stem cells are present in the stromal vascular fraction and in bone marrow [36]. Several studies demonstrated that the transcriptional regulator PR domain containing 16 (PRDM16) controls the development of brown adipocytes in BAT and brown-like adipocytes (known as beige or brite adipocytes) in WAT [37–39]. PRDM16 in WAT is activated by β3-adrenergic stimulation, peroxisome proliferator-activated receptor gamma (PPARγ) or cold environmental temperature [39–41]. It has been shown that PRDM16 is highly expressed in subcutaneous WAT depots, which results in a transdifferentiation of white adipocytes into brown fat-like adipocytes [42]. Although both brown adipocytes in BAT and white adipocytes in WAT express PRDM16, they have different cellular origin. Nevertheless, the origin of beige adipocytes continues to be controversial [43]. Moreover, uncoupling protein-1 (UCP1) is responsible for non-shivering thermogenesis and is located in the mitochondria of fat cells. In the same way, brown adipocytes and brown fat-like adipocytes present UCP1. Therefore, UCP1 is present in BAT and also in brown fat-like adipocytes of WAT [44] (**Figure 4**).

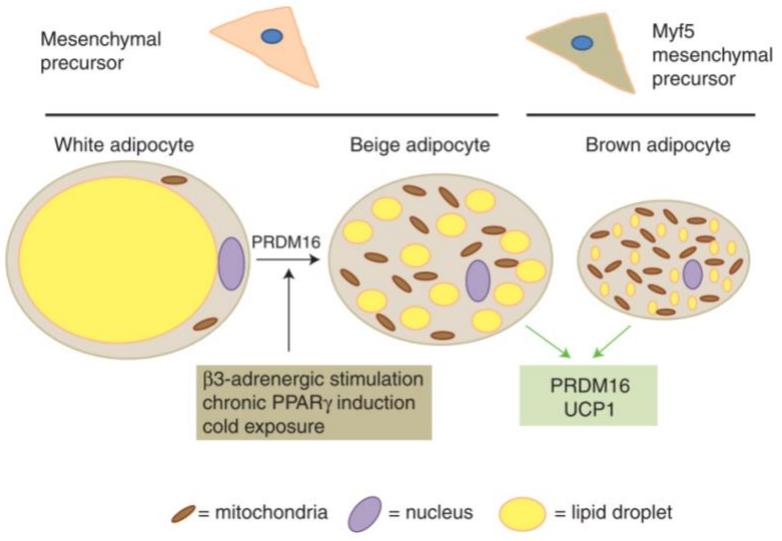

Figure 4. White and brown adipocyte are derived from distinct precursor cells and have distinct morphological characteristics. White adipocytes are derived from mesenchymal precursor cells; brown adipocytes are derived from Myf5-expressing precursor cells. White adipocytes contain one lipid droplet; brown adipocytes contain multilocular lipid droplets and are mitochondria rich. PRDM16 is present in both white and brown adipocytes and is an important factor in transforming white adipocytes to beige adipocytes. Figure obtained from [45].

Mature adipocytes are the predominant cell type in adipose tissue. Both white and brown adipocytes require key transcription factors to induce the differentiation from adipocyte precursor cells into mature adipocytes, process known as adipogenesis. A large variety of factors play a role on this highly orchestrated process through their activation or repression effects on adipocyte development. Adipogenesis is regulated by transcription factors, other proteins, hormones, cytokines and microRNAs (miRNAs) [46,47].

Transcription factor families which promote the first step of the adipogenesis, the clonal expansion, are activator protein 1 (AP-1), Krüppel-like transcription factors 4 and 5 (KLF 4 and 5), CCAAT/enhancer-binding proteins β and δ (C/EBP β and δ). The transcription factors which regulate the second step of the adipogenesis, involved in increasing lipid accumulation, insulin sensitivity and endocrine function are KLF 9 and 15, PPARγ, C/EBPα, signal transducer and

activator of transcription 5A (STAT5A) and sterol response element binding protein-1 (SREBP-1), among others. On the other hand, there are other transcription factors which inhibit the adipogenesis. These transcription factors are GATAs 2 and 3, KLFs 2, 3 and 7, and β-catenin, among others (**Figure 5**) [47].

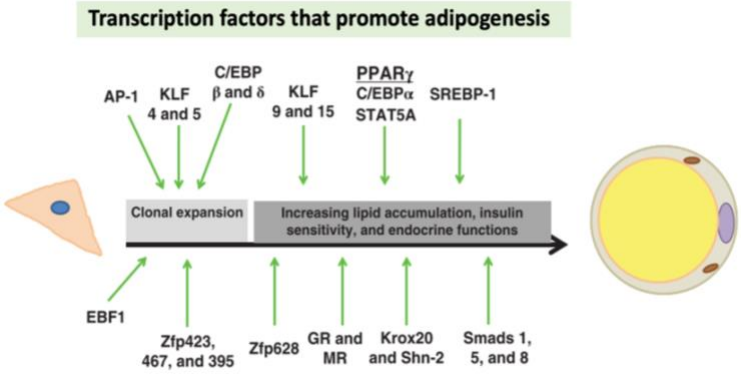

Figure 5. Transcription factors that promote adipogenesis. Many transcription factors are induced during adipocyte differentiation. Some of these are induced during clonal expansion. Others, like PPARγ and C/EBPα, are induced during adipocyte differentiation. Figure obtained from [47].

The major transcriptional factors which regulate adipogenesis are PPARγ and C/EBPs. PPARγ, the principal regulator of adipogenesis, is a ligand-dependent transcription factor that is a member of the nuclear receptor superfamily. PPARγ dimerize with retinoid X receptor alpha (RXRα) forming a heterodimer which modulates transcription of nearby genes [48]. PPARγ, apart from playing a huge role in adipogenesis, also contributes to the modulation of glucose homeostasis and insulin sensitivity [49,50]. The expression and activity of PPARγ proteins, and therefore adipogenesis, can be controlled by covalent modifications. These covalent modifications include phosphorylation, which inactivates PPARγ, acetylation and deacetylation by histone deacetylases (HDACs) [50,51,52,53]. As PPARγ has an important role in fat cell development and glucose and lipid metabolism, it is expected that its activity is regulated by multiple factors. One of these factors is sirtuin 1 (SIRT1), a highly conserved NAD^+-dependent protein deacetylase that has emerged as a metabolic sensor which its activity is regulated in response to environmental stimuli. SIRT1 represses

PPARγ, therefore inhibiting fat storage inside the adipocytes and increasing lipolysis [53].

Another important family of transcription factors are C/EBPs, which is involved in cell proliferation and differentiation. The family presents six members, C/EBPs α, β, γ, δ, ε, and ζ, which can form homodimers or heterodimers. They bind to promoter regions of genes with CCAAT sequence regulating gene expression. The most important members which regulate adipogenesis are C/EBPs α, β, and δ [54]. It is known that C/EBPs β and δ work together to trans-activate C/EBPα and PPARγ [55]. Studies have shown that the lack of transcription of C/EBPα suppresses adipocyte differentiation. Moreover, the deletion of C/EBPs β and δ, also suppresses adipogenesis, since both transcription factors are induced early during adipogenesis and modulate C/EBPα transcription [56]. C/EBPβ also plays a role inhibiting Wnt/β-catenin, which is a negative transcription factor that regulates adipogenesis and different processes important for adipocyte differentiation [57]. C/EBPs can also be modulated by translational and post-translational control mechanisms apart from transcriptional modulation. C/EBPα present two isoforms (full length and truncated), whereas C/EBPβ has three isoforms (full length longer, full length shorter and truncated) which their activity can be modulated by covalent modifications [58–60]. A lot of evidence demonstrates that C/EBPs play a crucial role on adipogenesis, and their control mechanisms could be of interest for future targets on adipogenesis regulation.

1.2.2. Lipid transport

Adipocytes in WAT store fat in form of TAGs, a molecule synthesized by one glycerol and three fatty acids. Most of the TAGs in fat cells originate from circulating lipids, which can be found as free fatty acids (FFA) or non-esterified

fatty acids (NEFA) bound to albumin, or they can be found in very-low density lipoproteins (VLDL) or chylomicrons. The lipoprotein lipase (LPL) hydrolyses TAG into glycerol and three fatty acids, which can be transported into the adipocyte through passive diffusion or by fatty acid transporter such as fatty acid translocase CD36 [61,62]. CD36 uptakes long-chain fatty acids. Once fatty acids are taken up, they can be converted into acyl-CoA derivatives which can be esterified with glycerol-3-phosphate and generate TAGs in the lipid droplets. The glycerol-3-phosphate is produced from glucose through glycolysis process in a fed state. In fact, lipogenesis pathway is regulated by insulin, therefore glucose metabolism plays an important role.

Moreover, fatty acid-binding proteins (FABPs), also known as intracellular lipid chaperones, present a potential action in fatty acid transport into adipocytes, and also in TAG storage and lipolysis. FABP4 was the first detected in adipocytes. FABP4 expression is tightly regulated by fatty acids, PPARγ agonists and insulin [63].

1.2.3. Glucose transport

In 1980, it was discovered that insulin stimulated the translocation of glucose from plasma membrane into adipocytes [64,65]. TAG in adipocytes can also be originated from endogenous synthesis from glucose, process known as de novo lipogenesis (DNL) [66,67]. Glucose enters fat cells through insulin-sensitive glucose transporter 4 (GLUT4) and non-insulin-sensitive GLUT1. Afterwards, some glucose is metabolized through glycolysis and converted into glycerol-3-phophate (glycerol-3-phosphate), which is the backbone of TAG. Moreover, glucose can be catabolized through glycolytic pathway followed by its oxidation in tricarboxylic acid cycle (TCA) and its conversion into citrate, which is required for DNL.

During fasting period, aerobic glycolysis is induced in adipocytes with the subsequent production of lactate. WAT is an important producer of lactate, contributing to systemic lactate turnover [68]. Lactate is an intermediate metabolite of TCA cycle for gluconeogenesis in most of the tissues, including the liver [69]. This process reduces whole-body glucose utilization and is involved in a complex regulation of glucose carbon fate in the fat cell.

Moreover, the uptake of glucose needs inulin signaling which begins with the binding of inulin to insulin receptor, that leads to the phosphorylation of insulin receptor substrate 2 (IRS2). This is followed by the recruitment of phosphoinositide 3-kinase (PI3K) and the activation of serine/threonine kinase (AKT) [70]. A deletion of IRS2 in the liver of mice induces insulin resistance due to the inhibition of AKT activity [71].

Another important enzyme in obese adipose tissue is glucose-6-phosphate dehydrogenase (G6PD). We could also talk about this enzyme in the inflammation section, however we decided to introduce it in the "glucose transport" section as it is the link between the hydrolysis of glucose, pentose phosphate pathway and redox regulation. G6PD is an enzyme that catalyzes the first reaction in the pentose phosphate pathway, which provides reducing power to cells in the form of NADPH; reduced form of nicotinamide adenine dinucleotide phosphate. NADPH enables cells to defense against oxidative damage [72]. Obesity is characterized by chronic inflammation which is related to many metabolic diseases. Therefore, the pentose phosphate pathway is an anabolic process which utilizes glucose to produce NADPH needed to fight against reactive oxygen species [73].

1.2.4. Lipogenesis

Adipose tissue is the major site of conversion of carbohydrates and proteins into fat. It has been shown that around 30% of the daily intake of carbohydrates is converted into fat in animal models [74]. Fatty acids provide a much higher energy reserve than glycogen, as fatty acids are the most calorically dense form of energy storage. Indeed, the regulation of fatty acid synthesis in adipose tissue is essential for the systemic energy balance.

Excess of carbon availability activates DNL, which induces the export of citrate from mitochondria to cytosol. Afterwards, citrate is converted to acetyl-CoA and this into malonyl-CoA by acetyl-CoA carboxylase (ACC or ACACA). Afterwards, fatty acid synthase (FAS or FASN) converts malonyl-CoA into fatty acids. It has been shown that lipogenic enzymes in WAT are positively correlated with insulin sensitivity, which suggests that DNL is important for adipocyte and systemic metabolism, specifically for insulin sensitivity [75,76].

The regulation of expression and activity of these enzymes is tightly controlled in a transcriptional and post-transcriptional level according to nutritional status (feeding and fasting), substrate availability and hormones. In fact, fatty acids inhibit DNL, while insulin stimulates fatty acid esterification by a sequential action of specific enzymes including glycerol-3-phosphate acyltransferase (GPAT) [77].

The major fatty acid synthesized by these enzymes and other enzymes, is palmitic acid (16:0), which can be elongated to stearic acid (18:0) and desaturated to form palmitoleic acid (16:1n7). Stearic acid can be desaturated and form oleic acid (18:1n9). DNL-derived fatty acids, apart from being stored as TAG in lipid droplets of adipocytes, they can also be part of phospholipids in cellular membranes or serve as extracellular signaling molecules [78].

The conversion of excess glucose into lipids protects against glucotoxicity. However, adipose organ is not the only organ which is responsible for DNL, but liver also is able to convert carbohydrates into fatty acids [79]. Indeed, an upregulation of DNL is associated with several pathologies such as type II diabetes, cardiovascular diseases and nonalcoholic fatty liver disease (NAFLD) [78–81]. In fact, most of these human studies determined the concentration of palmitic acid (16:0), palmitoleic acid (16:1n7), stearic acid (18:0) and oleic acid (18:1n9) on plasma or WAT to know the rate of DNL. Moreover, the length and saturation degree of dietary fat in circulation and WAT influence the systemic physiology. Indeed, the literature suggests that unsaturated fatty acids present benign effects on WAT, while long-chain saturated fat present harmful effects in WAT producing inflammatory responses [82,83].

1.2.5. Lipolysis

During periods of energy demands, like in fasting or physical activity, TAGs in WAT are hydrolyzed and mobilized to produce energy in required tissues. The breakdown of TAGs in WAT is known as lipolysis. This process is tightly regulated by hormones, including insulin, catecholamines and natriuretic peptides [84].

Three lipases are responsible for TAG lipolysis in adipocytes: adipose triglyceride lipase (ATGL), hormone-sensitive lipase (HSL) and monoglyceride lipase (MGL). ATGL hydrolysis TAG into diacylglycerol (DAG). Adipocyte-specific deletion of ATGL mice and humans showed reduced basal and stimulated lipolysis [85,86]. The following enzyme is HSL, which apart from hydrolyzing DAG, it also regulates TAG hydrolysis activity. A deficiency in HSL causes an accumulation of DAG in WAT and a reduction on stimulated lipolytic rate both in mice and humans [86–88]. Moreover, it has been shown that FABP4 also has an

important role in lipolysis, which bind to HSL in a 1 to 1 ratio in the cytosol. Indeed, FABP4 knockout mice presented a reduction on the lipolytic pathway [89]. The third enzyme of the lipolytic process is MGL which hydrolyses monoacylglycerol to glycerol and one fatty acid. HSL also present a role on regulating the last step of lipolysis [90].

The activity of these lipases depends on their intracellular localization and interactions with lipid droplet-associated proteins. Lipid droplets, which stored TAGs in adipocytes, are surrounded by phospholipids and some proteins. Perilipin 1 (PLIN1) is the major protein of adipocyte lipid droplet that regulates ATGL activity [91]. A member of the CIDE family of proteins, CIDEA, controls basal lipolysis when it is located in the lipid droplets, whereas when it is located in the nucleus acts as a transcription cofactor [92].

Carnitine palmitoyltransferase 1 (CPT1) is a key enzyme which controls fatty acid uptake into mitochondria regulating fatty acid β-oxidation pathway. It has been shown that CPT1 is inhibited by malonyl-CoA, the product of ACACA, which initiates lipogenesis [93]. Therefore, anabolic and catabolic pathways are highly reciprocally regulated.

A resume of lipid and glucose transport, lipogenesis and lipolysis is shown in **Figure 6**.

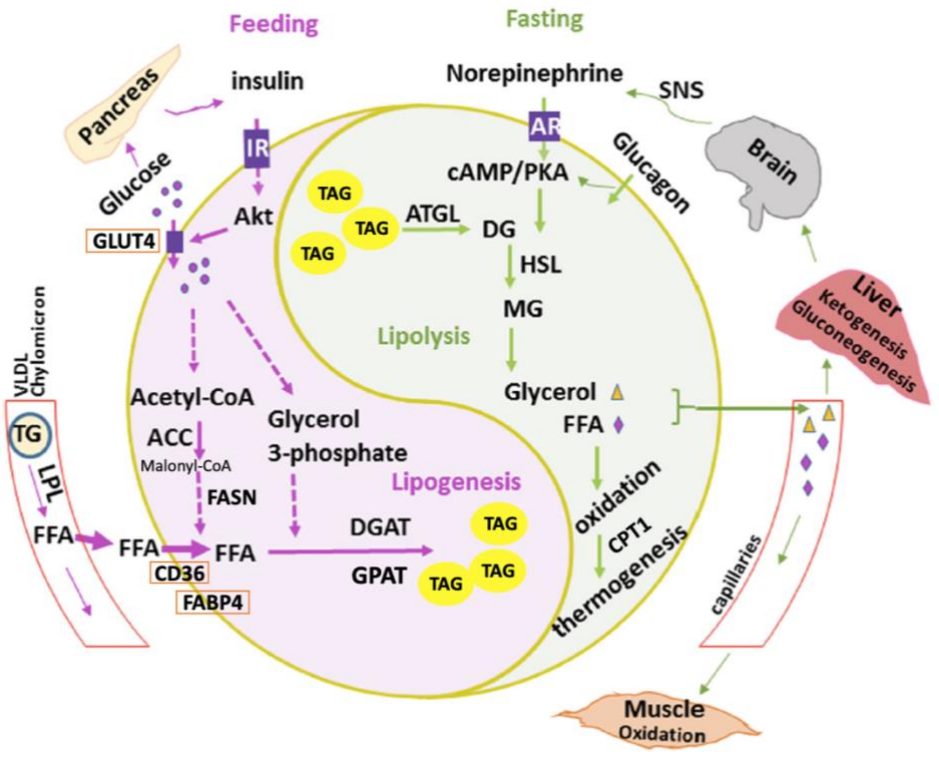

Figure 6. Lipid metabolism and mobilization controlled by adipose tissue. Lipogenesis is a process by which carbohydrates are converted into fatty acids, and promote the biosynthesis of TAG and expansion of lipid droplet in adipocytes. Lipolysis, in an opposite way, breaks down TAG to free fatty acid (FFA) and glycerol that can be either oxidized or released. The uptake of circulating FFA by liver, muscle and other tissues is a main pathway of lipid mobilization. Both lipogenic and lipolytic pathways are sensitive to nutrition as well as hormones such as insulin, norepinephrine and glucagon. Thus, a subtle regulation of lipogenesis and lipolysis is required for systemic energy homeostasis and insulin sensitivity. AR, adrenergic receptor; cAMP, cyclic adenosine monophosphate; IR, insulin receptor; PKA, protein kinase A. Adapted from [94].

1.2.6. Hormones

Adipose tissue produces and secretes adipocyte-derived molecules often known as adipokines. Their discoveries were the first indicators that adipose tissue was an endocrine organ with the control of systemic energy homeostasis. In the early 1990s, leptin and adiponectin were identified in adipose tissue and until now they have been extensively studied [95,96]. Leptin is secreted by adipocytes after feeding and acts primarily in the brain to inhibit food intake and balance energy expenditure [97]. In the hypothalamus, the hormone leptin binds to leptin or obesity receptor (Ob-R) isoform Ob-Rb, the only full-length isoform

out of six which is able to fully transduce the signal into the cell [98]. Leptin deficient ob/ob knockout mice presented profound obesity increasing the size of adipose tissue [95]. Apart from having an endocrine role, leptin also bind to leptin receptors in the adipocytes regulating adipose tissue metabolism through autocrine signaling [99].

Adiponectin is also expressed in fat cells and its role is to improve whole body glucose and lipid homeostasis. Adiponectin enhances adipocyte lipid storage with a healthy expansion of adipose tissue, thereby preventing ectopic fat accumulation. Therefore, adiponectin protects against diabetes, cardiovascular diseases, inflammation and metabolic syndrome [99].

1.2.7. Inflammation

Obesity is characterized by systemic chronic inflammation, which has been demonstrated to have an important role in the insulin resistance. The accumulation of lipids in adipose tissue and an imbalance between fatty acid uptake and β-oxidation in adipocytes contribute to inflammation and insulin resistance [100]. Monocytes are commonly differentiated into pro-inflammatory M1 macrophages in adipose tissue, although they can also be differentiated into anti-inflammatory M2 [101]. M1 macrophages release pro-inflammatory cytokines, like tumor necrosis factor alpha (TNF-α) under the stimulation of lipid or other factors, which cause insulin resistance through the inactivation of IRS1 [102]. Furthermore, it induces lipolysis, which leads to an increment of free fatty acid levels and creates a "pro-inflammatory vicious cycle" [103].

Specific lipids can activate kinases such as Jun amino-terminal kinase (JNK), IκB kinase (IKK), and protein kinase C (PKC) which phosphorylate the IRS1 in serine and suppresses insulin signaling [104]. Furthermore, excessive enlargement of adipocytes (hypertrophy) without enough neovascularization

could generate hypoxia in adipose tissue [105]. Altogether, these stimuli cause the infiltration of immune cells in adipose tissue.

Moreover, anther cytokine involved in the pathophysiology of obesity is interleukin 6 (IL-6). It is present in adipose tissue and in circulation, however it is not clear whether its role is beneficial or deleterious [106]. It has been shown that a chronic exposure of IL-6 in 3T3-L1 adipocytes, impairs insulin signaling [107]. While, a clinical study where diabetic participants were exposed to acute IL-6 levels increased fatty acid turnover [108]. Results showed opposite IL-6 effects since many variables may differ between the experiments. The principal divergence is that one experiment was *in vitro* and the other one was a clinical study.

Another pro-inflammatory chemokine present in adipose tissue and plasma in obese conditions is monocyte chemoattractant protein–1 (MCP-1). Indeed, mice fed a high-fat diet (HFD) showed higher mRNA levels of MCP-1 in adipose tissue and plasma, and presented insulin resistance, hepatic steatosis and macrophage accumulation in adipose tissue. On the other hand, MCP-1 homozygous knockout mice did not exhibit insulin resistance, hepatic steatosis neither macrophage infiltration in adipose tissue. These results suggests that MCP-1 contributes to these metabolic alterations [109].

1.2.8. Amino acid flux

The role of adipose tissue in lipid and glucose metabolism is strongly recognized, however its role in amino acid homeostasis is not highly known.

Adipose tissue presents the capacity to catabolize circulating branched chain amino acids (BCAA), leucine, isoleucine and valine, the three of nine essential amino acids and abundant in food supply accounting for 15 to 25% of total protein intake [110]. Adipose tissue plays a key role on regulating circulating

BCAA levels. It has been hypothesized that adipose tissue is the major site where excess BCAAs are store in form of lipids. Specifically, BCAA carbon skeletons are converted into new fatty acids [111]. The decrement of BCAA oxidation enzymes in adipose tissue, but not in muscle, leads to an increment of circulating BCAA levels. Moreover, the transplantation of adipose tissue into mice that are systemically defective in peripheral BCAA metabolism decreases BCAA levels by 30% in fasting state and 50% in fed state [111]. Obesity-related disorders including insulin resistance influences the metabolism of BCAA. It was observed that in humans with insulin resistance presented a downregulation of BCAA oxidation enzymes [112]. Therefore, the role of adipose tissue in regulating BCAA circulating levels is clear.

Moreover, adipose tissue also uptake glutamate and aspartate. In WAT, amino acids are metabolized, and the nitrogen removed from them is used to synthesized glutamine and alanine. These two amino acids are synthesized to avoid nitrogen toxification in WAT, since they can be liberated into circulation to be used for other tissues [113,114].

1.3. Expansion of adipose tissue

Cell size is a major determinant of WAT metabolism, whose alterations are associated with metabolic disorders. Adipose mass can expand in two ways, by adipose tissue hypertrophy or by adipose tissue hyperplasia. Hypertrophic WAT is characterized by large adipocytes through the storage of lipid on pre-existing adipocytes. On the other hand, hyperplastic WAT is characterized by an increment of smaller adipocyte number through the differentiation of progenitor cells. Around 10% of adipocytes in humans are renewed every year, while in mice 1-5% of adipocytes are replaced each day [115,116]. Adipocyte size varies

considerably within fat depots of the same individual and between individuals. Moreover, the average of adipocyte size increases during weight gain and decreases after weight loss [117].

However, obesity is usually characterized by a combination of hypertrophy and hyperplasia [118]. As we previously mentioned, adipocyte size is clinically important for its association with pathologic alterations. Hypertrophic morphology is associated with cardiometabolic disorders, including type II diabetes, insulin resistance, dyslipidemia and hypertension [119]. Furthermore, the anatomical location of fat depot influences adipose tissue morphology. The 80% of total body fat corresponds to subcutaneous fat, whereas the 10%-20% of the total fat in humans is visceral fat [120]. Although visceral fat depot is smaller compared to subcutaneous depot, visceral fat is considered more deleterious. Hypertrophic visceral fat is associated with insulin resistance and cardiometabolic disorders including dyslipidemia [119] [121]. Individuals that are unable to expand their sWAT in a healthy manner in response to a continuous energy income, are the ones in high risk of lipid accumulation in vWAT, inducing the first step for adipose tissue dysfunction. Moreover, TAG excess may accumulate in non-adipose organs including liver, muscle, heart inducing ectopic fat accumulation [122] .

1.3.1. Hypertrophy

In 1976, it was discovered that hypertrophic adipocytes presented defects on glucose metabolism [123]. Hypertrophic adipocytes present several characteristics that explain the deleterious metabolism of glucose. In obesity, hypertrophic WAT present dead adipocytes which impairs adipose tissue function and induces inflammation [101][124]. Hypertrophic adipocytes

synthesize and secrete pro-inflammatory cytokines including TNF-α, IL-6 and MCP-1 and recruit immune cells like macrophages. These high concentration of pro-inflammatory cytokines leads to serin phosphorylation of IRS1 causing the development of insulin resistance [125]. Hypertrophic WAT induces local adipose tissue hypoxia due to a relative deficiency of vasculature which accelerates tissue fibrosis [105,126]. Furthermore, basal lipolysis is elevated in hypertrophic adipocytes, leading to an increment of free fatty acid release into circulation which can be taken up by other tissues causing ectopic lipid accumulation [127,128]. Saturated fatty acids lead to chronic inflammation and insulin resistance [83,129]. Therefore, WAT hypertrophy impairs adipocyte function through inflammation, due to cell death and hypoxia, and excessive free fatty acids mobilization, exacerbating insulin resistance and disrupting energy metabolism.

1.3.2. Hyperplasia

Adipocyte hyperplasia protects against obesity-related comorbidities and occurs in greater extent in sWAT than vWAT [130,131]. In hyperplasia expansion, adipose precursor cells need to be differentiated into mature adipocytes by various transcription factors and hormones. PPARγ and C/EBPα regulate the induction and maintain the whole adipogenic process [132]. Overexpression of PPARγ induces adipogenic differentiation of new small adipocytes leading to an enhancement of insulin-dependent glucose uptake and providing higher capacity to store fat in the proper tissue [133].

Figure 7 shows the mechanisms of adipose tissue expansion and the corresponding health effects.

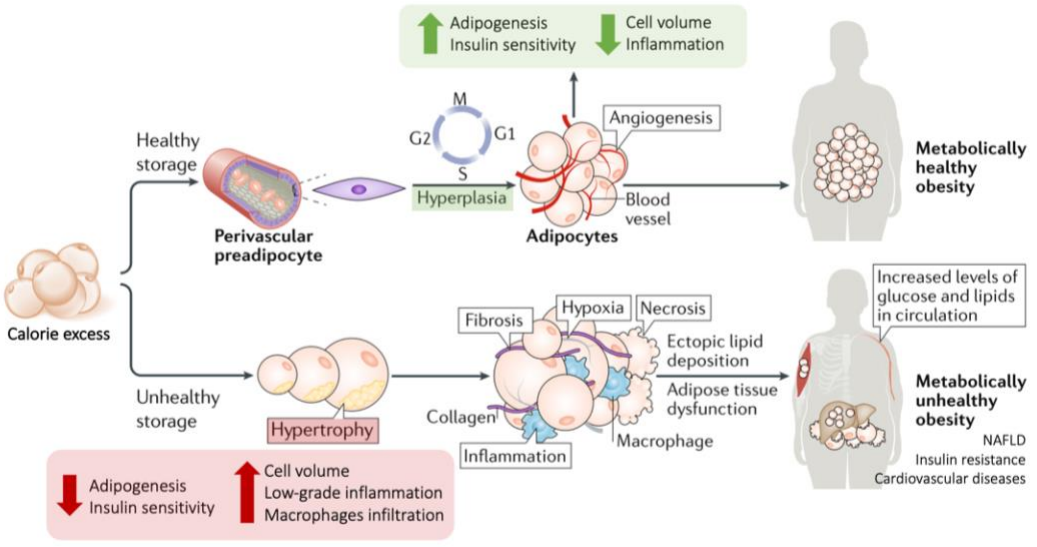

Figure 7. Mechanisms of adipose tissue expansion: through differentiation of resident tissue precursors to form new adipocytes (hyperplasia) or through enlargement of existing adipocytes (hypertrophy). Hyperplasia is generally considered healthy because adipose tissue maintains proper vascularization and levels of metabolism-modulatory adipokines. Hypertrophy of adipocytes is associated with an increase in hypoxia, which could lead to tissue fibrosis, necrosis, infiltration of immune cells and inflammation. These factors decrease adipose tissue function, leading to persistently elevated levels of nutrients (sugars and lipids) in the blood, contributing to earlier onset of metabolic disease and causing toxic lipid deposition in other tissues, such as muscle and liver. Adapted from [123].

2. Circadian rhythm

Most species are constantly exposed to predictable changes due to the Earth rotation which leads to light-dark cycle. To efficiently adapt and anticipate to daily recurring events, organisms have developed circadian clocks (from Latin *circa*, about; *dies*, day) that tightly regulate physiological processes. For example, some processes that oscillate throughout the day to respond better for near future actions or external cues are rest/activity cycle, fasting/feeding cycle, blood pressure, hormones secretion, body temperature, among others [134].

Environmental cues, synchronizers or time givers (zeitgebers) such as light, coordinate the circadian rhythm of organisms. Moreover, organisms present

intrinsic endogenous timing systems which control the circadian rhythm and could persist with the absence of environmental cues [135].

2.1. Molecular machinery of the circadian clock

The central clock is located in the suprachiasmatic nucleus (SCN) of the hypothalamus which orchestrates the clocks of peripheral tissues, including adipose tissue, via endocrine and nervous system. SCN is synchronized by light which is received by the eye and signals the status of the environmental light-dark to the master clock [136].

The endogenous circadian rhythms resulted from a series of interconnected positive and negative transcription-translation feedback loops. In mammals, the principal core clock components are circadian locomotor output cycles kaput (*Clock*) and brain and muscle Arnt-like 1 (*Bmal1,* or also known as *Arntl*), two transcription factors that form a heterodimer complex in the nucleus and activates the transcription of Period (*Per1-3*) and Cryptochrome (*Cry1,2*) by binding to the E-box elements of these genes [137]. Both resulting proteins would be accumulated in the cytoplasm which would induce the formation of a complex (PER-CRY) that enters the nucleus and represses CLOCK-BMAL1. Degradation of PER and CRY proteins is required to finish the repression phase and restart a new cycle of transcription, which is crucial in order to set the 24 hours period of the clock [137]. A secondary loop stabilizes these core-clock genes in which the nuclear receptor RAR-related orphan receptor alpha (RORα) and nuclear receptor subfamily 1 group D member 1 (NR1D1, also known as REV-ERBα) bind the ROR/REV-ERB-response element (RORE) in the promoter region of BMAL1. The expression of Bmal1 is activated by RORα and repressed by NR1D1 [138]. In addition to *Rorα*, PPARα is also a positive regulator of *Bmal1* expression. And interestingly, BMAL1 also regulates *Pparα* gene expression [139].

Several posttranslational regulators also play an important role on the modulation of circadian clock. Sirtuin 1 (SIRT1), a histone deacetylase dependent on the intracellular levels of nicotinamide adenine dinucleotide (NAD+), regulates CLOCK. The synthesis of the substrate NAD+ is regulated by the enzyme nicotinamide phosphoribosyltransferase (NAMPT), whose promoter is activated by CLOCK:BMAL1 dimer [140,141]. Therefore, circadian rhythms are directly linked with metabolism homeostasis (**Figure 8**).

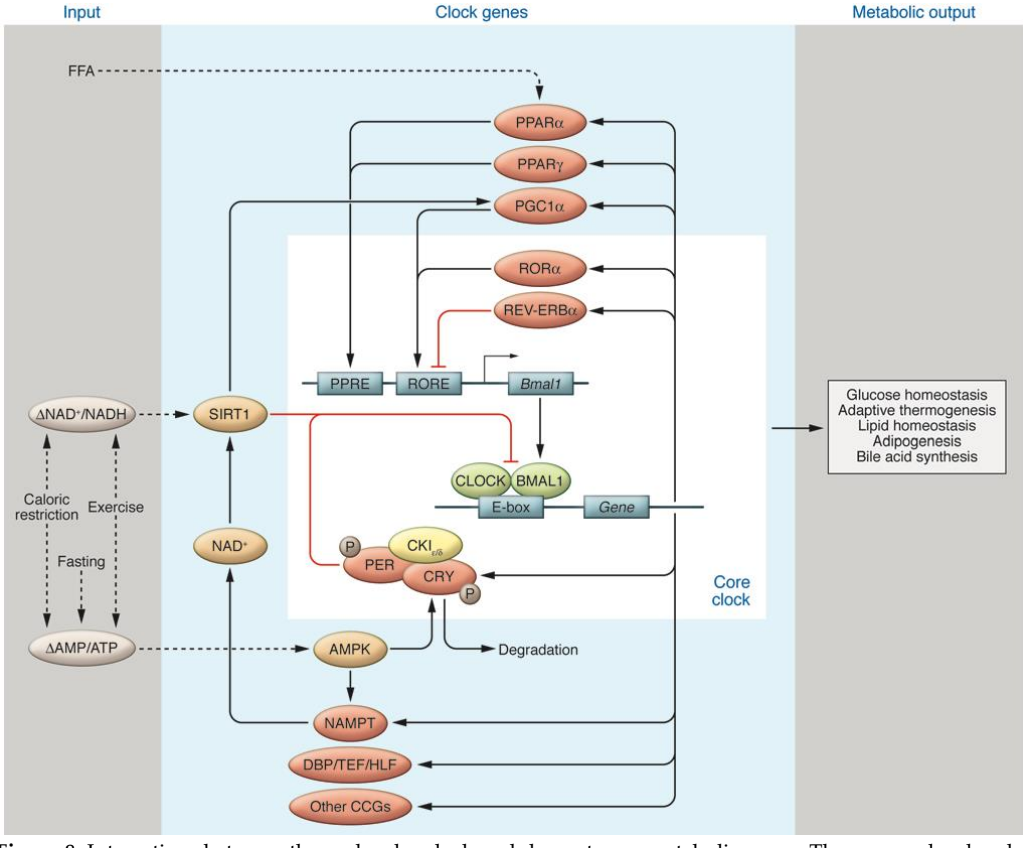

Figure 8. Interactions between the molecular clock and downstream metabolic genes. The core molecular clock consists of several transcription/translation feedback loops, including posttranscriptional regulation (yellow), that oscillate with an approximately 24-hour periodicity. CLOCK and BMAL1 heterodimerize to drive rhythmic expression of downstream target genes (shown in red), which in turn regulate diverse metabolic processes, including glucose metabolism, lipid homeostasis, and thermogenesis. Many of these clock target genes in turn reciprocally regulate the clock in response to changes in nutrient status (shown in blue) via cellular nutrient sensors (shown in orange), generating a complex network of interlocking feedback loops that fine-tune the clock and coordinate metabolic processes with the daily cycles of sleep/wakefulness and fasting/feeding. Dashed lines represent metabolic inputs; solid lines depict interactions among core clock genes, clock-controlled genes, and nutrient sensors. Figure obtained from [142].

Indeed, peripheral clocks are entrained by various factors, including feeding/fasting being the most important. An example is the food anticipatory activity where several tissues are ready for food ingestion as they present anticipatory rhythms which activate the secretion of enzymes and hormones, and the expression of certain genes necessary for the digestion process [143].

2.2. Rhythmic parameters

The study of circadian rhythm requires the evaluation of rhythmic parameters (**Figure 9**) [144,145].

- The principal rhythmic parameters are:
  - **Period**: The length of time that it takes a rhythm to repeat itself. Circadian rhythms have approximately 24-hours period.
  - **Mesor**: The mean of a rhythm or the central value around which the oscillation occurs.
  - **Amplitude**: The magnitude or strength of a rhythm. Half the range of excursion of the cycle with the given period.
  - **Peak**: The highest value of a rhythm.
  - **Trough or nadir**: The lowest value of a rhythm.
  - **Acrophase**: The time at which a rhythm peaks.
  - **Phase**: The relative displacement between the oscillation and a reference oscillation or the environmental light/dark cycle oscillation.

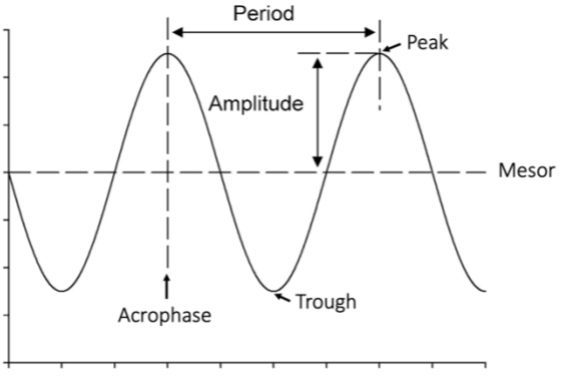

Figure 9. Diagram of an oscillatory process identifying rhythmic parameters: mesor, period, amplitude, acrophase, peak and trough. Adapted from [144].

- Other terms:
  - **Phase advance**: A shift in the timing of a rhythm such that it begins earlier.
  - **Phase delay**: A shift in the timing of a rhythm such that it begins later.
  - **Misalignment** or **desynchrony**: The state of having difference in phases between two rhythms.
  - **Transcriptional-Translational Feedback loop**: Series of feedback loops among circadian clock genes and proteins that maintain the 24-hour rhythms in nearly every cell of the body.
  - **Zeitgeber**: An external cue that entrains or influences the phase of a rhythm.
  - **Circadian rhythm**: Endogenously generated rhythms, even in the absence of light, with a period close to 24 hours.
  - **Diurnal rhythm**: A circadian rhythm that is synchronized with the day/night cycle.

2.3. Circadian clock and metabolism

Around 40% of all protein coding genes in mice present circadian rhythms, which are involved in the regulation of physiological and metabolic functions [146,147]. In adipocytes, the circadian clock controls adipogenesis, lipolysis, inflammation and expression and secretion of certain hormones. Indeed, *Bmal1* and *Rev-Erbα* activate adipocyte differentiation, while *Per2* and *RORα*, inhibit

adipogenesis through the reduction of *Pparα* gene expression [148–150]. Interestingly, the circadian rhythm of *Pparα* expression in adipocytes is damped under HFD in male mice [151].

The physiology of adipose tissue is tightly regulated by circadian rhythm since systemic energy demands fluctuate throughout the day. Fatty acid uptake and lipogenesis show diurnal oscillations in WAT reaching their maximum rates during active phase, while lipolysis rate presents its maximum during rest phase through *Atgl* and *Hsl*, the rate-limiting enzymes, which are controlled by CLOCK:BMAL1. Moreover, circulating levels of TAG, NEFA, cholesterol and glucose present diurnal oscillations that even persist during fasting [152,153].

A molecule implicated as a mediator between circadian rhythm and metabolism is NAD^+, an important cofactor involved in cellular redox reactions. The molecular clock directly regulates NAMPT, the rate-limiting enzyme of NAD^+ biosynthesis. Therefore, NAMPT synchronizes the circadian rhythm of NAD^+ levels in adipose tissue, even when animals are maintained in constant darkness [141,154]. Mice with mutations in the activator genes *Clock* and *Bmal1* present low NAD^+ levels, while those with mutations in the clock repressor genes *Cry1* and *Per2* exhibit high NAD^+ levels. This suggests that NAD^+ is directly regulated by the clock. The metabolic enzyme SIRT1 is a NAD^+-dependent deacetylase which its activity is also regulated by circadian rhythm. SIRT1 targets several transcription factors involved in the maintenance of nutrient flux, being a critical regulator of metabolic processes including gluconeogenesis, lipid metabolism and insulin sensitivity [154]. NAD^+ rhythmicity regulates SIRT1 activity, which coordinates the feeding/fasting cycle. Furthermore, SIRT1 also modulates CLOCK/BMAL1 activity generating a negative feedback loop [155].

To further demonstrate the interaction between metabolism and circadian clock in WAT, clock gene-mutant mice show changes in adiposity and adipocyte size. Indeed, *Clock-Δ19* mutant mice showed higher body weight, adiposity and adipocyte hypertrophy. Moreover, these mice present and alteration on feeding rhythms and an increment on food intake, and circulating cholesterol and TAG levels [156,157]. Mutations in other clock genes induce different effects. For example, *Cry* double-mutant STD diet-fed mice were leaner compared to wild-type mice despite of the dampened feeding rhythms. On other hand, *Cry* double-mutant HFD diet-fed mice rapidly gained weight although the food intake was lower [158]. The deflection of *Cry* in adipocytes potentiates lipid uptake and insulin-stimulated lipogenesis, which makes mice susceptible to diet-induced obesity. A mutation of *Per2* results in a higher body weight and food intake [159].

Adipocyte-specific mutation of *Bmal1* diminishes the concentration of polyunsaturated fatty acids (PUFA) in plasma and WAT. PUFAs inhibits appetite when reach the brain after crossing the blood-brain barrier [82,160]. Therefore, the higher hyperphagia observed in clock mutant mice could be induced by the reduced interaction PUFA-brain due to the low levels of PUFA.

Therefore, it exists a close interaction between circadian clock and metabolism. Thus, the disruption of circadian clock can alter the physiology and metabolism of WAT, affecting systemic homeostasis and increasing the risk to suffer metabolic disorders and obesity [161].

2.4. Disruption of the circadian rhythm

Endogenous circadian rhythms in organisms need to be synchronized with light/dark cycle. The time cues, known as time givers (zeitgebers (ZT)), such as

light, allow the biological clock – which present a slight longer period of 24-hours – to be reset and entrained to the 24-hour day [162]. Misalignment between endogenous circadian rhythms with daily photoperiodic cycles is a risk factor for developing negative health outcomes including impaired glucose tolerance, reduced insulin sensitivity and leptin levels, and increased body mass, blood pressure and ghrelin levels [163]. Indeed, the disruption of circadian rhythms could cause hypertriglyceridemia, hyperinsulinemia, inflammation, coronary heart diseases, obesity, diabetes, and other disorders [152,153].

Night shift workers, which present shift work sleep disorder, have a higher risk to develop dyslipidemia, diabetes, hypertension, heart diseases, depression, and infertility [164].

Circadian misalignment can also be induced by other factors than light. Diet, another zeitgeber, can modulate the circadian clock in peripheral tissues [165]. Time-restricted feeding (TRF), with 10 hours access to food during the active phase, improve metabolic health in clock mutant mice compare to *ad libitum*-fed mice. Indeed, TRF prevents fatty liver, dyslipidemia, glucose intolerance, obesity in clock mutant mice compared to *ad libitum* food intake in wild type and clockless mice [166–168].

Thus, the synchronization of physiological processes with light/dark cycle is an important aspect to maintain a healthy condition and to avoid certain diseases.

3. Bioactive compounds and health

3.1. Polyphenols

Polyphenols are secondary metabolites found in plants. These molecules are not essential for plant growth but are relevant to defense against stress factors including bacteria and fungi infections, herbivores, ultraviolet

irradiation, drought, extreme temperatures, among others [169,170]. Polyphenols are characterized to present at least one aromatic ring; phenol group (**Figure 10**), and one or more hydroxyl groups attached. Different combinations of phenol units and hydroxyl groups attached bring the existence of 8,000 different polyphenols identified [171].

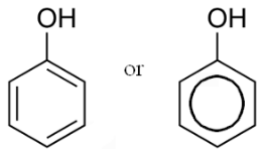

Figure 10. Phenol group.

Polyphenols are classified in flavonoids and nonflavonoids (phenolic acids, lignans and stilbenes) (**Figure 11**). Flavonoids are also subdivided in flavanols (flavan-3-ols), flavanones, flavones, isoflavones, flavonols and anthocyanidins [172].

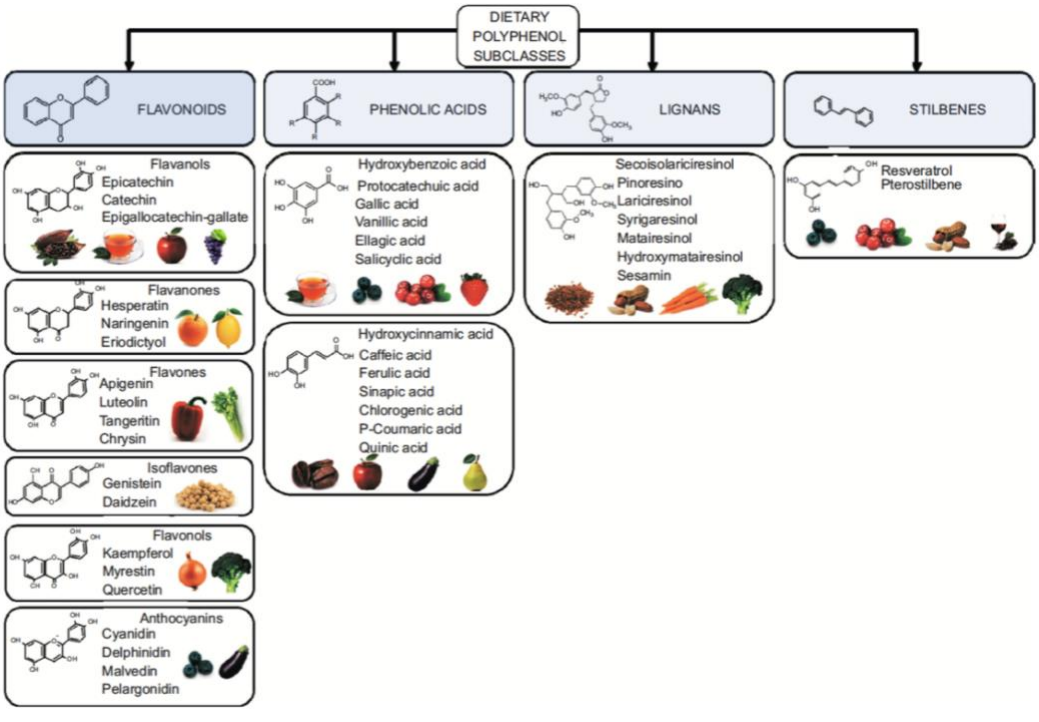

Figure 11. Dietary polyphenol subclasses, their basic chemical structure, and typical dietary sources. Adapted from [172].

Polyphenols are exclusively present in fruits and vegetables including grapes, strawberries, carrots, nuts, blackberries, apples, legumes, cocoa, broccoli, cereals, olives and beverages like tea, coffee and wine [169].

Phenolic compounds confer the color of vegetables ranging from orange to blue [169]. Moreover, polyphenols are known to be great antioxidant agents and have the capacity to prevent and ameliorate many health problems including inflammation, cancers, cardiometabolic diseases, diabetes, obesity, among others [173].

It is important to consider that the health effects of polyphenols are mainly attributed to the product of their metabolism. Indeed, when polyphenols reach the small intestine and the liver they are conjugated by certain enzymes and generate glucuronide, sulfate, and methylated derivatives. A high quantity of polyphenols is not absorbed by small intestine and reach the colon where they are metabolized by gut microbiota [174]. Thus, not only environmental, and agricultural factors affect the polyphenol content but endogenous metabolism including specific enzymes and microbiota are determinant for their effects.

3.1.1. Grape seed proanthocyanidin extract

Grape seed proanthocyanidin extract (GSPE) used in this Doctoral Thesis was composed by catechin, epicatechin, proanthocyanidin dimer B1, proanthocyanidin dimer B3, proanthocyanidin dimer B2, gallic acid, epicatechin gallate, dimer gallate, proanthocyanidin trimer, protocatechuic acid, vanillic acid, epigallocatechin, epigallocatechin gallate and proanthocyanidin tetramer; listed from highest concentration (121.32 ± 3.41 mg/g; catechin) to lowest concentration (0.05 ± 0.01 mg/g; proanthocyanidin tetramer). Polyphenols from GSPE were mainly classified as flavanols and phenolic acids [175]. Proanthocyanidins are

formed by oligomerization or polymerization of the flavan-3-ol monomers including catechin and epicatechin, and are the most abundant in human diets [173].

Proanthocyanidins are considered antioxidant molecules for its capacity to reduce free radicals through one electron donation by the phenolic OH group. However, it is not the unique mechanism by which proanthocyanidins exert their biological effects that result in beneficial health effects. It has been proposed proanthocyanidins modulate biological systems through different mechanisms of action, although the molecular interactions of these compounds with cell physiology remain mostly speculative. Proanthocyanidins can act through two major mechanisms:

- Basic biochemical mechanisms through specific interactions with proteins and enzymes which modify enzymatic activities and transcription factors. In this sense, proanthocyanidins can increase the expression or activity of several antioxidant enzymes, for example regulating the activity of nuclear factor-κB (NF- κB), which modulates the gene expression of pro-inflammatory factor cyclooxygenase (COX). Moreover, proanthocyanidins can induce the transcription of nuclear receptors including farnesoid X receptor (FXR), which regulates lipid homeostasis, and RORα, which regulates the molecular clock. Proanthocyanidins can also prevent apoptosis by modulating caspase-12 pathway.
- Epigenetic mechanisms including histone modifications, DNA methylation and microRNAs (miRNAs) modulation, which modulate the expression of mRNA. Several miRNAs play important regulatory roles in cell differentiation, insulin action and fat metabolism in adipocytes [173, 176].

Therefore, proanthocyanidins are able to modulate several pathways related to antioxidant mechanism, inflammation, apoptosis, lipid homeostasis and energy metabolism [173]. Due to the ability of proanthocyanidins to exert these effects through such a wide range of mechanisms, it was postulated that they could act in a higher level; which is the molecular clock. Indeed, in the recent years it has been shown that proanthocyanidins modulate the molecular clock changing the expression of core-clock genes. We will discuss this matter in the section 3.3. "Chronobiological effects of bioactive compounds".

Furthermore, due to the many beneficial properties of proanthocyanidins, it has been extensible studied their role on obesity. Previously, in our group it was found that physiological doses of GSPE reduced the size of visceral adipocytes and increased their number inducing a healthy expansion of WAT through hyperplasia [177]. It has been proposed that GSPE induces adipogenesis through a Sirt1-dependent upregulation of *Pparγ*, and inducing the expression of *Plin1*, *Fabp4* and *Adipoq* in WAT [177]. However, other studies suggest that GSPE interfere in the early stages of preadipocyte differentiation decreasing the expression of the PPAR-γ2 receptor, the main regulator of adipocyte differentiation, and downregulating the expression of lipid synthesis regulators including Pparγ, *C/EBPα*, FASN, PLIN1, FABP4 and *Adipoq* [178]. Furthermore, contradictory results are shown regarding the lipolytic effect of proanthocyanidins. Some studies showed that proanthocyanidins present an inhibitory effect against lipolytic enzymes including LPL and HSL and others suggest that proanthocyanidins induce the expression of *Hsl* and *Atgl* followed by an upregulation of genes involved in β-oxidation in visceral WAT depots [179–182].

Montagut *et al.* suggest that the ability of GSPE to modulate adipocyte differentiation depends on the physiological conditions and fat depot [183].

Indeed, in lean rats the protective effects of GSPE targets visceral WAT depot, while in obese rats GSPE mainly targets subcutaneous WAT [184]. Nevertheless, HFD-fed hamsters supplemented with GSPE for 15 days presented lower body weight and adiposity with a reduction of the weight of all visceral and subcutaneous WAT depots [180].

Moreover, other studies demonstrate that GSPE has an effect on the hypothalamus modifying anorexigenic and orexigenic genes, responsible for hunger regulation, and therefore food intake [185].

Obesity is closely related, among others, to the secretion of adipokines by WAT. Adipokines contribute to the peripheral insulin resistance and disorders related to lipid metabolism. In this context, GSPE exhibit beneficial effects on adipokine secretion and oxidative stress, which offers proanthocyanidins a substantial potential to fight against metabolic disorders and obesity [182,186].

GSPE can revert the BAT mitochondrial dysfunction present in obesity ameliorating the thermogenic capacity which would be beneficial as an anti-obesity effect [187,188]. In this sense, it has been suggest that proanthocyanidins might induce WAT browning, although no evidence has demonstrated this potential effect [189].

3.2. Bioactive multi-compound

Obesity is a multifactorial disease caused by the dysregulation of several organs and mechanisms, including the metabolism of WAT. These leads to several metabolic diseases including insulin resistance, cardiovascular diseases, NAFLD among others. Therefore, in the recent years it has increased the interest to combine different bioactive compounds in order to obtain additive or synergic effects that could tackle several pathways involved in obesity. In this sense, a bioactive multi-compound (MIX), which was based of GSPE, was created by our

group with the purpose of finding greater effects compared to individual-compound consumption for the management of obesity.

Indeed, a previous study in our group demonstrated that MIX reduces adiposity, specifically the weight of subcutaneous iWAT and visceral eWAT, inhibits lipogenesis and increases lipolysis [190].

MIX was based on proanthocyanidins extracted from grape-seed (GSPE; 25 mg/kg), anthocyanins from berries (100 mg/kg), conjugated linoleic acid (CLA; 100 mg/kg) and protein hydrolysate from chicken feet (Hpp11; 55 mg/kg).

Anthocyanins are a subgroup of flavonoids commonly found in fruits and vegetables. They exert metabolic effects beneficial for obesity and metabolic syndrome. In fact, HFD-fed mice supplemented daily for 8 weeks with 200 mg/kg of anthocyanins presented a reduction on body weight, serum glucose and a downregulation of *Tnfα*, *Il6* and *Pparγ* gene expression [191]. Moreover, other studies showed beneficial effects of anthocyanidins on insulin sensitivity [192].

Another component of MIX is CLA which is a fatty acid formed by the conjugation of isomers of polyunsaturated linoleic acid (18:2n6). CLA is found in meat and milk from cows and sheep. Two types of isomers can be found; *cis-9,trans-11* and *trans-10,cis-12* (**Figure 12**). The most abundant isomer in diet is *cis-9,trans-11* [193].

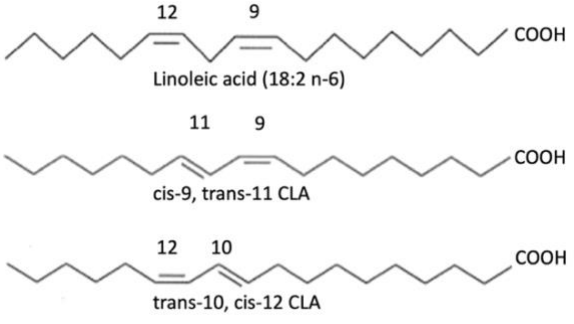

Figure 12. Structure of linoleic acid, *cis-9,trans-11* CLA and *trans-10,cis-12* CLA. Adapted from [194].

An interest in CLA arose due to its effects on reducing fat mass which led to its commercialization as a food supplement. The isomer *trans-10,cis-12* is the one mainly responsible for body fat reduction and the one that affects circulating lipids [193]. Specifically, it inhibits PPARγ which regulates the expression of genes responsible for lipid and glucose uptake including *Lpl* and *Glut4* [195]. Moreover, the *trans-10,cis-12* CLA, but not *cis-9,trans-11* CLA, increases adipocyte lipolysis [196]. Therefore, the increment of lipolysis and the reduction of lipid and glucose uptake into adipocytes leads to a reduction in fat mass by *trans-10,cis-12* CLA.

Nevertheless, it has been found that CLA also present side effects. The isoform *trans-10,cis-12* could induce insulin resistance and hepatic lipid accumulation [197]. Hepatic steatosis was associated with a decrement in body adiposity, which suggests that lipids accumulated in the liver come from the uptake of circulating fatty acids liberated from adipose tissue [198]. On the other hand, *cis-9,trans-11* could present beneficial effects on insulin sensitivity [197]. However, beneficial effects and side effects are still controversial as they seem to vary depending on the dose, species and metabolism [175,176]. In fact, a mixture of *cis-9,trans-11*, *trans-10,cis-12* and other CLA isomers increased *Pparγ* gene expression followed by an increment of adiponectin and fatty acid transporters [199].

Lastly, another component of MIX is Hpp11. Hpp11 is constituted by bioactive peptides obtained from proteins of chicken feet which are a by-product of the food industry. This hydrolysate is a patent product developed in our group with the aim to obtain a bioactive compound with antihypertensive properties [179,180]. Hpp11 inhibits angiotensin-converting enzyme (ACE), and therefore reduces vasoconstriction [200]. Thus, Hpp11 is a good candidate to ameliorate obesity related pathologies like cardiovascular diseases.

3.3. Chronobiological effects of bioactive compounds

Types of food, meal timing, nutrients and some bioactive compounds modulate the circadian clock which can help reset circadian rhythms attenuating metabolic diseases including obesity (**Figure 13**).

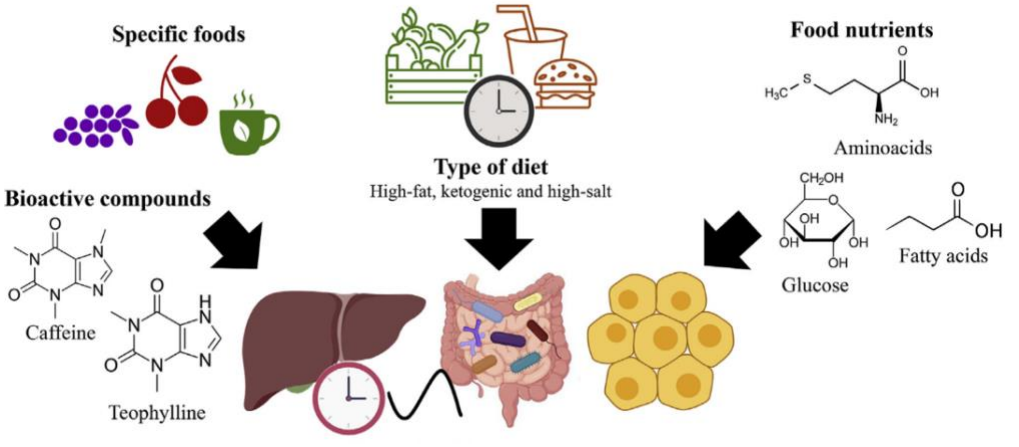

Figure 13. The interplay between circadian clock, nutrition and metabolism. Adapted from [201].

There is limited research on studying the chronobiological response of certain bioactive compounds, however some studies have been carried out and sustains the potential effect of some natural components on modulating biological clocks.

First, it has been shown that different nutritional diets affect the circadian clock. HFD induces changes in the period of locomotor activity rhythm and the expression of clock genes (*Clock*, *Bmal1* and *Per2*) and clock-controlled genes involved in energy homeostasis in adipose tissue [151]. Furthermore, meal timing is a key factor for the synchronization of endogenous clock. For example, time-limited food intervention leads to a reduction on adiposity [202].

Single nutrients including caffeine, cinnamic acid, nobiletin, palmitate, resveratrol can correct circadian disorders ameliorating metabolic comorbidities [203]. GSPE have the capacity to modulate peripheral molecular clocks by

synchronizing the expression of clock genes (*Clock*, *Bmal1*, *Per2*, *Rorα*, and *Rev-erb*) in liver and gut, and with lesser extent in WAT of lean and obese rats [204]. Polyphenols, such as resveratrol, restore the expression of clock genes, the circadian rhythm of circulating leptin, insulin and fasting glucose, and reduce the body weight of HFD-fed mice [205].

Therefore, polyphenols and other bioactive compounds from different natural sources can correct circadian disorders associated with metabolic diseases. However, time-of day compound administration must be evaluated to understand molecular mechanisms and to ameliorate the efficiency of the compounds. In fact, certain drugs such statins, which reduce low-density lipoproteins (LDL) levels, present higher efficacy when are taken in the evening since cholesterol biosynthesis present circadian rhythm reaching the peak at night in humans [206,207]. Thus, time-of-day administration is essential for the efficacy of drugs, bioactive compounds and nutraceuticals. Nevertheless, scare data is available regarding the effect of bioactive compounds depending on the time of administration. Therefore, further research is needed in the file of "chrononutrition" and "chrononutraceuticals".

4. References

[1] "World Health Organization (who.int), 2022.pdf."

[2] "World Obesity Federation (worldobesity.org), 2019.pdf."

[3] S. S. Choe, J. Y. Huh, I. J. Hwang, J. I. Kim, and J. B. Kim, "Adipose tissue remodeling: Its role in energy metabolism and metabolic disorders" *Front. Endocrinol. (Lausanne).*, vol. 7, pp. 1–16, 2016.

[4] G. H. Goossens, "The Metabolic Phenotype in Obesity: Fat Mass, Body Fat Distribution, and Adipose Tissue Function" *Obes. Facts*, vol. 10, no. 3, pp. 207–215, 2017.

[5] G. S. Hotamisligil, "Inflammation and metabolic disorders" *Insight Rev. - Nat.*, vol. 444, 2006.

[6] K. E. Wellen, G. S. Hotamisligil, K. E. Wellen, and G. S. Hotamisligil, "Inflammation, stress, and diabetes" vol. 115, no. 5, pp. 1111–1119, 2005.

[7] C. M. Phillips, "Metabolically healthy obesity: Definitions, determinants and clinical implications" *Rev. Endocr. Metab. Disord.*, vol. 14, no. 3, pp. 219–227, 2013.

[8] S. Cinti, "The adipose organ" *Prostaglandins Leukot. Essent. Fat. Acids*, vol. 73, no. 1 SPEC. ISS., pp. 9–15, 2005.

[9] B. Cannon and J. Nedergaard, "Brown Adipose Tissue: Function and Physiological Significance" *Physiol. Rev.*, vol. 84, no. 1, pp. 277–359, 2004.

[10] K. J. Suchacki and R. H. Stimson, "Nutritional regulation of human brown adipose tissue" *Nutrients*, vol. 13, no. 6, 2021.

[11] P. Boström *et al.*, "A PGC1-α-dependent myokine that drives brown-fat-like development of white fat and thermogenesis" *Nature*, vol. 481, no. 7382, pp. 463–468, 2012.

[12] S. Fabbiano *et al.*, "Caloric Restriction Leads to Browning of White Adipose Tissue through Type 2 Immune Signaling" *Cell Metab.*, vol. 24, no. 3, pp. 434–446, 2016.

[13] M. Saito, M. Matsushita, T. Yoneshiro, and Y. Okamatsu-Ogura, "Brown Adipose Tissue, Diet-Induced Thermogenesis, and Thermogenic Food Ingredients: From Mice to Men" *Front. Endocrinol. (Lausanne).*, vol. 11, no. April, 2020.

[14] K. Birsoy, W. T. Festuccia, and M. Laplante, "A comparative perspective on lipid storage in animals" *J. Cell Sci.*, vol. 126, no. 7, pp. 1541–1552, 2013.

[15] A. Drewnowski, "Sensory Properties of Fats and Fat Replacements" *Nutr. Rev.*, vol. 50, no. 4, pp. 17–20, 1992.

[16] F. Karpe and K. E. Pinnick, "Biology of upper-body and lower-body adipose tissue - Link to whole-body phenotypes" *Nat. Rev. Endocrinol.*, vol. 11, no. 2, pp. 90–100, 2015.

[17] L. Vishvanath and R. K. Gupta, "Contribution of adipogenesis to healthy adipose tissue expansion in obesity" *J. Clin. Invest.*, vol. 129, no. 10, pp. 4022–4031, 2019.

[18] A. Wronska and Z. Kmiec, "Structural and biochemical characteristics of various white adipose tissue depots" *Acta Physiol.*, vol. 205, no. 2, pp. 194–208, 2012.

[19] D. E. Chusyd, D. Wang, D. M. Huffman, and T. R. Nagy, "Relationships between Rodent White Adipose Fat Pads and Human White Adipose Fat Depots" *Front. Nutr.*, vol. 3, no. April, 2016.

[20] J. P. Després, "Body fat distribution and risk of cardiovascular disease: An update" *Circulation*, vol. 126, no. 10, pp. 1301–1313, 2012.

[21] L. Fontana, J. C. Eagon, M. E. Trujillo, P. E. Scherer, and S. Klein, "Visceral Fat Adipokine Secretion Is Associated With Systemic Inflammation in Obese Humans" *Diabetes*, vol. 56, no. April, pp. 1010–1013, 2007.

[22] K. N. Manolopoulos, F. Karpe, and K. N. Frayn, "Gluteofemoral body fat as a determinant of metabolic health" *Int. J. Obes.*, vol. 34, no. 6, pp. 949–959, 2010.

[23] G. Qiang *et al.*, "The obesity-induced transcriptional regulator TRIP-Br2 mediates visceral fat endoplasmic reticulum stress-induced inflammation" *Nat. Commun.*, vol. 7, pp. 1–14, 2016.

[24] L. E. Gyllenhammer, T. L. Alderete, C. M. Toledo-Corral, M. Weigensberg, and M. I. Goran, "Saturation of subcutaneous adipose tissue expansion and accumulation of ectopic fat associated with metabolic dysfunction during late and post-pubertal growth" *Int. J. Obes.*, vol. 40, no. 4, pp. 601–606, 2016.

[25] K. Frayn, "Adipose tissue as a buffer for daily lipid flux" *Diabetologia*, vol. 45, no. 9, pp. 1201–1210, 2002.

[26] P. Mathieu, P. Poirier, P. Pibarot, I. Lemieux, and J. P. Després, "Visceral obesity the link among inflammation, hypertension, and cardiovascular disease" *Hypertension*, vol. 53, no. 4, pp. 577–584, 2009.

[27] M. Hussain and F. R. Awan, "Hypertension regulating angiotensin peptides in the pathobiology of cardiovascular disease" *Clin. Exp. Hypertens.*, vol. 40, no. 4, pp. 344–352, 2018.

[28] S. K. Vasan *et al.*, "Comparison of regional fat measurements by dual-energy X-ray absorptiometry and conventional anthropometry and their association with markers of diabetes and cardiovascular disease risk" *Int. J. Obes.*, vol. 42, no. 4, pp. 850–857, 2018.

[29] S. Kurioka, Y. Murakami, M. Nishiki, M. Sohmiya, K. Koshimura, and Y. Kato, "Relationship between visceral fat accumulation and anti-lipolytic action of insulin in patients with type 2 diabetes mellitus" *Endocrine Journal*, vol. 49, no. 4. pp. 459–464, 2002.

[30] M. Rosenwald, A. Perdikari, T. Rülicke, and C. Wolfrum, "Bi-directional interconversion of brite and white adipocytes" *Nat. Cell Biol.*, vol. 15, no. 6, pp. 659–667, 2013.

[31] K. D. Nguyen *et al.*, "Alternatively activated macrophages produce catecholamines to sustain adaptive thermogenesis" *Nature*, vol. 480, no. 7375, pp. 104–108, 2011.

[32] and C. R. K. Thien T. Tran, Yuji Yamamoto, Stephane Gesta, "Beneficial Effects of Subcutaneous Fat Transplantation on Metabolism" *Cell Metab.*, vol. 7, no. 5, pp. 410–420, 2008.

[33] M. T. Foster, S. Softic, J. Caldwell, R. Kohli, A. D. DeKloet, and R. J. Seeley, "Subcutaneous adipose tissue transplantation in diet-induced obese mice attenuates metabolic dysregulation while removal exacerbates it" *Physiol. Rep.*, vol. 1, no. 2, pp. 1–12, 2013.

[34] P. Bora and A. S. Majumdar, "Adipose tissue-derived stromal vascular fraction in regenerative medicine: A brief review on biology and translation" *Stem Cell Res. Ther.*, vol. 8, no. 1, pp. 1–10, 2017.

[35] P. Seale *et al.*, "PRDM16 Controls a Brown Fat/Skeletal Muscle Switch" *Nature*, vol. 21, 454(7207), pp- 961-7.

[36] Q. Q. Tang and M. D. Lane, "Adipogenesis: From stem cell to adipocyte" *Annu. Rev. Biochem.*, vol. 81, pp. 715–736, 2012.

[37] M. Fessler, Michael B.; Rudel, Lawrence L.; Brown and Sheean, "Transcriptional Control of Brown Fat Determination by PRDM16" *Bone*, vol. 23, no. 1, pp. 1–7, 2008.

[38] S. Kajimura *et al.*, "Regulation of the brown and white fat gene programs through a PRDM16/CtBP transcriptional complex" *Genes Dev.*, vol. 22, no. 10, pp. 1397–1409, 2008.

[39] B. Cousin *et al.*, "Occurrence of brown adipocytes in rat white adipose tissue: Molecular and morphological characterization" *J. Cell Sci.*, vol. 103, no. 4, pp. 931–942, 1992.

[40] M. Ghorbani and J. Himms-Hagen, "Appearance of brown adipocytes in white adipose tissue during CL 316,243-induced reversal of obesity and diabetes in Zucker fa/fa rats" *Int. J. Obes.*, vol. 21, no. 6, pp. 465–475, 1997.

[41] N. Petrovic, T. B. Walden, I. G. Shabalina, J. A. Timmons, B. Cannon, and J. Nedergaard, "Chronic peroxisome proliferator-activated receptor γ (PPARγ) activation of epididymally

derived white adipocyte cultures reveals a population of thermogenically competent, UCP1-containing adipocytes molecularly distinct from classic brown adipocytes" *J. Biol. Chem.*, vol. 285, no. 10, pp. 7153–7164, 2010.

[42] P. Seale *et al.*, "Prdm16 determines the thermogenic program of subcutaneous white adipose tissue in mice" *J. Clin. Invest.*, vol. 121, no. 1, pp. 96–105, 2011.

[43] J. Sanchez-Gurmaches, C. M. Hung, and D. A. Guertin, "Emerging Complexities in Adipocyte Origins and Identity" *Trends Cell Biol.*, vol. 26, no. 5, pp. 313–326, 2016.

[44] G. Barbatelli *et al.*, "The emergence of cold-induced brown adipocytes in mouse white fat depots is determined predominantly by white to brown adipocyte transdifferentiation" *Am. J. Physiol. - Endocrinol. Metab.*, vol. 298, no. 6, pp. 1244–1253, 2010.

[45] K. Sarjeant and J. M. Stephens, "Adipogenesis" pp. 1–19.

[46] P. Arner and A. Kulyté, "MicroRNA regulatory networks in human adipose tissue and obesity" *Nat. Rev. Endocrinol.*, vol. 11, no. 5, pp. 276–288, 2015.

[47] P. M. de sá, A. J. Richard, H. Hang, and J. M. Stephens, "Transcriptional regulation of adipogenesis" *Compr. Physiol.*, vol. 7, no. 2, pp. 635–674, 2017.

[48] C. K. Glass, "Going nuclear in metabolic and cardiovascular disease" *J. Clin. Invest.*, vol. 116, no. 3, pp. 556–560, 2006.

[49] C. H. Lee *et al.*, "PPARδ regulates glucose metabolism and insulin sensitivity" *Proc. Natl. Acad. Sci. U. S. A.*, vol. 103, no. 9, pp. 3444–3449, 2006.

[50] H. D. H. Bryant Jeri L, Boughter John D, Gong Suzhen, LeDoux Mark S, "Inhibition of HDAC3 promotes ligand-independent PPARγ activation by protein acetylation" *Physiol. Behav.*, vol. 32, no. 1, pp. 41–52, 2010.

[51] K. A. Burns and J. P. Vanden Heuvel, "Modulation of PPAR activity via phosphorylation" *Biochim. Biophys. Acta - Mol. Cell Biol. Lipids*, vol. 1771, no. 8, pp. 952–960, 2007.

[52] C. Diradourian, J. Girard, and J. P. Pégorier, "Phosphorylation of PPARs: From molecular characterization to physiological relevance" *Biochimie*, vol. 87, no. 1 SPEC. ISS., pp. 33–38, 2005.

[53] T. T. Schug and X. Li, "Sirtuin 1 in lipid metabolism and obesity" *Ann. Med.*, vol. 43, no. 3, pp. 198–211, 2011.

[54] J. K. Hamm, B. H. Park, and S. R. Farmer, "A Role for C/EBPβ in Regulating Peroxisome Proliferator-activated Receptor γ Activity during Adipogenesis in 3T3-L1 Preadipocytes" *J. Biol. Chem.*, vol. 276, no. 21, pp. 18464–18471, 2001.

[55] Z. Cao, R. M. Umek, and S. L. McKnight, "Regulated expression of three C/EBP isoforms during adipose conversion of 3T3-L1 cells" *Genes Dev.*, vol. 5, no. 9, pp. 1538–1552, 1991.

[56] W. C. Yeh, Z. Cao, M. Classon, and S. L. McKnight, "Cascade regulation of terminal adipocyte differentiation by three members of the C/EBP family of leucine zipper proteins" *Genes Dev.*, vol. 9, no. 2, pp. 168–181, 1995.

[57] L. Guo *et al.*, "Transactivation of Atg4b by C/EBPβ Promotes Autophagy To Facilitate Adipogenesis" *Mol. Cell. Biol.*, vol. 33, no. 16, pp. 3180–3190, 2013.

[58] 2012 Morris et al., "Sumoylation and the function of CCAAT enhancer binding protein alpha (C/EBPα)" *Gerontology*, vol. 61, no. 6, pp. 515–525, 2015.

[59] J. Kim, C. A. Cantwell, P. F. Johnson, C. M. Pfarr, and S. C. Williams, "Transcriptional activity of CCAAT/enhancer-binding proteins is controlled by a conserved inhibitory domain that is a target for sumoylation" *J. Biol. Chem.*, vol. 277, no. 41, pp. 38037–38044, 2002.

[60] N. Wiper-Bergeron, H. A. Salem, J. J. Tomlinson, D. Wu, and R. J. G. Haché, "Glucocorticoid-stimulated preadipocytes differentiation is mediated through acetylation of C/EBPβ by GCN5" *Proc. Natl. Acad. Sci. U. S. A.*, vol. 104, no. 8, pp. 2703–2708, 2007.

[61] S. Kersten, "Physiological regulation of lipoprotein lipase" *Biochim. Biophys. Acta - Mol. Cell Biol. Lipids*, vol. 1841, no. 7, pp. 919–933, 2014.

[62] F. Acid, F. In, and C. L. Trafficking, "FATTY ACID FLUX IN ADIPOCYTES; THE IN'S AND OUT'S OF FAT CELL LIPID TRAFFICKING" vol. 318, pp. 24–33, 2011.

[63] S. M. Pauff and S. C. Miller, "Fatty acid-binding proteins: role in metabolic diseases and potential as drug targets" *Bone*, vol. 78, no. 2, pp. 711–716, 2012.

[64] S. W. Cushman and L. J. Wardzala, "Potential mechanism of insulin action on glucose transport in the isolated rat adipose cell. Apparent translocation of intracellular transport systems to the plasma membrane" *J. Biol. Chem.*, vol. 255, no. 10, pp. 4758–4762, 1980.

[65] K. Suzuki and T. Kono, "Evidence that insulin causes translocation of glucose transport activity to the plasma membrane from an intracellular storage site" *Proc. Natl. Acad. Sci. U. S. A.*, vol. 77, no. 5 I, pp. 2542–2545, 1980.

[66] G. Solinas, J. Borén, and A. G. Dulloo, "De novo lipogenesis in metabolic homeostasis: More friend than foe?" *Mol. Metab.*, vol. 4, no. 5, pp. 367–377, 2015.

[67] M. Wallace and C. M. Metallo, "Tracing insights into de novo lipogenesis in liver and adipose tissues" *Semin. Cell Dev. Biol.*, vol. 108, no. February, pp. 65–71, 2020.

[68] V. Sukonina *et al.*, "FOXK1 and FOXK2 regulate aerobic glycolysis" *Nature*, vol. 566, no. 7743, pp. 279–283, 2019.

[69] S. Hui *et al.*, "Glucose feeds the TCA cycle via circulating lactate" *Nature*, vol. 551, no. 7678, pp. 115–118, 2017.

[70] Leszek Szablewski, "Insulin signalling and the regulation of glucose and lipid metabolism" *Glucose Homeost. Insul. Resist.*, vol. 414, no. December, pp. 1–21, 2011.

[71] N. Kubota *et al.*, "Dynamic Functional Relay between Insulin Receptor Substrate 1 and 2 in Hepatic Insulin Signaling during Fasting and Feeding" *Cell Metab.*, vol. 8, no. 1, pp. 49–64, 2008.

[72] G. F. M. D. Cappellini, "Glucose-6-phosphate dehydrogenase deficiency" *Seminar*, vol. 371, pp. 64–74, 2008.

[73] Y. J. Park, S. S. Choe, J. H. Sohn, and J. B. Kim, "The role of glucose-6-phosphate dehydrogenase in adipose tissue inflammation in obesity" *Adipocyte*, vol. 6, no. 2, pp. 147–153, 2017.

[74] M. D. Albert I. Winegrad, M.D., Walter N. Shaw, Ph.D., F. D. W. Lukens, M.D., William C. Stadie, "Lipogenesis in adipose tissue" *Am. J. Clin. Nutr.*, vol. 8, no. 5, pp. 63–65, 1960.

[75] A. S. C. Morris, A. S. Denham, H. H. Bassett, and W. T. Curby, "De novo lipogenesis in human fat and liver is linked to ChREBP- β and metabolic health Leah" *Bone*, pp. 979–999, 2013.

[76] J. M. Collins, M. J. Neville, M. B. Hoppa, and K. N. Frayn, "De novo lipogenesis and stearoyl-

CoA desaturase are coordinately regulated in the human adipocyte and protect against palmitate-induced cell injury" *J. Biol. Chem.*, vol. 285, no. 9, pp. 6044–6052, 2010.

[77] B. Batchuluun, S. L. Pinkosky, and G. R. Steinberg, "Lipogenesis inhibitors: therapeutic opportunities and challenges" *Nat. Rev. Drug Discov.*, vol. 21, no. 4, pp. 283–305, 2022.

[78] F. Imamura *et al.*, "Fatty acids in the de novo lipogenesis pathway and incidence of type 2 diabetes: A pooled analysis of prospective cohort studies" *PLoS Med.*, vol. 17, no. 6, 2020.

[79] G. I. Smith *et al.*, "Insulin resistance drives hepatic de novo lipogenesis in nonalcoholic fatty liver disease" *J. Clin. Invest.*, vol. 130, no. 3, pp. 1453–1460, 2020.

[80] H. T. M. Lai *et al.*, "Serial Plasma Phospholipid Fatty Acids in the De Novo Lipogenesis Pathway and Total Mortality, Cause-Specific Mortality, and Cardiovascular Diseases in the Cardiovascular Health Study" *J. Am. Heart Assoc.*, vol. 8, no. 22, 2019.

[81] E. J. Lawitz *et al.*, "Acetyl-CoA Carboxylase Inhibitor GS-0976 for 12 Weeks Reduces Hepatic De Novo Lipogenesis and Steatosis in Patients With Nonalcoholic Steatohepatitis" *The Am. Gastroenterol. Ass.*, vol. 16, no. 12., 2018.

[82] D. E. Cintra *et al.*, "Unsaturated fatty acids revert diet-induced hypothalamic inflammation in obesity" *PLoS One*, vol. 7, no. 1, 2012.

[83] D. M. Rocha, A. P. Caldas, L. L. Oliveira, J. Bressan, and H. H. Hermsdorff, "Saturated fatty acids trigger TLR4-mediated inflammatory response" *Atherosclerosis*, vol. 244, pp. 211–215, 2016.

[84] D. Langin and P. Arner, "Importance of TNFα and neutral lipases in human adipose tissue lipolysis" *Trends Endocrinol. Metab.*, vol. 17, no. 8, pp. 314–320, 2006.

[85] G. Schoiswohl *et al.*, "Impact of reduced ATGL-mediated adipocyte lipolysis on obesity-associated insulin resistance and inflammation in male mice" *Endocrinology*, vol. 156, no. 10, pp. 3610–3624, 2015.

[86] V. Bezaire *et al.*, "Contribution of adipose triglyceride lipase and hormone-sensitive lipase to lipolysis in hMADS adipocytes" *J. Biol. Chem.*, vol. 284, no. 27, pp. 18282–18291, 2009.

[87] G. Haemmerle *et al.*, "Hormone-sensitive lipase deficiency in mice causes diglyceride accumulation in adipose tissue, muscle, and testis" *J. Biol. Chem.*, vol. 277, no. 7, pp. 4806–4815, 2002.

[88] J. S. Albert *et al.*, "Null Mutation in Hormone-Sensitive Lipase Gene and Risk of Type 2 Diabetes" *N. Engl. J. Med.*, vol. 370, no. 24, pp. 2307–2315, 2014.

[89] L. Scheja *et al.*, "Altered insulin secretion associated with reduced lipolytic efficiency in aP2(-/-) mice" *Diabetes*, vol. 48, no. 10, pp. 1987–1994, 1999.

[90] U. Taschler *et al.*, "Monoglyceride lipase deficiency in mice impairs lipolysis and attenuates diet-induced insulin resistance" *J. Biol. Chem.*, vol. 286, no. 20, pp. 17467–17477, 2011.

[91] J. G. Granneman, H. P. H. Moore, R. Krishnamoorthy, and M. Rathod, "Perilipin controls lipolysis by regulating the interactions of AB-hydrolase containing 5 (Abhd5) and adipose triglyceride lipase (Atgl)" *J. Biol. Chem.*, vol. 284, no. 50, pp. 34538–34544, 2009.

[92] A. Kulyté *et al.*, "CIDEA interacts with liver X receptors in white fat cells" *FEBS Lett.*, vol. 585, no. 5, pp. 744–748, 2011.

[93] M. Schreurs, F. Kuipers, and F. R. Van Der Leij, "Regulatory enzymes of mitochondrial β-oxidation as targets for treatment of the metabolic syndrome" *Obes. Rev.*, vol. 11, no. 5, pp.

380–388, 2010.

[94] L. Luo and M. Liu, "Adipose tissue in control of metabolism" *J. Endocrinol.*, vol. 231, no. 3, pp. R77–R99, 2016.

[95] Y. Zhang, R. Proenca, M. Maffei, M. Barone, L. Leopold, and J. M. Friedman, "Positional cloning of the mouse obese gene and its human homologue" *Nature*, vol. 374, no. 6521, p. 479, 1995.

[96] E. Hu, P. Liang, and B. M. Spiegelman, "AdipoQ is a novel adipose-specific gene dysregulated in obesity" *J. Biol. Chem.*, vol. 271, no. 18, pp. 10697–10703, 1996.

[97] M. W. Schwartz, R. J. Seeley, L. A. Campfield, P. Burn, and D. G. Baskin, "Identification of targets of leptin action in rat hypothalamus" *J. Clin. Invest.*, vol. 98, no. 5, pp. 1101–1106, 1996.

[98] E. C. Cottrell and J. G. Mercer, "Leptin receptors" *Handb. Exp. Pharmacol.*, vol. 209, pp. 3–21, 2012.

[99] J. H. Stern, J. M. Rutkowski, and P. E. Scherer, "Adiponectin, Leptin, and Fatty Acids in the Maintenance of Metabolic Homeostasis through Adipose Tissue Crosstalk" *Cell Metab.*, vol. 23, no. 5, pp. 770–784, 2016.

[100] M. Tschöp and G. Thomas, "Fat fuels insulin resistance through Toll-like receptors" *Nat. Med.*, vol. 12, no. 12, pp. 1359–1361, 2006.

[101] S. Cinti *et al.*, "Adipocyte death defines macrophage localization and function in adipose tissue of obese mice and humans" *J. Lipid Res.*, vol. 46, no. 11, pp. 2347–2355, 2005.

[102] S. B. Csehi *et al.*, "Tumor necrosis factor (TNF) interferes with insulin signaling through the p55 TNF receptor death domain" *Biochem. Biophys. Res. Commun.*, vol. 329, no. 1, pp. 397–405, 2005.

[103] W. P. Cawthorn and J. K. Sethi, "TNF-α and adipocyte biology" *FEBS Lett.*, vol. 582, no. 1, pp. 117–131, 2008.

[104] L. Zhang, W. Keung, V. Samokhvalov, W. Wang, and G. D. Lopaschuk, "Role of fatty acid uptake and fatty acid β-oxidation in mediating insulin resistance in heart and skeletal muscle" *Biochim. Biophys. Acta - Mol. Cell Biol. Lipids*, vol. 1801, no. 1, pp. 1–22, 2010.

[105] P. Trayhurn, "Hypoxia and adipose tissue function and dysfunction in obesity" *Physiol. Rev.*, vol. 93, no. 1, pp. 1–21, 2013.

[106] M. Maachi *et al.*, "Systemic low-grade inflammation is related to both circulating and adipose tissue TNFα, leptin and IL-6 levels in obese women" *Int. J. Obes.*, vol. 28, no. 8, pp. 993–997, 2004.

[107] C. Lagathu, J. P. Bastard, M. Auclair, M. Maachi, J. Capeau, and M. Caron, "Chronic interleukin-6 (IL-6) treatment increased IL-6 secretion and induced insulin resistance in adipocyte: Prevention by rosiglitazone" *Biochem. Biophys. Res. Commun.*, vol. 311, no. 2, pp. 372–379, 2003.

[108] E. W. Petersen *et al.*, "Acute IL-6 treatment increases fatty acid turnover in elderly humans in vivo and in tissue culture in vitro" *Am. J. Physiol. - Endocrinol. Metab.*, vol. 288, no. 1 51-1, pp. 155–162, 2005.

[109] H. Kanda *et al.*, "MCP-1 contributes to macrophage infiltration into adipose tissue, insulin resistance, and hepatic steatosis in obesity" *J. Clin. Invest.*, vol. 116, no. 6, pp. 1494–1505,

2006.

[110] D. K. Layman, "The role of leucine in weight loss diets and glucose homeostasis" *J. Nutr.*, vol. 133, no. 1, pp. 261–267, 2003.

[111] M. A. Herman, P. She, O. D. Peroni, C. J. Lynch, and B. B. Kahn, "Adipose tissue Branched Chain Amino Acid (BCAA) metabolism modulates circulating BCAA levels" *J. Biol. Chem.*, vol. 285, no. 15, pp. 11348–11356, 2010.

[112] P. She *et al.*, "TDisruption of BCATm in mice leads to increased energy expenditure associated with the activation of a futile protein turnover cycle" *Cell*, vol. 6, no. 3, pp. 181–194, 2009.

[113] K. N. Frayn, K. Khan, S. W. Coppack, and M. Elia, "Amino acid metabolism in human subcutaneous adipose tissue in vivo" *Clin. Sci.*, vol. 80, no. 5, pp. 471–474, 1991.

[114] T. J. Kowalski, W. U. Guoyao, and M. Watford, "Rat adipose tissue amino acid metabolism in vivo as assessed by microdialysis and arteriovenous techniques" *Am. J. Physiol.*, vol. 273, no. 3 PART 1, 1997.

[115] K. L. Spalding *et al.*, "Dynamics of fat cell turnover in humans" *Nature*, vol. 453, no. 7196, pp. 783–787, 2008.

[116] A. Rigamonti, K. Brennand, F. Lau, and C. A. Cowan, "Rapid cellular turnover in adipose tissue" *PLoS One*, vol. 6, no. 3, 2011.

[117] K. G. Stenkula and C. Erlanson-Albertsson, "Adipose cell size: Importance in health and disease" *Am. J. Physiol. - Regul. Integr. Comp. Physiol.*, vol. 315, no. 2, pp. R284–R295, 2018.

[118] P. Arner and K. L. Spalding, "Fat cell turnover in humans" *Biochem. Biophys. Res. Commun.*, vol. 396, no. 1, pp. 101–104, 2010.

[119] P. Tandon, R. Wafer, and J. E. N. Minchin, "Adipose morphology and metabolic disease" *J. Exp. Biol.*, vol. 121, 2018.

[120] G. E. Walker, P. Marzullo, R. Ricotti, G. Bona, and F. Prodam, "The pathophysiology of abdominal adipose tissue depots in health and disease" *Horm. Mol. Biol. Clin. Investig.*, vol. 19, no. 1, pp. 57–74, 2014.

[121] J. Hoffstedt *et al.*, "Regional impact of adipose tissue morphology on the metabolic profile in morbid obesity" *Diabetologia*, vol. 53, no. 12, pp. 2496–2503, 2010.

[122] I. Despres, Jean-Pierre & Lemieux, "Abdominal obesity and metabolic syndrome" *Nature*, vol. 444, pp. 881–887, 2006.

[123] A. L. Ghaben and P. E. Scherer, "Adipogenesis and metabolic health" *Nat. Rev. Mol. Cell Biol.*, vol. 20, no. 4, pp. 242–258, 2019.

[124] K. J. Strissel *et al.*, "Adipocyte death, adipose tissue remodeling, and obesity complications" *Diabetes*, vol. 56, no. 12, pp. 2910–2918, 2007.

[125] Y. S. Kang, "Obesity associated hypertension: New insights into mechanism," *Electrolyte Blood Press.*, vol. 11, no. 2, pp. 46–52, 2013.

[126] J. Ye, Z. Gao, J. Yin, and Q. He, "Hypoxia is a potential risk factor for chronic inflammation and adiponectin reduction in adipose tissue of ob/ob and dietary obese mice" *Am. J. Physiol. - Endocrinol. Metab.*, vol. 293, no. 4, pp. 1118–1128, 2007.

[127] S. Wueest, R. A. Rapold, J. M. Rytka, E. J. Schoenle, and D. Konrad, "Basal lipolysis, not the

degree of insulin resistance, differentiates large from small isolated adipocytes in high-fat fed mice" *Diabetologia*, vol. 52, no. 3, pp. 541–546, 2009.

[128] J. M. Rutkowski, J. H. Stern, and P. E. Scherer, "The cell biology of fat expansion" *J. Cell Biol.*, vol. 208, no. 5, pp. 501–512, 2015.

[129] J. Y. Lee *et al.*, "Reciprocal modulation of toll-like receptor-4 signaling pathways involving MyD88 and phosphatidylinositol 3-kinase/AKT by saturated and polyunsaturated fatty acids" *J. Biol. Chem.*, vol. 278, no. 39, pp. 37041–37051, 2003.

[130] R. Drolet *et al.*, "Hypertrophy and hyperplasia of abdominal adipose tissues in women" *Int. J. Obes.*, vol. 32, no. 2, pp. 283–291, 2008.

[131] M. Longo *et al.*, "Adipose Tissue Dysfunction as Determinant of Obesity-Associated Metabolic Complications" 2019.

[132] A. T. Ali, W. E. Hochfeld, R. Myburgh, and M. S. Pepper, "Adipocyte and adipogenesis" *Eur. J. Cell Biol.*, vol. 92, no. 6–7, pp. 229–236, 2013.

[133] Y. J. Koh *et al.*, "Activation of PPARγ induces profound multilocularization of adipocytes in adult mouse white adipose tissues" *Exp. Mol. Med.*, vol. 41, no. 12, pp. 880–895, 2009.

[134] S. M. Pauff and S. C. Miller, "Regulation of Metabolism: The Circadian Clock dictates the Time" *Bone*, vol. 78, no. 2, pp. 711–716, 2012.

[135] S. M. Pauff and S. C. Miller, "Circadian Clocks and Metabolism" *Bone*, vol. 78, no. 2, pp. 711–716, 2012.

[136] J.-T. Kiehn, C. E. Koch, M. Walter, A. Brod, and H. Oster, "Circadian rhythms and clocks in adipose tissues: current insights" *ChronoPhysiology Ther.*, vol. Volume 7, pp. 7–17, 2017.

[137] F. R. Cagampang and K. D. Bruce, "The role of the circadian clock system in nutrition and metabolism" *Br. J. Nutr.*, vol. 108, no. 3, pp. 381–392, 2012.

[138] F. Guillaumond, H. Dardente, V. Giguère, and N. Cermakian, "Differential control of Bmal1 circadian transcription by REV-ERB and ROR nuclear receptors" *J. Biol. Rhythms*, vol. 20, no. 5, pp. 391–403, 2005.

[139] L. Canaple *et al.*, "Reciprocal regulation of brain and muscle Arnt-like protein 1 and peroxisome proliferator-activated receptor α defines a novel positive feedback loop in the rodent liver circadian clock" *Mol. Endocrinol.*, vol. 20, no. 8, pp. 1715–1727, 2006.

[140] Y. Nakahata, S. Sahar, G. Astarita, M. Kaluzova, and P. Sassone-Corsi, "Circadian Control of the NAD+ Salvage Pathway by CLOCK-SIRT1" *Science (80-.).*, vol. 324, no. 5927, pp. 654–657, 2009.

[141] K. M. Ramsey *et al.*, "Circadian Clock Feedback Cycle Through NAMPT-Mediated NAD+ Biosynthesis" vol. 324, no. 5927, pp. 651–654, 2010.

[142] E. Maury, K. M. Ramsey, and J. Bass, "Sleep, circadian rhythms and metabolism" *Metab. Basis Obes.*, vol. 121, no. 6, pp. 229–255, 2011.

[143] J. E. Oosterman, A. Kalsbeek, S. E. La Fleur, and D. D. Belsham, "Impact of nutrients on circadian rhythmicity" *Am. J. Physiol. - Regul. Integr. Comp. Physiol.*, vol. 308, no. 5, pp. R337–R350, 2015.

[144] R. Refinetti, G. Cornélissen, and F. Halberg, "Procedures for numerical analysis of circadian rhythms" *Bio Rhythm Res.* vol. 38, no. 4. 2007.

[145] E. Poggiogalle, H. Jamshed, and C. M. Peterson, "Circadian regulation of glucose, lipid, and energy metabolism in humans" *Metabolism.*, vol. 84, pp. 11–27, 2018.

[146] S. Panda *et al.*, "Coordinated transcription of key pathways in the mouse by the circadian clock" *Cell*, vol. 109, no. 3, pp. 307–320, 2002.

[147] E. Challet, "Circadian aspects of adipokine regulation in rodents" *Best Pract. Res. Clin. Endocrinol. Metab.*, vol. 31, no. 6, pp. 573–582, 2017.

[148] S. Shimba *et al.*, "Brain and muscle Arnt-like protein-1 (BMAL1), a component of the molecular clock, regulates adipogenesis" *Proc. Natl. Acad. Sci. U. S. A.*, vol. 102, no. 34, pp. 12071–12076, 2005.

[149] B. Grimaldi *et al.*, "PER2 Controls Lipid Metabolism by Direct Regulation of PPARγ" *Cell Metab.*, vol. 12, no. 5, pp. 509–520, Nov. 2010.

[150] H. Duez *et al.*, "Inhibition of adipocyte differentiation by RORα," *FEBS Lett.*, vol. 583, no. 12, pp. 2031–2036, 2009.

[151] A. Kohsaka *et al.*, "High-Fat Diet Disrupts Behavioral and Molecular Circadian Rhythms in Mice" *Cell Metab.*, vol. 6, no. 5, pp. 414–421, 2007.

[152] C. Escobar, M. Díaz-Muñoz, F. Encinas, and R. Aguilar-Roblero, "Persistence of metabolic rhythmicity during fasting and its entrainment by restricted feeding schedules in rats" *Am. J. Physiol. - Regul. Integr. Comp. Physiol.*, vol. 274, no. 5 43-5, pp. 1309–1316, 1998.

[153] K. Fukagawa, H. M. Gou, R. Wolf, and P. Tso, "Circadian rhythm of serum and lymph apolipoprotein AIV in ad libitum-fed and fasted rats" *Am. J. Physiol. - Regul. Integr. Comp. Physiol.*, vol. 267, no. 5 36-5, 1994.

[154] S. Sahar, V. Nin, M. T. Barbosa, E. N. Chini, and P. Sassone-Corsi, "Altered behavioral and metabolic circadian rhythms in mice with disrupted NAD+ oscillation" *Aging (Albany. NY).*, vol. 3, no. 8, pp. 794–802, 2011.

[155] R. S. Stawski, D. M. Almeida, M. E. Lachman, and C. B. Rosnick, "The NAD+ -Dependent Deacetylase SIRT1 Modulates CLOCK- Mediated Chromatin Remodeling and Circadian Control" *NIH Public Access*, vol. 61, no. 6, pp. 515–525, 2015.

[156] A. Shostak, J. Meyer-Kovac, and H. Oster, "Circadian regulation of lipid mobilization in white adipose tissues" *Diabetes*, vol. 62, no. 7, pp. 2195–2203, 2013.

[157] F. W. Turek *et al.*, "Obesity and Metabolic Syndrome in Circadian Clock Mutant Mice" vol. 308, no. 5724, pp. 1043–1045, 2013.

[158] J. L. Barclay *et al.*, "High-fat diet-induced hyperinsulinemia and tissue-specific insulin resistance in Cry-deficient mice" *Am. J. Physiol. - Endocrinol. Metab.*, vol. 304, no. 10, pp. 1053–1063, 2013.

[159] R. Dallmann, C. Touma, R. Palme, U. Albrecht, and S. Steinlechner, "Impaired daily glucocorticoid rhythm in Per1Brd mice" *J. Comp. Physiol. A Neuroethol. Sensory, Neural, Behav. Physiol.*, vol. 192, no. 7, pp. 769–775, 2006.

[160] T. K. T. Lam *et al.*, "Hypothalamic sensing of circulating fatty acids is required for glucose homeostasis" *Nat. Med.*, vol. 11, no. 3, pp. 320–327, 2005.

[161] M. S. Bray and M. E. Young, "Circadian rhythms in the development of obesity: Potential role for the circadian clock within the adipocyte" *Obesity Reviews*, vol. 8, no. 2. pp. 169–181, 2007.

[162] J. Aschoff, "Circadian rhythms in man" *Science*, vol. 148, no. 3676, pp. 1427–1432, 1965.

[163] Benjamin Chun-Kit Tong, "Effects of poor and short sleep on glucose metabolism and obesity risk" *Physiol. Behav.*, vol. 176, no. 5, pp. 139–148, 2017.

[164] N. Deng, T. P. Kohn, L. I. Lipshultz, and A. W. Pastuszak, "The Relationship Between Shift Work and Men's Health" *Sex. Med. Rev.*, vol. 6, no. 3, pp. 446–456, 2018.

[165] D. Arul and P. Subramanian, "Circadian rhythms of plasma lipid and protein levels in daytime food-restricted rats" *Biol. Rhythm Res.*, vol. 45, no. 2, pp. 157–166, 2014.

[166] A. Chaix, T. Lin, H. D. Le, M. W. Chang, and S. Panda, "Time-Restricted Feeding Prevents Obesity and Metabolic Syndrome in Mice Lacking a Circadian Clock" *Cell Metab.*, vol. 29, no. 2, pp. 303-319.e4, 2019.

[167] S. M. Pauff and S. C. Miller, "Time-restricted feeding is a preventative and therapeutic intervention against diverse nutritional challenges" *Bone*, vol. 78, no. 2, pp. 711–716, 2012.

[168] A. Zarrinpar, A. Chaix, and S. Panda, "Daily Eating Patterns and Their Impact on Health and Disease" *Trends Endocrinol. Metab.*, vol. 27, no. 2, pp. 69–83, 2016.

[169] A. Crozier, T. Yokota, I. B. Jaganath, S. Marks, M. Saltmarsh, and M. N. Clifford, "Secondary Metabolites in Fruits, Vegetables, Beverages and Other Plant-based Dietary Components" *Plant Second. Metab. Occur. Struct. Role Hum. Diet*, pp. 208–302, 2007.

[170] T. Løvdal, K. M. Olsen, R. Slimestad, M. Verheul, and C. Lillo, "Synergetic effects of nitrogen depletion, temperature, and light on the content of phenolic compounds and gene expression in leaves of tomato" *Phytochemistry*, vol. 71, no. 5–6, pp. 605–613, 2010.

[171] K. B. Pandey and S. I. Rizvi, "Plant polyphenols as dietary antioxidants in human health and disease" *Oxid. Med. Cell. Longev.*, vol. 2, no. 5, pp. 270–278, 2009.

[172] K. A. Woodward, R. Draijer, D. H. J. Thijssen, and D. A. Low, "Polyphenols and Microvascular Function in Humans: A Systematic Review" *Curr. Pharm. Des.*, vol. 24, no. 2, pp. 203–226, 2018.

[173] C. Bladé *et al.*, "Proanthocyanidins in health and disease" *BioFactors*, vol. 42, no. 1, pp. 5–12, 2016.

[174] Nurgiyantoro, "Absorption and metabolism of polyphenols in the gut and impact on health" *Biomed Pharmacother*, vol. 56, no. 6, pp. 1–11, 2002.

[175] M. Margalef, Z. Pons, L. Iglesias-Carres, F. I. Bravo, B. Muguerza, and A. Arola-Arnal, "Lack of Tissue Accumulation of Grape Seed Flavanols after Daily Long-Term Administration in Healthy and Cafeteria-Diet Obese Rats" *J. Agric. Food Chem.*, vol. 63, no. 45, pp. 9996–10003, 2015.

[176] L. Baselga-Escudero *et al.*, "Chronic supplementation of proanthocyanidins reduces postprandial lipemia and liver miR-33a and miR-122 levels in a dose-dependent manner in healthy rats" *J. Nutr. Biochem.*, vol. 25, no. 2, pp. 151–156, 2014.

[177] A. Pascual-Serrano *et al.*, "Grape seed proanthocyanidin supplementation reduces adipocyte size and increases adipocyte number in obese rats" *Int. J. Obes.*, vol. 41, no. 8, pp. 1246–1255, 2017.

[178] Y. S. Jeong, J. H. Hong, K. H. Cho, and H. K. Jung, "Grape skin extract reduces adipogenesis- and lipogenesis-related gene expression in 3T3-L1 adipocytes through the peroxisome proliferator-activated receptor-γ signaling pathway" *Nutr. Res.*, vol. 32, no. 7, pp. 514–521,

2012.

[179] D. A. Moreno, N. Ilic, A. Poulev, D. L. Brasaemle, S. K. Fried, and I. Raskin, "Inhibitory effects of grape seed extract on lipases" *Nutrition*, vol. 19, no. 10, pp. 876–879, 2003.

[180] A. Caimari, J. M. Del Bas, A. Crescenti, and L. Arola, "Low doses of grape seed procyanidins reduce adiposity and improve the plasma lipid profile in hamsters" *Int. J. Obes.*, vol. 37, pp. 576–583, 2013.

[181] S. Wei, Y. Zheng, M. Zhang, H. Zheng, and P. Yan, "Grape seed procyanidin extract inhibits adipogenesis and stimulates lipolysis of porcine adipocytes in vitro" *J. Anim. Sci.*, vol. 96, no. 7, pp. 2753–2762, 2018.

[182] K. Kowalska, A. Olejnik, J. Rychlik, and W. Grajek, "Cranberries (Oxycoccus quadripetalus) inhibit lipid metabolism and modulate leptin and adiponectin secretion in 3T3-L1 adipocytes" *Food Chem.*, vol. 185, pp. 383–388, 2015.

[183] G. Montagut *et al.*, "Differential effects of grape-seed derived procyanidins on adipocyte differentiation markers in different in vivo situations" *Genes Nutr.*, vol. 2, no. 1, pp. 101–103, 2007.

[184] A. Ardévol, M. J. Motilva, A. Serra, M. Blay, and M. Pinent, "Procyanidins target mesenteric adipose tissue in Wistar lean rats and subcutaneous adipose tissue in Zucker obese rat" *Food Chem.*, vol. 141, no. 1, pp. 160–166, 2013.

[185] M. Ibars, A. Ardid-Ruiz, M. Suárez, B. Muguerza, C. Bladé, and G. Aragonès, "Proanthocyanidins potentiate hypothalamic leptin/STAT3 signalling and Pomc gene expression in rats with diet-induced obesity" *Int. J. Obes.*, vol. 41, no. 1, pp. 129–136, 2017.

[186] M. C. Gonçalves, M. C. F. Passos, C. F. de Oliveira, J. B. Daleprane, and J. C. Koury, "Effects of proanthocyanidin on oxidative stress biomarkers and adipokines in army cadets: a placebo-controlled, double-blind study" *Eur. J. Nutr.*, vol. 56, no. 2, pp. 893–900, 2017.

[187] D. Pajuelo *et al.*, "Acute administration of grape seed proanthocyanidin extract modulates energetic metabolism in skeletal muscle and BAT mitochondria" *J. Agric. Food Chem.*, vol. 59, no. 8, pp. 4279–4287, 2011.

[188] D. Pajuelo *et al.*, "Chronic dietary supplementation of proanthocyanidins corrects the mitochondrial dysfunction of brown adipose tissue caused by diet-induced obesity in Wistar rats" *Br. J. Nutr.*, vol. 107, no. 2, pp. 170–178, 2012.

[189] M. Liu, P. Yun, Y. Hu, J. Yang, R. B. Khadka, and X. Peng, "Effects of Grape Seed Proanthocyanidin Extract on Obesity" *Obes. Facts*, vol. 13, no. 2, pp. 279–291, 2020.

[190] A. Gibert-Ramos, M. Z. Martín-González, A. Crescenti, and M. Josepa Salvadó, "A mix of natural bioactive compounds reduces fat accumulation and modulates gene expression in the adipose tissue of obese rats fed a cafeteria diet" *Nutrients*, vol. 12, no. 11, pp. 1–17, 2020.

[191] T. Wu, Z. Jiang, J. Yin, H. Long, and X. Zheng, "Anti-obesity effects of artificial planting blueberry (Vaccinium ashei) anthocyanin in high-fat diet-treated mice" *Int. J. Food Sci. Nutr.*, vol. 67, no. 3, 2016.

[192] P. Solverson, "Anthocyanin Bioactivity in Obesity and Diabetes : The Essential Role of Glucose Transporters in the Gut and Periphery" *Cells*, vol. 9, pp. 1–21, 2020.

[193] I. Churruca, A. Fernández-Quintela, and M. P. Portillo, "Conjugated linoleic acid isomers: Differences in metabolism and biological effects" *BioFactors*, vol. 35, no. 1, pp. 105–111, 2009.

[194] M. E. Evans, J. M. Brown, and M. K. McIntosh, "Isomer-specific effects of conjugated linoleic acid (CLA) on adiposity and lipid metabolism" *J. Nutr. Biochem.*, vol. 13, no. 9, pp. 508–516, 2002.

[195] T. E. Lehnen, M. R. da Silva, A. Camacho, A. Marcadenti, and A. M. Lehnen, "A review on effects of conjugated linoleic fatty acid (CLA) upon body composition and energetic metabolism" *J. Int. Soc. Sports Nutr.*, vol. 12, no. 1, 2015.

[196] S. M. Pauff and S. C. Miller, "Trans-10,cis-12 CLA increases adipocyte lipolysis and alters lipid droplet-associated proteins: role of mTOR and ERK signaling" *Bone*, vol. 78, no. 2, pp. 711–716, 2012.

[197] D. Rubin *et al.*, "Influence of different CLA isomers on insulin resistance and adipocytokines in pre-diabetic, middle-aged men with PPARc2 Pro12Ala polymorphism" *Genes Nutr.*, vol. 7, no. 4, pp. 499–509, 2012.

[198] D. Vyas, A. K. G. Kadegowda, and R. A. Erdman, "Dietary conjugated linoleic acid and hepatic steatosis: Species-specific effects on liver and adipose lipid metabolism and gene expression" *J. Nutr. Metab.*, vol. 2012, no. 232, 2012.

[199] X. R. Zhou, C. H. Sun, J. R. Liu, and D. Zhao, "Dietary conjugated linoleic acid increases PPARγ gene expression in adipose tissue of obese rat, and improves insulin resistance" *Growth Horm. IGF Res.*, vol. 18, no. 5, pp. 361–368, 2008.

[200] F. I. Bravo, A. Mas-Capdevila, M. Margalef, A. Arola-Arnal, and B. Muguerza, "Novel Antihypertensive Peptides Derived from Chicken Foot Proteins" *Mol. Nutr. Food Res.*, vol. 63, no. 12, 2019.

[201] E. Dufoo-Hurtado, A. Wall-Medrano, and R. Campos-Vega, "Naturally-derived chronobiotics in chrononutrition" *Trends Food Sci. Technol.*, vol. 95, pp. 173–182, 2020.

[202] R. Antoni, T. M. Robertson, M. D. Robertson, and J. D. Johnston, "A pilot feasibility study exploring the effects of a moderate time-restricted feeding intervention on energy intake, adiposity and metabolic physiology in free-living human subjects" *J. Nutr. Sci.*, pp. 1–6, 2018-

[203] H. Oike, "Modulation of circadian clocks by nutrients and food factors" *Biosci. Biotechnol. Biochem.*, vol. 81, no. 5, pp. 863–870, 2017.

[204] A. Ribas-Latre *et al.*, "Chronic consumption of dietary proanthocyanidins modulates peripheral clocks in healthy and obese rats" *J. Nutr. Biochem.*, vol. 26, pp. 112–119, 2015.

[205] L. Sun *et al.*, "Resveratrol restores the circadian rhythmic disorder of lipid metabolism induced by high-fat diet in mice" *Biochem. Biophys. Res. Commun.*, vol. 458, no. 1, pp. 86–91, 2015.

[206] K. Awad *et al.*, "Effects of morning vs evening statin administration on lipid profile: A systematic review and meta-analysis" *J Clin Lipidol*, vol. 11, no. 4, 2017.

[207] K. Awad and M. Banach, "The optimal time of day for statin administration: A review of current evidence" *Curr. Opin. Lipidol.*, vol. 29, no. 4, pp. 340–345, 2018.

Hypothesis and objectives

Obesity is a public health issue worldwide which its prevalence is dramatically increasing. White adipose tissue (WAT) plays a critical role in obesity-related metabolic disorders. The localization of excessive WAT, the adipocyte size, the alteration of the metabolism of adipocytes and immune cells that composed WAT determine the physiology of WAT and the risk to suffer insulin resistance, hyperglycemia, dyslipidemia, and cardiovascular diseases. In addition, mammals present endogenous circadian clocks which are synchronized by external cues. The central clock is regulated by light/dark cycle, while peripheral clocks are regulated by diet. This synchronization is highly important in WAT to efficiently adapt and anticipate to daily recurring events, including secretion of hormones, lipogenesis, lipolysis, inflammation, among other metabolic pathways. The disruption of the clock, through cafeteria diet or high-fat diet, shift work or late-night activity, could lead to physiologic alterations affecting systemic homeostasis and body weight management.

Polyphenols and other bioactive compounds have been studied during the last decades as a prevention and treatment against obesity-related pathologies. In the present Doctoral Thesis, it has particularly been used proanthocyanidins from grape seed (GSPE) which possesses large number of benefits, including antioxidant and antihypertensive properties and the amelioration of dyslipidemia, insulin sensitivity and chronic inflammation. Specifically in WAT, GSPE consumption reduces adiposity and adipocyte size (hypertrophy) in subcutaneous and visceral WAT, increases PPARγ gene expression in visceral WAT leading to expansion through hyperplasia and increases insulin sensitivity. Additionally, proanthocyanidins are potential modulators of circadian rhythm which can improve clock disruption attenuating obesity-related metabolic alterations.

In this context, it is plausible to speculate that the effects of GSPE consumption on WAT metabolism and clock system could depend on time-of-day administration since several metabolic outcomes present circadian rhythm in this tissue. Therefore, we **hypothesized that proanthocyanidins counteract diet-induced alterations in WAT metabolism and rhythmicity according to time-of-day administration.**

Thus, the **main objective** of this thesis was **to determine whether proanthocyanidins exert different effects on the metabolism and circadian rhythm of WAT in obese rodents depending on the time-of-day they are consumed.** To this end, specific objectives were proposed:

1. **To evaluate the time-of-day dependent effect of GSPE consumption on subcutaneous and visceral WAT in rats with diet-induced obesity.** To accomplish this objective, rats were fed with cafeteria diet for 9 weeks to induce obesity. From week 6 on, animals were supplemented with GSPE (25 mg/kg) at two different zeitgeber times (ZT): at the beginning of the light/rest phase (ZT0) or at the beginning of the dark/active phase (ZT12) (**Manuscript 1**).

2. **To challenge the ability of GSPE to restore the circadian rhythm of subcutaneous WAT lost in obesity in a time-of-day dependent manner.**

    a. **To evaluate the effect of GSPE consumption on the diurnal rhythm of WAT metabolites in rats with diet-induced obesity.** Cafeteria diet-fed animals were supplemented with vehicle or GSPE (25 mg/kg) either at the beginning of the light/rest phase (ZT0) or at the beginning of the dark/active

phase (ZT12) for 4 weeks. Animals were sacrificed at 6-hour intervals to analyze the diurnal rhythms of subcutaneous WAT metabolites assessed by nuclear magnetic resonance spectrometry (**Manuscript 2**).

b. **To determine the effect of GSPE-derived serum metabolites on *PER2* circadian rhythm in WAT explants**. To assess this objective subcutaneous WAT explants from lean and obese *PER2::LUC* or wild-type mice were treated with GSPE serum metabolites (GSPM) at two different time points; at the peak or trough of *PER2::LUC* bioluminescence (**Manuscript 3**).

3. **To determine the time-of-day dependent effect of the consumption of a bioactive multi-compound (MIX) based on GSPE on subcutaneous and visceral WAT in rats with diet-induced obesity.** To achieve this aim rats were fed with cafeteria diet for 9 weeks. From week 6 on, animals were supplemented with MIX at the beginning of the light/rest phase (ZT0) or at the beginning of the dark/active phase (ZT12) (**Manuscript 4**).

Experimental designs

Different experimental designs were used in the present Doctoral Thesis to assess the main hypothesis and reach the experimental objectives previously described.

1. **Evaluation of GSPE effects depending on time-of-day consumption on subcutaneous and visceral WAT metabolism of cafeteria diet obese rats (Manuscript 1).**

Male Wistar rats were fed a CAF diet for 9 weeks. After 5 weeks, the animals were supplemented with 25 mg GSPE/kg for 4 weeks at the beginning of the light/rest phase (ZT0) or of the dark/active phase (ZT12). Body weight and food intake were recorded weekly and body fat content was determined by nuclear magnetic resonance. Biochemical parameters were evaluated and histological analyses (hematoxylin and eosin staining) were performed in visceral epididymal (eWAT) and subcutaneous inguinal (iWAT) fat depots to determine adipocyte size and number. In addition, the expression of genes related to adipose metabolism and circadian clock function were analyzed by qPCR (Figure 1).

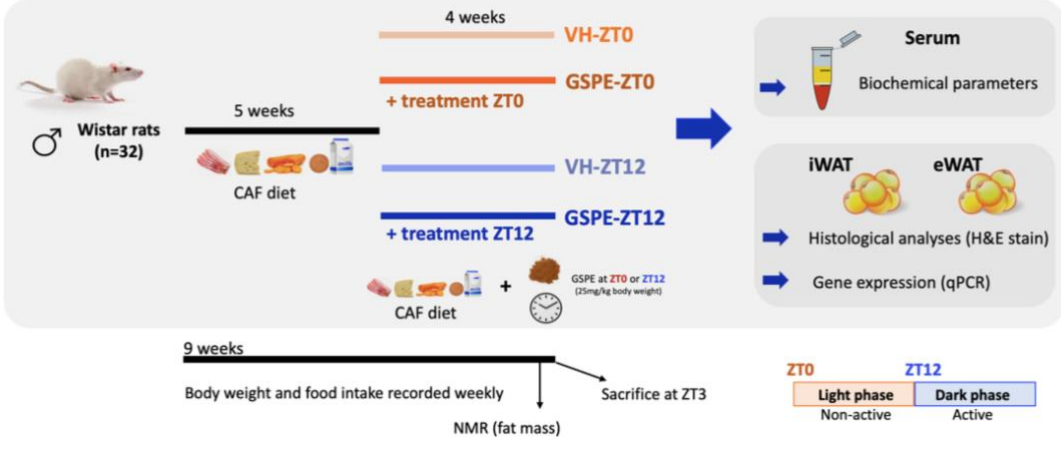

Figure 1. Experimental design to evaluate GSPE effects depending on time-of-day consumption on subcutaneous and visceral WAT metabolism of cafeteria diet obese rats.

2. Determination of GSPE effects depending on time-of-day consumption on the diurnal rhythm of subcutaneous WAT metabolites in cafeteria diet obese rats (Manuscrip 2).

Ninety-six male Fischer rats were fed STD (two groups) or CAF (four groups) diet for 9 weeks (n = 16 each group). From week 6 on, CAF diet animals were supplemented with vehicle or 25 mg GSPE/kg of body weight either at the beginning of the light/rest phase (ZT0) or at the beginning of the dark/active phase (ZT12). The two STD groups were also supplemented with vehicle at ZT0 or ZT12. Body weight and food intake were recorded weekly. In week 9, animals were sacrificed at 6 h intervals (n = 4) to determine biochemical parameters, the histology of iWAT (hematoxylin and eosin staining) and to analyze the diurnal rhythms of iWAT metabolites by nuclear magnetic resonance spectrometry (Figure 2).

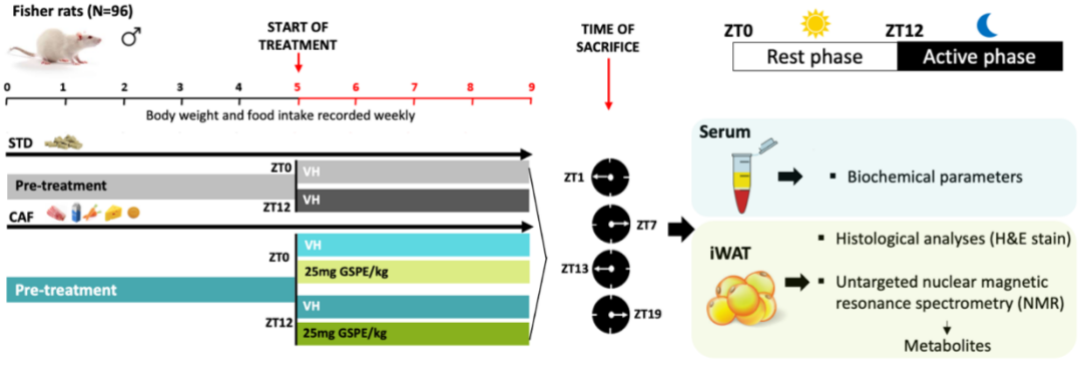

Figure 2. Experimental design to determine GSPE effects depending on time-of-day consumption on the diurnal rhythm of subcutaneous WAT metabolites of cafeteria diet obese rats.

3. Evaluation of the effect of GSPE-derived serum metabolites on *PER2* circadian rhythm in obese subcutaneous WAT explants according to time-of-day treatment (Manuscript 3).

Rats from the GSPE group were administered 1 ml of 1 g/kg of body weight of GSPE by oral gavage. The control group was orally administered 1 ml of water. Two hours after the treatment, the rats were sacrificed by decapitation and trunk blood was collected. To obtain the metabolized proanthocyanidins from rat serum, serum samples were pretreated by off-line micro-solid-phase extraction (μSPE). Afterwards, samples were evaporated and redissolved in recording medium (Figure 3a).

PER2::LUC knockin C57BL/6J mice were fed with STD or HFD diet for 5 weeks. Mice were sacrificed and iWAT explants were prepared to treat with GSPE metabolites at peak of *PER2* bioluminiscence or at trough. Samples were placed in the LumiCycle luminometer for five days. Afterwards, circadian rhythm of *PER2* bioluminiscence was analyzed. Wild-type C57BL/6J mice were also fed with STD or HFD diet. iWAT explants were treated with GSPE metabolites at peak or trough of *PER2* bioluminiscence for 10 hours. Afterwards, samples were frozen for gene expression analysis. Moreover, glycerol content was analyzed in the medium after a GSPE treatment of 24 hours (Figure 3b).

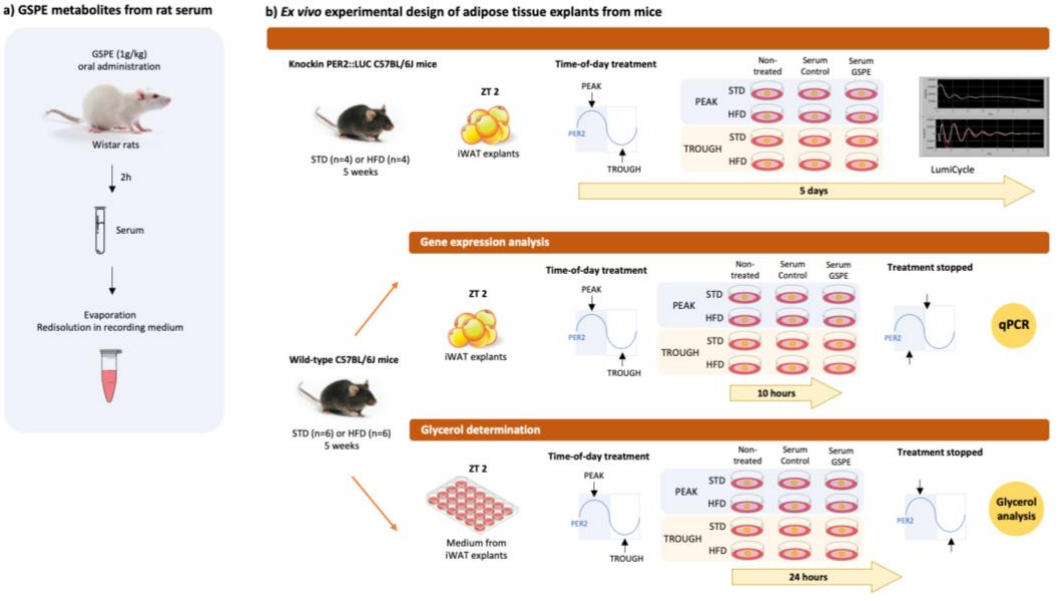

Figure 3. Experimental design to determine the effect of GSPE serum metabolites on PER2 circadian rhythm in obese subcutaneous WAT explants according to time-of-day treatment.

4. Determination of the effects of a bioactive multi-compound (based on GSPE) consumption on subcutaneous and visceral WAT metabolism depending on time-of-day administration in cafeteria diet obese rats (Manuscript 4).

Male Wistar rats (n=32) fed a CAF diet for 9 weeks were orally supplemented the last 4 weeks with MIX or vehicle when the lights turned on (ZT0) or turned off (ZT12). Body weight and food intake were recorded weekly and body fat content was determined by nuclear magnetic resonance. Biochemical parameters were determined. Histological analyses (hematoxylin and eosin staining) were performed in eWAT and iWAT depots to evaluate adipocyte size and number. In addition, the expression of genes related to adipose metabolism and circadian clock function were analyzed by qPCR (Figure 4).

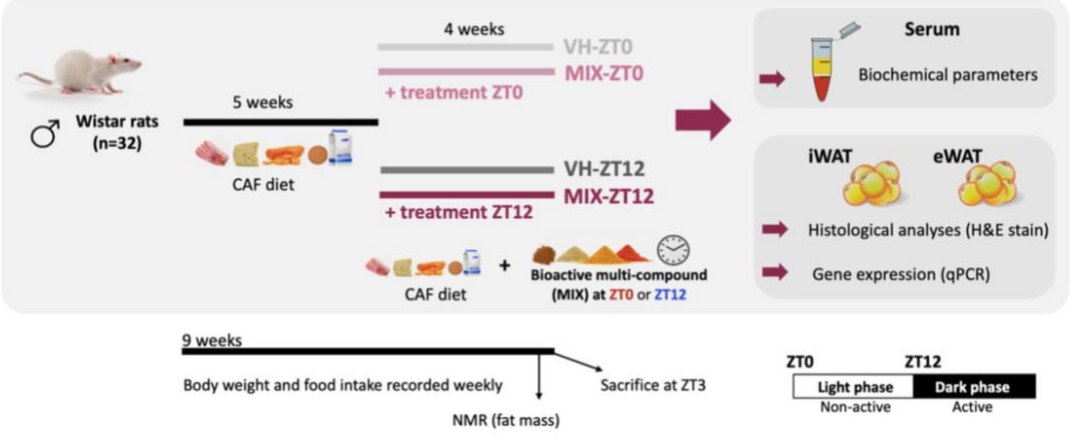

Figure 4. Experimental design to evaluate the impact of the bioactive multi-compound (MIX; based on GSPE) depending on time-of-day consumption on subcutaneous and visceral WAT metabolism of cafeteria diet obese rats.

Results

Manuscript 1

Time-of-day dependent effect of proanthocyanidins on adipose tissue metabolism in rats with diet-induced obesity

Marina Colom-Pellicer[1], Romina M Rodríguez[1], Èlia Navarro-Masip[1], Francisca Isabel Bravo[1], Miquel Mulero[1], Lluís Arola[1], and Gerard Aragonès[1] ✉

[1] Universitat Rovira i Virgili, Department of Biochemistry and Biotechnology, Nutrigenomics Research Group, Tarragona, Spain.

The authors declare no competing interests in relation to this manuscript.

Published in *International Journal of Obesity*
Received: 21 October 2021. Accepted: 21 April 2022. Published: 25 April 2022

Abstract: Grape-seed proanthocyanidin extract (GSPE) improve white adipose tissue (WAT) expansion during diet-induced obesity. However, because adipose metabolism is synchronized by circadian rhythms, it is plausible to speculate that the bioactivity of dietary proanthocyanidins could be influenced by the time-of-day in which they are consumed. Therefore, the aim of the present study was to determine the interaction between zeitgeber time (ZT) and GSPE consumption on the functionality of WAT in rats with diet-induced obesity. Male Wistar rats were fed a cafeteria diet for 9 weeks. After 5 weeks, the animals were supplemented with 25 mg GSPE/kg for 4 weeks at the beginning of the light/rest phase (ZT0) or of the dark/active phase (ZT12). Body fat content was determined by nuclear magnetic resonance and histological analyses were performed in the epididymal (EWAT) and inguinal (IWAT) fat depots to determine adipocyte size and number. In addition, the expression of genes related to adipose metabolism and circadian clock function were analyzed by qPCR. GSPE consumption at ZT0 was associated with a potential antidiabetic effect without affecting adiposity and energy intake and downregulating the gene expression of inflammatory markers in EWAT. In contrast, GSPE consumption at ZT12 improve adipose tissue expansion decreasing adipocyte size in IWAT. In accordance with this adipogenic activity, the expression of genes involved in fatty acid metabolism were downregulated at ZT12 in IWAT. In turn, GSPE consumption at ZT12, but not at ZT0, repressed the expression of the clock gene *Cry1* in IWAT. The interaction between ZT and GSPE consumption influenced the metabolic response of WAT in a tissue-specific manner. Understanding the impact of circadian clock on adipose metabolism and how this is regulated by polyphenols will provide new insights for the management of obesity.

1. Introduction

The obesity epidemic is a major metabolic health problem, mainly characterized by excessive adiposity, which disrupts whole-body energy balance and body composition [1]. In mammals, white adipose tissue (WAT) is increasingly recognized as a major player in maintaining metabolic homeostasis by regulating energy metabolism [2]. In general, feeding stimulates the lipogenic pathway and storage of triglycerides in WAT, while fasting and physical activity induce lipolytic pathway activation and promote triglycerides breakdown and fatty acids release into the bloodstream to meet the needs of other tissues [3]. In addition, to properly accommodate triglycerides, WAT needs to remodel and expand itself by inducing the proliferation and differentiation of pre-adipocytes to adipocytes via adipogenesis [4]. This process is controlled by an interacting network of transcription factors, such as *peroxisome proliferator-activated receptor gamma* (PPARγ) and members of the *CCAAT/enhancer-binding proteins* (C/EBPs), operating together to coordinate the expression of many hundreds of genes responsible for establishing the phenotype of mature fat cells [5]. However, WAT expandability is not infinite and, once the limit is reached, fat is deposited in visceral adipocyte depots resulting in local and systemic metabolic alterations such as insulin resistance, dyslipidemia and chronic inflammation [6].

In this context, dietary and lifestyle interventions have been shown to be adequate to improve WAT functionality and, therefore, improve its metabolic health [7, 8]. In this sense, natural dietary polyphenols and specifically proanthocyanidins, the most structurally complex subclass of flavonoids, have exhibited, over the last few years, to play an important role in the regulation of the main metabolic transcriptional networks in WAT [9,10]. Specifically, consumption of a proanthocyanidins mixture extracted from grape seeds was shown to exert anti-hypertrophic and adipogenic activity by increasing the

capacity of WAT to store and mobilize triglycerides and, consequently, inducing a healthier expansion of this tissue to match the surplus of energy provided by the cafeteria diet [11, 12].

Nevertheless, the main metabolic processes in mammals are influenced by the circadian clock, which is a complex biological timing system. This system coordinates cellular and physiological functions in periodical cycles of approximately 24 hours [13]. In fact, several studies in rodents and humans revealed that approximately 10-20% of genes in WAT have a circadian rhythm expression [14,15]. In addition, one of the most important molecular components of the mammalian circadian clock system such as *brain and muscle ARNT-like* (BMAL1), has been shown to modulate the expression of key enzymes involved in lipolysis and lipid transport in WAT, including *adipose triglyceride lipase* (ATGL), *hormone-sensitive lipase* (HSL) and *lipoprotein lipase* (LPL) [16,17]. Therefore, cellular and physiological circadian mechanisms define the moment in which metabolic processes are more active in WAT [18] and, presumably, more susceptible to be modulated [19]. In this context, it is plausible to speculate that the effectiveness of dietary polyphenols in the prevention of diet-induced obesity could depend substantially on the time-of-day in which they are consumed. Therefore, the aim of the present study was to investigate whether the functionality of WAT in response to proanthocyanidins was significantly influenced by the time-of-day of their consumption.

2. Methods

2.1. Proanthocyanidins extract

The grape seed extract enriched in proanthocyanidins (GSPE) was kindly provided by *Les Dérivés Résiniques et Terpéniques* (Dax, France). According to the manufacturer, the GSPE composition used in this study contained monomers

(21.3%), dimers (17.4%), trimers (16.3%), tetramers (13.3%), and oligomers (5-13 units; 31.7%) of proanthocyanidins. The phenolic composition of this extract was further analysed by Margalef et al [20].

2.2. Study design and dosage information

Thirty-two male Wistar rats weighing 250-290 g, 8 weeks of age, were purchased from *Charles River Laboratories* (Barcelona, Spain). Animals were housed in pairs under a 12 h light-dark cycle, at 22°C and fed *ad libitum* with a standard chow diet (Panlab A04, Barcelona, Spain) and tap water. After one week of adaptation, animals were fed everyday *ad libitum* with cafeteria diet for 9 weeks. The cafeteria diet was previously described by Ribas-Latre et al [21]. During the last 4 weeks of the cafeteria diet intervention, animals were randomly divided into four groups of 8 animals each and were orally supplemented at two different time points with GSPE (25 mg/kg of body weight/day) or vehicle (VH). According to Zeitgeber time (ZT), two groups were supplemented at ZT0, when the light turn on (VH-ZT0 and GSPE-ZT0 groups), and the other two were supplemented at ZT12, when lights turned off (VH-ZT12 and GSPE-ZT12 groups). GSPE was dissolved in 450 μL of commercial sweetened skim condensed milk (Nestle; 100 g: 8.9 g protein, 0.4 g fat, 60.5 g carbohydrates, 1175 kJ). VH groups were supplemented with the same volume of sweetened skim condensed milk. Two or three days before administration, rats were trained to voluntarily lick the milk to avoid oral gavage.

One week prior to sacrifice, total body fat content was analysed by quantitative magnetic resonance using an EchoMRI-700 (*Echo Medical Systems*, LLC., TX, USA) without anaesthesia.

To avoid differences related to circadian rhythms in gene expression, all animals were sacrificed by decapitation 3 hours after the lights turn on (ZT3). Afterwards,

blood from neck was collected and centrifuged (1 500 x g, 15 min, 4°C) to obtain serum. In addition, epididymal and inguinal WAT depots (EWAT and IWAT, respectively) were excised, weighted and immediately frozen in liquid nitrogen. Serum and adipose depots were stored at −80°C until further use.

The Animal Ethics Committee of Universitat Rovira i Virgili approved all procedures (reference number 9495 by Generalitat de Catalunya). All the above-mentioned experiments were performed as authorized (European Directive 86/609/CEE and Royal Decree 223/1988 of the Spanish Ministry of Agriculture, Fisheries and Food, Madrid, Spain).

2.3. Measurement of circulating biomarkers

Serum levels of insulin, leptin, adiponectin, and monocyte chemoattractant protein-1 (MCP-1) were measured using mouse/rat-specific immunometric sandwich enzyme-linked immunosorbent assay (ELISA) kit purchased from Millipore Ibérica (Madrid, Spain).

Enzymatic colorimetric kits were used for the determination of serum glucose, triglycerides and total cholesterol (QCA, Barcelona, Spain) and non-esterified fatty acids (NEFA, or free fatty acids) (Wako, CA, USA). Homeostasis model assessment-estimated insulin resistance (HOMA-IR) index was calculated from insulin and glucose serum levels.

2.4. Adipose tissue histology

This study focuses on two key white adipose depots: inguinal subcutaneous WAT (IWAT) and visceral WAT derived from the epididymal (gonadal) fat pad (EWAT). IWAT and EWAT have an important role in metabolic homeostasis. In fact, in rodent models, surgical removal of IWAT can lead to metabolic dysfunction [22,23]. In contrast, transplantation of IWAT into the visceral cavity

of mice leads to improved glucose homeostasis and body composition [24]. In addition, EWAT is one of the most used adipose tissues because it makes up the largest portion of the total adipose tissue of an abdominal cavity and allows more accurate weighing due to easy extraction. Small pieces of frozen IWAT and EWAT were thawed and fixed in 4% formaldehyde. Paraffin blocks, hematoxylin-eosin staining and the calculations for area, volume and number of adipocytes were performed following Gibert-Ramos et al [25]. The frequency of adipocyte size distribution across the tissue was calculated by distributing all counted cells of each sample into two groups according to their area, <3 000μm^2 or >3 000μm^2; then, the number of total counted adipocytes was used to calculate the percentage of adipocytes in both categories.

2.5. Gene expression analysis

Total RNA from IWAT and EWAT was extracted and quantified following Gibert-Ramos et al [25]. The integrity of the RNA was evaluated by RNA integrity number (RIN) through 2100 Bioanalyzer Instrument (Agilent Technologies). cDNA was synthesized and amplified following Ibars et al [26]. The candidate genes were selected based on previous studies [12,21,25] as well as on their implication on the most important metabolic pathways of adipose tissue including adipogenesis, lipid metabolism, thermogenesis, adipokine expression, inflammation and glucose uptake. The primers used for the different genes are described in **Supplementary Information Table S1** and were obtained from *Biomers.net* (Ulm, Germany). The relative expression of each gene was calculated according to *Cyclophilin peptidylprolyl isomerase A* (*Ppia*) mRNA levels and normalized to the levels measured in the corresponding control group. The ΔΔCt method was used and corrected for primer efficiency [27].

2.6. Statistical analysis

Data are expressed as the mean±SEM (n=6-8). Grubbs' test was used to detect outliers, which were discarded before subsequent analyses. Treatment (T), administration time (ZT) and treatment × administration time interaction (T×ZT) effects within groups were determined by performing two-way analysis of variance (ANOVA) followed by Tukey's post-hoc test when F was significant [2×2 factorial designs: treatment (GSPE or VH) x administration time (ZT0 or ZT12)]. Only significant F values were shown in the text as well as in Supplementary information. Statistical tests were performed using XL-Stat 2017 software (Addinsoft, Paris, France) and graphics were prepared using GraphPad Prism 6 (GraphPad Software, San Diego, CA, USA). A P value ≤0.05 was considered statistically significant.

3. Results

3.1. GSPE consumption at ZT0 improved insulin sensitivity without affecting adiposity and energy intake

As shown in Table 1, final body weight, body weight gain, body fat content and energy intake were not significantly affected by GSPE consumption and only animals supplemented with VH or GSPE at ZT12 showed lower energy intake values than animals at ZT0 [ZT effect; F (1,27)=5.57; P=0.025]. In contrast, GSPE consumption significantly reduced insulin values [T effect; F (1,23)=4.74; P=0.039] (Table 2). In fact, HOMA-IR values were significantly improved in response to GSPE only at ZT0 [ZTxT effect; F (1,19)=4.51; P=0.046], indicating that GSPE consumption could restore insulin sensitivity in animals with obesity when it was consumed at the beginning of the light phase. No effects were observed in triglyceride, total cholesterol, non-esterified fatty acids (NEFA), proinflammatory

monocyte chemoattractant protein-1 (MCP-1), leptin and adiponectin blood levels driven by GSPE administration (Table 2).

Table 1. Body weight and adiposity in rats fed a CAF diet and supplemented with GSPE or vehicle (VH) when the lights turn on (ZT0) or when then the lights turn off (ZT12).

	VH-ZT0	GSPE-ZT0	VH-ZT12	GSPE-ZT12	Two-way ANOVA
Final body weight (g)	484.88 ± 9.3	483.69 ± 10.0	483.81 ± 21.4	485.21 ± 12.1	ns
Body weight gain [a] (g)	55.26 ± 2.6	54.50 ± 5.2	54.56 ± 4.0	52.64 ± 4.5	ns
Body fat content [b] (%)	17.78 ± 1.3	18.39 ± 1.3	21.93 ± 0.7	18.34 ± 1.2	ns
IWAT (%)	2.20 ± 0.2	2.19 ± 0.2	2.40 ± 0.3	2.11 ± 0.2	ns
EWAT (%)	3.53 ± 0.2	3.73 ± 0.4	3.85 ± 0.5	3.62 ± 0.3	ns
Energy intake [c] (kJ/day)	2099.98 ± 172.8	1842.42 ± 72.8	1746.69 ± 85.1	1666.58 ± 71.4	ZT

ns no significant differences, ZT effect of supplementation time using two-way ANOVA (P < 0.05), CAF cafeteria, EWAT epididymal white adipose tissue, GSPE grape-seed proanthocyanidins extract, IWAT inguinal white adipose tissue, VH vehicle.

[a] Body weight gain was calculated as the difference between body weight measured at the beginning and at the end of the treatment period (from week 6 to week 9).

[b] Body fat content was assessed by quantitative magnetic resonance one week prior to sacrifice.

[c] Accumulated food intake was calculated as the difference between food intake at week 9 and food intake at week 6.

Table 2. Serum metabolic variables in rats fed a CAF diet and supplemented with GSPE or vehicle (VH) when the lights turn on (ZT0) or when then the lights turn off (ZT12).

	VH-ZT0	GSPE-ZT0	VH-ZT12	GSPE-ZT12	Two-way ANOVA
Glucose (mM)	8.16 ± 0.3 ab	8.49 ± 0.2 a	7.32 ± 0.2 b	8.05 ± 0.4 ab	ZT
Insulin (ng/mL)	8.60 ± 1.0	5.53 ± 0.9	7.44 ± 0.6	6.51 ± 0.6	T
HOMA-IR	76.13 ± 11.8 [a]	38.93 ± 9.7 [b]	54.55 ± 4.9 [ab]	57.01 ± 7.5 [ab]	ZT x T
Triglycerides (mg/dL)	200.2 ± 10.5	182.9 ± 18.8	187.6 ± 8.8	218.4 ± 26.1	ns
Cholesterol (mg/dL)	150.6 ± 9.2	152.4 ± 6.4	138.7 ± 3.8	153.7 ± 12.2	ns
NEFA (mg/dL)	31.78 ± 4.3	30.48 ± 2.5	22.95 ± 2.6	25.85 ± 2.4	ZT
MCP-1 (pg/mL)	343.7 ± 33.4	287.1 ± 24.0	375.3 ± 20.4	381.3 ± 25.0	ns
Adiponectin (μg/mL)	26.89 ± 2.4	25.06 ± 1.9	29.49 ± 2.8	26.48 ± 2.4	ns
Leptin (ng/mL)	35.81 ± 4.7	40.62 ± 2.8	35.86 ± 3.4	33.79 ± 3.6	ns

[a,b] Indicates significant differences (P < 0.05) using Tukey's post hoc test. ZT effect of supplementation time, T effect of treatment, ZTxT interaction of the supplementation time and treatment, ns no significant differences using two-way ANOVA (P < 0.05), CAF cafeteria, GSPE grape-seed proanthocyanidins extract, HOMA-IR homeostatic model assessment-insulin resistance, MCP-1 Monocyte chemoattractant protein-1, NEFA non-esterified fatty acids; VH, vehicle.

3.2. GSPE consumption reduced adipocyte size and increased adipocyte number in IWAT but not in EWAT

Knowing that the functionality of the adipose tissue can determine metabolic disturbances associated with obesity, we next explored whether GSPE consumption could modulate adipocyte histology and WAT expansion in rats with obesity. There are important metabolic differences between WAT depots which depend on their localization (in or outside of the abdominal cavity). Hence, in this study, both size and number of adipocytes were studied in two fat pads: inguinal subcutaneous WAT (IWAT) and visceral WAT derived from the epididymal fat pad (EWAT). A representative histological image of IWAT and EWAT for each group of animals is shown at **Supplementary Information Fig. S1.** When a two-way ANOVA test was conducted, a significant effect of GSPE consumption (T effect) was observed in IWAT histology in comparison with VH animals regardless of administration time (Fig. 1A). However, when Tukey's post hoc test was used, animals supplemented with GSPE at ZT12 significantly presented lower adipocyte area and lower frequency of larger adipocytes distribution (> 3 000 μm^2) with respect to VH-ZT12 animals (**Fig. 1A**). Interestingly, comparisons between VH-ZT0 and VH-ZT12 did not result in any significant differences in IWAT, reinforcing the results obtained in response to GSPE consumption. In contrast, in EWAT, GSPE treatment did not produce any significant change in adipocyte morphology in any group of animals (**Fig. 1B**).

3.3. GSPE consumption at ZT12 resulted in decreased gene expression of positive regulators of adipogenesis, fatty acid metabolism and glucose uptake in IWAT

We next investigated the metabolic gene expression profile of several key regulators of adipocyte metabolism in IWAT (**Fig. 2 and Supplementary information Table S2**) and EWAT (**Fig. 3 and Supplementary information Table**

S3). Additionally, the differential gene expression heatmap for each fat depot is also shown in **Supplementary Information Fig. S2.**

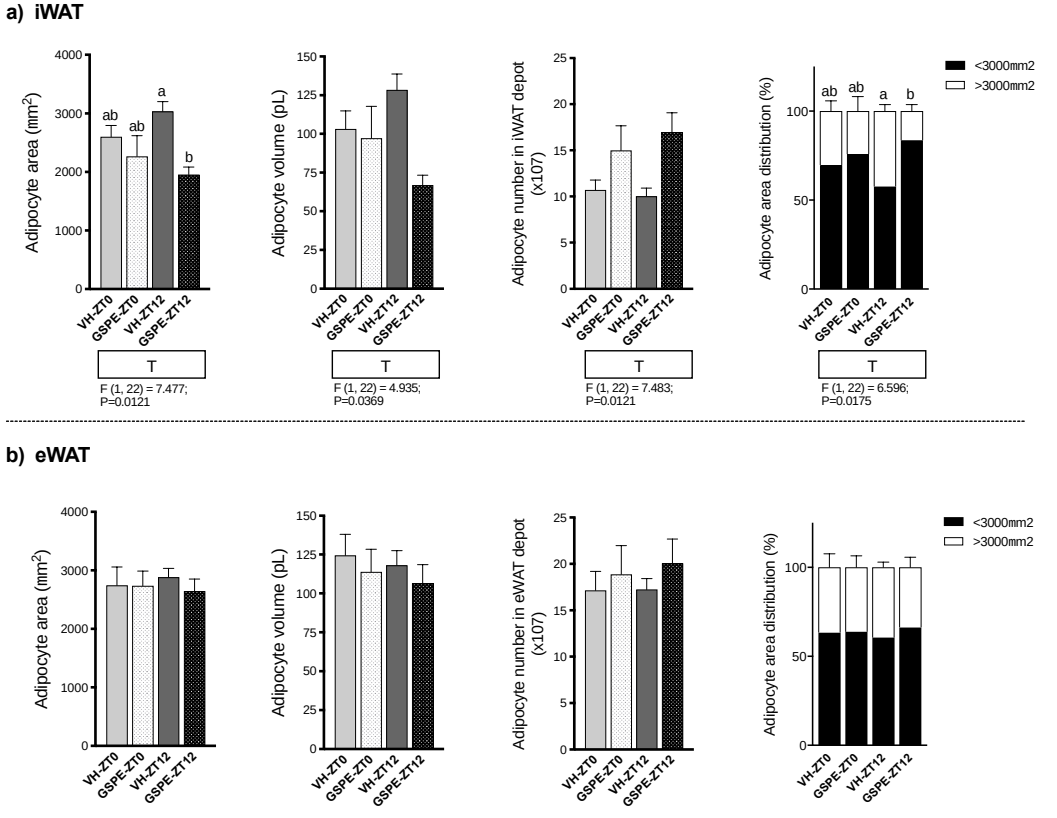

Fig. 1 Adipose tissue histology. *Histological analysis of IWAT (a) and EWAT (b) of animals fed a cafeteria diet for 9 weeks and treated with GSPE (25 mg/kg of body weight) or vehicle (VH) the last 4 weeks of the study when the lights turned on (ZT0) or when the lights turned off (ZT12). For adipocyte area distribution, adipocytes were divided in two groups according to their areas (<3000 or >3000 μm2). Results are presented as the mean ± SEM. (n = 6). T indicates treatment effect using two-way ANOVA (P < 0.05) and a, b denotes significant differences between groups using Tukey's post hoc test.*

As illustrated in **Fig. 2**, the consumption of GSPE produced a different pattern of gene expression in IWAT depending on the ZT in which GSPE was consumed (ZTxT effect). In fact, GSPE consumption at ZT0 did not significantly affect the relative gene expression of these genes. In contrast, GSPE consumption at ZT12 produced a significant downregulation of the adipogenic factor *Pparγ* [ZTxT effect, F (1,23)=7.94; P=0.009] as well as of several genes involved in fatty acid

metabolism including *Mgl* [ZTxT effect, F (1,22)=9.86; P=0.004], *Cpt1b* [ZTxT effect; F (1,21)=8.07; P=0.009] and *Cd36* [ZTxT effect, F (1,21)=7.41; P=0.012]. In addition, in this tissue, GSPE consumption at ZT12 also decreased the gene expression of *Adipoq* [ZTxT effect, F (1,21)=5.85; P=0.024] and the insulin-signaling effector *Glut4* [ZTxT effect, F (1,22)=11.25; P=0.002]. Interestingly, when VH-ZT0 and VH-ZT12 groups were compared, only a significant upregulation of *Glut4* gene expression was observed in animals supplemented at ZT12 with respect to ZT0.

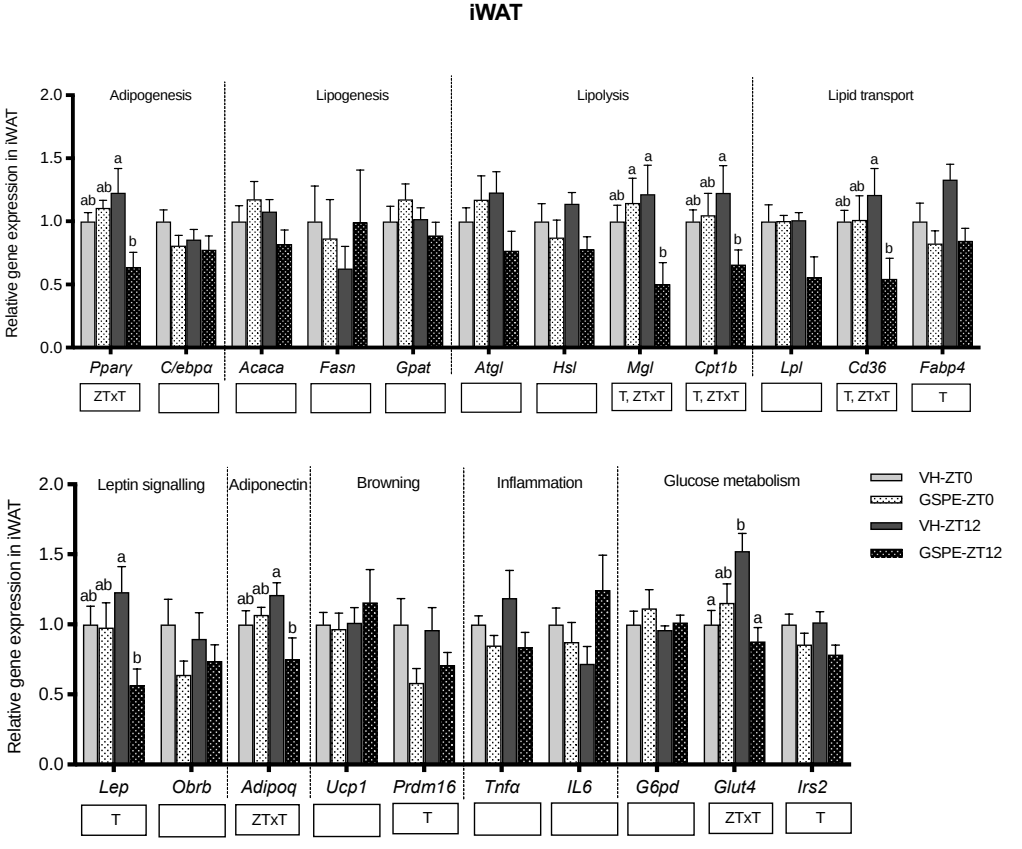

Fig. 2 Effects of GSPE on the expression of genes related to adipose metabolism in IWAT. *Animals were fed with a cafeteria diet for 9 weeks and treated with GSPE (25 mg/kg of body weight) or vehicle (VH) the last 4 weeks of the study when the lights turned on (ZT0) or when the lights turned off (ZT12). The gene expression was measured by qPCR and normalized by Ppia gene expression. The relative expression (presented as fold-change) was normalized to VH-ZT0 group. Results are presented as the mean ± SEM (n = 6–8). T indicates treatment effect, ZT x T indicates interaction of the supplementation time and treatment effect using two-way ANOVA (P < 0.05). a,b denotes significant differences between groups using Tukey's post hoc test. Pparγ peroxisome proliferator-activated receptor γ, C/ebp α CCAAT/enhancer-binding protein alpha, Acaca acetyl-CoA carboxylase alpha, Fasn fatty acid synthase, Gpat glycerol-3-phosphate acyltransferase, Atgl adipose triglyceride lipase, Hsl hormone-sensitive lipase, Mgl monoacylglycerol lipase, Cpt1b carnitine*

palmitoyltransferase 1B, Lpl lipoprotein Lipase, Cd36 cluster of differentiation 36, Fabp4 fatty Acid Binding Protein 4, Lep leptin, Obrb leptin receptor, Adipoq adiponectin, Ucp1 uncoupling protein 1, Prdm16 PR domain containing 16, Tnfα tumor necrosis factor alpha, Il6 interleukin 6, G6pd glucose-6 phosphate dehydrogenase, Glut4 glucose transporter 4, Irs2 insulin receptor substrate 2.

3.4. GSPE consumption at ZT0 reduced the gene expression of inflammatory and thermogenic markers in EWAT

In EWAT, as observed in IWAT, the consumption of GSPE also produced a different pattern of expression depending on the ZT in which GSPE was consumed. However, contrary to the results observed in IWAT, GSPE consumption at ZT0 resulted in a downregulation of genes involved in lipid metabolism including *Gpat* [ZTxT effect, F (1,23)=20.75; P=0.0001] and *Ucp1* [ZTxT effect, F (1,24)=6.27; P=0.019] (**Fig. 3**). Interestingly, GSPE consumption at ZT0 also caused a significant decrease of the proinflammatory cytokine *Il6* [F (1,23)=5.69; P=0.025]. In contrast, at ZT12, a significant upregulation of *C/ebpa* [ZTxT effect, F (1,24)=17.04; P=0.0004], *Gpat* [ZTxT effect, F (1,23)=20.75; P=0.0001] and *Hsl* [ZTxT effect, F (1,24)=7.926; P=0.012] was detected in response to GSPE consumption, while no significant changes were observed in the expression of genes involved in lipid transport and glucose metabolism. Comparing VH-ZT0 and VH-ZT12 groups, the mRNA levels of *Gpat* and *Il6* were significantly downregulated at ZT12 with respect to ZT0, while A*dipoq* was significantly upregulated at ZT12.

3.5. GSPE consumption upregulated Cry1 gene expression in IWAT at ZT12 but not at ZT0

Different components of the circadian clock system have been shown to modulate the expression of key genes involved in adipogenesis, and lipid and glucose metabolism in WAT. Therefore, we further studied whether these changes in gene

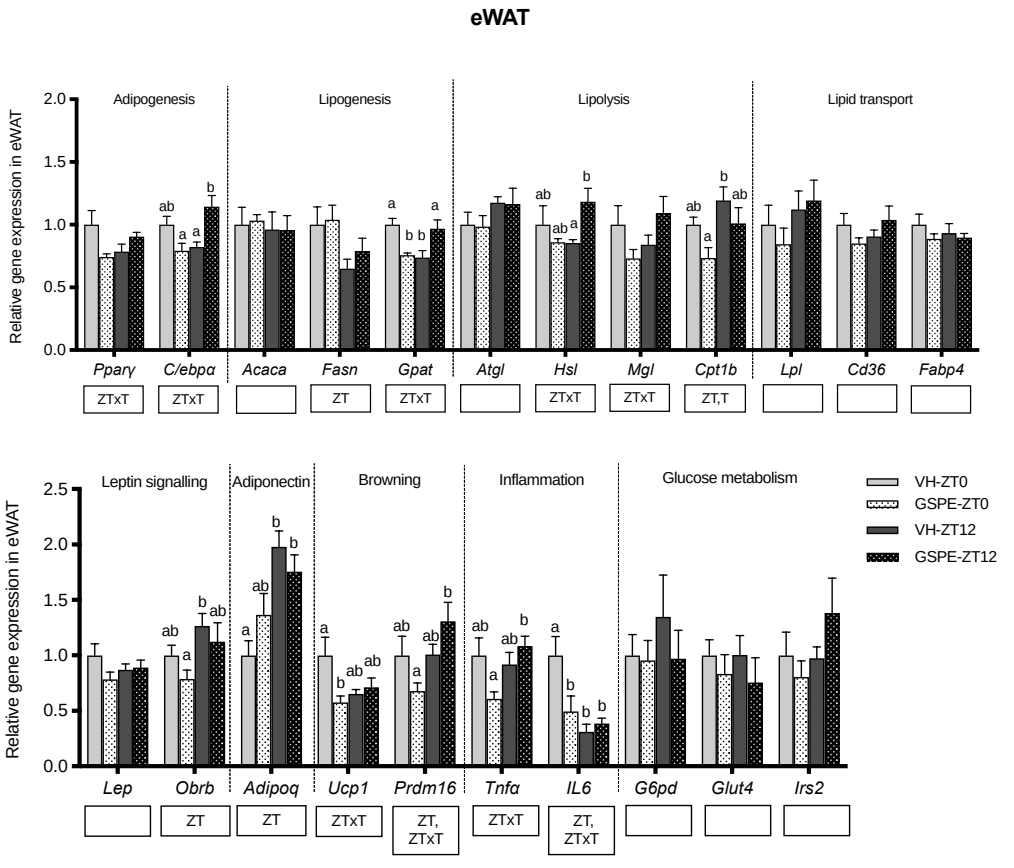

Fig. 3 Effects of GSPE on the expression of genes related to adipose metabolism in EWAT. *Animals were fed with a cafeteria diet for 9 weeks and treated with GSPE (25 mg/kg of body weight) or vehicle (VH) the last 4 weeks of the study when the lights turned on (ZT0) or when the lights turned off (ZT12). The gene expression was measured by qPCR and normalized by Ppia gene expression. The relative expression (presented as fold-change) was normalized to VH-ZT0 group. Results are presented as the mean ± SEM (n = 6–8). ZT indicates effect of supplementation time, T treatment effect and ZT x T interaction of the supplementation time and treatment effect using two-way ANOVA (P < 0.05). a,b denotes significant differences between groups using Tukey's post hoc test. Pparγ peroxisome proliferator-activated receptor γ, C/ebp α CCAAT/enhancer-binding protein alpha, Acaca acetyl-CoA carboxylase alpha, Fasn fatty acid synthase, Gpat glycerol-3-phosphate acyltransferase, Atgl adipose triglyceride lipase, Hsl hormone-sensitive lipase, Mgl monoacylglycerol lipase, Cpt1b carnitine palmitoyltransferase 1B, Lpl lipoprotein Lipase, Cd36 cluster of differentiation 36, Fabp4 fatty Acid Binding Protein 4, Lep leptin, Obrb leptin receptor, Adipoq adiponectin, Ucp1 uncoupling protein 1, Prdm16 PR domain containing 16, Tnfα tumor necrosis factor alpha, Il6 interleukin 6, G6pd glucose-6-phosphate dehydrogenase, Glut4 glucose transporter 4, Irs2 insulin receptor substrate 2.*

expression driven by GSPE consumption were associated with clock gene expression profiles in IWAT and EWAT. Therefore, we evaluated the expression pattern of *Bmal1* (clock-core gene), *Per2*, *Cry1* and *Rev-erb-a* (components of the negative loop of the circadian clock) in response to GSPE consumption (**Fig. 4 and Supplementary information Table S4**). In IWAT, GSPE consumption was able to modulate the mRNA levels of *Bmal1*, *Cry1* and *Rev-erb-a* depending on the ZT in which GSPE was consumed. Specifically, GSPE consumption at ZT12 significantly upregulated the gene expression of *Cry1* [ZTxT effect, F (1,20)=5.23; P=0.033]. In EWAT, the consumption of GSPE also produced a different pattern of the gene expression of *Bmal1* [ZTxT effect; F (1,24)=7.66; P=0.010] and *Per2* [ZTxT effect; F (1,24)=4.33; P=0.048], while *Cry1* was upregulated at ZT0 regardless of GSPE administration.

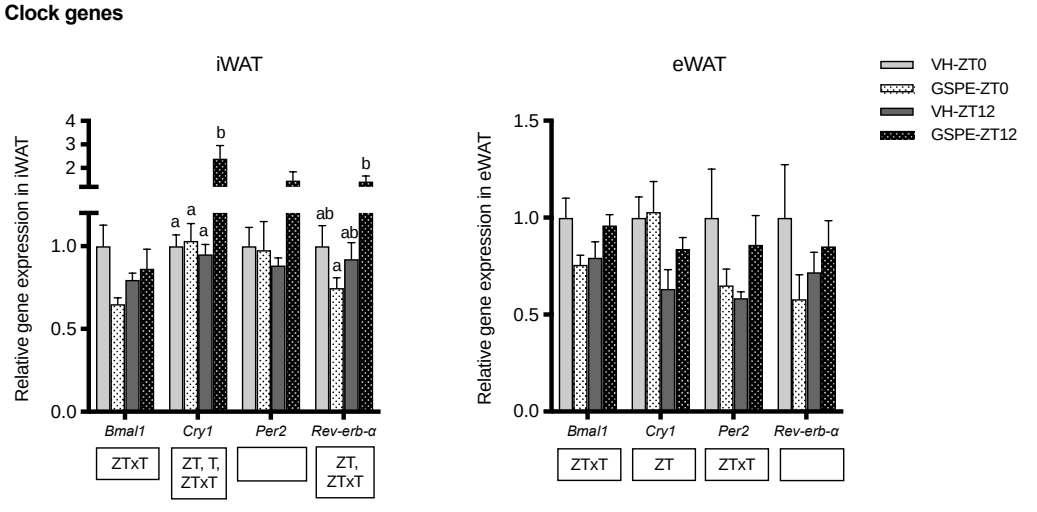

Fig. 4 Effects of GSPE on the expression of clock genes. *Animals were fed with a cafeteria diet for 9 weeks and treated with GSPE (25 mg/kg of body weight) or vehicle (VH) the last 4 weeks of the study when the lights turned on (ZT0) or when the lights turned off (ZT12). The gene expression was measured by qPCR and normalized by Ppia gene expression. The relative expresión (presented as fold-change) was normalized to VH-ZT0 group. Results are presented as the mean ± SEM (n = 6–8). ZT indicates effect of supplementation time, T treatment effect and ZT x T interaction of the supplementation time and treatment effect using two-way ANOVA (P < 0.05). a,b denotes significant differences between groups using Tukey's post hoc test. Bmal1 brain and muscle ARNT-Like 1 (aryl hydrocarbon receptor nuclear translocator-like), Cry1 cryptochrome circadian regulator 1, Per2 period circadian regulator 2, Rev-erb-α nuclear receptor subfamily 1, group D, member 1 (Nr1d1).*

4. Discussion

The health effects of polyphenols are usually determined without considering the time-of-day of their consumption. However, it seems evident that biological rhythms should be considered in preclinical and clinical nutritional studies as many physiological and metabolic processes in mammals present circadian oscillations. In this sense, similar to other peripheral tissues studied from a circadian context, WAT is a metabolic organ with a tremendous plasticity that is directly influenced by circadian clock [14-19]. In addition, previous studies have demonstrated that a long-term consumption of GSPE induced a healthier expansion of WAT to match the surplus energy provided by the cafeteria diet by reducing adipocyte size and increasing fat cell number [11,12]. Unfortunately, to the best of our knowledge, any study has addressed the interaction between circadian WAT metabolism and GSPE consumption. In this context, our study was specifically designed to investigate whether the metabolic response of WAT to GSPE consumption was significantly influenced by the time-of-day in which it was consumed. For this purpose, GSPE was administered to rats with obesity during 4 weeks at the beginning of the light phase (ZT0) or, on the contrary, at the beginning of dark phase (ZT12). Our results provide, for the first time, evidence that the biological effect of GSPE on WAT metabolism depends on the ZT point of its consumption.

Although various studies have shown that polyphenols and polyphenolic extracts could prevent body weight gain and fat accumulation, there are scarce data about the effect of polyphenols at different ZT points on body fat content. In addition, in most of these studies performed with animals, the body-lowering effect in response to polyphenolic consumption has been mainly observed after the administration for a long time (<10 weeks) and/or using high doses of polyphenolic compounds (<200 mg/kg of body weight) [28,29]. Here, although our

data did not demonstrate an effect of GSPE on body fat content, we report for the first time that the administration of GSPE during 4 weeks at dose of 25 mg/kg of body weight significantly altered the pattern of expansion of IWAT by decreasing adipocyte size only when GSPE was consumed at the beginning of the dark phase (ZT12), while this effect was not observed when GSPE was consumed at the beginning of the light phase (ZT0). In contrast, in EWAT, GSPE consumption did not modulate adipocyte morphology in any ZT point, indicating that subcutaneous fat could be more sensitive than visceral fat to GSPE. In mammals, when energy intake is higher than energy expenditure, WAT can expand by generating more adipocytes (hyperplasia) or by storing more fat in existing adipocytes (hypertrophy). Several studies have shown that hyperplasia protects against insulin resistance and inflammation, whereas adipocyte hypertrophy causes an overproduction of adipokines that decreases tissue insulin sensitivity and induces oxidative stress and inflammation [30]. In our model of obesity using CAF diet-fed rats, subcutaneous IWAT could act as a buffer for the daily excess of food intake, protecting against visceral fat accumulation which is closely correlated with unhealthy metabolic complications such as inflammation and insulin resistance [31].

Although GSPE consumption at ZT0 did not display significant changes in the histologic analysis of WAT, the pro-inflammatory gene *IL-6* was notably downregulated in visceral EWAT when GSPE was consumed at ZT0. In fact, visceral adipose tissue secretes more proinflammatory factors than subcutaneous adipose tissue [32], and TNF-α and IL-6 may lead to insulin resistance by increasing free fatty acid produced by adipocytes and reducing adiponectin synthesis [33]. In addition, both TNF-α and IL-6 exhibit circadian rhythmicity in their gene expression, being highest in the rest phase and lowest in the active phase [34]. Our results indicate that GSPE consumption downregulated the gene

expression of *IL-6* only when their expression levels reach its maximum during the rest time (light phase) and did not exert any anti-inflammatory effect at ZT12 when their gene expression levels are physiologically reduced during the active phase (dark phase). Consistent with these results, acute resveratrol (RSV) administration in male Wistar rats also showed opposite effects on proinflammatory and lipid peroxidation levels depending on the time-of-day of its administration [35]. Although blood concentration of MCP-1, another pro-inflammatory chemokine with a well-established systemic role in the regulation of metabolism and insulin resistance in mammals [36], did not show significant changes in GSPE-treated animals, its concentrations were reduced when GSPE was administered at ZT0, reinforcing the putative anti-inflammatory and antidiabetic role of this polyphenolic extract when it is consumed during the rest phase.

Glucose and lipid metabolism also present circadian regulation in order to prepare the metabolic functions for the outcoming situations during the day. In this sense, it was reported that insulin sensitivity in mammals displays a circadian rhythm and that it reaches its maximum around noon and its minimum during rest phase [37]. It has been recently demonstrated that an acute ingestion of catechin-rich green tea reduces postprandial blood glucose concentrations when it was consumed in the evening but not in the morning in healthy young men [38]. Accordingly, our data demonstrated that GSPE consumption restores HOMA-IR values in animals with diet-induced obesity only when it was administered at ZT0 (the beginning of rest phase in Wistar rats) suggesting that GSPE could enhance insulin sensitivity only when it reaches its minimum during the rest time. Although several studies have previously demonstrated that GSPE consumption properly restore insulin levels in animals with obesity [39,40], our study is the first reporting such differential effects between ZT points and GSPE consumption. By

contrast, in our experiment, GSPE consumption did not prevent the hyperlipidemia induced by the CAF diet in any ZT point. Several works have reported a decrement in the circulating levels of triglycerides and cholesterol in response to GSPE consumption, but others have found no significant effects [41]. These discrepancies may rely either on the differences among polyphenolic extracts, the length of treatment, the dose of polyphenols or the animal models used in the different studies.

Other important effects of polyphenols in adipose tissue lead to a decrease in adiposity by reducing adipogenesis and the release of adipokines such as leptin [42]. In our study, when GSPE was consumed at ZT12, a significant decrease in the gene expression of *Leptin* and the adipogenic gene *Pparγ* was observed in IWAT, reinforcing the robust metabolic correlation between leptin and fat mass and contributing to the enhancement of leptin sensitivity. The mechanisms that control adipogenesis have been studied mainly *in vitro*, and little information is known under *in vivo* conditions. However, in a previous study of our group [12], the adipose tissue of rats supplemented with GSPE showed an increase in the expression of *Pref-1*, suggesting that GSPE supplementation could increase the number of adipocyte precursors in this tissue. However, further research is worthy to be conducted to assess the impact of GSPE in the proliferation of pre-adipocytes in order to elucidate its potential effect on adipogenesis.

In addition, GSPE consumption at ZT12 also resulted in a downregulation of all genes related to lipolysis, fatty acid oxidation (*Cpt1b*) and lipid transport, strongly suggesting that GSPE could prevent fat accumulation in this tissue through the reduction of adipocyte lipid uptake. In fact, it is well-established that body fat mass loss is mainly driven by lower rate of lipid uptake rather than by changes in lipid removal through lipolysis [43]. Our results suggest that GSPE consumption downregulated the expression of lipolytic genes in IWAT only when their

expression levels reach its maximum at dark phase, compared with ZT0 when the expression of these lipolytic genes reaches the trough. Additionally, our results also reported a significant upregulation of *Cry1* gene in IWAT, but not in visceral EWAT, in response to GSPE consumption at ZT12. *Cry*-deficient mice increase lipid storage in adipose tissue suggesting that *Cry1* regulates lipid transport and lipolysis [44]. In addition, several authors have demonstrated that *Rev-erb-a* is an essential positive regulator of adipogenesis [45], reinforcing the hyperplasic effect of GSPE on WAT expansion when it was consumed at ZT12 compared to ZT0. In contrast, the mRNA expression of *Adipoq* gene and the glucose transporter gene *Glut4* were simultaneously decreased in response to GSPE consumption at ZT12 in this tissue. This effect of GSPE consumption had previously been reported by others in mesenteric WAT [40].

Finally, in visceral EWAT, a significant increase in the expression of both *Gpat* and *Hsl* genes was observed when GSPE was consumed at ZT12. This simultaneous activation of both catabolic and anabolic lipid pathways in response to GSPE consumption was previously reported in visceral fat depots and *in vitro* adipocytes [46,47]. However, the metabolic meaning of this apparently futile cycle induced by GSPE consumption is still unclear.

However, as in this study the gene expression is only measured at one time point but not over time, it is not plausible to determine changes in the circadian expression profile of these genes. In addition, the potential circadian entrainment effect of the sweetened skim condensed milk used to help animals to consume GSPE properly for 4 weeks cannot also be discarded. Consequently, further studies are needed to assess whether the modification of the expression of clock genes in response to GSPE consumption was due to a phase shift, a period enlargement, or a modification in the amplitude.

In conclusion, our results indicated that the beneficial effects associated with the consumption of GSPE in animals with obesity are strongly influenced in a tissue-specific manner by the time-of-day in which it was consumed. Particularly, GSPE consumption at the beginning of light phase (ZT0) was associated with a potential antidiabetic and anti-inflammatory effect in EWAT, whereas its consumption at the beginning of the dark phase (ZT12) resulted in a hyperplasic expansion of IWAT. Therefore, it is plausible to speculate that the consumption of polyphenols at the most optimal time-of-day could properly potentiate the metabolic response of adipose tissue and therefore affect the whole-body energy metabolism contributing to the management of overweight and obesity.

Acknowledgements: We gratefully acknowledge the aid of laboratory technicians Niurka Dariela Llópiz and Rosa Pastor from Universitat Rovira i Virgili.

Funding: This research was supported by a grant (AGL2013-40707-R and AGL2016-77105-R) from the Spanish government. MC-P received a pre-doctoral fellowship from the government of Catalonia (2021 FI_B2 00105). RMR and EN-M received a grant for PhD students from the Universitat Rovira i Virgili (2018PMF-PIPF-11 and 2019PMF-PIPF-73, respectively). GA, MM and FIB are Serra-Húnter fellows at the Universitat Rovira i Virgili.

Author contribution: MC-P, MM, FIB, LA, and GA designed the research; MC-P and RMR performed the experiments and collected the data; MC-P, MM, FIB, LA and GA analyzed the data and interpreted the results; MC-P, EN-M and GA wrote the manuscript. All authors read and approved the final manuscript.

Competing interests: The authors declare no competing interests in relation to this manuscript.

Additional information: Supplementary information is available on International Journal of Obesity's website. Correspondence and requests for materials should be addressed to Gerard Aragonès.

References

1. Conway B, Rene A. Obesity as a disease: No lightweight matter. *Obes Rev*. 2004;5(3):145-151. doi:10.1111/j.1467-789X.2004.00144.x

2. Coelho M, Oliveira T, Fernandes R. Biochemistry of adipose tissue: an endocrine organ. *Arch Med Sci*. 2013;20:9(2):191-200. doi:10.5114/aoms.2013.33181

3. Ducharme NA, Bickel PE. Minireview: Lipid droplets in lipogenesis and lipolysis. *Endocrinology*. 2008;149(3):942-949. doi:10.1210/en.2007-1713

4. Kuri-Harcuch W, Velez-delValle C, Vazquez-Sandoval A, Hernández-Mosqueira C, Fernandez-Sanchez V. A cellular perspective of adipogenesis transcriptional regulation. *J Cell Physiol*. 2019;234(2):1111-1129. doi:10.1002/jcp.27060

5. Madsen MS, Siersbaek R, Boergesen M, Nielsen R, Mandrup S. Peroxisome Proliferator-Activated Receptor and C/EBP Synergistically Activate Key Metabolic Adipocyte Genes by Assisted Loading. *Mol Cell Biol*. 2014;34(6):939-954. doi:10.1128/mcb.01344-13

6. Chait A, den Hartigh LJ. Adipose Tissue Distribution, Inflammation and Its Metabolic Consequences, Including Diabetes and Cardiovascular Disease. *Front Cardiovasc Med*. 2020;7:1-41. doi:10.3389/fcvm.2020.00022

7. Stanford KI, Middelbeek RJW, Goodyear LJ. Exercise effects on white adipose tissue: Beiging and metabolic adaptations. *Diabetes*. 2015;64(7):2361-2368. doi:10.2337/db15-0227

8. Palou A, Picó C, Luisa Bonet M. Nutritional potential of metabolic remodelling of white adipose tissue. *Curr Opin Clin Nutr Metab Care*. 2013;16(6):650-656. doi:10.1097/MCO.0b013e328365980f

9. Peng J, Jia Y, Hu T, et al. GC-(4→8)-GCG, A Proanthocyanidin Dimer from Camellia ptilophylla, Modulates Obesity and Adipose Tissue Inflammation in High-Fat Diet Induced Obese Mice. *Mol Nutr Food Res*. 2019;63(11):1-12. doi:10.1002/mnfr.201900082

10. Ardévol A, Motilva MJ, Serra A, Blay M, Pinent M. Procyanidins target mesenteric adipose tissue in Wistar lean rats and subcutaneous adipose tissue in Zucker obese rat. *Food Chem*. 2013;141(1):160-166. doi:10.1016/j.foodchem.2013.02.104

11. Pascual-Serrano A, Bladé C, Suárez M, Arola-Arnal A. Grape Seed Proanthocyanidins Improve White Adipose Tissue Expansion during Diet-Induced Obesity Development in Rats. *Int J Mol Sci*. 2018;19(9):2632. doi:10.3390/ijms19092632

12. Pascual-Serrano A, Arola-Arnal A, Suárez-García S, Bravo FI, Suárez M, Arola L, et al. Grape seed proanthocyanidin supplementation reduces adipocyte size and increases adipocyte number in obese rats. *Int J Obes*. 2017;41(8):1246-1255. doi:10.1038/ijo.2017.90

13. Patke A, Young MW, Axelrod S. Molecular mechanisms and physiological importance of circadian rhythms. *Nat Rev Mol Cell Biol*. 2020;21(2):67-84. doi:10.1038/s41580-019-0179-2

14. Ptitsyn AA, Zvonic S, Conrad SA, Scott LK, Mynatt RL, Gimble JM. Circadian clocks are resounding in peripheral tissues. *PLoS Comput Biol*. 2006;2(3):126-135. doi:10.1371/journal.pcbi.0020016

15. Zvonic S, Ptitsyn AA, Conrad SA, Scott LK, Floyd ZE, Kilroy G, et al. Characterization of Peripheral Circadian Clocks in Adipose Tissues. *Diabetes*. 2006;55(4):962-70. doi: 10.2337/diabetes.55.04.06.db05-0873.

16. Shostak A, Meyer-Kovac J, Oster H. Circadian Regulation of Lipid Mobilization in White Adipose Tissues. *Diabetes*. 2013;62(7):2195-203. doi:10.2337/db12-1449

17. Stenvers DJ, Scheer FAJL, Schrauwen P, la Fleur SE, Kalsbeek A. Circadian clocks and insulin resistance. *Nat Rev Endocrinol*. 2019;15(2):75-89. doi:10.1038/s41574-018-0122-1

18. Ribas-latre A, Santos RB, Fekry B, Tamim YM, Shivshankar S, Mohamed AMT, et al. Cellular and physiological circadian mechanisms drive diurnal cell proliferation and expansion of white adipose tissue. *Nat Commun*. 2021;12(1):3482. doi:10.1038/s41467-021-23770-0

19. Dollet L, Zierath JR. Interplay between diet, exercise and the molecular circadian clock in orchestrating metabolic adaptations of adipose tissue. *J Physiol*. 2019;597(6):1439-1450. doi:10.1113/JP276488

20. Margalef M, Pons Z, Iglesias-Carres L, Bravo FI, Muguerza B, Arola-Arnal A. Lack of tissue accumulation of grape seed flavanols after daily long-term administration in healthy and cafeteria-diet obese rats. *J Agric Food Chem*. 2015;63(45):9996-10003. doi:10.1021/acs.jafc.5b03856

21. Ribas-Latre A, Baselga-Escudero L, Casanova E, Arola-Arnal A, Salvadó MJ, Arola L, et al. Chronic consumption of dietary proanthocyanidins modulates peripheral clocks in healthy and obese rats. *J Nutr Biochem*. 2015;26:112-119. doi:10.1016/j.jnutbio.2014.09.006

22. Foster MT, Softic S, Caldwell J, Kohli R, DeKloet AD, Seeley RJ. Subcutaneous adipose tissue transplantation in diet-induced obese mice attenuates metabolic dysregulation while removal exacerbates it. *Physiol Rep*. 2013;1(2):1-12. doi:10.1002/phy2.15

23. Cox-York K, Wei Y, Wang D, Pagliassotti MJ, Foster MT. Lower body adipose tissue removal decreases glucose tolerance and insulin sensitivity in mice with exposure to high fat diet. *Adipocyte*. 2015;4(1):32-43. doi:10.4161/21623945.2014.957988

24. Tran TT, Yamamoto Y, Gesta S, Kahn CR. Beneficial Effects of Subcutaneous Fat Transplantation on Metabolism. *Cell Metab*. 2008;7(5):410-420. doi:10.1016/j.cmet.2008.04.004.Beneficial

25. Gibert-Ramos A, Palacios-Jordan H, Salvadó MJ, Crescenti A. Consumption of out-of-season orange modulates fat accumulation, morphology and gene expression in the adipose tissue of Fischer 344 rats. *Eur J Nutr*. 2020;59(2):621-631. doi:10.1007/s00394-019-01930-9

26. Ibars M, Aragonès G, Ardid-Ruiz A, Gibert-Ramos A, Arola-Arnal A, Suárez M, et al. Seasonal consumption of polyphenol-rich fruits affects the hypothalamic leptin signaling system in a photoperiod-dependent mode. *Sci Rep*. 2018;8(1):13572. doi:10.1038/s41598-018-31855-y

27. Pfaffl MW. Relative quantification. *Real-time PCR*. 2007:64-82.

28. Pons Z, Margalef M, Bravo FI, Arola-Arnal A, Muguerza B. Chronic administration of grape-seed polyphenols attenuates the development of hypertension and improves other cardiometabolic risk factors associated with the metabolic syndrome in cafeteria diet-fed rats. *Br J Nutr*. 2017;117(2):200-208. doi:10.1017/S0007114516004426

29. Serrano J, Casanova-Martí À, Gual A, Pérez-Vendrell AM, Blay MT, Terra X, et al. A specific dose of grape seed-derived proanthocyanidins to inhibit body weight gain limits food intake and increases energy expenditure in rats. *Eur J Nutr*. 2017;56(4):1629-1636. doi:10.1007/s00394-016-1209-x

30. Longo M, Zatterale F, Naderi J, Parrillo L, Formisano P, Raciti GA, et al. Adipose Tissue

Dysfunction as Determinant of Obesity-Associated Metabolic Complications. *Int J Mol Sci*. 2019;20(9):2358. doi:10.3390/ijms20092358

31. Manolopoulos KN, Karpe F, Frayn KN. Gluteofemoral body fat as a determinant of metabolic health. *Int J Obes*. 2010;34(6):949-959. doi:10.1038/ijo.2009.286

32. Hamdy O, Porramatikul S, Al-Ozairi E. Metabolic Obesity: The Paradox Between Visceral and Subcutaneous Fat. *Curr Diabetes Rev*. 2006;2(4):367-373. doi:10.2174/1573399810602040367

33. Medina EA, Afsari RR, Ravid T, Sianna Castillo S, Erickson KL, Goldkorn T. Tumor necrosis factor-α decreases Akt protein levels in 3T3-L1 adipocytes via the caspase-dependent ubiquitination of Akt. *Endocrinology*. 2005;146(6):2726-2735. doi:10.1210/en.2004-1074

34. Cermakian N, Lange T, Golombek D, Sarkar D, Nakao A, Shibata S, et al. Crosstalk between the circadian clock circuitry and the immune system. *Chronobiol Int*. 2013;30(7):870-888. doi:10.3109/07420528.2013.782315

35. Gadacha W, Ben-attia M, Bonnefont-Rousselot D, Aouani E, Chanem-Boughanmi N, Touitou Y. Resveratrol opposite effects on rat tissue lipoperoxidation: pro-oxidant during day-time and antioxidant at night. *Redox Rep*. 2009;14(4):154-8. doi:10.1179/135100009X466131

36. Rull A, Camps J, Alonso-villaverde C, Joven J. Insulin Resistance, Inflammation, and Obesity: Role of Monocyte Chemoattractant Protein-1 (or CCL2) in the Regulation of Metabolism. *Mediators Inflamm*. 2010;2010:326580. doi:10.1155/2010/326580

37. Carrasco-benso MP, Rivero-gutierrez B, Lopez-Minguez J, Anzola A, Diez-Noguera A, Madrid JA, et al. Human adipose tissue expresses intrinsic circadian rhythm in insulin sensitivity. *FASEB J*. 1026;20(9):3117-3123. doi:10.1096/fj.201600269RR

38. Takahashi M, Ozaki M, Miyashita M, Fukazawa M, Nakaoka T, Wakisaka T, et al. Effects of timing of acute catechin-rich green tea ingestion on postprandial glucose metabolism in healthy men. *J Nutr Biochem*. 2019;73:108221. doi:10.1016/j.jnutbio.2019.108221

39. Montagut G, Onnockx S, Vaqué M, Bladé C, Blay M, Fernández-Larrea J, et al. Oligomers of grape-seed procyanidin extract activate the insulin receptor and key targets of the insulin signaling pathway differently from insulin. *J Nutr Biochem*. 2010;21(6):476-481. doi:10.1016/j.jnutbio.2009.02.003

40. Montagut G, Bladé C, Blay M, Fernández-Larea J, Pujadas G, Salvadó MJ, et al. Effects of a grapeseed procyanidin extract (GSPE) on insulin resistance. *J Nutr Biochem*. 2010;21(10):961-967. doi:10.1016/j.jnutbio.2009.08.001

41. Arola L, Salvado M. Hypolipidemic effects of proanthocyanidins and their underlying biochemical and molecular mechanisms. *Mol Nutr Food Res*. 2010:54(1):37-59. doi:10.1002/mnfr.200900476

42. Sandoval V, Sanz-Lamora H, Arias G, Marrero PF, Haro D, Relat J. Metabolic impact of flavonoids consumption in obesity: From central to peripheral. *Nutrients*. 2020;12(8):1-55. doi:10.3390/nu12082393

43. Arner P, Bernard S, Appelsved L, Fu KY, Andersson DP, Salehpour M, et al. Adipose lipid turnover and long-term changes in body weight. *Nat Med*. 2019;25(9):1385-1389. doi:10.1038/s41591-019-0565-5

44. Barclay JL, Shostak A, Leliavski A, Tsang AH, Jöhren O, Müller-Fielitz H, et al. High-fat diet-

induced hyperinsulinemia and tissue-specific insulin resistance in Cry-deficient mice. *Am J Physiol Endocrinol Metab*. 2013;304:1053-1063. doi:10.1152/ajpendo.00512.2012.-Perturbation

45. Kumar N, Solt LA, Wang Y, Rogers PM, Bhattacharyya G, Kamenecha TM, et al. Regulation of adipogenesis by natural and synthetic REV-ERB ligands. *Endocrinology*. 2010;151(7):3015-3025. doi:10.1210/en.2009-0800

46. Caimari A, Del Bas JM, Crescenti A, Arola L. Low doses of grape seed procyanidins reduce adiposity and improve the plasma lipid profile in hamsters. *Int J Obes*. 2013;37:576-583. doi:10.1038/ijo.2012.75

47. Pinent M, Bladé MC, Salvadó MJ, Arola L, Ardévol A. Intracellular mediators of procyanidin-induced lipolysis in 3T3-L1 adipocytes. *J Agric Food Chem*. 2005;53(2):262-266. doi:10.1021/jf048947y

GRAPHICAL ABSTRACT

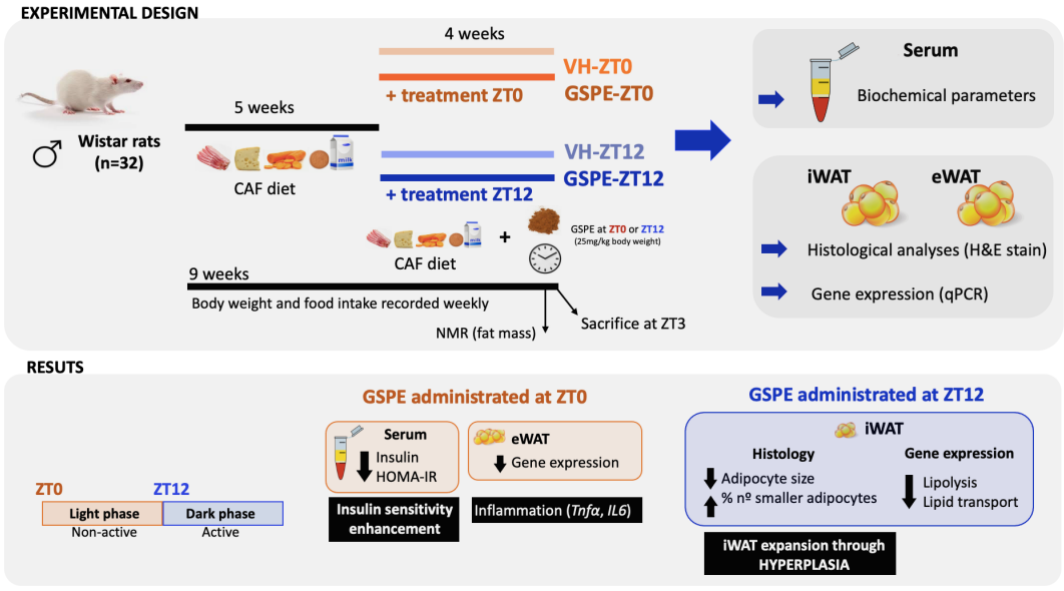

SUPPLEMENTARY MATERIAL

Table S1. Primers for the Q-PCR analysis.

	Forward (5'...3')	**Reverse (5'...3')**
Acacα	GCGGCTCTGGAGGTATATGT	TCTGTTTAGCGTGGGGATGT
Adipoq	GTTCCAGGACTCAGGATGCT	CGTCTCCCTTCTCTCCCTTC
Atgl	GAAGACCCTGCCTGCTGATT	CACATAGCGCACCCCTTGAA
Bmal1	GTAGATCAGAGGGCGACGGCTA	CTTGTCTGTAAAACTTGCCTGTGAC
C/ebpα	TGTACTGTATGTCGCCAGCC	TGGTTTAGCATAGACGCGCA
Cd36	CAGTGCAGAAACAGTGGTTGTCT	TGACATTTGCAGGTCCATCTATG
Cpt1b	GCAAACTGGACCGAGAAGAG	CCTTGAAGAAGCGACCTTTG
Cry1	TGGAAGGTATGCGTGTCCTC	TCCAGGAGAACCTCCTCACG
Fabp4	GAAAGAAGTGGGAGTTGGCT	TACTCTCTGACCGGATGACG
Fasn	TAAGCGGTCTGGAAAGCTGA	CACCAGTGTTTGTTCCTCGG
G6pd	ACCAGGCATTCAAAACGCAT	CAGTCTCAGGGAAGTGTGGT
Glut4	TGGTCTCGGTGCTCTTAGTAGA	ATAACTCATGGATGGAACCCGC
Gpat	GAATACAGCCTTGGCCGATG	GAGGCGTGCATGAATAGCAA
Hsl	AGTTCCCTCTTTACGGGTGG	GCTTGGGGTCAGAGGTTAGT
IL6	GCTTCCCTCAGGATGCTTGT	ATTAACTGGGGTGCCTGCTC
Irs2	TATACCGAGATGGCCTTTGG	CCATGAGACTTAGCCGCTTC
Lep	ATTTCACACACGCAGTCGGTAT	CCCGGGAATGAAGTCCAAA
Lpl	GGCCCAGCAACATTATCCAG	ACTCAAAGTTAGGCCCAGCT
Mgl	ATCATCCCCGAGTCAGGACA	TGACTCCCCTAGACCACGAG
Obrb	CCA GTA CCC AGA GCC AAA GT	GGA TCG GGC TTC ACA ACA AGC
Per2	CGGACCTGGCTTCAGTTCAT	AGGATCCAAGAACGGCACAG
Pparγ	AGGGCGATCTTGACAGGAAA	CGAAACTGGCACCCTTGAAA
Ppia	CTTCGAGCTGTTTGCAGACAA	AAGTCACCACCCTGGCACATG
Prdm16	GTTCTGCGTGGATGCCAATC	TGGCGAGGTTTTGGTCATCA
Rev-erb-α	CTGCTCGGTGCCTAGAATCC	GTCTTCACCAGCTGGAAAGCG
Tnfα	GCTGCACTTTGGAGTGATCG	GTGTGCCAGACACCCTATCT
Ucp1	GGTACCCACATCAGGCAACA	TCTGCTAGGCAGGCAGAAAC

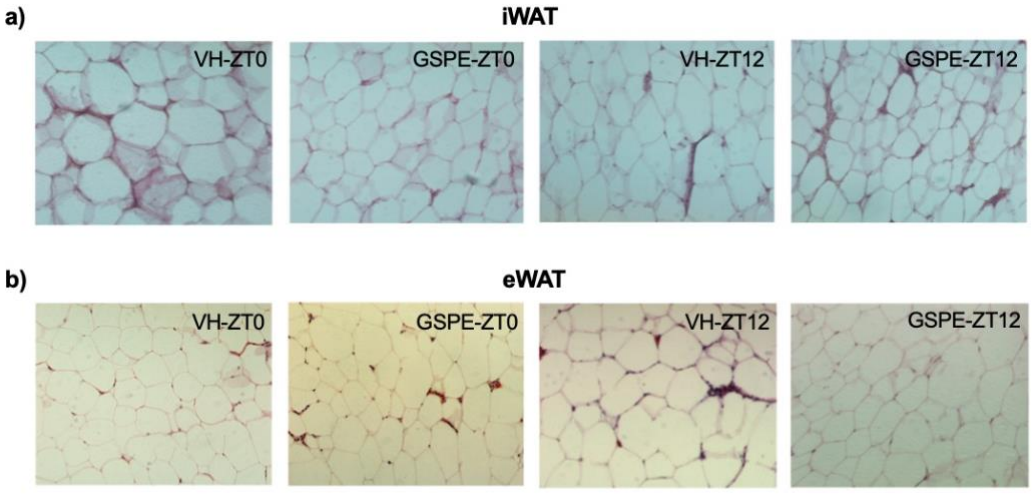

Figure S1. *Hematoxylin and eosin (H&E) staining of inguinal (a) and epididymal (b) white adipose tissue. H&E magnification, x10. VH-ZT0, vehicle group treated at ZT0; GSPE-ZT0, GSPE group treated at ZT0; VH-ZT12, vehicle group treated at ZT12; GSPE-ZT12, GSPE group treated at ZT12.*

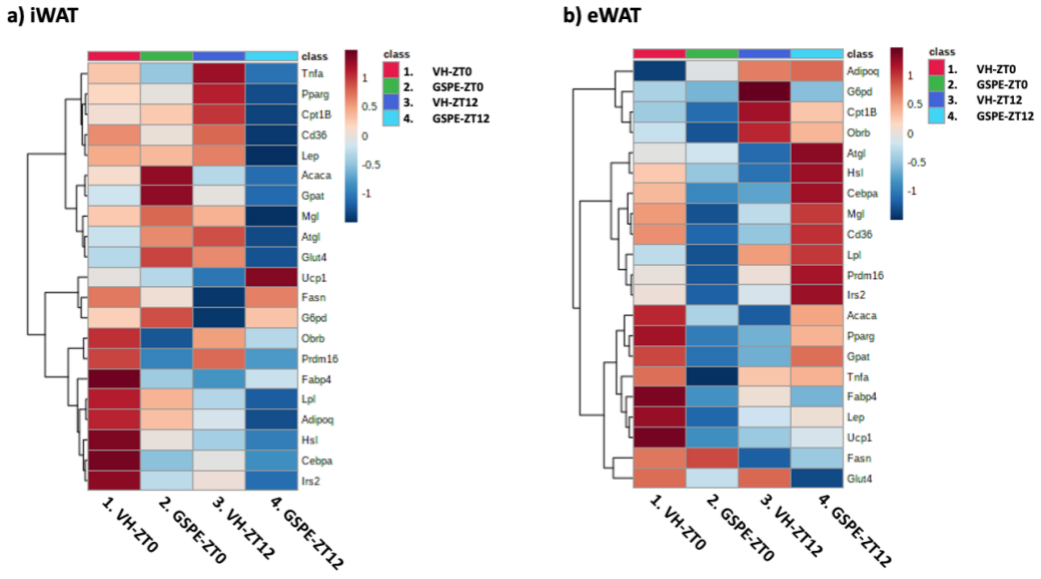

Figure S2. *Heatmap illustrating the differential gene expression upon grape seed proanthocyanidin extract (GSPE) consumption at different zeitgeber time points; when the lights turn on (ZT0) and when the lights turn off (ZT12) in inguinal white adipose tissue (iWAT) (a) and epididymal (eWAT) (b) of CAF diet-induced obese rats. Wistar rats were fed with cafeteria diet for 9 weeks and treated with GSPE (25 mg/kg body weight) or vehicle (VH) the last 4 weeks of the study at ZT0 or ZT12. VH-ZT0, vehicle group treated at ZT0; GSPE-ZT0, GSPE group treated at ZT0; VH-ZT12, vehicle group treated at ZT12; GSPE-ZT12, GSPE group treated at ZT12.*

Pparγ, peroxisome proliferator-activated receptor γ; C/ebp α, CCAAT/enhancer-binding protein alpha; Acaca, acetyl-CoA carboxylase alpha; Fasn, fatty acid synthase; Gpat, glycerol-3-phosphate acyltransferase; Atgl, adipose triglyceride lipase; Hsl, hormone-sensitive lipase; Mgl, monoacylglycerol lipase; Cpt1b, carnitine palmitoyltransferase 1B; Lpl, lipoprotein lipase; Cd36, cluster of differentiation 36; Fabp4, fatty Acid Binding Protein 4; Lep, leptin; Obrb, leptin receptor; Adipoq, adiponectin; Ucp1, uncoupling protein 1; Prdm16, PR domain containing 16; Tnfα, tumor necrosis factor alpha; Il6, interleukin 6; G6pd, glucose-6 phosphate dehydrogenase; Glut4, glucose transporter 4; Irs2, insulin receptor substrate 2.

Table S2. F, degrees of freedom (DF) and P value of two-way ANOVA corresponding to Figure 2.

Gene	**Source of variation**	**F (DFn, DFd)**	**P value**
Pparγ	ZTxT	F (1, 23) = 7.940	P=0.0098
Mgl	T	F (1, 22) = 5.155	P=0.0333
Mgl	ZTxT	F (1, 22) = 9.862	P=0.0048
Cpt1b	T	F (1, 22) = 6.315	P=0.0198
Cpt1b	ZTxT	F (1, 22) = 8.077	P=0.0095
Cd36	T	F (1, 21) = 7.010	P=0.0151
Cd36	ZTxT	F (1, 21) = 7.413	P=0.0128
Fabp4	T	F (1, 21) = 6.853	P=0.0161
Lep	T	F (1, 22) = 4.695	P=0.0414
Adipoq	ZTxT	F (1, 21) = 5.856	P=0.0247
Prdm16	T	F (1, 23) = 5.346	P=0.0301
Glut4	ZTxT	F (1, 22) = 11.25	P=0.0029
Irs2	T	F (1, 23) = 6.338	P=0.0192

Statistical data of iWAT gene expression comparing four groups (ZT0-VH, ZT0-GSPE, ZT12-VH, ZT12-GSPE) showing "F", degrees of freedom (DF) and p value ($p < 0.05$) using two-way ANOVA (ZT, time treatment effect; T, treatment effect; ZTxT, interaction between time treatment and treatment).

Table S3. F, degrees of freedom (DF) and p value of two-way ANOVA correspondin to Figure 3.

Gene	Source of variation	F (DFn, DFd)	P value
Pparγ	ZTxT	F (1, 24) = 7.968	P=0.0094
Cebpα	ZTxT	F (1, 24) = 17.05	P=0.0004
Fasn	ZT	F (1, 24) = 7.453	P=0.0117
Gpat	ZTxT	F (1, 23) = 20.75	P=0.0001
Hsl	ZTxT	F (1, 24) = 7.268	P=0.0126
Mgl	ZTxT	F (1, 23) = 5.057	P=0.0344
Cpt1b	ZT	F (1, 23) = 5.882	P=0.0236
Cpt1b	T	F (1, 23) = 5.325	P=0.0304
Obrb	ZT	F (1, 24) = 6.805	P=0.0154
Adipoq	ZT	F (1, 21) = 16.87	P=0.0005
Ucp1	ZTxT	F (1, 24) = 6.272	P=0.0195
Prdm16	ZT	F (1, 24) = 5.905	P=0.0229
Prdm16	ZTxT	F (1, 24) = 5.591	P=0.0265
Tnfα	ZTxT	F (1, 23) = 6.135	P=0.0210
Il6	ZT	F (1, 23) = 10.89	P=0.0031
Il6	ZTxT	F (1, 23) = 5.699	P=0.0256

Statistical data of eWAT gene expression comparing four groups (ZT0-VH, ZT0-GSPE, ZT12-VH, ZT12-GSPE) showing "F", degrees of freedom (DF) and p value ($p < 0.05$) using two-way ANOVA (ZT, time treatment effect; T, treatment effect; ZTxT, interaction between time treatment and treatment).

Table S4. F, degrees of freedom (DF) and P value of two-way ANOVA corresponding to Figure 4.

Tissue	*Gene*	Source of variation	F (DFn, DFd)	P value
IWAT	*Bmal1*	ZTxT	F (1, 22) = 4.834	P=0.0387
	Cry1	ZT	F (1, 20) = 4.528	P=0.0460
	Cry1	T	F (1, 20) = 5.702	P=0.0269
	Cry1	ZTxT	F (1, 20) = 5.234	P=0.0332
	Rev-erb-α	ZT	F (1, 22) = 4.535	P=0.0446
	Rev-erb-α	ZTxT	F (1, 22) = 7.237	P=0.0134
EWAT	*Bmal1*	ZTxT	F (1, 24) = 7.669	P=0.0107
	Cry1	ZT	F (1, 21) = 5.347	P=0.0310
	Per2	ZTxT	F (1, 24) = 4.335	P=0.0482

Statistical data of iWAT and eWAT gene expression comparing four groups (ZT0-VH, ZT0-GSPE, ZT12-VH, ZT12-GSPE) showing "F", degrees of freedom (DF) and p value ($p < 0.05$) using two-way ANOVA (ZT, time treatment effect; T, treatment effect; ZTxT, interaction between time treatment and treatment).

Manuscript 2

Proanthocyanidins Restore the Metabolic Diurnal Rhythm of Subcutaneous White Adipose Tissue According to Time-Of-Day Consumption

Marina Colom-Pellicer[1], Romina M Rodríguez[1], Jorge R. Soliz-Rueda[1], Leonardo Vinícius Monteiro de Assis[2], Èlia Navarro-Masip[1], Sergio Quesada-Vázquez[3], Xavier Escoté[1], Henrik Oster[2], Miquel Mulero[1] and Gerard Aragonès[1,*]

[1] Nutrigenomics Research Group, Department of Biochemistry and Biotechnology, Universitat Rovira i Virgili, 43007 Tarragona, Spain.
[2] Center of Brain, Behavior and Metabolism, Institute of Neurobiology, University of Lübeck, Marie Curie Street, 23562 Lübeck, Germany.
[3] Unitat de Nutrició i Salut, Centre Tecnològic de Catalunya, Eurecat, 43204 Reus, Spain.
* Correspondence: gerard.aragones@urv.cat; Tel.: +34-977-558-188

Published in *Nutrients*
Received: 26 April 2022. Accepted: 25 May 2022. Published: 27 May 2022

Abstract: Consumption of grape seed proanthocyanidin extract (GSPE) has beneficial effects on the functionality of white adipose tissue (WAT). However, although WAT metabolism shows a clear diurnal rhythm, whether GSPE consumption could affect WAT rhythmicity in a time-dependent manner has not been studied. Ninety-six male Fischer rats were fed standard (STD, two groups) or cafeteria (CAF, four groups) diet for 9 weeks (n = 16 each group). From week 6 on, CAF diet animals were supplemented with vehicle or 25 mg GSPE/kg of body weight either at the beginning of the light/rest phase (ZT0) or at the beginning of the dark/active phase (ZT12). The two STD groups were also supplemented with vehicle at ZT0 or ZT12. In week 9, animals were sacrificed at 6 h intervals (n = 4) to analyze the diurnal rhythms of subcutaneous WAT metabolites by nuclear magnetic resonance spectrometry. A total of 45 metabolites were detected, 19 of which presented diurnal rhythms in the STD groups. Although most metabolites became arrhythmic under CAF diet, GSPE consumption at ZT12, but not at ZT0, restored the rhythmicity of 12 metabolites including compounds involved in alanine, aspartate, and glutamate metabolism. These results demonstrate that timed GSPE supplementation may restore, at least partially, the functional dynamics of WAT when it is consumed at the beginning of the active phase. This study opens an innovative strategy for time-dependent polyphenol treatment in obesity and metabolic diseases.

Keywords: acrophase; circacompare; chronobiology; chrononutrition; flavonoids; metabolomics; zeitgeber

1. Introduction

Most species have developed circadian clocks in order to anticipate recurring and, thus, predictable environmental changes associated with the 24 h day/night cycle. In mammals, the main synchronizer for these clocks is light, although food intake, sleep/wake, and body temperature cycles also help to maintain an organism's proper timekeeping. Circadian clocks regulate the expression of many metabolic genes across the day and clock disruption increases the risk of metabolic disorders [1–3]. The central regulator of circadian clocks in mammals is located in the suprachiasmatic nucleus (SCN) of the hypothalamus, which orchestrates subordinate clocks in peripheral tissues including white adipose tissue (WAT) [4]. SCN-controlled cues such as hormones and food intake together regulate important functions of WAT including adipocyte differentiation, lipid metabolism, and adipokine expression. Adipokines, in turn, can modulate circadian appetite and energy metabolism rhythms in the brain. Such circadian adipocyte–brain crosstalk plays a crucial role in energy homeostasis [4].

Hypercaloric diets disrupt circadian rhythms in a tissue-specific manner [5]. In addition to food composition, the timing of food intake has a strong impact on circadian WAT homeostasis. When nocturnal rodents have access to food only during the light phase, they gain more weight compared with dark phase-fed animals [6,7]. In fact, light phase-fed animals present phase shifts in lipogenic gene expression rhythms, loss of rhythmicity in lipolytic gene expression in WAT, as well as alterations in leptin and insulin circadian profiles and body temperature rhythms compared with animals with access to food only during the dark phase [6,8,9]. In contrast, dark phase-fed animals exhibit lower circulating leptin and WAT pro-inflammatory cytokine levels than animals eating during the light phase [10].

Moreover, metabolite rhythms in blood are boosted by time-restricted feeding, even when endogenous clocks are disrupted such as in liver-specific *Bmal1* knock-out mice [11]. Interestingly, these rhythmic metabolites are mostly amino acids with the highest expression levels right after feeding, suggesting that the timing of food intake determines amino acid daily rhythms [11]. In this sense, amino acid metabolism could play a crucial role in the pathophysiology of metabolic abnormalities associated with obesity. Observational studies show associations between diurnal variations in amino acid plasma concentrations (including branched-chain amino acids (BCAA), aromatic amino acids, alanine, and glutamine) and insulin resistance and diabetes [12,13]. In fact, under insulin resistance and non-alcoholic fatty liver disease, BCAA oxidation enzymes are downregulated in WAT, but not in skeletal muscle, demonstrating the impact of WAT metabolism on BCAA circulating levels [14–16].

Proanthocyanidins are a class of polyphenolic compounds that are attracting considerable interest in the nutraceutical field due to their potential health benefits. They are ubiquitous and present as the second most abundant natural phenolic after lignin. Structurally, proanthocyanidins are phenolic compounds that belong to the class of flavonoids and are oligomers of monomeric (epi)catechin units that can be differentiated into A-type or B-type depending on their interflavanic linkages [17,18]. Specifically, previous studies demonstrated that grape seed proanthocyanidins, which are B-type, have beneficial effects on both WAT physiology and WAT clock regulation [19,20]. This prompted us to ask whether consumption of a grape seed extract enriched in proanthocyanidins (GSPE) could affect WAT rhythmicity in a time-dependent manner. To test this, we evaluated the effect of GSPE consumption on rhythmic metabolites of subcutaneous WAT by administration either at the beginning of the light/rest

phase or at the beginning of the dark/active phase in rats with diet-induced obesity.

2. Materials and Methods

2.1. Proanthocyanidin Extract

The grape seed proanthocyanidin extract (GSPE) used in this study was composed of monomers (21.3%), dimers (17.4%), trimers (16.3%), tetramers (13.3%), and oligomers (5–13 units; 31.7%) of proanthocyanidins according to the manufacturer (Les Dérivés Résiniques et Terpéniques, Dax, France). The phenolic composition of this extract was further analyzed by Margalef et al. [21].

2.2. Study Design and Dosage Information

Ninety-six 12-week old male Fischer 344 rats were purchased from Charles River Laboratories (Barcelona, Spain). Animals were housed in pairs under a 12 h:12 h light:dark cycle, at 22 °C, 55% of humidity and fed ad libitum with a standard chow diet (STD) (Panlab A04, Barcelona, Spain) and tap water for one week of adaptation. Then, animals were randomly divided into two groups according to their diet. Thirty-two rats were fed with STD and 64 rats with cafeteria diet (CAF) for 9 weeks. The composition of STD was 76% carbohydrates, 20% protein, and 4% fat. CAF consisted of biscuits with cheese and paté, bacon, ensaïmada (sweetened pastry), carrots, and milk with sucrose 20% (*w*/*v*), and its composition was 51% carbohydrates, 35% fat, and 14% proteins. The treatment period started in week 5 and continued for 4 weeks. STD-fed rats received 450 μL of vehicle at the beginning of the light phase (*zeitgeber* time 0; ZT0; $n = 16$) or at the beginning of the dark phase (ZT12; $n = 16$). CAF animals were divided into four groups ($n = 16$ each) receiving either vehicle or 25 mg of GSPE/kg of body weight at either ZT0 or ZT12. GSPE was dissolved in 450 μL of commercial sweetened skim condensed milk (Nestle; 100 g: 8.9 g protein, 0.4 g fat, 60.5 g carbohydrates,

1175 kJ). Vehicle groups were supplemented with the same volume of sweetened skim condensed milk. Two or three days before administration, rats were trained to voluntarily lick the milk to avoid oral gavaging. Treatment was orally administered daily using a syringe.

Body weight and food intake were recorded weekly during the whole experiment. At the end of the experiment, each group of 16 animals was randomly divided into 4 sub-groups of 4 rats in order to sacrifice them at four different time points across the day at ZT1 (9 a.m.), ZT7 (3 p.m.), ZT13 (9 p.m.) and ZT19 (3 a.m.). Prior to the sacrifice, animals were fasted for 3 h and sacrificed by decapitation. Trunk blood was collected and centrifuged (2000 × *g*, 15 min, 4 °C) to obtain serum. In addition, adipose tissue depots were excised and weighed; inguinal WAT fat pads (iWAT) were snap-frozen in liquid nitrogen. Serum and adipose samples were stored at −80 °C until further use.

Animal experiments were approved by the Animal Ethics Committee of Universitat Rovira i Virgili (reference number 9495) and carried out in accordance with Directive 86/609/CEE of the Council of the European Union and the procedures established by the Departament d'Agricultura, Ramaderia i Pesca of Generalitat de Catalunya (Spain).

2.3. Biometric Parameters and Circulating Biomarkers

Body weight gain was calculated by comparing body weight at the beginning of the treatment period and at the end of the experiment. Body fat content was determined by summarizing the weight of all fat pads. Relative weights of iWAT were calculated dividing fat pad weight by total body weight. Food intake was determined weekly by calculating the weight difference between food prior to placement in the cage and food leftovers after 24 h. Energy intake was calculated according to the caloric content of each diet provided by the manufacturer. Accumulated food intake represents all the calories eaten during

the treatment period. Enzymatic colorimetric assays were used for the determination of serum glucose, triglycerides, total cholesterol (QCA, Barcelona, Spain), and non-esterified fatty acids (Wako, Neuss, Germany).

2.4. Adipose Tissue Histology

This study focused on inguinal subcutaneous WAT (iWAT). Rats sacrificed at ZT1 and ZT7 (n = 4 each) in the six different groups were used for the histological analysis. Small pieces of frozen iWAT were thawed and fixed in 4% formaldehyde. Paraffin embedding and sectioning, hematoxylin-eosin staining, and calculations for the area, volume, and number of adipocytes were performed following Gibert-Ramos et al. [22]. The distribution of adipocyte sizes across the tissue was calculated by distributing all counted cells of each sample into two groups according to their area (<3000 μm^2 or >3000 μm^2); then, the number of total counted adipocytes was used to calculate the percentage of adipocytes in both categories.

2.5. Adipose Tissue Preparation for 1H NMR-Based Metabolomics Assay

Metabolites from iWAT were analyzed by untargeted nuclear magnetic resonance spectrometry (NMR). Hydrophilic and lipophilic metabolites were extracted from the fat pad following the procedure described by Castro et al. [23]. Two hundred mg of adipose tissue was homogenized with 800 μL of methanol, 1600 μL of chloroform, and 800 μL of Milli-Q water using vortex. Homogenates were centrifuged at 4000 × g for 10 min at 4 °C in 15 mL Falcon tubes. Supernatants (hydrophilic metabolites) were separated from pellets (lipophilic metabolites). Pellets were washed following the previous procedure. Lipophilic metabolites were separated and dried using a nitrogen stream. Hydrophilic metabolites were frozen overnight at −80 °C and lyophilized. Both hydrophilic and lipophilic phases were stored at −80 °C.

2.6. NMR Analysis

NMR measurements of hydrophilic and lipophilic extracts were performed following the protocol of Palacios-Jordan [24]. For metabolite identification, the acquired ^{1}H NMR spectra were compared to references of pure compounds from the metabolic profiling AMIX spectra database (Bruker), HMDB, Chenomx NMR suite 8.4 software (Chenomx Inc., Edmonton, AN, Canada). Metabolites were assigned by ^{1}H–^{1}H homonuclear correlation (COSY and TOCSY), ^{1}H–^{13}C heteronuclear (HSQC) 2D NMR experiments, and by correlation with pure compounds run in-house. After pre-processing, specific ^{1}H NMR regions identified in the spectra were integrated using the AMIX 3.9 software package. A data matrix was generated with absolute concentrations derived from, both, lipophilic and hydrophilic extracts. Data were scaled to the same units for all the identified metabolites.

2.7. Statistical Analysis

Statistical tests were performed using XL-Stat 2017 software (Addinsoft, Paris, France), and graphics were prepared using GraphPad Prism 9 (GraphPad Software, San Diego, CA, USA). A p-value < 0.05 was considered statistically significant. Data were analyzed using one-way analysis of variance (ANOVA) or Kruskal–Wallis test, depending on whether data were parametric or non-parametric (tested by Shapiro–Wilk test), followed by Bonferroni post-hoc test when comparing individual time points between the different treatment groups. Student's t-test or Mann–Whitney tests were used for pairwise comparisons. For correlation analysis, Spearman correlation was performed using the Harrell Miscellaneous package (version 4.6) and significant correlations were classified when p-value < 0.05. Corrplot package (version 0.9) was used for visualization of the correlations for each group. Diurnal (i.e., 24 h) rhythmicity was evaluated using a sample number of 4 animals per timepoint on absolute values. Diurnal

parameters such as rhythmicity, mesor, amplitude, and acrophase were calculated using CircaCompare algorithm [25]. Rhythmic parameters were compared in a pairwise fashion using CircaCompare. Presence of metabolite rhythmicity was considered when a p-value < 0.05 was found. Comparison of amplitudes and mesors was performed by fitting cosine curve regardless of the rhythmicity (p-value = 1). This method allows for an estimation of mesor and amplitude between rhythmic and non-rhythmic metabolites. Phase estimation was performed only when both metabolites were considered rhythmic (CircaCompare p-value < 0.05). Graphs showing diurnal rhythm and acrophase were created using the Python package based on Cosinor and MetaboAnalyst 5.0 (v11.0, Wishart Research Group, University of Alberta, Edmonton, Canada) was used to analyze metabolic pathway involvement (https://www.metaboanalyst.ca accessed on January 18th, 2022) [26].

3. Results

3.1. GSPE Administration at ZT12 Reduces Body Weight Gain and Accumulated Food Intake

Our experiment confirmed that cafeteria diet is a robust model of diet-induced obesity in rats. After 9 weeks of obesogenic diet, final body weight and body weight gain of CAF animals were significantly higher compared with STD animals (Table 1). STD-VH (STD supplemented with vehicle) and CAF-GSPE animals supplemented at night (ZT12) presented lower final body weight, and lower body weight gain in CAF-GSPE, compared with the respective groups supplemented in the morning (ZT0). Interestingly, when GSPE was administrated at night, body weight gain was as low as in the STD-VH group and different from CAF-VH animals. Moreover, body fat content was significantly higher in CAF rats compared with STD-fed rats in both ZT0 and ZT12 animals. However, iWAT relative weight in CAF-VH supplemented at night was not statistically different

compared to STD or CAF-GSPE. As expected, food intake was higher in CAF groups irrespective of the time of supplementation. CAF-GSPE supplemented at night presented lower accumulated food intake compared with CAF-GSPE supplemented in the morning. Interestingly, CAF-GSPE rats presented lower final food intake compared with CAF-VH only at ZT12 supplementation.

Table 1. Biometric parameters of rats fed standard or cafeteria diet supplemented with vehicle or GSPE at ZT0 or ZT12 during the last 4 weeks of the experiment.

	ZT0 SDT-VH	ZT0 CAF-VH	ZT0 CAF-GSPE	ZT12 STD-VH	ZT12 CAF-VH	ZT12 CAF-GSPE
Body weight (g)	514.7 ± 7.5 ^{a}	591.1 ± 7.8 ^{b}	573.1 ± 9.2 ^{b}	481.8 ± 7.1 ^{a*}	569.3 ± 8.4 ^{b}	546.8 ± 7.8 ^{b*}
Body weight gain (g)	47.3 ± 3.4 ^{a}	74.4 ± 3.9 ^{b}	65.3 ± 4.3 ^{b}	40.9 ± 3.1 ^{a}	72.7 ± 3.3 ^{b}	50.4 ± 3.1 ^{a*}
Body fat content (%)	8.1 ± 0.3 ^{a}	13.7 ± 0.4 ^{b}	12.9 ± 0.6 ^{b}	9.3 ± 0.6 ^{a}	14.4 ± 0.6 ^{b}	13.4 ± 0.5 ^{b}
iWAT (%)	0.9 ± 0.1 ^{a}	1.7 ± 0.1 ^{b}	1.8 ± 0.1 ^{b}	1.3 ± 0.1 ^{a*}	1.6 ± 0.2 ^{ab}	2.1 ± 0.2 ^{b}
Acc. food intake [1] (kJ)	1239.5± 36.5 ^{a}	2598.3 ± 80.5 ^{b}	2696.9 ± 36.6 ^{b}	1226.5 ± 40.1 ^{a}	2793.0 ± 132.6 ^{b}	2513.5 ± 71.1 ^{b*}
Food intake [2] (kJ/day)	338.1 ± 18.2 ^{a}	592.0 ± 12.7 ^{b}	576.1 ± 32.5 ^{b}	308.1 ± 4.9 ^{a}	791.4 ± 77.7 ^{b*}	578.1 ± 20.3 ^{c}

*Data represent mean ± SEM (n = 12–16). ^{a}, ^{b}, ^{c} represent significant differences among same-ZT groups using one-way ANOVA ($p < 0.05$) followed by Bonferroni post-hoc test. * effect of ZT treatment, comparison between two groups with the same diet and supplementation but different ZT treatment determined by Student's t-test. [1] Accumulated food intake during treatment period; [2] final food intake calculated at week 9. Abbreviations: ZT0, treatment administration at the beginning of the light phase; ZT12, treatment administration at the beginning of the dark phase; STD-VH, standard diet group supplemented with vehicle; CAF-VH, cafeteria diet group supplemented with vehicle; CAF-GSPE, cafeteria diet group supplemented with grape-seed procyanidin extract; iWAT, inguinal white adipose tissue; Acc, accumulated.*

3.2. Adipocyte Size Is Modified According to Time-of-Day GSPE Administration

Subcutaneous adipose tissue expansion is associated with metabolic health. In fact, in rodent models, surgical removal of iWAT can eventually lead to metabolic dysfunction and ectopic lipid accumulation [27, 28]. Conversely, transplantation of iWAT into the visceral cavity of mice leads to improved glucose homeostasis and a reduction in body weight and total fat mass [29]. Therefore, in this study, we also evaluated the effect of GSPE administration on the histology of iWAT. Accordingly, CAF diet consumption resulted in larger adipocytes compared with STD-VH groups (Supplementary materials, Figure S1).

Specifically, CAF animals presented higher adipocyte area and volume, and lower percentage of smaller adipocytes in both ZT0 and Z12 animals compared to STD groups. Importantly, GSPE consumption resulted in a stronger effect on adipocyte histology, lowering the area and volume of adipocytes, when it was supplemented at ZT0 compared with animals supplemented with GSPE at ZT12.

3.3. GSPE Administration at ZT12 Recovers the Diurnal Rhythmic Concentration of Serum TAG That is Lost in Diet-Induced Obesity

The CircaCompare algorithm was used to evaluate the effect of GSPE supplementation on the diurnal rhythmicity of triglyceride (TAG), glucose, cholesterol and non-esterified fatty acid (NEFA) serum concentrations. Rhythm parameters including rhythmicity, mesor, amplitude, and acrophase were calculated and compared in a pairwise fashion (Table 2). STD animals treated at ZT0 showed significant rhythmicity only in TAG, while CAF animals presented a diurnal rhythm in most of the biochemical parameters. However, in the ZT12 groups, TAG (p-value = 0.002) and cholesterol (p-value = 0.035) serum concentrations presented a significant rhythmicity in STD conditions that was completely lost in response to CAF diet. Importantly, GSPE administration recovered the diurnal rhythm of TAG concentrations (p-value = 0.019) when it was consumed at ZT12. In addition, CAF diet resulted in higher TAG and glucose mesor concentrations compared with the respective STD groups. However, no effect of GSPE was observed in these parameters. In contrast, cholesterol mesor concentrations and TAG amplitude estimations were significantly increased in response to CAF diet only in ZT0 treated animals and GSPE consumption restored cholesterol levels to STD conditions only when it was consumed at ZT0.

Table 2. Rhythm variables of main metabolic parameters in serum of rats fed standard or cafeteria diet treated with vehicle or GSPE at ZT0 or ZT12.

	Group	ZT0 Glucose	ZT0 TAG	ZT0 CHOL	ZT0 NEFA	ZT12 Glucose	ZT12 TAG	ZT12 CHOL	ZT12 NEFA
Rhythmicity (*p* value)	**STD-VH**	NS	0.001	NS	NS	NS	0.002	0.035	NS
	CAF-VH	0.017	0.001	NS	0.048	NS	NS	NS	NS
	CAF-GSPE	NS	0.007	0.002	0.001	NS	0.019	NS	NS
Mesor (mg/dL)	**STD-VH**	87.19	71.38	91.37	25.49	84.87	90.71	111.98	29.98
	CAF-VH	103.64 *	191.58 *	110.03 *	29.29	117.33 *	211.44 *	116.02	30.70
	CAF-GSPE	102.73 #	163.68 #	102.03	30.59	113.53 #	228.02 #	122.68	32.91
Amplitude estimation	**STD-VH**	4.92	34.38	7.89	5.37	3.14	52.06	22.48	2.13
	CAF-VH	10.51	104.54 *	20.42	4.15	11.05	62.78	16.51	3.59
	CAF-GSPE	9.23	81.10	32.14 #	6.89	9.96	93.45	17.16	2.10
Acrophase (ZT)	**STD-VH**	NA	6.39	NA	NA	NA	5.71	5.32	NA
	CAF-VH	10.06	8.83	NA	11.83	NA	NA	NA	NA
	CAF-GSPE	NA	7.39	5.52	12.65	NA	7.04	NA	NA

*Table shows the presence of rhythm, in a 24 h period, of each biochemical parameter with a p value ($p < 0.05$ indicates significant rhythm), circadian mean concentration (mesor), amplitude, and acrophase in ZT (time of highest concentration within the day) followed by comparisons between two groups using CircaCompare (p value < 0.05). * indicates significant difference between CAF-VH and STD-VH; # indicates significant difference between CAF-GSPE and STD-VH. NA indicates not-available acrophase values in non-rhythmic metabolites, and NS indicates not significant. Abbreviations: ZT0, treatment administration at the beginning of the light phase; ZT12, treatment administration at the beginning of the dark phase; STD-VH, standard diet group supplemented with vehicle; CAF-VH, cafeteria diet group supplemented with vehicle; CAF-GSPE, cafeteria diet group supplemented with grape-seed procyanidin extract; TAG, tryacilglicerides; CHOL, cholesterol; NEFA, non-esterified fatty acids.*

3.4. Metabolite Concentrations in iWAT Are Restored in Response to GSPE Administration in a Time-Dependent Manner

Next, ^{1}H NMR was performed to determine whether the metabolite profile of iWAT in response to GSPE was significantly influenced by the time-of-day of its consumption. After alignment and normalization of the spectra, a total of 45 metabolites were identified and integrated, 10 in the lipid phase and 35 in the

aqueous phase. Tables 3 and 4 show the 24 h mean concentrations of all metabolites detected in this tissue.

In the lipid phase (Table 3), CAF diet induced changes in the 24 h mean concentrations of omega-3, oleic acid, linoleic acid, PUFAs, and total fatty acids compared with STD-VH and, when GSPE was administered, only the levels of total fatty acids decreased partially to basal levels in both ZT0 and ZT12 groups. Interestingly, a similar pattern was observed for TAGs, but their concentrations only decreased in response to GSPE when it was administered at ZT12.

Table 3. Daily (24-h mean) concentrations (μmol/g) of individual lipophilic metabolites identified in iWAT.

	ZT0 STD-VH	ZT0 CAF-VH	ZT0 CAF-GSPE	ZT12 STD-VH	ZT12 CAF-VH	ZT12 CAF-GSPE
Omega-3	189.7 ± 8.1 [a]	137.0 ± 6.1 [b]	156.3 ± 9.3 [b]	210.0 ± 10.7 [a]	145.5 ± 5.5 [b]	161.5 ± 8.8 [b]
Oleic Acid (18:1)	1641.2 ± 106.7 [a]	2402.5 ± 109.3 [b]	2285.6 ± 125.7 [b]	1553.2 ± 128.7 [a]	2457.2 ± 105.8 [b]	2196.3 ± 119.7 [b]
Linoleic Acid (18:2)	528.8 ± 24.8 [a]	383.0 ± 19.8 [b]	361.5 ± 18.4 [b]	456.5 ± 38.6 [a]	354.0 ± 20.3 [b]	352.2 ± 23.4 [b]
PUFAs	523.2 ± 26.9 [a]	269.2 ± 12.4 [b]	276.6 ± 24.0 [b]	500.9 ± 21.8 [a]	252.1 ± 9.7 [b]	294.5 ± 16.5 [b]
Total Fatty Acid	2905.8 ± 122.9 [a]	3262.3 ± 148.9 [b]	3121.7 ± 111.8 [ab]	2587.7 ± 231.8 [a]	3279.1 ± 121.9 [b]	3108.5 ± 158.4 [ab]
Diglycerides	3.4 ± 0.5	5.0 ± 0.4	3.9 ± 0.6	3.3 ± 0.5	4.6 ± 0.4	4.0 ± 0.4
Triglycerides	1467.5 ± 62.1	1636.0 ± 65.6	1601.1 ± 59.7	1338.9 ± 93.5 [a]	1658.5 ± 62.9 [b]	1557.0 ± 66.5 [ab]
Sphingomyelin	0.3 ± 0.05	0.2 ± 0.04	0.2 ± 0.03	0.3 ± 0.06	0.2 ± 0.02	0.2 ± 0.07
Cholesterol	5.9 ± 0.4	5.5 ± 0.5	6.5 ± 0.8	5.8 ± 0.6	6.0 ± 0.4	6.0 ± 0.4
MUFAs	4265.6 ± 162.1	4271.7 ± 180.1	4167.9 ± 132.7	3941.3 ± 229.2	4263.5 ± 133.6	4077.3 ± 147.8

Data represent mean ± SEM (n = 12–16). [a], [b]; represent significant differences among same ZT groups using Kruskal–Wallis ($p < 0.05$) followed by Bonferroni post-hoc test. Metabolites are sorted starting from the lowest p value comparing the groups treated at ZT0. Abbreviations: ZT0, treatment administration at the beginning of the light phase; ZT12, treatment administration at the beginning of the dark phase; STD-VH, standard diet group supplemented with vehicle; CAF-VH, cafeteria diet group supplemented with vehicle; CAF-GSPE, cafeteria diet group supplemented with grape seed procyanidin extract.

In contrast, in the aqueous phase (Table 4), CAF diet decreased the 24-h mean concentrations of aspartate, lysine, carnitine, taurine, propionate, glycerophosphocholine, choline, inosine, histamine, and glucose compared to STD-VH in the ZT0 group but not at ZT12. In addition, in ZT0 animals, GSPE administration increased the concentrations of lysine, propionate,

glycerophosphocholine, choline, inosine, histamine, and glucose. Similarly, when GSPE was administrated at ZT12, propionate concentrations achieved values not significantly different from STD-VH.

Table 4. Daily (24 h mean) concentrations (μmol/g) of individual hydrophilic metabolites identified in iWAT.

	ZT0 STD-VH	ZT0 CAF-VH	ZT0 CAF-GSPE	ZT12 STD-VH	ZT12 CAF-VH	ZT12 CAF-GSPE
Aspartate	0.11 ± 0.017 [a]	0.04 ± 0.004 [b]	0.05 ± 0.006 [b]	0.08 ± 0.010	0.05 ± 0.006	0.05 ± 0.008
Lysine	0.11 ± 0.016 [a]	0.06 ± 0.016 [b]	0.07 ± 0.015 [ab]	0.09 ± 0.011	0.06 ± 0.008	0.06 ± 0.010
Carnitine	0.01 ± 0.001 [a]	0.005 ± 0.001 [b]	0.01 ± 0.001 [b]	0.01 ± 0.001	0.00 ± 0.000	0.01 ± 0.001
Taurine	1.05 ± 0.110 [a]	0.68 ± 0.058 [b]	0.78 ± 0.094 [b]	0.97 ± 0.080	0.70 ± 0.055	0.73 ± 0.072
Propionate	0.02 ± 0.003 [a]	0.01 ± 0.002 [b]	0.01 ± 0.002 [ab]	0.02 ± 0.002 [a]	0.01 ± 0.001 [b]	0.01 ± 0.002 [ab]
GPC	0.11 ± 0.018 [a]	0.06 ± 0.012 [b]	0.07 ± 0.013 [ab]	0.09 ± 0.012	0.08 ± 0.011	0.07 ± 0.001
Choline	0.01 ± 0.001 [a]	0.01 ± 0.001 [b]	0.01 ± 0.001 [ab]	0.01 ± 0.001	0.01 ± 0.001	0.01 ± 0.001
Inosine	0.08 ± 0.011 [a]	0.05 ± 0.006 [b]	0.06 ± 0.007 [ab]	0.07 ± 0.006	0.05 ± 0.005	0.05 ± 0.007
Histamine	0.07 ± 0.011 [a]	0.04 ± 0.011 [b]	0.04 ± 0.008 [ab]	0.06 ± 0.008	0.03 ± 0.005	0.03 ± 0.007
Glucose	0.31 ± 0.037 [a]	0.19 ± 0.017 [b]	0.26 ± 0.04 [ab]	0.27 ± 0.034	0.22 ± 0.021	0.21 ± 0.024
Glutamine	0.96 ± 0.127	0.61 ± 0.078	0.72 ± 0.116	0.85 ± 0.091	0.64 ± 0.069	0.64 ± 0.085
Lactate	1.05 ± 0.149	0.64 ± 0.089	0.74 ± 0.120	0.93 ± 0.145	0.71 ± 0.116	0.63 ± 0.100
Leucine	0.07 ± 0.011	0.04 ± 0.007	0.04 ± 0.008	0.06 ± 0.008	0.04 ± 0.005	0.04 ± 0.005
Creatine	0.15 ± 0.043	0.08 ± 0.011	0.10 ± 0.022	0.11 ± 0.022	0.07 ± 0.006	0.09 ± 0.019
Isoleucine	0.03 ± 0.005	0.02 ± 0.003	0.02 ± 0.003	0.03 ± 0.004	0.02 ± 0.002	0.02 ± 0.003
Glycogen	0.46 ± 0.156	0.17 ± 0.033	0.22 ± 0.06	0.20 ± 0.085 *	0.31 ± 0.114	0.20 ± 0.065
Glutamate	0.23 ± 0.034	0.15 ± 0.017	0.18 ± 0.022	0.21 ± 0.025	0.16 ± 0.015	0.16 ± 0.019
Succinate	0.04 ± 0.006	0.03 ± 0.003	0.03 ± 0.003	0.03 ± 0.004	0.03 ± 0.003	0.03 ± 0.005
Valine	0.05 ± 0.008	0.03 ± 0.004	0.04 ± 0.006	0.05 ± 0.006	0.04 ± 0.003	0.03 ± 0.004
Uridine	0.03 ± 0.005	0.02 ± 0.003	0.02 ± 0.004	0.03 ± 0.004	0.02 ± 0.002	0.03 ± 0.004

Alanine	0.31 ± 0.051	0.20 ± 0.029	0.23 ± 0.033	0.28 ± 0.032	0.21 ± 0.023	0.21 ± 0.027
Myo-inositol	0.59 ± 0.141	0.32 ± 0.078	0.37 ± 0.086	0.52 ± 0.083	0.37 ± 0.074	0.34 ± 0.077
Asparagine	0.03 ± 0.005	0.01 ± 0.002	0.02 ± 0.004	0.03 ± 0.005	0.02 ± 0.002	0.02 ± 0.003
ChoP	0.07 ± 0.013	0.05 ± 0.007	0.06 ± 0.008	0.07 ± 0.011	0.05 ± 0.006	0.06 ± 0.011
Glycerol	0.09 ± 0.008	0.09 ± 0.006	0.10 ± 0.009	0.10 ± 0.010	0.08 ± 0.005	0.09 ± 0.007
Phenylalanine	0.03 ± 0.006	0.02 ± 0.003	0.02 ± 0.005	0.03 ± 0.006	0.02 ± 0.002	0.02 ± 0.003
Tyrosine	0.03 ± 0.007	0.02 ± 0.004	0.02 ± 0.004	0.03 ± 0.004	0.02 ± 0.002	0.02 ± 0.003
Niacinamide	0.02 ± 0.004	0.01 ± 0.002	0.01 ± 0.003	0.02 ± 0.002	0.01 ± 0.002	0.02 ± 0.002
AMP	0.03 ± 0.005	0.03 ± 0.008	0.03 ± 0.004	0.02 ± 0.003 *	0.02 ± 0.004	0.02 ± 0.004
Uracil	0.01 ± 0.002	0.01 ± 0.002	0.01 ± 0.003	0.01 ± 0.002	0.01 ± 0.001	0.01 ± 0.002
Fumarate	0.003 ± 0.001	0.003 ± 0.001	0.002 ± 0.000	0.004 ± 0.001	0.002 ± 0.000	0.003 ± 0.001
3-OHB	0.02 ± 0.003	0.03 ± 0.003	0.03 ± 0.006	0.03 ± 0.007	0.02 ± 0.004	0.03 ± 0.005
Acetate	0.05 ± 0.006	0.05 ± 0.004	0.05 ± 0.008	0.06 ± 0.006	0.04 ± 0.003	0.05 ± 0.004
Sarcosine	0.02 ± 0.002	0.02 ± 0.002	0.02 ± 0.002	0.02 ± 0.003	0.01 ± 0.002	0.02 ± 0.005
Formate	0.01 ± 0.001	0.01 ± 0.001	0.01 ± 0.002	0.01 ± 0.001	0.01 ± 0.001	0.01 ± 0.001

*Data represent mean ± SEM (n = 12–16). [a, b]; represent significant differences among same ZT groups using Kruskal–Wallis ($p < 0.05$) followed by Bonferroni post-hoc test, * indicates differences between ZTS STD-VH vs ZT12 STD-VH using Mann–Whitney ($p < 0.05$). Metabolites are sorted starting from the lowest p value comparing the groups treated at ZT0. Abbreviations: ZT0, treatment administration at the beginning of the light phase; ZT12, treatment administration at the beginning of the dark phase; STD-VH, standard diet group supplemented with vehicle; CAF-VH, cafeteria diet group supplemented with vehicle; CAF-GSPE, cafeteria diet group supplemented with grape seed procyanidin extract; GPC, glycerophosphocholine; ChoP, phosphorylcholine; 3-OHB, 3-hydorxybutyrate.*

To further evaluate the effect of GSPE administration on the global functionality of iWAT, we also performed a global correlation analysis between the 24 h mean concentrations of all detected metabolites and the biometric parameters collected in the last week of the experiment (Supplementary Materials, Figure S2). Collectively, CAF diet resulted in a clear reduction in the number of correlations (26.2% lower in the ZT0 and 22.1% lower in the ZT12 groups) while

GSPE supplementation restored the correlation network to similar levels as in the STD group for both ZTs.

3.5. GSPE Administration at ZT12 Re-Establishes the Number of Rhythmic Metabolites in iWAT

To specifically evaluate the diurnal rhythm of detected iWAT metabolites, each group of animals was divided into four subgroups according to time of sacrifice (ZT1, ZT7, ZT13, or ZT19). The CircaCompare algorithm was used to model the oscillation profiles of these metabolites across 24 h, and rhythm parameters including rhythmicity, mesor, amplitude, and acrophase were calculated and compared in a pairwise fashion (Supplementary Materials, Tables S1 and S2).

As summarized in Figure 1a, STD animals at ZT0 presented four metabolites (glutamate, asparagine, uracil, and valine) with diurnal rhythmic concentrations, and only valine concentrations preserved rhythmicity in the CAF group. Moreover, leucine, isoleucine, glycogen, glycerol, tyrosine, and fumarate also presented rhythmic concentrations in this group of animals. Interestingly, the supplementation of GSPE resulted in loss of seven rhythmic metabolites found in CAF animals, and only concentrations of 3-hydroxybutyrate (3-OHB) became rhythmic in response to GSPE administration. In contrast, the STD animals treated at ZT12 presented 18 metabolites with rhythmic concentrations. However, under CAF diet, 16 metabolites lost rhythmicity and only fumarate and lactate concentrations kept stable diurnal rhythms in this group of animals. Importantly, GSPE supplementation at ZT12 restored the rhythm of 12 of 16 metabolites. In total, GSPE administration at ZT12 resulted in 27 rhythmic metabolites (Figure 1b).

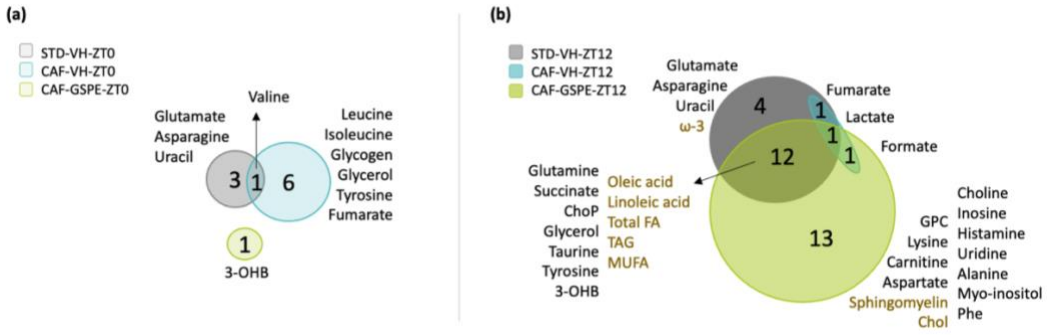

Figure 1. *Overlap diagram of rhythmic metabolite concentrations presented in ZT0 (**a**) and ZT12 groups (**b**). Rats were fed standard or cafeteria diet for 9 weeks. At week 6, rats received a daily oral dose of GSPE or vehicle for 4 weeks at ZT0 or ZT12. Rats from each group were sacrificed at four different time points: ZT1, ZT7, ZT13, and ZT19 in order to analyze the diurnal rhythm of these metabolites. Forty-five metabolites detected by NMR were analyzed using CircaCompare algorithm based on Cosinor ($p < 0.05$). Metabolites from aqueous phase are shown in black color and metabolites from lipidic phase in brown color. Abbreviations: iWAT, inguinal adipose tissue; ZT0, beginning of the light phase; ZT12, beginning of the dark phase; STD-VH-ZT0; standard diet vehicle group treated at ZT0; CAF-VH-ZT0, cafeteria diet vehicle group treated at ZT0; CAF-GSPE-ZT0, cafeteria diet treated with grape-seed procyanidin extract at ZT0; STD-VH-ZT12; standard diet vehicle group treated at ZT12; CAF-VH-ZT12, cafeteria diet vehicle group treated at ZT12; CAF-GSPE-ZT12, cafeteria diet treated with grape seed procyanidin extract at ZT12; 3-OHB, 3-Hydroxybutyrate; Chol, cholesterol; Total FA, total fatty acids; TAG, triacylglyceride; MUFA, monounsaturated fatty acids; ω-3, omega-3; GPC, glycerophosphocholine; Phe, phenylalanine; ChoP, phosphorylcholine.*

Five of these twelve rhythmic metabolites that were restored by GSPE administration at ZT12 (oleic acid, linoleic acid, total fatty acids, triglycerides, and mono-unsaturated fatty acids (MUFAs)) were detected in the lipid phase (Figure 2). MUFAs did not show any difference in the rhythmic parameters comparing CAF-GSPE and STD-VH animals. However, oleic acid, linoleic acid, total fatty acids, and triglycerides concentrations differed on mesor value, being higher in all of them except for linoleic acid, which was lower in CAF-GSPE compared with STD-VH. Moreover, GSPE supplementation also resulted in a phase delay of 5 h in oleic acid compared with the STD-VH group. In the aqueous phase, lactate presented rhythmicity in all animal groups at ZT12 and formate was rhythmic in both CAF-VH and CAF-GSPE groups and, interestingly, GSPE caused a phase advance of 9 h. Notably, glutamine, succinate, phosphorylcholine, glycerol, taurine, tyrosine, and 3-OHB restored diurnal rhythmicity only when GSPE was

administered at ZT12 (Figure 3). Among these, phase advances of 6, 5, and 3 h were detected in tyrosine, phosphorylcholine, and 3-OHB concentrations, respectively.

In summary, 19 of 45 detected metabolites in iWAT were rhythmic in the STD-VH group and 18 of these 19 metabolites were rhythmic in STD animals treated at ZT12. Only 4 metabolites of these 19 were rhythmic at ZT0. In response to CAF diet, the number of rhythmic metabolites decreased dramatically, however, GSPE recovered their rhythmicity when it was administrated at ZT12.

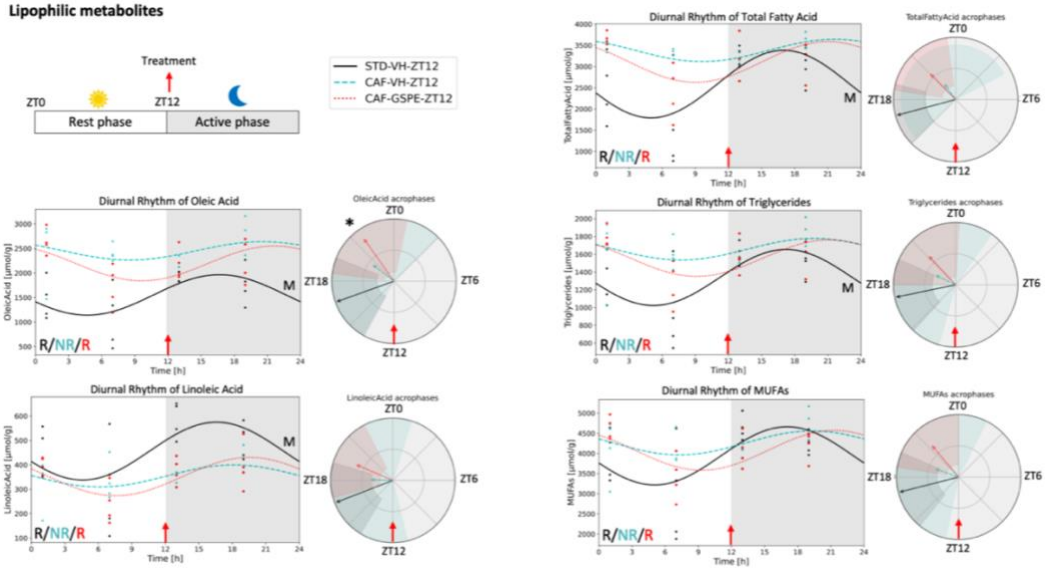

Figure 2. *Lipophilic metabolites that recovered their diurnal rhythm loss under cafeteria diet in response to GSPE administration at ZT12. Circadian parameters such as rhythmicity, mesor, amplitude, and acrophase were calculated using the CircaCompare algorithm based on Cosinor. Graphs showing diurnal rhythm and acrophase were performed using the Python package based on Cosinor. R indicates significant rhythmicity; NR indicates non-rhythmic; M indicates significant mesor difference between STD-VH-ZT12 and both cafeteria diet groups; * indicates significant acrophase difference between STD-VH-ZT vs CAF-GSPE-ZT12. None of the metabolites presented differences between groups for amplitude.*

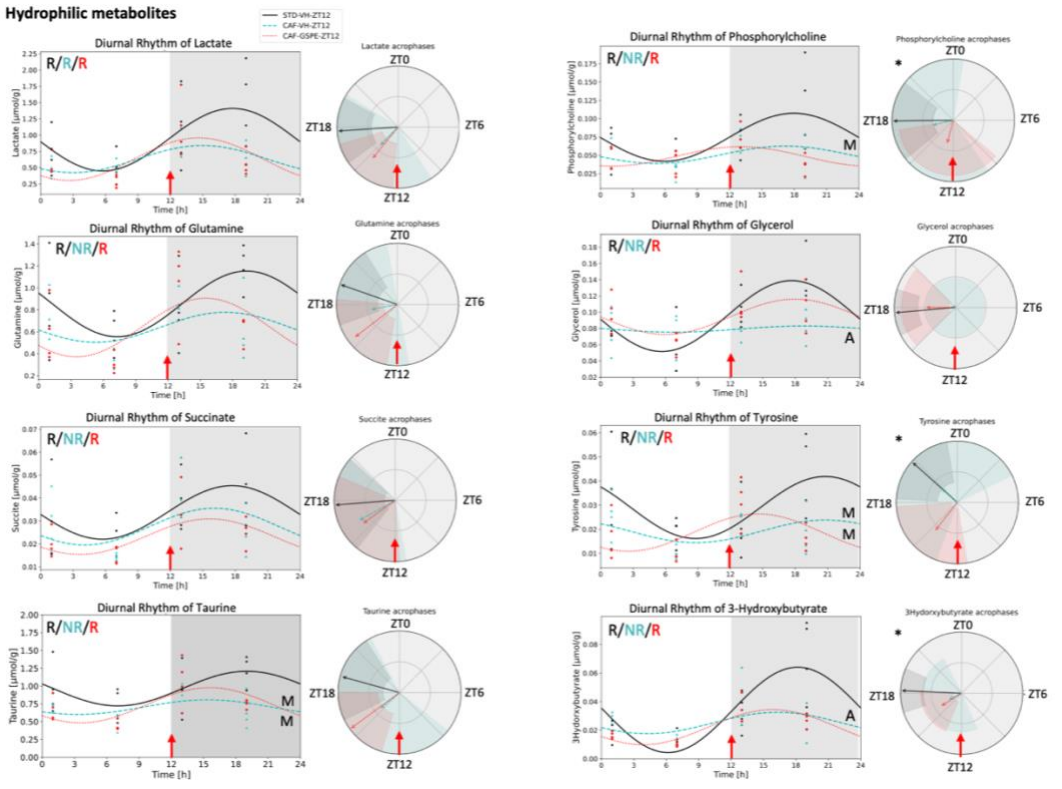

Figure 3. *Hydrophilic metabolites which recovered their diurnal rhythm lost under cafeteria diet through GSPE administration in ZT12. Circadian parameters such as rhythmicity, mesor, amplitude, and acrophase were calculated using the CircaCompare algorithm based on Cosinor. Graphs showing diurnal rhythm and acrophase were performed using the Python package based on Cosinor. R, indicates significant rhythmicity; NR, indicates non-rhythmic; M, denotes significant mesor difference against STD-VH-ZT12; A, denotes significant amplitude difference against STD-VH-ZT12; * indicates significant acrophase difference between STD-VH-ZT vs CAF-GSPE-ZT12.*

3.6. GSPE Administration at ZT12 Restores the Rhythmicity of Alanine, Aspartate and Glutamate Metabolism Pathways in iWAT

Next, to test whether the identified rhythmic metabolites at ZT12 were biologically meaningful, we performed a pathway analysis using MetaboAnalyst 5.0 software of the 12 hydrophilic rhythmic metabolites detected in STD group as well as the 20 rhythmic hydrophilic metabolites detected in response to GSPE administration at ZT12.

As shown in Table 5, rhythmic metabolites in the STD group were significantly enriched for alanine, aspartate and glutamate metabolism (*p*-value = 1.10 E-06), arginine biosynthesis (*p*-value = 1.30 E-04), and D-glutamine and D-glutamate metabolism (*p*-value = 8.50 E-04). Notably, in animals supplemented with GSPE at ZT12, rhythmic metabolites were enriched for alanine, aspartate, and glutamate metabolism (*p*-value = 3.80 E-04) suggesting that GSPE administration at ZT12 restored the rhythmicity of this metabolic pathway in iWAT that was lost in response to CAF diet. In fact, succinate and glutamine, the most important metabolites involved in the alanine, aspartate, and glutamate metabolism pathway, were rhythmic in both STD-VH-ZT12 and CAF-GSPE-ZT12 groups (Figure 4 a,b). In addition, rhythmic hydrophilic metabolites of animals supplemented with GSPE at ZT12 also presented an enrichment for the phenylalanine, tyrosine, and tryptophan biosynthetic pathway (*p*-value = 9.90E-04), suggesting that the 13 rhythmic hydrophilic metabolites exclusively detected in animals supplemented with GSPE, and not in the STD group, could be associated with this biosynthetic pathway.

Table 5. Rhythmic metabolic pathways detected at ZT12 in iWAT.

Group	Metabolic Pathway with Diurnal Rhythm	Total	Hits	*p* value	FDR	Impact
STD-VH	Alanine, aspartate, and glutamate metabolism	28	5	1.10 E-06	9.20 E-05	3.10 E-01
	Arginine biosynthesis	14	3	1.30 E-04	4.60 E-03	1.20 E-01
	D-Glutamine and D-glutamate metabolism	6	2	8.50 E-04	1.20 E-02	5.00 E-01
CAF-GSPE	Alanine, aspartate, and glutamate metabolism	28	4	3.80 E-04	1.60 E-02	3.40 E-01
	Phenylalanine, tyrosine, and tryptophan biosynthesis	4	2	9.90 E-04	2.80 E-02	1.00 E+00

Abbreviations: STD-VH-ZT12, standard diet supplemented with vehicle at the beginning of the dark phase; CAFGSPE-ZT12, cafeteria diet supplemented with grape seed procyanidin extract at the beginning of the dark phase. Hydrophilic metabolites with significant rhythmicity were analyzed for pathway enrichment using MetaboAnalyst. p-value < 0.05, FDR < 0.05 and impact > 0.1 was considered significant.

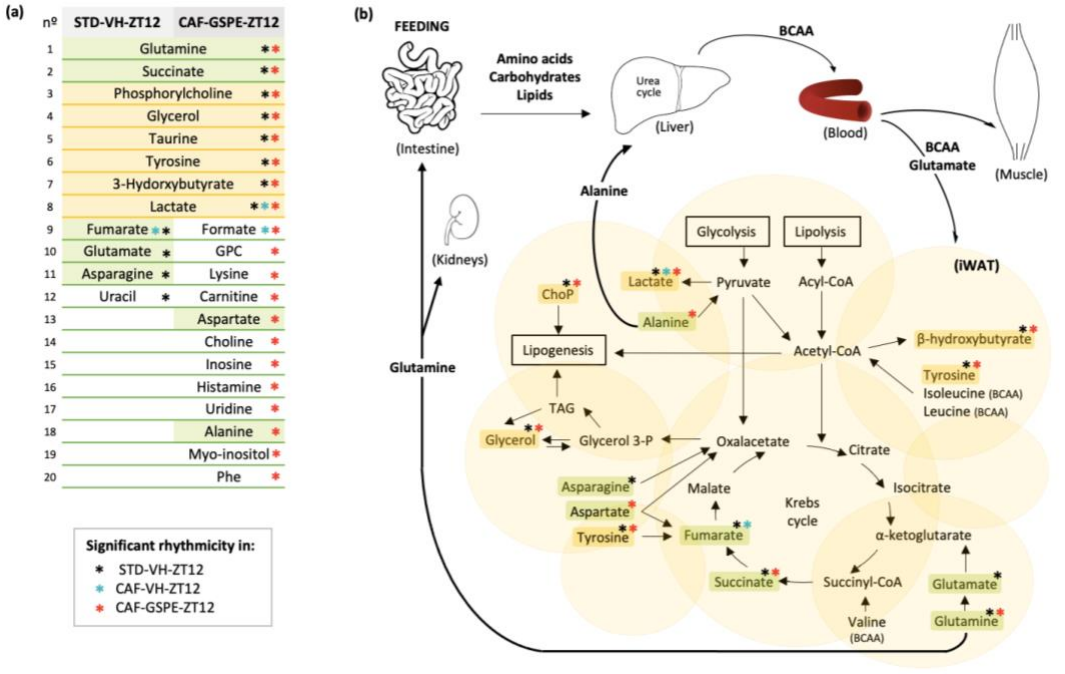

Figure 4. *Metabolic network analysis of identified rhythmic metabolites in iWAT. Hydrophilic metabolites with diurnal rhythm in the corresponding groups, (**a**) inter-tissue amino acid flux and alanine, aspartate, and glutamate metabolism pathway (**b**). Green boxes indicate metabolites involved in alanine, aspartate, and glutamate metabolism that are rhythmic in STD-VH-ZT12, CAF-GSPE-ZT12, or both groups; yellow boxes indicate metabolites that are rhythmic in both STD-VH-ZT12 and CAF-GSPE-ZT12 that are not involved in alanine, aspartate, and glutamate metabolism. Abbreviations: ChoP, phosphorylcholine; GPC, glycerophosphocholine; Phe, phenylalanine; TAG, triacylglyceride; Glycerol 3-P, glycerol 3-phosphate.*

4. Discussion

The health effects of proanthocyanidins are usually determined without considering biological rhythms. However, it seems evident that they should be considered in chrononutrition studies as proanthocyanidins can significantly modulate the circadian system. In fact, previous studies demonstrated that GSPE alters the expression profile of clock genes in the rat hypothalamus and modulates the serum melatonin concentrations when it was administered at the beginning of the light phase [30]. In addition, GSPE critically modulates hepatic BMAL1 acetylation, *Nampt* expression, and nicotinamide adenine dinucleotide (NAD)

availability in mice as well as the expression of *Clock* and *Per2* genes in white adipose tissue [20,31]. Nevertheless, other mechanisms cannot be discarded because GSPE was also shown to increase endothelial nitric oxide synthase (eNOS), 5′-AMP-activated protein kinase (AMPK), and SIRT1 expression in the light cycle of rats [32]. However, to the best of our knowledge, no study so far has addressed the effect of GSPE consumption on the diurnal rhythmicity of subcutaneous WAT. In this context, we investigated the effect of GSPE administration on the diurnal oscillations of adipose tissue metabolites (assessed by NMR) in rats with diet-induced obesity. Our results provide evidence that grape seed proanthocyanidins, essentially B-type proanthocyanidins, are able to restore the diurnal rhythm of alanine, aspartate, and glutamate metabolic pathway in iWAT when they are administered at ZT12.

4.1. Biometric Parameters and Circulating Biomarkers

Although various studies have shown that grape seed proanthocyanidins could prevent body weight gain and fat accumulation, there are scarce data about the effect on body fat content at different ZT points. In this study, although our data did not demonstrate an effect of GSPE on body fat content, we report that the administration of GSPE reduced body weight gain and accumulated food intake when it was consumed at the beginning of the dark phase. In fact, our group recently observed very similar results in Wistar rats supplemented with GSPE at dose of 25 mg/kg of body weight for 4 weeks [33]. Consistent with these previous results, our data also demonstrated that GSPE consumption significantly altered the pattern of expansion of iWAT by decreasing adipocyte size and increasing adipocyte number. In addition, our data showed for the first time that GSPE consumption recovered the diurnal rhythmic concentrations of serum TAG that were lost in diet-induced obesity only when it was administered at ZT12. Glucose and lipid metabolism present circadian regulation to prepare the metabolic

functions for the outcoming situations. Although several studies have previously demonstrated that GSPE consumption properly restore blood lipid concentrations in animals with obesity, our study showed that GSPE enhanced the diurnal rhythm of TAG and cholesterol concentrations according to time-of-day consumption. By contrast, in our experiment, both glucose and NEFA serum concentrations did not display diurnal rhythmicity in response to GSPE consumption. However, as we evaluated rhythm variables only at 6 h intervals, we cannot be completely sure that the consumption of GSPE exclusively affected the diurnal rhythm of TAG and cholesterol concentrations. Thus, more studies with a 4 h interval evaluation are needed to elucidate the effects of GSPE consumption on the circadian concentrations of other circulating biomarkers.

4.2. Lipophilic Metabolites in Adipose Tissue

As expected, the concentration of detected lipophilic metabolites in iWAT was much higher compared to hydrophilic metabolites. Although we did not observe a significant effect of treatment time on the concentration of lipophilic metabolites in iWAT, CAF diet affected significantly its concentrations. In fact, CAF diet determined the degree of unsaturation of fatty acids resulting in lower concentrations of polyunsaturated fatty acids (omega-3, linoleic acid and PUFAs) and higher concentrations of monounsaturated oleic acid compared with STD diet animals. In addition, it is known that CAF disrupts circadian rhythms [34]. In this sense, our findings support a study demonstrating an increase in TAG containing lower degree of unsaturation of fatty acids in subcutaneous WAT of mice with adipocyte-specific deletion of the clock gene *Arntl* (also known as *Bmal1*) compared with control mice [35]. BMAL1 is essential for the function of the molecular circadian clock and regulates circadian transcription of metabolic genes. In our study, MUFAs and omega-3, linoleic and oleic fatty acids presented diurnal rhythms in STD-VH and CAF-GSPE groups treated at ZT12, suggesting a

metabolically active subcutaneous fat pad when GSPE was supplemented at the beginning of the dark phase. Consistent with these results, Castro et al. [35] also detected clear changes of lipids across light/dark cycle in brown adipose tissue, while in WAT significant differences were not detected. These results were expected for the authors as brown adipose tissue has a higher dynamic metabolic role in comparison with WAT. However, it is known that subcutaneous WAT also may develop brown-like adipocytes. Thus, further research is warranted to elucidate the clinical relevance of these lipidic rhythmic oscillations in response to GSPE consumption in this tissue.

4.3. Lipid Metabolism in Adipose Tissue

Lipolysis and lipogenesis are mainly influenced by the light/dark cycle and fasting/feeding states. The light/dark cycle regulates melatonin, which is a hormone that plays a key role in many physiological processes such as lipid metabolism [36]. In our study, total fatty acids, TAGs, lactate, glycerol, and phosphorylcholine presented higher concentrations during the dark phase in STD-VH and CAF-GSPE animals treated at ZT12. The acrophase in the dark phase of these metabolites indicates an activation of lipid synthesis during the dark phase and lipid oxidation during the light phase, respectively [35]. In fact, after feeding, glucose and fatty acids are taken up by WAT to synthesize acetyl-CoA for fatty acid synthesis [37]. Glycerol, another product of glycolysis, is needed for TAG formation in WAT when it is converted into glycerol-3-phosphate [38]. Lactate, for which we also found its acrophase in the dark phase, increases its production in WAT after glucose intake [37,38]. Moreover, we expected to find 3-OHB increased during the light phase because of its association with β-oxidation [35]. However, in our study, this metabolite was increased during the dark phase in STD animals and in response to GSPE administration at ZT12 when lipogenesis

is active in this tissue, suggesting that 3-OHB could play an alternative role as a substrate for ATP generation during prolonged catabolic periods [35].

4.4. Hydrophilic Metabolites in Adipose Tissue

Whereas the role of adipose tissue in glucose and lipid homeostasis is widely recognized, its role in systemic protein and amino acid metabolism is less well-appreciated. Mammals obtain energy from proteins only in extreme situations such as long-term starvation and, in normal conditions, amino acids are recycled for new proteins. Interestingly, protein-associated metabolic pathways also present circadian rhythms in human subcutaneous WAT with higher activity during the day such as branched-chain amino acid (BCAA) metabolism [39]. In fact, WAT may be the primary tissue which uptakes BCAAs from liver after feeding as insulin action and glucose uptake increase BCAA uptake in WAT [40]. BCAAs can be taken up by WAT through direct BCAA transport or, depending on BCAA levels, inside the adipocyte, exchanging internal glutamine, alanine, and asparagine for external BCAA and glutamate, which occurs immediately after feeding [41]. BCAA uptake and metabolism in WAT are reduced under insulin resistance and inflammation in humans and rodents and, consequently, are associated with elevated blood BCAA levels. A previous study reported a significant reduction on BCAA levels in WAT under a high-fat diet compared to STD [5,40]. Although in our study the reduction of BCAA levels in CAF groups was not significant in iWAT, our findings demonstrated important differences in the diurnal rhythm of amino acids in response to CAF diet as well as in response to GSPE administration at ZT12. Specifically, from the 18 rhythmic metabolites found in STD animals, 16 lost their rhythm under CAF diet, and importantly, most of them restored the rhythmicity only when GSPE was administrated at ZT12. In addition, these metabolites, including alanine, asparagine, aspartate, fumarate, glutamate, glutamine, and succinate, were significantly involved in alanine,

aspartate, and glutamate metabolism, suggesting that this metabolic pathway could prevent the metabolic abnormalities associated with an obesogenic diet.

4.5. Alanine, Aspartate and Glutamate Metabolism

Glutamine and alanine are involved in a mechanism to avoid nitrogen toxification in WAT. The regeneration of proteins drives to nitrogen removal. In fact, the way to remove nitrogen in WAT and skeletal muscle is through the synthesis of glutamine and alanine. During starvation state, some authors reported significant release of glutamine, alanine, taurine, and tyrosine by subcutaneous WAT probably due to protein breakdown [41,42]. Glutamine can be synthesized and kept in WAT for lipid synthesis or liberated in the circulation to be uptaken for other tissues including kidney and intestine, which consume glutamine as source of energy through the TCA cycle. Thus, WAT plays a significant role in whole-body glutamine homeostasis as it releases 20% of net amounts of glutamine. Alanine can also be synthesized and liberated by WAT. The synthesis and transport of alanine to the liver, where the urea cycle takes place, is a mechanism to ensure the prevention of nitrogen toxification. In the liver, alanine could also be converted to glucose through gluconeogenesis, a substrate for muscle, brain, erythrocytes, and other glucose-dependent cells. A previous study in mice reported that BCAA production in WAT is higher during the light phase, which matches with the timing of alanine production [5]. However, in our study, alanine concentrations were higher during the dark phase in response to GSPE administration at ZT12. Indeed, in these animals, all the metabolites involved in alanine, aspartate, and glutamate metabolism showed an acrophase during the dark phase. In contrast, STD animals presented acrophases of asparagine and glutamate during the light phase with peaks around ZT3, but the administration of GSPE at ZT0 could not restore the rhythmicity of these metabolites under CAF diet conditions. Therefore, timing of supplementation is

crucial for affecting the acrophase of alanine, aspartate, and glutamate metabolism, and only GSPE supplementation at ZT12 restored the rhythmicity lost in response to CAF diet. Glutamine and succinate in WAT also attenuate the expression of pro-inflammatory genes and macrophage infiltration [43,44]. Pro-inflammatory genes, such as TNF-α and IL-6, exhibit circadian rhythmicity with the highest concentrations during the light phase when glutamate and succinate concentrations are low in iWAT in response to GSPE administration at ZT12 [45]. In human WAT, oxidoreductase activity was shown to be higher in the evening, at the beginning of the rest phase for humans [39]. Therefore, the observed diurnal rhythm of glutamine and succinate is in coherence with pro-inflammatory gene expression in STD animals and also in response to GSPE administration at ZT12. However, further studies are needed to analyze the inflammatory status of this tissue and and confirm these results

5. Conclusions

Cafeteria diet induced greater accumulation of monounsaturated than polyunsaturated fatty acids in iWAT compared with non-obese animals. Although GSPE supplementation did not present any effect on the degree of (un)saturation of fatty acids, its consumption restored the diurnal rhythm of 12 metabolites only when it was administered at the beginning of the dark/activity phase (ZT12). Diet-induced obesity is associated with metabolic disruption of adipose tissue including diurnal rhythm misalignment. Therefore, the amelioration of diurnal rhythmicity could enhance the functionality of this tissue. Our results demonstrated for the first time that timed GPSE administration specifically at ZT12 restored the rhythmic metabolism of alanine, aspartate, and glutamate that was lost in response to CAF diet. This pathway plays a pivotal role in the metabolism of nitrogen-containing compounds, BCAA metabolism, and pro-inflammatory state in mammals. However, further studies are needed to

elucidate the metabolic pathways and processes involved in these events and better understand the interaction of diurnal rhythms and proanthocyanidins on the circadian biology of WAT.

Supplementary Materials: The following supporting information can be downloaded at: www.mdpi.com/xxx/s1, Figure S1: iWAT histology parameters; Figure S2: Correlation analysis; Table S1: Circadian parameters of lipophilic iWAT metabolites; Table S2: Circadian parameters of hydrophilic iWAT metabolites.

Author Contributions: Conceptualization, M.C.-P. and G.A.; methodology, M.C.-P., R.M.R., J.R.S.-R., M.M. and G.A.; software, M.C.-P., J.R.S.-R. and L.V.M.d.A.; validation, M.C.-P., L.V.M.d.A. and G.A.; formal analysis, M.C.-P., L.V.M.d.A. and J.R.S.-R.; investigation, M.C.-P., R.M.R.; resources, M.C.-P., R.M.R., J.R.S.-R.; data curation, M.C.-P., L.V.M.d.A. and J.R.S.-R.; writing—original draft preparation, M.C.-P.; writing—review and editing, È.N.-M., S.Q.-V., X.E., L.V.M.d.A., H.O. and G.A.; visualization, M.C.-P.; supervision, L.V.M.d.A., H.O. and G.A.; funding acquisition, M.M. and G.A. All authors have read and agreed to the published version of the manuscript.

Funding: This research was funded by the Spanish Ministry of Economy and Competitiveness (MINECO) (AGL2016-77105-R). M.C.-P. is recipient of a predoctoral fellowship from the Catalan Government (2021FI_B2 00150). R.M.R. and È.N.-M. are recipients of predoctoral fellowships from Universitat Rovira i Virgili (2018PMF-PIPF-11 and 2019PMF-PIPF-73, respectively). J.R.S.-R. is supported by the Ministry of Science and Innovation and the European Social Fund (BES-2017-080919). S.Q.-V. is supported by a fellowship from the Vicente Lopez Program (Eurecat). G.A. and M.M. are Serra-Hunter fellows. H.O. and L.A. receive funding by the German Research Foundation (DFG; CRC/TR296, P13).

Institutional Review Board Statement: All animal care and experimental protocols involving animals were approved by the Ethics Review Committee for Animal Experimentation of the Universitat Rovira i Virgili (reference number 9495, 18 September 2019) and were carried out in accordance with Directive 86/609EEC of the Council of the European Union and the procedure established by the Departament d'Agricultura, Ramaderia i Pesca of the Generalitat de Catalunya.

Data Availability Statement: The data presented in this study are available on request from the corresponding author. The data are not publicly available due to lack of platform to publish them.

Acknowledgments: We gratefully acknowledge the aid of laboratory technicians Niurka Dariela Llópiz and Rosa Pastor from Universitat Rovira i Virgili.

Conflicts of Interest: The authors declare no conflict of interest. The funders had no role in the design of the study; in the collection, analyses, or interpretation of data; in the writing of the manuscript, or in the decision to publish the results.

References

1. Brown, S.A. Circadian Metabolism: From Mechanisms to Metabolomics and Medicine. *Trends Endocrinol. Metab.* **2016**, *27*, 415–426. https://doi.org/10.1016/j.tem.2016.03.015.
2. Gamble, K.L.; Berry, R.; Frank, S.J.; Young, M.E. Circadian clock control of endocrine factors. *Nat. Rev. Endocrinol.* **2014**, *10*, 466–475. https://doi.org/10.1038/nrendo.2014.78.
3. de Assis, L.V.M.; Oster, H. The circadian clock and metabolic homeostasis: Entangled networks. *Cell. Mol. Life Sci.* **2021**, *78*, 4563–4587. https://doi.org/10.1007/s00018-021-03800-2.
4. Kiehn, J.-T.; Koch, C.E.; Walter, M.; Brod, A.; Oster, H. Circadian rhythms and clocks in adipose tissues: Current insights. *ChronoPhysiology Ther.* **2017**, *7*, 7–17. https://doi.org/10.2147/cpt.s116242.
5. Dyar, K.A.; Lutter, D.; Artati, A.; Ceglia, N.J.; Liu, Y.; Armenta, D.; Jastroch, M.; Schneider, S.; de Mateo, S.; Cervantes, M.; et al. Atlas of Circadian Metabolism Reveals System-wide Coordination and Communication between Clocks. *Cell* **2018**, *174*, 1571–1585.e11. https://doi.org/10.1016/j.cell.2018.08.042.
6. Bray, M.S.; Ratcliffe, W.F.; Grennet, M.H.; Brewer, R.A.; Gamble, K.L.; Young, M.E. Quantitative Analysis of Light-Phase Restricted Feeding Reveals Metabolic Dyssynchrony in Mice. *Int. J. Obes.* **2013**, *37*, 843–852. https://doi.org/10.1038/ijo.2012.137.Quantitative.
7. Arble, D.M.; Bass, J.; Laposky, A.D.; Vitaterna, M.H.; Turek, F.W. Circadian timing of food intake contributes to weight gain. *Obesity* **2009**, *17*, 2100–2102. https://doi.org/10.1038/oby.2009.264.
8. Satoh, Y.; Kawai, H.; Kudo, N.; Kawashima, Y.; Mitsumoto, A. Time-restricted feeding entrains daily rhythms of energy metabolism in mice. *Am. J. Physiol. Regul. Integr. Comp. Physiol.* **2006**, *290*, 1276–1283. https://doi.org/10.1152/ajpregu.00775.2005.
9. Arble, D.M.; Vitaterna, M.H.; Turek, F.W. Rhythmic leptin is required for weight gain from circadian desynchronized feeding in the mouse. *PLoS ONE* **2011**, *6*, e25079. https://doi.org/10.1371/journal.pone.0025079.
10. Ng Chee Ping Time-restricted feeding is a preventative and therapeutic intervention against diverse nutritional challenges. *Cell Metab.* **2014**, *2*, 991–1005. https://doi.org/10.1016/j.cmet.2014.11.001.Time-restricted.
11. Chaix, A.; Lin, T.; Le, H.D.; Chang, M.W.; Panda, S. Time-Restricted Feeding Prevents Obesity and Metabolic Syndrome in Mice Lacking a Circadian Clock. *Cell Metab.* **2019**, *29*, 303–319.e4. https://doi.org/10.1016/j.cmet.2018.08.004.

12. Fiehn, O.; Timothy Garvey, W.; Newman, J.W.; Lok, K.H.; Hoppel, C.L.; Adams, S.H. Plasma metabolomic profiles reflective of glucose homeostasis in non-diabetic and type 2 diabetic obese African-American women. *PLoS ONE* **2010**, *5*, e15234. https://doi.org/10.1371/journal.pone.0015234.

13. Wurtz, P.; Soininen, P.; Kangas, A.J.; Rönnemaa, T.; Lehtimäki, T.; Kähönen, M.; Viikari, J.S.; Raitakari, O.T.; Ala-Korpela, M. Branched-chain and aromatic amino acidsare predictors of insulinresistance in young adults. *Diabetes Care* **2013**, *36*, 648–655. https://doi.org/10.2337/dc12-0895.

14. Herman, M.A.; She, P.; Peroni, O.D.; Lynch, C.J.; Kahn, B.B. Adipose tissue Branched Chain Amino Acid (BCAA) metabolism modulates circulating BCAA levels. *J. Biol. Chem.* **2010**, *285*, 11348–11356. https://doi.org/10.1074/jbc.M109.075184.

15. Frayn, K.N.; Khan, K.; Coppack, S.W.; Elia, M. Amino acid metabolism in human subcutaneous adipose tissue in vivo. *Clin. Sci.* **1991**, *80*, 471–474. https://doi.org/10.1042/cs0800471.

16. Cheng, S.; Wiklund, P.; Autio, R.; Borra, R.; Ojanen, X.; Xu, L.; Törmäkangas, T.; Alen, M. Adipose tissue dysfunction and altered systemic amino acid metabolism are associated with non-alcoholic fatty liver disease. *PLoS ONE* **2015**, *10*, e0138889. https://doi.org/10.1371/journal.pone.0138889.

17. C. Constabel. Molecular controls of proanthocyanidin synthesis and structure: Prospects for genetic engineering in crop plants. *J. Agric. Food Chem.* **2018**, *66*, 9882–9888. https://doi.org/10.1021/acs.jafc.8b02950.

18. Mannino G.; Chinigò, G.; Serio, G.; Genova, T.; Gentile, C.; Munaron, L.; Bertea, C.M. Proanthocyanidins and where to find them: A meta-analytic approach to investigate their chemistry, biosynthesis, distribution, and effect on human health. *Antioxidants* **2021**, *10*, 1229. https://doi.org/10.3390/antiox10081229.

19. Pascual-Serrano, A.; Bladé, C.; Suárez, M.; Arola-Arnal, A. Grape Seed Proanthocyanidins Improve White Adipose Tissue Expansion during Diet-Induced Obesity Development in Rats. *Int. J. Mol. Sci.* **2018**, *19*, 2632. https://doi.org/10.3390/ijms19092632.R.

20. Ribas-Latre A.; Baselga-Escudero, L.; Casanova, E.; Arola-Arnal, A.; Salvado, J.; Arola, L.; Bladé, C. Chronic consumption of dietary proanthocyanidins modulates peripheral clocks in healthy and obese rats. *J. Nutr. Biochem*. **2015**, *26*, 112–119. https://doi.org/10.1016/j.jnutbio.2014.09.006.

21. Margalef, M.; Pons, Z.; Iglesias-Carres, L.; Bravo, F.I.; Muguerza, B.; Arola-Arnal, A. Lack of Tissue Accumulation of Grape Seed Flavanols after Daily Long-Term Administration in Healthy and Cafeteria-Diet Obese Rats. *J. Agric. Food Chem.* **2015**, *63*, 9996–10003. https://doi.org/10.1021/acs.jafc.5b03856.

22. Gibert-Ramos, A.; Palacios-Jordan, H.; Salvadó, M.J.; Crescenti, A. Consumption of out-of-season orange modulates fat accumulation, morphology and gene expression in the adipose tissue of Fischer 344 rats. *Eur. J. Nutr.* **2020**, *59*, 621–631. https://doi.org/10.1007/s00394-019-01930-9.

23. Castro, C.; Briggs, W.; Paschos, G.K.; Fitzgerald, G.A.; Griffin, J.L. A metabolomic study of adipose tissue in mice with a disruption of the circadian system. *Mol. Biosyst.* **2015**, *11*, 1897–1906. https://doi.org/10.1039/c5mb00032g.

24. Palacios-Jordan, H.; Martín-González, M.Z.; Suárez, M.; Aragonès, G.; Mugureza, B.; Rodríguez, M.A.; Bladé, C. The disruption of liver metabolic circadian rhythms by a cafeteria diet is sex-dependent in fischer 344 rats. *Nutrients* **2020**, *12*, 1085. https://doi.org/10.3390/nu12041085.

25. Parsons, R.; Parsons, R.; Garner, N.; Oster, H.; Rawashdeh, O. CircaCompare: A method to estimate and statistically support differences in mesor, amplitude and phase, between circadian rhythms. *Bioinformatics* **2020**, *36*, 1208–1212.. https://doi.org/10.1093/bioinformatics/btz730.

26. Moškon, M. CosinorPy: A python package for cosinor-based rhythmometry. *BMC Bioinformatics* **2020**, *21*, 485. https://doi.org/10.1186/s12859-020-03830-w.

27. Foster, M.T.; Softic, S.; Caldwell, J.; Kohli, R.; DeKloet, A.D.; Seeley, R.J. Subcutaneous adipose tissue transplantation in diet-induced obese mice attenuates metabolic dysregulation while removal exacerbates it. *Physiol. Rep.* **2013**, *1*, e00015. https://doi.org/10.1002/phy2.15.

28. Cox-York, K.; Wei, Y.; Wang, D.; Pagliassotti, M.J.; Foster, M.T. Lower body adipose tissue removal decreases glucose tolerance and insulin sensitivity in mice with exposure to high fat diet. *Adipocyte* **2015**, *4*, 32–43. https://doi.org/10.4161/21623945.2014.957988.

29. Tran, T.T.; Yamamoto, Y.; Gesta, S.; Kahn, C.R. Beneficial Effects of Subcutaneous Fat Transplantation on Metabolism. *Cell Metab.* **2008**, *7*, 410–420. https://doi.org/10.1016/j.cmet.2008.04.004.

30. Ribas-Latre, A.; Del Bas, J.M.; Baselga-Escudero, L.; Casanova, E.; Arola-Arnal, A.; Salvado, J.; Arola, L.; Bladé, C. Dietary proanthocyanidins modulate melatonin levels in plasma and the expression pattern of clock genes in the hypothalamus of rats. *Mol. Nutr. Food Res.* **2015**, *59*, 865–878. https://doi.org/10.1002/mnfr.201400571.

31. Ribas-Latre, A.; Baselga-Escudero, L.; Casanova, E.; Arola-Arnal, A.; Salvadó, M., Bladé, C.; Arola, L. Dietary proanthocyanidins modulate BMAL1 acetylation, Nampt expression and NAD levels in rat liver." *Sci. Rep.* **2015**, *5*, 10954. https://doi.org/10.1038/srep10954.

32. Cui, X.; Liu, X.; Feng, H.; Zhao, S.; Gao, H. Grape seed proanthocyanidin extracts enhance endothelial nitric oxide synthase expression through 5'-AMP activated protein kinase/Surtuin 1-Krüpple like factor 2 pathway and modulate blood pressure in ouabain induced hypertensive rats. *Biol. Pharm. Bull.* **2012**, *35*, 2192–2197. https://doi.org/10.1248/bpb.b12-00598.

33. Colom-Pellicer,M.; Rodríguez, R.M.; Navarro-Masip, È.; Bravo, F.I.; Mulero, M.; Arola, L.; Aragonès, G. Time-of-day dependent effect of proanthocyanidins on adipose tissue metabolism in rats with diet-induced obesity. *Int. J. Obes.* **2022**, in press. https://doi.org/10.1038/s41366-022-01132-0.

34. Wang, S.; Lin, Y.; Gao, L.; Yang, Z.; Lin, J.; Ren, S.; Li, F.; Chen, J.; Wang, Z.; Dong, Z.; et al. PPAR-γ integrates obesity and adipocyte clock through epigenetic regulation of Bmal1. *Theranostics* **2022**, *12*, 1589–1606. https://doi.org/10.7150/thno.69054.

35. Castro, C.; Briggs, W.; Paschos, G.K.; FitzGerald, G.A.; Griffin, J.L. A metabolomic study of adipose tissue in mice with a disruption of the circadian system. *Mol. Bio. Syst.* 2015, *11*, 1897–1906. https://doi.org/10.1039/c5mb00032g.

36. Hong, F.; Pan, S.; Xu, P.; Xue, T.; Wang, J.; Guo, Y.; Jia, L.; Qiao, X.; Li, L.; Zhai, Y. Melatonin Orchestrates Lipid Homeostasis through the Hepatointestinal Circadian Clock and Microbiota during Constant Light Exposure. *Cells* **2020**, *9*, 1–22. https://doi.org/10.3390/cells9020489.

37. Upadhyay, S.K.; Eckel-Mahan, K.L.; Mirbolooki, M.R.; Tjong, I.; Griffey, S.M.; Schmunk, G.; Koehne, A.; Halbout, B.; Iadonato, S.; Pedersen, B.; et al. Selective Kv1.3 channel blocker as therapeutic for obesity and insulin resistance. *Proc. Natl. Acad. Sci. USA* **2013**, *110*, E2239–E2248. https://doi.org/10.1073/pnas.1221206110.

38. Possik, E.; Al-Mass, A.; Peyot, M.L.; Ahmad, R.; Al-Mulla, F.; Madiraju, S.R.M.; Prentki, M. New Mammalian Glycerol-3-Phosphate Phosphatase: Role in β-Cell, Liver and Adipocyte Metabolism. *Front. Endocrinol.* **2021**, *12*, 706607. https://doi.org/10.3389/fendo.2021.706607.

39. Christou, S.; Wehrens, S.M.T.; Isherwood, C.; Möller-Levet, C.S.; Wu, H.; Revell, V.L.; Bucca, G.; Skene, D.J.; Laing, E.E.; Archer, S.N.; et al. Circadian regulation in human white adipose tissue revealed by transcriptome and metabolic network analysis. *Sci. Rep.* **2019**, *9*, 2641. https://doi.org/10.1038/s41598-019-39668-3.

40. Lackey, D.E.; Lynch, C.J.; Olson, K.C.; Mostaedi, R.; Ali, M.; Smith, W.H.; Karpe, F.; Humphreys, S.; Bedinger, D.H.; Dunn, T.N.; et al. Regulation of adipose branched-chain amino acid catabolism enzyme expression and cross-adipose amino acid flux in human obesity. *Am. J. Physiol. Endocrinol. Metab.* **2013**, *304*, 1175–1187. https://doi.org/10.1152/ajpendo.00630.2012.

41. Kowalski, T.J.; Guoyao, W.U.; Watford, M. Rat adipose tissue amino acid metabolism in vivo as assessed by microdialysis and arteriovenous techniques. *Am. J. Physiol.* **1997**, *273*, E613.

42. Burrill, J.S.; Long, E.K.; Reilly, B.; Deng, Y.; Armitage, I.M.; Scherer, P.E.; Bernlohr, D.A. Inflammation and ER stress regulate branched-chain amino acid uptake and metabolism in adipocytes. *Mol. Endocrinol.* **2015**, *29*, 411–420. https://doi.org/10.1210/me.2014-1275.

43. Stumvoll, M.; Perriello, G.; Meyer, C.; Gerich, J. Role of glutamine in human carbohydrate metabolism in kidney and other tissues. *Kidney Int.* **1999**, *55*, 778–792. https://doi.org/10.1046/j.1523-1755.1999.055003778.x.

44. Kowalski, T.J.; Watford, M. Production of glutamine and utilization of glutamate by rat subcutaneous adipose tissue in vivo. *Am. J. Physiol. Endocrinol. Metab.* **1994**, *266*, 51–54. https://doi.org/10.1152/ajpendo.1994.266.1.e151.

45. Petrus, P.; Lecoutre, S.; Dollet, L.; Wiel, C.; Sulen, A.; Gao, H.; Tavira, B.; Laurencikiene, J.; Rooyackers, O.; Checa, A.; et al. Glutamine Links Obesity to Inflammation in Human White Adipose Tissue. *Cell Metab.* **2020**, *31*, 375–390.e11. https://doi.org/10.1016/j.cmet.2019.11.019.

GRAPHICAL ABSTRACT

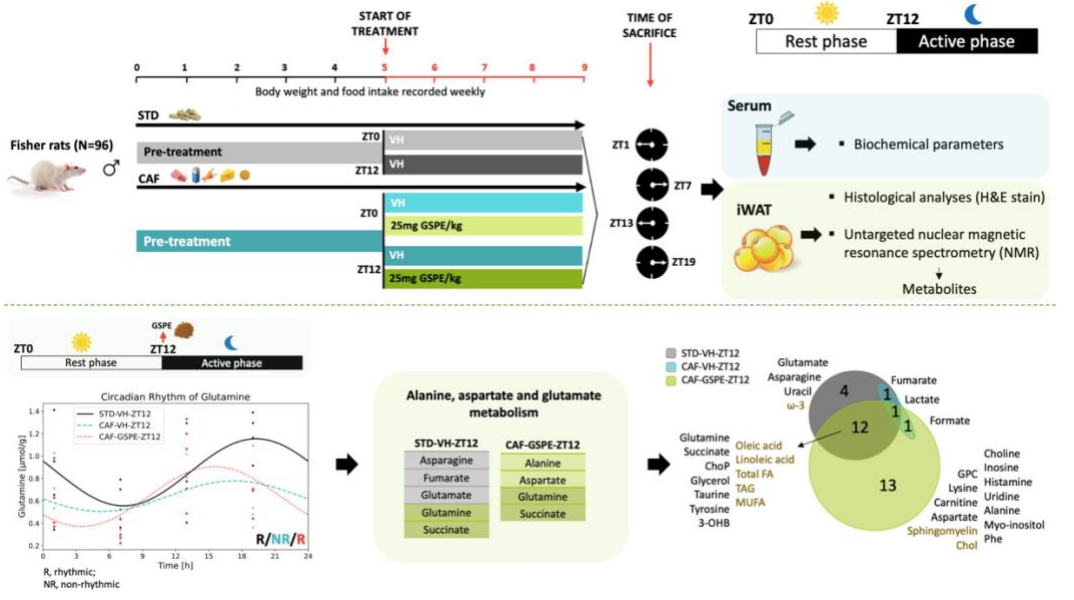

SUPPLEMENTARY MATERIAL

Table S1. Rhythmicity, mesor, amplitud and peak time of lipophilic metabolites in iWAT of rats fed standard or cafeteria diet treated with vehicle or GSPE at ZT0 or ZT12.

Metabolites	Rhythmicity (p value)			Mesor (μmol/g)			Amplitude estimate			Acrophase (ZT)			Period estimate
ZT0	STD-VH	CAF-VH	CAF-GSPE	STD-VH	CAF-VH	CAF-GSPE	STD-VH	CAF-VH	CAF-GSPE	STD-VH	CAF-VH	CAF-GSPE	
Cholesterol	0.247	0.278	0.267	5.923	5.494	6.326	0.739	0.803	1.444	NA	NA	NA	24
Diglycerides	0.622	0.180	0.403	3.408 *	5.018	3.968	0.378	0.867	0.757	NA	NA	NA	24
Linoleic Acid	0.585	0.506	0.129	528.776 *	383.035	357.343 #	20.853	20.158	42.033	NA	NA	NA	24
MUFAs	0.302	0.686	0.387	4265.558	4271.734	4150.951	253.755	112.354	179.005	NA	NA	NA	24
Oleic Acid	0.331	0.615	0.390	1641.234 *	2402.484	2281.759 #	157.541	84.727	167.141	NA	NA	NA	24
Omega-3	0.067	0.840	0.085	189.677 *	136.957	154.970 #	21.158	1.913	23.484	NA	NA	NA	24
PUFAs	0.072	0.231	0.176	523.170 *	269.154	272.586 #	70.387	22.410	49.355	NA	NA	NA	24
Sphingomyelin	0.381	0.644	0.305	0.313	0.234	0.178	0.078	0.033	0.054	NA	NA	NA	24
Total Fatty Acid	0.401	0.699	0.519	2905.779	3262.330	3112.816	157.513	88.895	113.099	NA	NA	NA	24
Triglycerides	0.377	0.662	0.414	1467.509	1635.971	1594.813	83.620	44.292	76.088	NA	NA	NA	24
ZT12	STD-VH	CAF-VH	CAF-GSPE	STD-VH	CAF-VH	CAF-GSPE	STD-VH	CAF-VH	CAF-GSPE	STD-VH	CAF-VH	CAF-GSPE	
Cholesterol	0.159	0.082	0.005	5.770	5.991	5.960	1.183	0.887	1.443	NA	NA	18.105	24
Diglycerides	0.070	0.444	0.078	3.340	4.586	4.046	1.374	0.449	0.916	NA	NA	NA	24
Linoleic Acid	0.030	0.121	0.015	456.528 *	354.638	352.156 #	118.545	45.229	78.542	16.587	NA	19.541	24
MUFAs	0.025	0.121	0.016	3941.272	4261.909	4077.310	721.686	297.093	493.209	17.052	NA	21.310	24
Oleic Acid	0.022	0.233	0.037	1553.215 *	2452.311	2196.257 #	413.037	186.833	354.565	16.688	NA	21.639 #	24
Omega-3	0.004	0.213	0.367	209.956 *	144.753	161.455 #	40.961 *	10.682	12.097	5.627	NA	NA	24
PUFAs	0.722	0.175	0.090	500.925 *	252.456 $	294.490 #	11.977	19.138	40.961	NA	NA	NA	24
Sphingomyelin	0.380	0.691	0.032	0.297	0.164	0.226	0.078	0.013 $	0.212	NA	NA	14.340	24
Total Fatty Acid	0.012	0.241	0.032	2587.671 *	3283.056	3108.460 #	796.237	210.882	479.950	16.997	NA	21.023	24
Triglycerides	0.015	0.187	0.028	1338.868 *	1657.022	1556.984 #	315.445	121.114	205.413	17.222	NA	21.129	24

*Table shows the presence of rhythm of each metabolite with a p value, circadian mean concentration (mesor), amplitude and acrophase (time of highest concentration within the day) followed by comparisons between two groups using CircaCompare (p value < 0.05). * indicates significant difference between STD-VH vs CAF-VH; $ indicates significant difference between CAF-VH vs CAF-GSPE; # indicates significant difference between CAF-GSPE vs STD-VH. NA, not available acrophase values in non-rhythmic metabolites. iWAT, inguinal white adipose tissue; STD-VH, standard diet vehicle group; CAF-VH, cafeteria diet vehicle group; CAF-GSPE, cafeteria diet treated with grape-seed procyanidin extract. Rats were fed standard or cafeteria diet for 9 weeks. At week 6, rats received a daily oral dose of GSPE or vehicle for 4 weeks at ZT0 or ZT12. Rats from each group were sacrificed at four different time points; ZT1, ZT7, ZT13 and ZT19 in order to analyse the circadian rhythm of lipophilic metabolites.*

Table S2. Rhythmicity, mesor, amplitud and peak time of hydrophilic metabolites in iWAT of rats fed standard or cafeteria diet treated with vehicle or GSPE at ZT0 or ZT12.

Metabolites	Rhythmicity (p value)			Mesor (μmol/g)			Amplitude estimate			Acrophase (ZT)			Period estimate
ZT0	STD-VH	CAF-VH	CAF-GSPE	STD-VH	CAF-VH	CAF-GSPE	STD-VH	CAF-VH	CAF-GSPE	STD-VH	CAF-VH	CAF-GSPE	
3-Hydorxybutyrate	0.549	0.133	0.002	0.024	0.026	0.036 #	0.002	0.007 $	0.022 #	NA	NA	20.155	24
Acetate	0.162	0.292	0.154	0.053	0.048	0.051	0.013	0.006	0.017	NA	NA	NA	24
Alanine	0.096	0.141	0.096	0.306	0.204	0.240	0.124	0.064	0.082	NA	NA	NA	24
AMP	0.520	0.086	0.245	0.030	0.030	0.028	0.005	0.020	0.008	NA	NA	NA	24
Asparagine	0.019	0.068	0.313	0.025 *	0.013	0.016	0.016	0.006	0.006	2.377	NA	NA	24
Aspartate	0.125	0.117	0.200	0.106 *	0.038 $	0.054 #	0.039	0.010	0.012	NA	NA	NA	24
Carnitine	0.078	0.175	0.112	0.007 *	0.005	0.005	0.002	0.001	0.002	NA	NA	NA	24
Choline	0.073	0.563	0.116	0.011 *	0.007	0.009	0.003	0.001	0.003	NA	NA	NA	24
Creatine	0.242	0.582	0.079	0.153	0.081	0.100	0.076	0.010	0.054	NA	NA	NA	24
Formate	0.417	0.180	0.391	0.013	0.013	0.014	0.002	0.003	0.002	NA	NA	NA	24
Fumarate	0.060	0.003	0.454	0.003	0.003	0.002	0.001	0.002	0.000	NA	1.455	NA	24
Glucose	0.325	0.513	0.149	0.308 *	0.191	0.272	0.055	0.017	0.086	NA	NA	NA	24
Glutamate	0.046	0.122	0.078	0.226 *	0.147	0.186	0.096	0.039	0.056	3.241	NA	NA	24
Glutamine	0.086	0.349	0.065	0.962 *	0.612	0.750	0.317	0.111	0.313	NA	NA	NA	24
Glycerol	0.327	0.047	0.076	0.092	0.091	0.102	0.013	0.017	0.024	NA	22.297	NA	24
Glycerophosphocholine	0.348	0.069	0.076	0.113 *	0.061	0.077	0.026	0.032	0.034	NA	NA	NA	24
Glycogen	0.813	0.012	0.175	0.465	0.168	0.226	0.058	0.115	0.123	NA	10.590	NA	24
Histamine	0.148	0.149	0.084	0.066	0.038	0.045	0.023	0.023	0.020	NA	NA	NA	24
Inosine	0.179	0.709	0.151	0.081 *	0.048	0.061	0.022	0.003	0.015	NA	NA	NA	24
Isoleucine	0.080	0.048	0.101	0.031 *	0.021	0.022	0.012	0.008	0.008	NA	4.228	NA	24
Lactate	0.187	0.209	0.178	1.052 *	0.637	0.757	0.294	0.167	0.244	NA	NA	NA	24
Leucine	0.072	0.046	0.129	0.068 *	0.042	0.045	0.028	0.020	0.018	NA	4.828	NA	24
Lysine	0.188	0.178	0.111	0.111 *	0.062	0.074	0.031	0.032	0.035	NA	NA	NA	24
Myo-inositol	0.202	0.152	0.113	0.589	0.319	0.388	0.271	0.167	0.205	NA	NA	NA	24
Niacinamide	0.196	0.091	0.347	0.017	0.010	0.014	0.008	0.005	0.004	NA	NA	NA	24
Phenylalanine	0.052	0.088	0.151	0.030	0.019	0.021	0.017	0.008	0.010	NA	NA	NA	24
Phosphorylcholine	0.096	0.248	0.283	0.074	0.050	0.060	0.031	0.013	0.014	NA	NA	NA	24
Propionate	0.155	0.320	0.123	0.018 *	0.009	0.013	0.006	0.003	0.006	NA	NA	NA	24
Sarcosine	0.076	0.243	0.302	0.019	0.018	0.021	0.005	0.003	0.002	NA	NA	NA	24
Succinate	0.232	0.846	0.069	0.039	0.027	0.033	0.010	0.001	0.008	NA	NA	NA	24
Taurine	0.092	0.159	0.160	1.048 *	0.683	0.796	0.271	0.125	0.201	NA	NA	NA	24
Tyrosine	0.051	0.031	0.067	0.032	0.020	0.023	0.018	0.012	0.011	NA	5.798	NA	24
Uracil	0.046	0.051	0.264	0.012	0.009	0.010	0.007	0.006	0.005	2.180	NA	NA	24
Uridine	0.104	0.618	0.127	0.032	0.022	0.024	0.011	0.002	0.009	NA	NA	NA	24
Valine	0.046	0.048	0.114	0.052	0.035	0.039	0.024	0.013	0.013	2.422	4.538	NA	24

ZT12	STD-VH	CAF-VH	CAF-GSPE	STD-VH		CAF-VH		CAF-GSPE		STD-VH		CAF-VH		CAF-GSPE		STD-VH	CAF-VH	CAF-GSPE	
3-Hydorxybutyrate	0.000	0.158	0.009	0.034		0.025		0.026		0.030	*	0.007		0.019		18.169	NA	14.718 #	24
Acetate	0.307	0.099	0.234	0.057	*	0.042		0.049		0.009		0.006		0.007		NA	NA	NA	24
Alanine	0.124	0.242	0.032	0.276		0.214		0.208		0.072		0.039		0.083		NA	NA	14.229	24
AMP	0.221	0.686	0.180	0.016		0.023		0.022		0.007		0.003		0.008		NA	NA	NA	24
Asparagine	0.045	0.495	0.129	0.026		0.017		0.018		0.013		0.002		0.008		18.262	NA	NA	24
Aspartate	0.130	0.209	0.016	0.077	*	0.051		0.054		0.023		0.011		0.028		NA	NA	18.422	24
Carnitine	0.056	0.427	0.037	0.006	*	0.004		0.005		0.002		0.000		0.002		NA	NA	16.251	24
Choline	0.059	0.283	0.023	0.009	*	0.006		0.007	#	0.003		0.001		0.003		NA	NA	14.659	24
Creatine	0.228	0.458	0.096	0.109		0.071		0.091		0.041		0.006		0.047		NA	NA	NA	24
Formate	0.221	0.046	0.024	0.012		0.011		0.014		0.002		0.003		0.004		NA	22.912 $	13.071	24
Fumarate	0.032	0.003	0.175	0.004		0.002		0.002		0.002		0.001		0.001		19.300	16.831	NA	24
Glucose	0.196	0.152	0.206	0.273		0.219		0.209		0.065		0.046		0.046		NA	NA	NA	24
Glutamate	0.016	0.456	0.083	0.210		0.159		0.161		0.082		0.017		0.047		18.876	NA	NA	24
Glutamine	0.019	0.181	0.026	0.854		0.642		0.639		0.299		0.137		0.267		19.286	NA	15.499	24
Glycerol	0.000	0.648	0.032	0.095		0.079		0.094		0.044	*	0.004		0.022		17.666	NA	17.992	24
Glycerophosphocholine	0.184	0.385	0.038	0.093		0.076		0.066		0.024		0.014		0.030		NA	NA	14.738	24
Glycogen	0.493	0.067	0.165	0.208		0.335		0.196		0.090		0.314		0.132		NA	NA	NA	24
Histamine	0.228	0.341	0.033	0.056		0.035		0.035		0.015		0.008		0.022		NA	NA	14.147	24
Inosine	0.099	0.523	0.017	0.070	*	0.053		0.052	#	0.014		0.005		0.023		NA	NA	14.478	24
Isoleucine	0.067	0.446	0.119	0.029		0.021		0.018	#	0.011		0.002		0.006		NA	NA	NA	24
Lactate	0.017	0.017	0.018	0.930		0.733		0.630		0.481		0.396		0.327		17.750	14.002	14.615	24
Leucine	0.056	0.493	0.093	0.060		0.041		0.039	#	0.023		0.005		0.013		NA	NA	NA	24
Lysine	0.143	0.241	0.021	0.086		0.058		0.057		0.025		0.014		0.033		NA	NA	14.275	24
Myo-inositol	0.255	0.509	0.038	0.520		0.374		0.337		0.143		0.074		0.228		NA	NA	13.563	24
Niacinamide	0.286	0.518	0.079	0.015		0.012		0.016		0.004		0.002		0.005		NA	NA	NA	24
Phenylalanine	0.065	0.206	0.027	0.032	*	0.018		0.017	#	0.015		0.004		0.009		NA	NA	14.328	24
Phosphorylcholine	0.029	0.177	0.049	0.075	*	0.051		0.057		0.033		0.012		0.031		17.958	NA	12.996 #	24
Propionate	0.470	0.079	0.243	0.016	*	0.009		0.011		0.002		0.003		0.003		NA	NA	NA	24
Sarcosine	0.206	0.629	0.260	0.017		0.013		0.023		0.005		0.001		0.009		NA	NA	NA	24
Succinate	0.040	0.119	0.031	0.034		0.028		0.027		0.012		0.008		0.014		17.705	NA	14.393	24
Taurine	0.033	0.225	0.013	0.965	*	0.704		0.731	#	0.243		0.103		0.247		19.029	NA	15.573	24
Tyrosine	0.030	0.170	0.041	0.029	*	0.019		0.019	#	0.013		0.005		0.008		20.783	NA	14.554 #	24
Uracil	0.015	0.153	0.062	0.013		0.010		0.010		0.008		0.003		0.005		19.481	NA	NA	24
Uridine	0.147	0.342	0.028	0.032		0.023		0.026		0.008		0.003		0.012		NA	NA	13.476	24
Valine	0.058	0.577	0.120	0.050		0.036		0.034	#	0.016		0.003		0.010		NA	NA	NA	24

*Table shows the presence of rhythm of each metabolite with a p value, circadian mean concentration (mesor), amplitude and acrophase (time of highest concentration within the day) followed by comparisons between two groups using CircaCompare (p value < 0.05). * indicates significant difference between STD-VH vs CAF-VH; $ indicates significant difference between CAF-VH vs CAF-GSPE; # indicates significant difference between CAF-GSPE vs STD-VH. NA, not available acrophase values in non-rhythmic metabolites. iWAT, inguinal white adipose tissue; STD-VH, standard diet vehicle group; CAF-VH, cafeteria diet vehicle group; CAF-GSPE, cafeteria diet treated with grape-seed procyanidin extract. Rats were fed standard or cafeteria diet for 9 weeks. At week 6, rats received a daily oral dose of GSPE or vehicle for 4 weeks at ZT0 or ZT12. Rats from each group were sacrificed at four different time points; ZT1, ZT7, ZT13 and ZT19 in order to analyse the circadian rhythm of hydrophilic metabolites.*

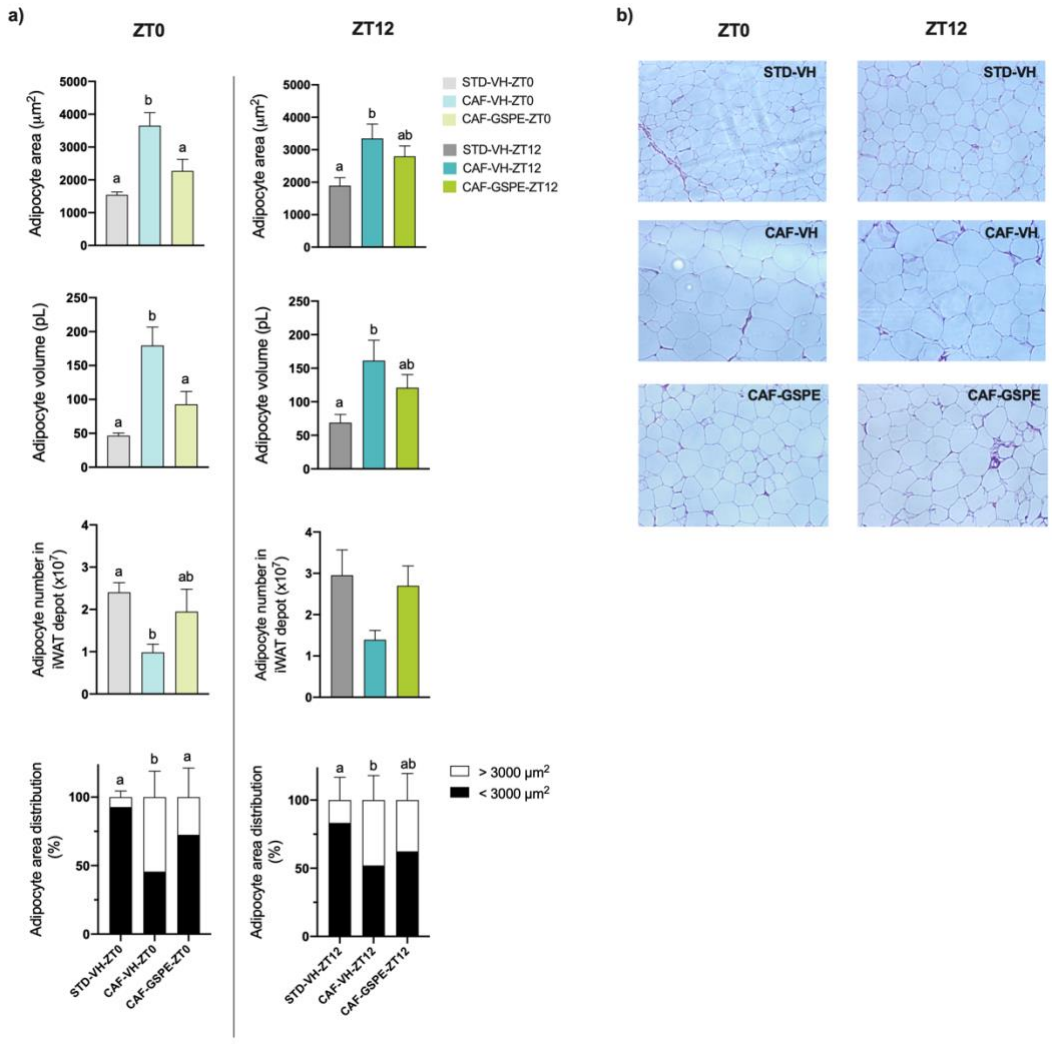

Figure S1. *iWAT histology. Histology parameters (a) and representative images of hematoxilin & eosin staining (b). a, b; represent significant differences using one-way ANOVA ($p < 0.05$) followed by Bonferroni post hoc test (n=6, rats sacrificed at ZT1 and ZT7).*

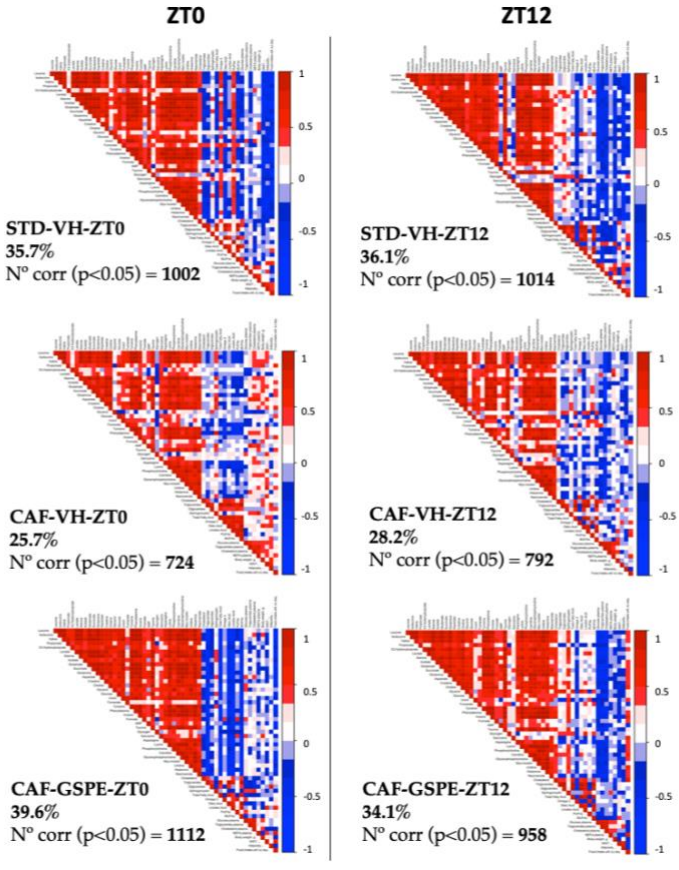

Figure S2. *Correlation analysis among iWAT metabolites, final body weight, iWAT relative weight, adiposity and food intake at week 9. * significant correlation analysis using Spearman method (p < 0.05). Red and blue mean positive and negative correlations, respectively.*

Manuscript 3

Proanthocyanidins modulate PER2 circadian rhythm and metabolic gene expression in mice adipose tissue explants in a time-dependent manner

Marina Colom-Pellicer[1]*, Leonardo Vinícius Monteiro de Assis[2]*, Romina M Rodríguez[1], Miquel Mulero[1], Anna Arola-Arnal[1], Henrik Oster[2], Gerard Aragonès[1, $]

* authors with equal contribution

[1] Universitat Rovira i Virgili, Department of Biochemistry and Biotechnology, Nutrigenomics Research Group, 43007 Tarragona, Spain.
[2] University of Lübeck, Institute of Neurobiology, Center of Brain, Behavior and Metabolism, Marie Curie Street, 23562 Lübeck, Germany.
[$] Correspondence: gerard.aragones@urv.cat

Submitted to *Frontiers in Nutrition*
June 2022

Abstract: The disruption of circadian clocks in mammals is associated with the development of metabolic disorders, including obesity. Under high-fat diet conditions, the consumption of grape seed proanthocyanidin extract (GSPE) ameliorates molecular clock desynchrony and energy metabolism in white adipose tissue (WAT). We hypothesized that proanthocyanidins effects could be influenced by the time of administration as many functions of WAT display circadian rhythms. To this end, inguinal WAT explants from lean (STD) and obese (i.e., kept for 5 weeks on a high-fat diet (HFD)) *PER2::LUC* mice were treated with metabolites present in the serum of GSPE-administered rats (GSPM) at the peak or trough of PER2::LUC bioluminescence. iWAT explants obtained from obese animals presented a lower amplitude, longer period, and phase delay compared to explants from lean animals. In response to GSPM treatment, iWAT explants of both lean and obese mice increased PER2::LUC amplitude and period compared to untreated explants only when GSPM was given at the trough of the luminescence rhythm. Interestingly, GSPM treatment upregulated the expression of genes involved in lipogenesis (*Acaca*), lipolysis (*Atgl*), and appetite regulation (*Lep*) in iWAT explants from lean mice, while lipid metabolism genes such as *Lpl* were affected in explants from obese mice mainly when GSPM was given at the peak of the PER2::LUC signal. These results show that physiological metabolites derived from GSPE consumption affect molecular clock rhythm and lipid metabolism of iWAT in a time-dependent manner. Therefore, chrono-utilization of food bioactive compounds warrants further investigation as potential strategy for the management of metabolic disruptions such as obesity.

Keywords: adipocyte, circadian clock, obesity, proanthocyanidin, time-of-day.

1. Introduction

Many physiological processes in mammals are regulated by endogenous circadian clocks. The resulting 24-hour rhythms are an important adaption in anticipation of predictable environmental changes. Mammals have a hierarchical circadian system with a central oscillator, the suprachiasmatic nucleus (SCN), which is localized in the hypothalamus. CN clocks receive external light information from melanopsin-expressing retinal ganglion cells to align internal with external time. Through different pathways, such as core body temperature, nervous input, and hormones, the SCN resets subordinate clocks throughout the body – a process that is essential for systemic metabolic homeostasis (1).

At the molecular level, circadian clocks consist of interlocked transcription-translation feedback loops. The transcriptional activators circadian locomotor output cycles kaput (CLOCK) and brain and muscle ARNT-like protein 1 (ARNTL or BMAL1) form a heterodimer which activates the transcription of the period (*Per1-3*) and cryptochrome (*Cry1/2*) genes. PER and CRY proteins form complexes that migrate to the nucleus and inhibit the activity of CLOCK/BMAL1, which leads to a reduction of *Per* and *Cry* gene expression. In a secondary loop, the CLOCK/BMAL1 heterodimer enhances the transcription of retinoic acid-related orphan receptors (*Rorα-γ* or *Nr1f1-3*) and the nuclear receptor subfamily 1, group D (*Nr1d1/2* or *Rev-erbα/β*). ROR and REV-ERB proteins increase and decrease *Bmal1* transcription, respectively (1, 2). Disruption of the clock machinery, e.g., by rotating shift work, results in various health problems, including metabolic disorders such as obesity, since energy metabolism and the circadian clock are highly interlocked (3, 4).

The worldwide prevalence of obesity has dramatically increased over the last years. This disease is characterized by excessive fat accumulation due to an

imbalance between energy intake and expenditure. White adipose tissue (WAT) plays a crucial role in energy homeostasis (2). In obesity WAT function is impaired with increased inflammation, insulin resistance, and circadian rhythm disruption (5, 6).

Besides light, sleep/wake, temperature, and fasting/feeding cycles can act as time signals (*zeitgeber*) for peripheral tissue clocks (1, 7). Dietary components, such as polyphenols, have been shown to modulate circadian clock gene expression in different experimental models. Proanthocyanidins, a type of polyphenols found in grape seed extract (GSPE), were shown to upregulate expression of *Per2*, *Clock* and *Bmal1*, and downregulate *Rorα* and *Rev-erbα* in adipose tissue of Wistar rats (8). Furthermore, GSPE effects depend on their administration time since tissue responses are tightly linked to their circadian rhythm (9, 10). In rats, GSPE administration at the beginning of the active phase (i.e., when the lights are turned off, ZT12) reduces adipocyte size, increased the percentage of smaller fat cells, and downregulates the expression levels of genes involved in lipid transport, lipolysis, adipogenesis. These effects are not observed when GSPE is administrated at the beginning of the resting phase (i.e., when the lights are turned on, ZT0) (11).

However, it remains unknown whether GSPE effects on WAT function are due to a direct effect on adipocytes or, in contrast, represent a less specific and more systemic response. Therefore, in the current study we hypothesized that the physiological metabolites that are present in the serum of GSPE-administered animals (GSPM) could directly affect the iWAT circadian clock and key genes involved in iWAT physiology. Thus, iWAT explants from lean and obese mice were treated with GSPM at two different time points. We show that treatment of GSPM has a clear time-dependent effect. The effects in the clock gene machinery

are more pronounced when GSPM is given at the trough of *PER2* expression. However, the effects of GSPM on lipid metabolism-related gene expression are higher when GSPM is provided at the peak of *PER2*. These differential results lend further support to the therapeutic potential of polyphenols in the treatment of obesity in humans.

2. **Materials and methods**

2.1. Proanthocyanidin extract

Grape seed proanthocyanidin extract (GSPE) used in this study was composed of monomers (21.3%), dimers (17.4%), trimers (16.3%), tetramers (13.3%), and oligomers (5-13 units; 31.7%) of proanthocyanidins. GSPE was kindly provided by Les Dérivés Résiniques et Terpéniques (Dax, France). The phenolic composition of this extract was further analysed by Margalef et al (12).

2.2. Production of GSPE metabolites in rat serum

In this study, 13-14-week-old male Wistar rats that weighed 400–480 g were purchased from Charles River Laboratories (Spain). Animals were housed in animal quarters at 22 °C under a 12-hour:12-hour light:dark cycle (lights on from 9:00 a.m. to 9:00 p.m.). The animals consumed tap water and a standard chow diet (Panlab A04, Spain) *ad libitum* throughout the experiment. Rats were randomly divided into two groups: control (n=6) and GSPE (n=7). The rats from the GSPE group were administered 1 g/kg of body weight of GSPE by oral gavage in 1 ml of water. The control group was orally administered 1 ml of water. Treatments were administered between 9 and 10 a.m. after overnight fasting. Two hours later, the rats were sacrificed by decapitation and trunk blood was collected. The blood was maintained at room temperature for 30 min. Once the blood coagulated, it was centrifuged at 2,000 × g and 4 °C for 15 min to obtain

serum which was stored at −80 °C until analysis. The Animal Ethics Committee of the University Rovira i Virgili (Tarragona, Spain) approved all procedures (reference number 11464 by Generalitat de Catalunya).

2.3. Extraction of serum proanthocyanidins

To obtain the metabolized proanthocyanidins from rat serum, serum samples were pretreated by off-line micro-solid-phase extraction (μSPE) following the methodology that was previously described by Martí et al. (13) using 30-μm OASIS HLB μElution plates (186001828BA; Waters, Spain). Briefly, the microcartridges were sequentially conditioned with 250 μl of methanol and 250 μl of 0.2 % acetic acid. Prior to extraction, the serum was centrifuged at 2,000 × g and 4 °C for 5 min. Two serum aliquots (each of 350 μl) were mixed, each of them, with 350 μl of 4 % phosphoric acid and 50 μl of pyrocatechol (2,000 ppb) and then loaded onto the plate. The loaded plate was washed with 200 μl of Milli-Q water and 200 μl of 0.2 % acetic acid. The retained flavanols on the plate were eluted with 2 × 50 μl of an acetone/Milli-Q water/acetic acid solution (70:29.5:0.5, v:v:v). The two eluates were mixed to obtain a final volume of 200 μl. Part of the solution (25 μl) was evaporated to dryness using a SpeedVac Concentrator SPD 2010 SAVANT (Thermo Scientific, Germany) at room temperature and redissolved in 25 μl of an acetone/Milli-Q water/acetic acid solution (70:29.5:0.5, v:v:v). A chromatographic analysis for the determination of the compounds of serum metabolites of GSPE-administered rats was analyzed by Guerrero et al. (14). The remaining 175 μl of the semi-purified serum was evaporated to dryness at room temperature using the same procedure described above and then stored at −80 °C.

2.4. *Experimental design of adipose tissue explant cultures from mice*

A summary of the experimental design is shown in Figure 1.

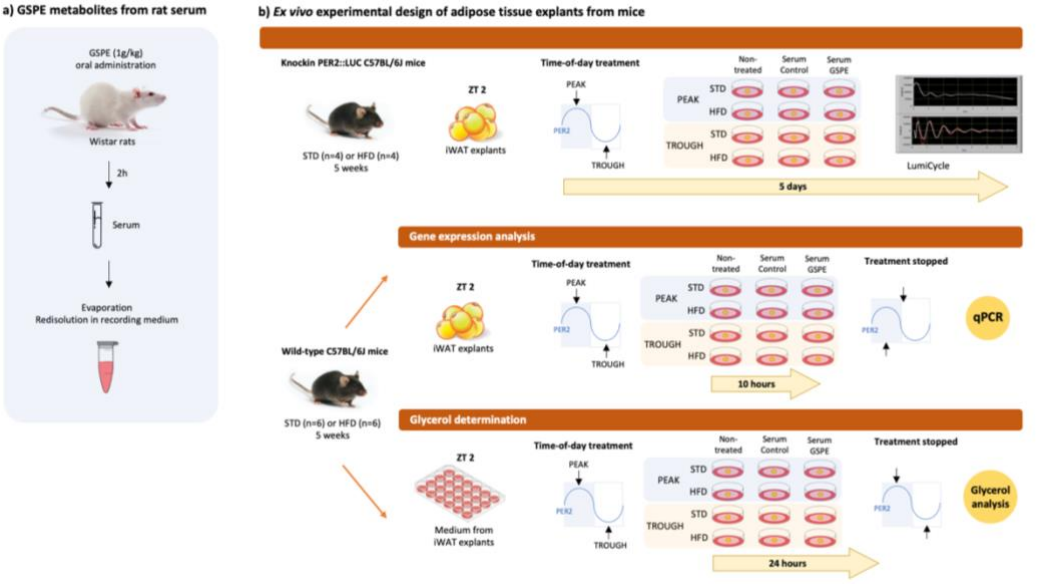

Figure 1. *Experimental design. a) Isolation of GSPM metabolites from rat serum; b) treatment of murine adipose tissue explants with GSPM extracts.*

2.4.1. *Treatment*

Each dried purified serum was redissolved in 4.8 mL of recording culture medium. The composition of recording medium was 1 L autoclaved double-distilled water, 1 g of DMEM low-glucose medium powder (Sigma-Aldrich, Germany), 4 g of glucose powder, 4.7 mL of sodium bicarbonate (7.5 %), 10 mL of HEPES buffer (1 M), and 10 mL penicillin/streptomycin (1 %) (all items from ThermoFisher, Germany). At indicated times, adipose tissue explants were treated with a dilution of 1:20 (v:v) plus B-27 (2 %) (ThermoFisher, Germany). For LumiCycle analyses luciferin (200 μM, AppliChem, Germany) was added at the time of treatment.

2.4.2. *LumiCycle analysis of PER2::LUC explants*

Eight 8-week-old heterozygous *PERIOD2::LUCIFERASE* (*PER2::LUC*) knockin C57BL/6J mice (15) were housed under a 12-hour:12-hour light:dark cycle (lights on at 7 a.m.) at 22 °C, 55 % of humidity and fed *ad libitum* with standard chow diet (1314, Altromin, Germany) and tap water for one week of adaptation. For five weeks, 4 mice were fed with standard chow diet and 4 mice with high-fat diet (E15742 EF D12492, 60 % kJ fat, Sniff Laboratories, Germany). Body weight was determined weekly. At the end of the experiment, mice were sacrificed at ZT2 by cervical dislocation. iWAT was collected and kept in HBSS (ThermoFisher, Germany) aerated with carbogen. A small piece of iWAT (around 3 μm in diameter) was placed onto floating inserts (0.4 μm, Merck, USA, PICM0RG50) for each condition, previously cleaned and sterilized by UV radiation, in a 35-mm dish containing culture medium supplemented with 2 % of B-27 and 200 μM of luciferin. Dishes were sealed with round coverslips and incubated at 32.5 °C. Animal experiments were performed with the approval of the ethics committee of the Ministry of Consumer Protection, Agriculture and Energy Change of the state of Schleswig-Holstein, DE.

The acrophase of the *PER2::LUC* luminescence rhythm was detected around 13 hours after the sacrifice, therefore half of the samples were treated at this moment (peak treatment). The following trough was at around 27 hours after the sacrifice. Therefore, the other half of the samples were treated at this moment (trough treatment). 100 μL of medium were removed from the dish and replaced by 100 μL of B-27-supplemented recording medium with serum metabolites from control (Ct) and GSPE animals (GSPM). Samples were placed in the LumiCycle luminometer (Actimetrics, USA) for five days at 32.5 °C. Bioluminescence recordings were performed for 1 min each at 10-min intervals.

2.4.3. Gene expression analysis of wild-type C57BL/6J mice

Twelve 8-week-old wild-type C57BL/6J mice were purchased from Janvier (Germany). Animals were fed and housed as described in 2.4.2. Body weight was determined weekly. At the end of the experiment, mice were sacrificed at ZT2 by cervical dislocation. iWAT was collected and kept in HBSS (ThermoFisher, Germany) aerated with carbogen. Small pieces of iWAT (around 3 μm in diameter) were placed into 24-well plates with 1 mL of culture medium supplemented with 2 % of B-27 per well. Afterwards, the plates were incubated at 32.5 °C.

Samples were treated with extracts at two times as described above. 50 μL of medium was removed from the wells and replaced with 50 μL of B-27 supplemented culture medium with serum metabolites from control (Ct) or GSPE (GSPM) animals. Samples were placed back in the incubator for 10 hours and frozen at -80 °C afterwards for gene expression analysis.

2.4.4. Medium glycerol determination

Explants of eight wildtype C57BL/6J mice (4 mice fed STD and 4 fed HFD) used for gene expression analysis of iWAT explants were also used for glycerol determination. Explants were prepared as described and treated at peak or trough. All culture medium was removed and replaced by B-27 supplemented medium with 2 % of bovine serum albumin (BSA) previously filtered with a syringe. Immediately, 50 μL of B-27 supplemented culture medium with serum metabolites from control (Ct) or GSPE (GSPM) animals were added in each sample. Samples were collected after 24 hours. The piece of iWAT was weighed to normalize medium glycerol content to tissue mass. Medium was collected and stored at 4 °C for glycerol determination following the protocol of the manufacturer (Glycerol Assay Kit, Abcam, United Kingdom).

2.5. Gene expression analysis

For gene expression analysis, iWAT was processed to isolate total RNA using TRIzol. RNA quantity and purity were measured with a NanoDrop 1000 spectrophotometer (Thermo Scientific, Germany). Reverse transcription was performed to obtain cDNA using the High-Capacity Complementary DNA Reverse Transcription Kit (Thermo Fisher, Germany). Gene expression was analyzed by quantitative PCR using the iTaq Universal SYBR Green Supermix (Bio-Rad, USA) in real-time PCR system (Applied Biosystems, Germany) using primers obtained from Eurofins (Germany). The PCR protocol consisted of 95 °C for 3 min, followed by 40 cycles of 94 °C for 15 s, 60 °C for 15 s, 72 °C for 20 s. Primer specificity was confirmed by the presence of single peaks in the melting curve. Forward and reverse primers used in this study are listed in Table 1. The relative expression of each gene compared to eukaryotic elongation factor 1 alpha (*eEF1α*) mRNA levels and normalized to the levels measured in the corresponding control group was determined. The ΔΔCt method was used and corrected for primer efficiency (16).

Table 1. Primers for the qPCR analysis.

Gene	Forward primer (5'...3')	Reverse primer (5'...3')
Acaca	GCCTTTCACATGAGATCCAGC	CTGCAATACCATTGTTGGCGA
Adipoq	CTCCACCCAAGGGAACTTGT	TAGGACCAAGAAGACCTGCATC
Atgl	TTCGCAATCTCTACCGCCTC	AGCAAAGGGTTGGGTTGGTT
Cd36	TGAATGGTTGAGACCCCGTG	TAGAACAGCTTGCTTGCCCA
Eef1α	CAC ATC CCA GGC TGA CTG T	TCG GTG GAA TCC ATT TTG TT
Glut4	GGCATCAATGCTGTTTTCTACTATT	TCTACTAAGAGCACCGAGACCAAC
Hsl	TGTCACGCTACACAAAGGCT	AATCGGCCACCGGTAAAGAG
Lep	GAGACCCCTGTGTCGGTTC	CTGCGTGTGTGAAATGTCATTG
Lpl	GAAAGGGCTCTGCCTGAGTT	TAGGGCATCTGAGAGCGAGT
Mgl	AAGACTAATGGAAACAGGGCCTA	TGGGACACAAAGATGAGGGC
Pparγ	TACTGTCGGTTTCAGAAATGCC	GTCAGCGGACTCTGGATTCAG
Sirt1	GATGACAGAACGTCACACGC	ATTGTTCGAGGATCGGTGCC
Tnfα	GAAAAGCAAGCAGCCAACCA	CGGATCATGCTTTCTGTGCTC

2.6. Rhythm analyzes

Samples were treated at the peak or trough of *PER2* bioluminescence, which corresponded to 13 or 27 h after the experiment started. Every 10 min, baseline-subtracted (24-hour running average) bioluminescence data were collected for 5 days. The first 36 h were removed from the analyzes. Minimal and maximal mean values from chow were used to normalize the bioluminescence data. For GSPM treatment, values from Ct treated at the peak were used to normalize the data. Rhythmicity was assessed using the CircaSingle algorithm as previously described (17). Rhythm parameters (phase, amplitude, period, dampening rate) were exported to Prism 9 (GraphPad, USA) and two-way ANOVA followed by Bonferroni post-tests was used for statistical evaluation. A p-value < 0.05 was considered statistically significant. In the figures, values are shown as mean ± SEM.

2.7. Non-rhythm-related statistical analyzes

Data are expressed as mean ± SEM (n = 4-6). Grubbs' test (alpha = 0.1) was applied to detect outliers. Statistical tests and graphs were done with GraphPad Prism 9. Data were analyzed using Student's *t* test with Welch correction or two-way ANOVA followed by Bonferroni post-hoc test. A p-value < 0.05 was considered statistically significant.

3. Results

3.1. HFD results in amplitude reduction, increased period, and phase delay of PER2 in iWAT

HFD-fed animals presented higher body weight compared to STD-fed animals from week 3 onwards. At the end of the experiment (5th week), a body weight increment of 15.6 % was found in obese mice compared to lean animals (**Figure S1**). In the 5th week, mice were sacrificed and *PER2* bioluminescence was evaluated in iWAT explants. iWAT explants obtained from HFD-fed animals showed a significant longer period (24.3 *vs.* 22.5 h), phase delay (13.1 *vs.* 10.4 h), a reduction of amplitude (50 %), and a reduced dampening rate of 33 % compared to explants of STD-fed animals (Figure 2 a – e).

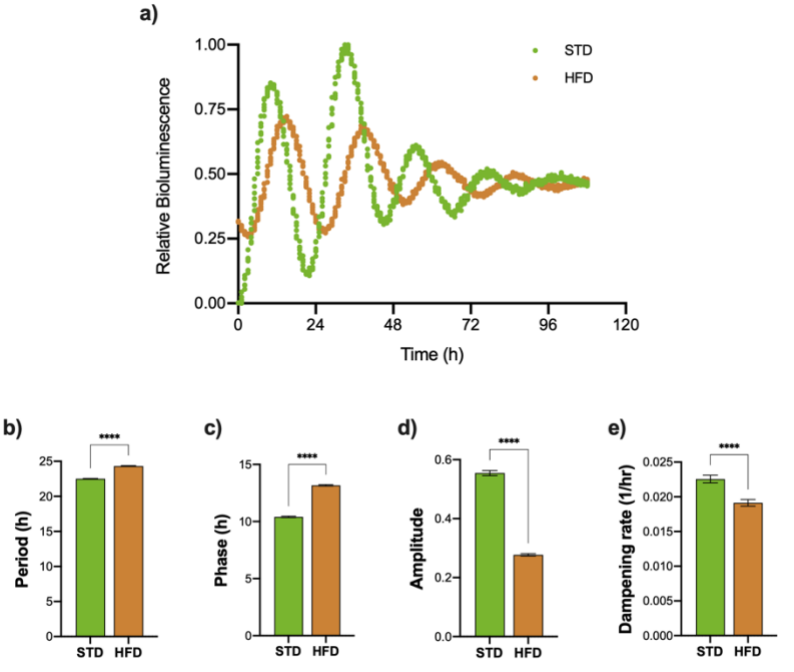

Figure 2. *PER2::LUC circadian rhythm analysis of STD- or HFD-fed iWAT explants. a) Average of normalized bioluminescence data. b – e) Rhythmic parameter evaluation (CircaSingle). n = 7 - 8. Unpaired Student's t test with Welch correction was applied. **** = p < 0.0001.*

3.2. *In response to GSPM treatment, iWAT explants obtained from lean animals exhibit increased period and higher amplitude only when treatment was given at the trough of PER2 bioluminescence*

In iWAT explants from STD animals, GSPM treatment at the peak of *PER2* bioluminescence resulted in a reduced period (25.9 *vs.* 21.6 h), but significant alterations in amplitude and phase were not detected. In addition, decreased dampening rates (40 %) were observed in response to peak GSPM treatment. In contrast, GSPM treatment at the trough of *PER2* bioluminescence significantly resulted in increased period (22.6 *vs.* 24.5 h) and higher amplitudes (40 %) without any effect on phase and dampening rates (Figure 3 a - e).

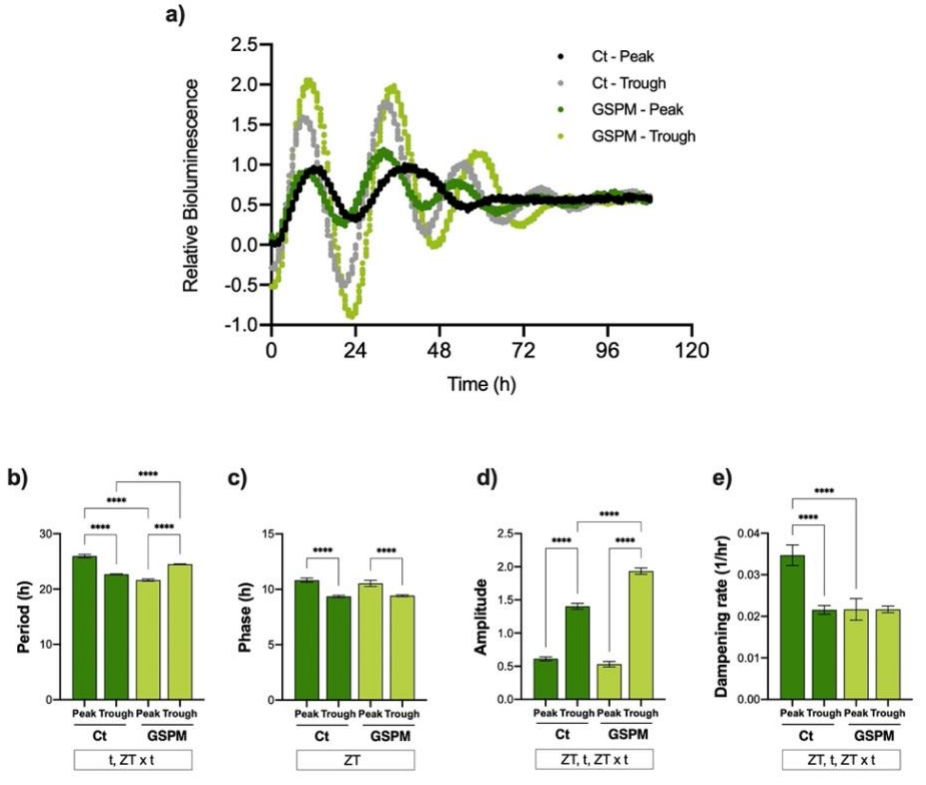

Figure 3. *PER2::LUC circadian rhythm analysis of serum control-treated (Ct) and serum GSPM-treated groups of STD iWAT explants which were treated at peak or trough of PER2. a) Average of normalized bioluminescence data. b – e) Rhythmic parameter evaluation (CircaSingle). n = 3 - 4. Two-way ANOVA followed by Bonferroni post-hoc test; t, treatment effect; ZT, time-of-day treatment; ZT x t, interaction between treatment and time-of-day treatment. **** = p < 0.0001.*

3.3. *In response to GSPM treatment, iWAT explants obtained from obese animals present increased period, phase advance and higher amplitude only when treatment was given at the trough of PER2 bioluminescence*

GSPM treatment at the peak of *PER2* bioluminescence in iWAT explants obtained from obese animals did not affect period, but led to a marked phase delay (9.6 *vs.* 17 h), reduced amplitude (60 %), and a higher dampening rate (20 %) compared to untreated explants. Interestingly, treatment at the trough of *PER2* bioluminescence resulted in increased period (24.2 *vs.* 25.1 h), a slight phase advance (12.9 *vs.* 11.5 h), and a marked amplitude increase (320 %) without any effect on dampening of the PER2::LUC rhythm (Figure 4 a – e).

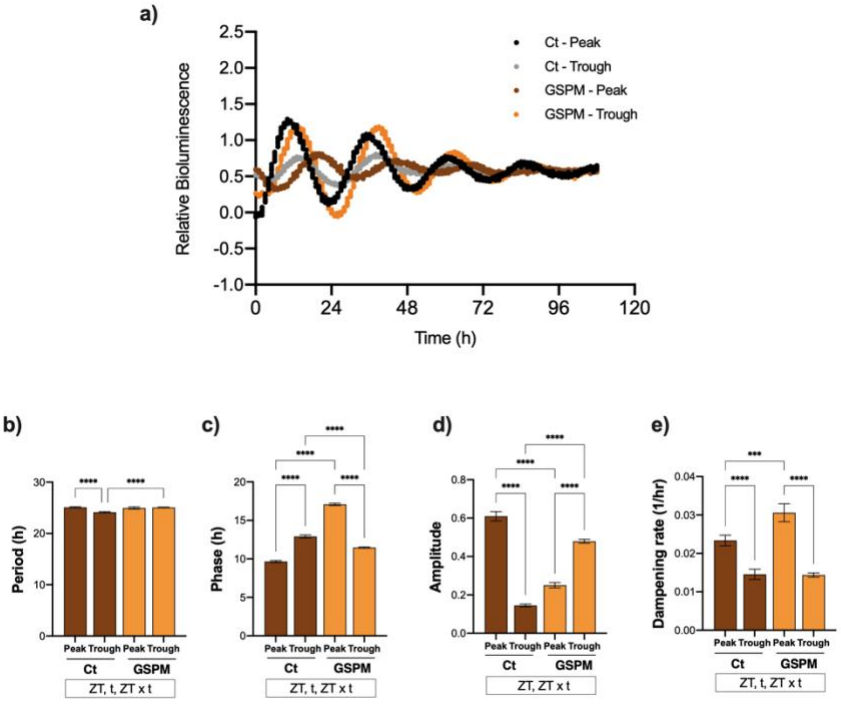

Figure 4. *PER2::LUC circadian rhythm analysis of serum control-treated (Ct) and serum GSPM-treated groups of HFD iWAT explants which were treated at peak or trough of PER2. a) Average of normalized bioluminescence data. b – e) Rhythmic parameters evaluation (CircaSingle). n = 3 - 4. Two-way ANOVA followed by Bonferroni post-hoc test; t, treatment effect; ZT, time-of-day treatment; ZT x t, interaction between treatment and time-of-day treatment. *** = p < 0.001; **** = p < 0.0001.*

3.4. Gene expression analysis in iWAT explants obtained from wild-type C57BL/6J mice

Diet effects on body weight in wild-type mice were also recorded weekly. As expected, HFD-fed animals presented significant higher body weight (14 % increase) compared to STD-fed animals at the last week of the experiment (Figure S2). iWAT explants obtained from HFD-fed animals presented a downregulation of the expression of important mRNA transcripts including *Acaca*, *Lep* and *Tnfα* compared to lean mice. In addition, *Pparγ*, *Atgl* and *Adipoq* gene expression presented an interaction between diet and time-of-day experiment preparation. Specifically, obese explants prepared at the peak of *PER2* showed an upregulation of *Atgl* and *Adipoq* expression levels, while a downregulation in the expression levels of these genes was observed when experiment started at the through of *PER2* bioluminescence (Figure S3 a – i).

3.4.1. GSPM treatment upregulates lipogenesis, lipolysis and leptin-related gene expression in iWAT explants obtained from STD animlas with a more evident effect when treatment was given at peak of PER2 bioluminescence

GSPM treatment upregulated the expression of transcripts associated with lipogenesis (*Acaca*), glucose transport (*Glut4*), lipolysis (*Atgl*, *Hsl* and *Mgl*), and leptin (*Lep*) in iWAT explants obtained from lean animals. For *Acaca*, *Atgl* and *Lep* genes, this upregulation in response to GSPM incubation was significantly higher when explants were treated at peak (Figure 5 a - i).

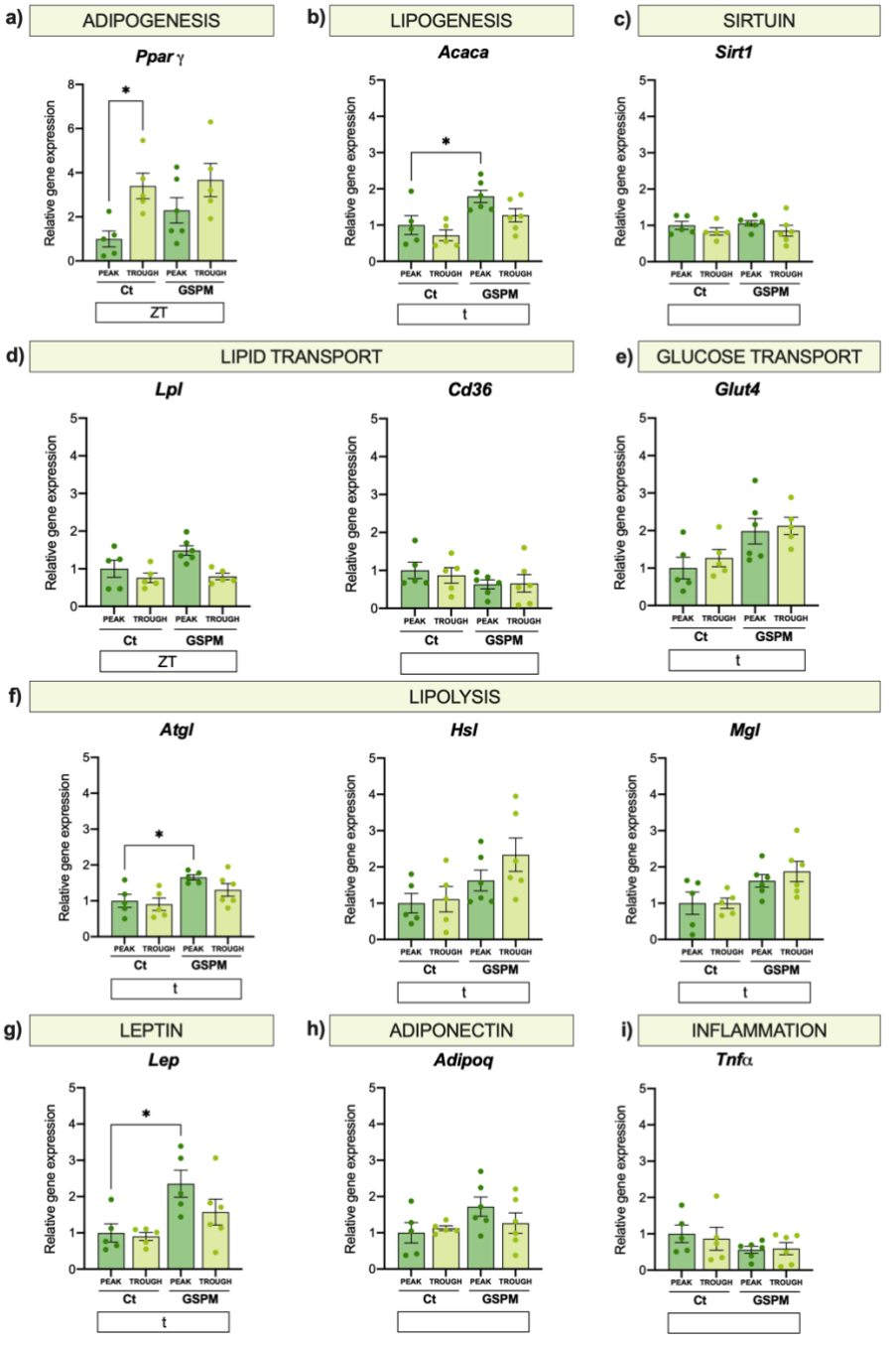

Figure 5. *Expression of metabolism-associated transcripts in serum control-treated and serum GSPM-treated groups of STD iWAT explants which were treated at peak or trough of PER2. Expression of genes related to adipogenesis (a), lipogenesis (b), sirtuin (c), lipid transport (d), glucose transport (e), lipolysis (f), leptin (g), adiponectin (h) and inflammation (i). Ct, explants treated with serum metabolites from control; GSPM, explants treated with serum metabolites from GSPE. n = 5 - 6. Two-way ANOVA followed by Bonferroni post-hoc test; t, treatment effect; ZT, time-of-day treatment. * = p < 0.05.*

3.4.2. *GSPM treatment upregulates Lpl gene expression in iWAT explants obtained from obese animals mainly when treatment was given at the peak of PER2 bioluminescence*

iWAT explants from HFD-fed animals treated at trough presented an upregulation of transcripts associated with adipogenesis (*Pparγ*) and a downregulation of sirtuin 1 (*Sirt1*), lipid transport (*Lpl*), and leptin (*Lep*) compared to peak independently of treatment. However, GSPM upregulated the expression of genes involved in lipid transport (*Lpl*) and lipolysis (*Atgl*) with more significant impact when GSPM was given at peak (Figure 6 a - i). However, when glycerol concentrations (product of TAG lipolysis) were analyzed in the culture medium of iWAT explants, no significant differences were observed between the groups (Figure S4**)**.

4. Discussion

In this study, we used an established circadian luminescence reporter, PER2::LUC, to determine the effects of obesity on the regulation of the circadian clock of iWAT and to evaluate the therapeutical value of proanthocyanidins in this context. We demonstrated a potential effect of physiological metabolites that are present in the serum of GSPE-administered animals (GSPM) according to time-of-day treatment. The GSPM effects on clock gene machinery were more noticeable when it was given at the trough of PER2::LUC expression, while GSPM effects on lipid metabolism-related gene expression were more pronounced when GSPM was provided at the peak of PER2::LUC (Table S1).

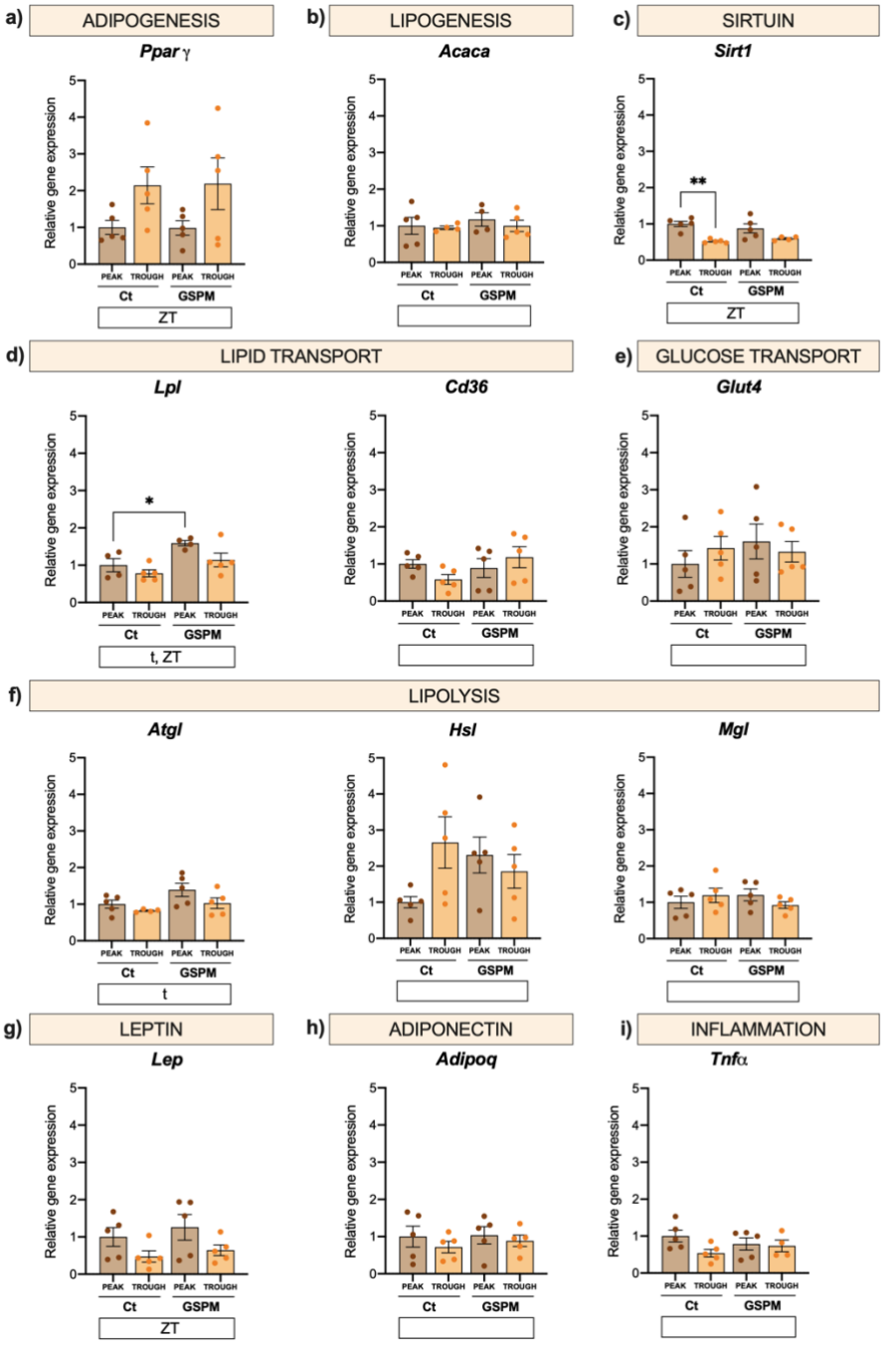

Figure 6. *Gene expression of serum control-treated and serum GSPM-treated groups of HFD iWAT explants which were treated at peak or trough of PER2. Expression of genes related to adipogenesis (a), lipogenesis (b), sirtuin (c), lipid transport (d), glucose transport (e), lipolysis (f), leptin (g), adiponectin (h) and inflammation (i). Ct, explants treated with serum metabolites from control; GSPM, explants treated with serum metabolites from GSPE. n = 4 - 5. Two-way ANOVA followed by Bonferroni post-hoc test; t, treatment effect; ZT, time-of-day treatment. * = p < 0.05.*

Our results demonstrate that adipose tissue explants from obese animals show a longer period, a phase delay, and lower amplitude compared to adipose tissue from STD-fed mice. Different studies reported that *Per2* rhythms in adipose tissue present a phase delay under insulin stimuli (18) and that HFD alters circadian clock and circadian clock-controlled gene expression in the liver and kidneys with a phase advance of 4-5 hours for *Per2* mRNA in liver (19-21). Interestingly, another study showed that a significant portion of liver metabolites are phase advanced, while *Per2* is phase delayed, in obese mice compared to chow animals (22). Mice under chow diet eat mostly during the dark with some activity and meal bouts in the light phase. However, introduction of HFD for 1 week leads to an increase in light phase food intake and desynchronized eating patterns (20). Among different organs, the liver is the only tissue that shows a marked effect in response to HFD. However, it is not yet clear whether liver rhythms shift is due to the observed change in eating behavior or as a direct effect of HFD on the tissue (20). Controversy exists whether circadian rhythm disruption is caused by an obesogenic diet or obesity itself. Some authors demonstrated that HFD leads to a marked alteration in the clock functioning in many tissues (21-23). Nevertheless, others postulate that obesity, and not diet itself, promotes *Bmal1* rhythm disruption. One potential mechanism involves adipose tissue release of the proinflammatory cytokine *Tnfα* which inhibits *PPARγ* expression via the suppression of its activator *C/EBPδ* (24). This reduction in *PPARγ* results in a reduction of glutamine and methionine in adipocytes, two epigenetic regulators of *Bmal1*. This leads to a downregulation in the expression of *Bmal1* and other clock genes causing a clock disfunction in adipose tissue (25). In humans, *PER2* expression between obese and lean individuals is not affected, but reduced amplitudes for *CRY2* and *NR1D1* were found in adipose tissue (26). In mice, 6 weeks of HFD do not affect the phase, but lead to a marked reduction in amplitude

of *Per2* (27). To the best of our knowledge, this is the first report in which adipose tissue explants from HFD-fed mice show a significant reduction in amplitude, phase delays, and reduced period length of *PER2* bioluminescence rhythms. Interestingly, weakened *PER2* rhythms were associated with a slight decrease in dampening, which argues that, although the rhythms are weaker, individual period length variation between cells may be smaller, thus increasing coherence across the specimen, at least *in vitro*.

Another aim of this study was to determine whether GSPM could restore the changes in circadian rhythms produced by HFD and whether GSPM effects were dependent on the time of treatment. It is important to consider that the molecular forms of GSPE that reach the circulation and tissues are different from those that are present in GSPE before its consumption. Proanthocyanidins are metabolized by intestinal cells, microbiota and liver, and cause the modification of these molecules (28). Therefore, to evaluate *in vitro* the effects of GSPE on WAT explants, it is important to use the metabolites found in serum of GSPE-administered rodents.

Interestingly, our data show an important role of treatment time: responses to GSPM treatment were higher when it was given around the trough of *PER2* bioluminescence, which roughly corresponds to the normal rest phase *in vivo*. In both STD- and HFD-fed iWAT explants, GSPM treatment significantly increased rhythm period and amplitude. Only in iWAT explants obtained from HFD-fed animals, a phase advance was observed. Treatment did not affect the dampening rate suggesting a specific time-of-day dependent effect of GSPM in modulating the adipose circadian clock. Corroborating literature shows that GSPE consumption at ZT1 in male Wistar rats upregulates *Per2* gene expression in mesenteric WAT under STD (50 mg/kg of GSPE) and HFD (25 mg/kg of GSPE)

compared to STD vehicle group (8). However, it is still speculative how GSPE or GSPM could affect *Per2* or other clock genes in *in vivo*.

We also studied whether GSPM affected the expression of genes involved in lipid and glucose metabolism in a time-of-day dependent manner in iWAT explants from lean and obese mice. We observed that iWAT explants from HFD-fed mice presented a lower expression of genes involved in lipogenesis, leptin signaling, and inflammation compared to lean animals. Lower expression of lipogenesis may indicate increased insulin resistance (29). When glucose is not taken up by WAT, lipogenesis is reduced. Moreover, leptin is a hormone secreted by adipocytes in response to food intake which acts in the hypothalamus upregulating energy expenditure and stimulating satiety (30). Circulating leptin is elevated in obesity (31). Therefore, we expected to find an overexpression of *Lep* in HFD explants. Furthermore, the stable expression levels of the inflammatory gene *Tnfα* were unexpected as increased *Tnfα* has previously correlated with adiposity and insulin resistance (32). However, it is important to take into consideration that gene expression data in this study only reports from a single time point. Therefore, it is plausible that HFD induced a phase shift as it is known that *Tnfα* mRNA presents circadian rhythm (33). Interestingly, in iWAT explants obtained from lean animals - but not from obese ones – GSPM upregulated lipogenesis (*Acaca*), glucose transport (*Glut4*), lipolysis (*Atgl*, *Hsl* and *Mgl*) and leptin related transcripts. This effect was more significant when GSPM was treated at peak, specifically for *Acaca*, *Atgl*, and *Lep*. In obese explants, GSPM upregulated the expression of genes associated with lipid transport (*Lpl*) and lipolysis (*Atgl*). The upregulation of *Lpl* was clearer when GSPM was treated at peak in obese explants (or when samples were collected at ZT1). It is known that GSPE affects lipid and glucose metabolism inducing a beneficial effect on HFD-fed animals.

Specifically, it was demonstrated that GSPE consumption increases the capacity to store and mobilize fat from WAT. This simultaneous activation of anabolic and catabolic pathways in WAT in response to GSPE consumption has been demonstrated in *in vivo* and *in vitro* experiments, suggesting an activation of lipid metabolism (34-37).

It is plausible to speculate that GSPE affects clock gene expression, such as *Per2*, which in turn modulates lipid metabolism since the regulation of lipid metabolic pathways by the molecular clock is well documented (38). Indeed, *Per2* null mice show an increment in fatty acid transport which may be compensated by a higher oxidative capability observed in the expression levels of genes involved in fatty acid oxidation in WAT, suggesting the involvement of *Per2* in lipid transport and oxidation (39). However, most of the studies so far did not investigate whether the effects of GSPE depend on the time of treatment. We previously demonstrated that GSPE consumption at ZT12 downregulates lipid transport and lipolysis genes in cafeteria diet-fed rats, which appears in opposite to the results from the current study (11). Such differences could be explained by different effects of GSPE on subcutaneous and visceral fat depots and between lean and obese animals (40). Other explanations could be differences in the animal species, genetic background, sex, GSPE dosage, and differences in the experimental setup.

Interestingly, most of the effects on PER2::LUC circadian parameters in response to GSPM treatment were observed when lean and obese iWAT explants were treated at PER2::LUC trough. However, metabolic gene expression data revealed marked effects when treatment was given at the peak. It should be highlighted that gene expression data reflect more acute effects (10 h) while bioluminescence data was obtained over longer periods (5 days). Taking into consideration that the duration between bioluminescence and qPCR experiments

were different, one could speculate that differential responses in fact may corroborate time-dependent effects of GSPM on iWAT, as were also shown by Ribas-Latre, et al. (10).

Although we provide interesting results, some limitations of our study are present. We studied the expression of genes at a single time point; therefore, it is not clear whether the differences found are due to changes in rhythmic parameters for the transcripts. With regard to luminescence data, some acute GSPM effects might not be preserved over the long cultivation period.

Taken altogether, our study provides novel data regarding the effects of HFD on iWAT clock functioning and the beneficial effects of GSPE metabolites on regulating the adipose circadian clock as well as key metabolic genes. We also provide a perspective on a chrono-utilization of GSPE and other polyphenols for the management of obesity, which warrants further validation in preclinical and in clinical studies.

Acknowledgments: This work was supported by grants of the German Research Foundation (DFG) to HO 353-10/1, HO 353-11/1, GRK-1957, and CRC-296 "LocoTact" (TP13), and we gratefully acknowledge the aid of laboratory technicians Niurka Dariela Llópiz and Rosa Pastor from Universitat Rovira i Virgili.

Supplementary Materials: Figure S1: Body weight during 5 weeks of STD or HFD-fed PER2::LUC mice; Figure S2: Body weight during 5 weeks of STD or HFD-fed wile-type mice; Figure S3: Gene expression of leam and obese iWAT explants which were prepared at two different times – peak or trough of PER2; Figure S4: Glycerol content in the medium of adipose tissue explants from STD or HFD-fed mice treated at peak or trough; Table S1: Summary of gene expression analysis.

Author Contributions: M.C-P., L.V.M.A, G.A., A.A., M.M. and H.O.: conceptualization; M.C-P. and L.V.M.A.: data curation, formal analysis, and investigation; M.C-P., L.V.M.A. and R.M.R.: methodology; H.O. and G.A.: funding acquisition; H.O.: project administration and supervision; M.C-P. and L.V.M.A.: writing - original draft.; all authors: text review & editing.

Conflicts of Interest: The authors declare no conflict of interest. The funders had no role in the design of the study; in the collection, analyses, or interpretation of data; in the writing of the manuscript, or in the decision to publish the results.

References

1. de Assis LVM, Oster H. The Circadian Clock and Metabolic Homeostasis: Entangled Networks. *Cell Mol Life Sci* (2021). Epub 2021/03/09. doi: 10.1007/s00018-021-03800-2.
2. Lekkas D, Paschos GK. The Circadian Clock Control of Adipose Tissue Physiology and Metabolism. *Auton Neurosci* (2019) 219:66-70. Epub 20190508. doi: 10.1016/j.autneu.2019.05.001.
3. Green CB, Takahashi JS, Bass J. The Meter of Metabolism. *Cell* (2008) 134(5):728-42. Epub 2008/09/09. doi: 10.1016/j.cell.2008.08.022.
4. Gooley JJ, Chua EC. Diurnal Regulation of Lipid Metabolism and Applications of Circadian Lipidomics. *J Genet Genomics* (2014) 41(5):231-50. Epub 20140421. doi: 10.1016/j.jgg.2014.04.001.
5. Goossens GH. The Metabolic Phenotype in Obesity: Fat Mass, Body Fat Distribution, and Adipose Tissue Function. *Obes Facts* (2017) 10(3):207-15. Epub 20170601. doi: 10.1159/000471488.
6. Froy O, Garaulet M. The Circadian Clock in White and Brown Adipose Tissue: Mechanistic, Endocrine, and Clinical Aspects. *Endocr Rev* (2018) 39(3):261-73. Epub 2018/03/01. doi: 10.1210/er.2017-00193.
7. Finger AM, Kramer A. Mammalian Circadian Systems: Organization and Modern Life Challenges. *Acta Physiol (Oxf)* (2020):e13548. Epub 2020/08/28. doi: 10.1111/apha.13548.
8. Ribas-Latre A, Baselga-Escudero L, Casanova E, Arola-Arnal A, Salvadó MJ, Arola L, et al. Chronic Consumption of Dietary Proanthocyanidins Modulates Peripheral Clocks in Healthy and Obese Rats. *J Nutr Biochem* (2015) 26(2):112-9. Epub 20141013. doi: 10.1016/j.jnutbio.2014.09.006.
9. Rodríguez RM, Cortés-Espinar AJ, Soliz-Rueda JR, Feillet-Coudray C, Casas F, Colom-Pellicer M, et al. Time-of-Day Circadian Modulation of Grape-Seed Procyanidin Extract (Gspe) in Hepatic Mitochondrial Dynamics in Cafeteria-Diet-Induced Obese Rats. *Nutrients* (2022) 14(4). Epub 20220212. doi: 10.3390/nu14040774.
10. Ribas-Latre A, Del Bas JM, Baselga-Escudero L, Casanova E, Arola-Arnal A, Salvadó MJ, et al. Dietary Proanthocyanidins Modulate Melatonin Levels in Plasma and the Expression

Pattern of Clock Genes in the Hypothalamus of Rats. *Mol Nutr Food Res* (2015) 59(5):865-78. Epub 20150323. doi: 10.1002/mnfr.201400571.

11. Colom-Pellicer M, Rodríguez RM, Navarro-Masip È, Bravo FI, Mulero M, Arola L, et al. Time-of-Day Dependent Effect of Proanthocyanidins on Adipose Tissue Metabolism in Rats with Diet-Induced Obesity. *Int J Obes (Lond)* (2022). Epub 20220506. doi: 10.1038/s41366-022-01132-0.

12. Margalef M, Pons Z, Iglesias-Carres L, Bravo FI, Muguerza B, Arola-Arnal A. Lack of Tissue Accumulation of Grape Seed Flavanols after Daily Long-Term Administration in Healthy and Cafeteria-Diet Obese Rats. *J Agric Food Chem* (2015) 63(45):9996-10003. Epub 20151110. doi: 10.1021/acs.jafc.5b03856.

13. Martí MP, Pantaleón A, Rozek A, Soler A, Valls J, Macià A, et al. Rapid Analysis of Procyanidins and Anthocyanins in Plasma by Microelution Spe and Ultra-Hplc. *J Sep Sci* (2010) 33(17-18):2841-53. doi: 10.1002/jssc.201000274.

14. Guerrero L, Margalef M, Pons Z, Quiñones M, Arola L, Arola-Arnal A, et al. Serum Metabolites of Proanthocyanidin-Administered Rats Decrease Lipid Synthesis in Hepg2 Cells. *J Nutr Biochem* (2013) 24(12):2092-9. doi: 10.1016/j.jnutbio.2013.08.001.

15. Yoo SH, Yamazaki S, Lowrey PL, Shimomura K, Ko CH, Buhr ED, et al. Period2::Luciferase Real-Time Reporting of Circadian Dynamics Reveals Persistent Circadian Oscillations in Mouse Peripheral Tissues. *Proc Natl Acad Sci U S A* (2004) 101(15):5339-46. Epub 20040212. doi: 10.1073/pnas.0308709101.

16. Pfaffl MW. *Relative Quantification*: International University Line (2007).

17. Ungefroren H, Thürling I, Färber B, Kowalke T, Fischer T, De Assis LVM, et al. The Quasimesenchymal Pancreatic Ductal Epithelial Cell Line Panc-1&Mdash;a Useful Model to Study Clonal Heterogeneity and Emt Subtype Shifting. *Cancers* (2022) 14(9):2057.

18. Sato M, Murakami M, Node K, Matsumura R, Akashi M. The Role of the Endocrine System in Feeding-Induced Tissue-Specific Circadian Entrainment. *Cell Rep* (2014) 8(2):393-401. Epub 20140710. doi: 10.1016/j.celrep.2014.06.015.

19. Branecky KL, Niswender KD, Pendergast JS. Disruption of Daily Rhythms by High-Fat Diet Is Reversible. *PLoS One* (2015) 10(9):e0137970. Epub 20150914. doi: 10.1371/journal.pone.0137970.

20. Pendergast JS, Branecky KL, Yang W, Ellacott KL, Niswender KD, Yamazaki S. High-Fat Diet Acutely Affects Circadian Organisation and Eating Behavior. *Eur J Neurosci* (2013) 37(8):1350-6. Epub 2013/01/22. doi: 10.1111/ejn.12133.

21. Hsieh MC, Yang SC, Tseng HL, Hwang LL, Chen CT, Shieh KR. Abnormal Expressions of Circadian-Clock and Circadian Clock-Controlled Genes in the Livers and Kidneys of Long-Term, High-Fat-Diet-Treated Mice. *Int J Obes (Lond)* (2010) 34(2):227-39. Epub 20091110. doi: 10.1038/ijo.2009.228.

22. Eckel-Mahan KL, Patel VR, de Mateo S, Orozco-Solis R, Ceglia NJ, Sahar S, et al. Reprogramming of the Circadian Clock by Nutritional Challenge. *Cell* (2013) 155(7):1464-78. doi: 10.1016/j.cell.2013.11.034.

23. Dyar KA, Lutter D, Artati A, Ceglia NJ, Liu Y, Armenta D, et al. Atlas of Circadian Metabolism Reveals System-Wide Coordination and Communication between Clocks. *Cell* (2018) 174(6):1571-85 e11. Epub 2018/09/08. doi: 10.1016/j.cell.2018.08.042.

24. Cawthorn WP, Sethi JK. Tnf-Alpha and Adipocyte Biology. *FEBS Lett* (2008) 582(1):117-31. Epub 20071126. doi: 10.1016/j.febslet.2007.11.051.

25. Wang S, Lin Y, Gao L, Yang Z, Lin J, Ren S, et al. Ppar-Γ Integrates Obesity and Adipocyte Clock through Epigenetic Regulation of Bmal1. *Theranostics* (2022) 12(4):1589-606. Epub 20220116. doi: 10.7150/thno.69054.

26. Vieira E, Ruano E, Figueroa AL, Aranda G, Momblan D, Carmona F, et al. Altered Clock Gene Expression in Obese Visceral Adipose Tissue Is Associated with Metabolic Syndrome. *PLoS One* (2014) 9(11):e111678. Epub 20141103. doi: 10.1371/journal.pone.0111678.

27. Kohsaka A, Laposky AD, Ramsey KM, Estrada C, Joshu C, Kobayashi Y, et al. High-Fat Diet Disrupts Behavioral and Molecular Circadian Rhythms in Mice. *Cell Metab* (2007) 6(5):414-21. doi: 10.1016/j.cmet.2007.09.006.

28. Scalbert A, Williamson G. Dietary Intake and Bioavailability of Polyphenols. *The Journal of Nutrition* (2000) 130(8):2073S-85S. doi: 10.1093/jn/130.8.2073S.

29. Smith U, Kahn BB. Adipose Tissue Regulates Insulin Sensitivity: Role of Adipogenesis, De Novo Lipogenesis and Novel Lipids. *J Intern Med* (2016) 280(5):465-75. Epub 20161003. doi: 10.1111/joim.12540.

30. Münzberg H, Flier JS, Bjørbaek C. Region-Specific Leptin Resistance within the Hypothalamus of Diet-Induced Obese Mice. *Endocrinology* (2004) 145(11):4880-9. Epub 20040722. doi: 10.1210/en.2004-0726.

31. Stern JH, Rutkowski JM, Scherer PE. Adiponectin, Leptin, and Fatty Acids in the Maintenance of Metabolic Homeostasis through Adipose Tissue Crosstalk. *Cell Metab* (2016) 23(5):770-84. doi: 10.1016/j.cmet.2016.04.011.

32. Cottam DR, Mattar SG, Barinas-Mitchell E, Eid G, Kuller L, Kelley DE, et al. The Chronic Inflammatory Hypothesis for the Morbidity Associated with Morbid Obesity: Implications and Effects of Weight Loss. *Obes Surg* (2004) 14(5):589-600. doi: 10.1381/096089204323093345.

33. Cermakian N, Lange T, Golombek D, Sarkar D, Nakao A, Shibata S, et al. Crosstalk between the Circadian Clock Circuitry and the Immune System. *Chronobiol Int* (2013) 30(7):870-88. Epub 20130522. doi: 10.3109/07420528.2013.782315.

34. Pascual-Serrano A, Arola-Arnal A, Suárez-García S, Bravo FI, Suárez M, Arola L, et al. Grape Seed Proanthocyanidin Supplementation Reduces Adipocyte Size and Increases Adipocyte Number in Obese Rats. *Int J Obes (Lond)* (2017) 41(8):1246-55. Epub 20170404. doi: 10.1038/ijo.2017.90.

35. Caimari A, del Bas JM, Crescenti A, Arola L. Low Doses of Grape Seed Procyanidins Reduce Adiposity and Improve the Plasma Lipid Profile in Hamsters. *Int J Obes (Lond)* (2013) 37(4):576-83. Epub 20120515. doi: 10.1038/ijo.2012.75.

36. Pinent M, Bladé MC, Salvadó MJ, Arola L, Ardévol A. Metabolic Fate of Glucose on 3t3-L1 Adipocytes Treated with Grape Seed-Derived Procyanidin Extract (Gspe). Comparison with the Effects of Insulin. *J Agric Food Chem* (2005) 53(15):5932-5. doi: 10.1021/jf050601f.

37. Ardévol A, Bladé C, Salvadó MJ, Arola L. Changes in Lipolysis and Hormone-Sensitive Lipase Expression Caused by Procyanidins in 3t3-L1 Adipocytes. *Int J Obes Relat Metab Disord* (2000) 24(3):319-24. doi: 10.1038/sj.ijo.0801130.

38. Li Y, Ma J, Yao K, Su W, Tan B, Wu X, et al. Circadian Rhythms and Obesity: Timekeeping Governs Lipid Metabolism. *J Pineal Res* (2020) 69(3):e12682. Epub 20200807. doi: 10.1111/jpi.12682.

39. Grimaldi B, Bellet MM, Katada S, Astarita G, Hirayama J, Amin RH, et al. Per2 Controls Lipid Metabolism by Direct Regulation of Pparγ. *Cell Metab* (2010) 12(5):509-20. doi: 10.1016/j.cmet.2010.10.005.

40. Ardévol A, Motilva MJ, Serra A, Blay M, Pinent M. Procyanidins Target Mesenteric Adipose Tissue in Wistar Lean Rats and Subcutaneous Adipose Tissue in Zucker Obese Rat. *Food Chem* (2013) 141(1):160-6. Epub 20130307. doi: 10.1016/j.foodchem.2013.02.104.

SUPPLEMENTARY MATERIAL

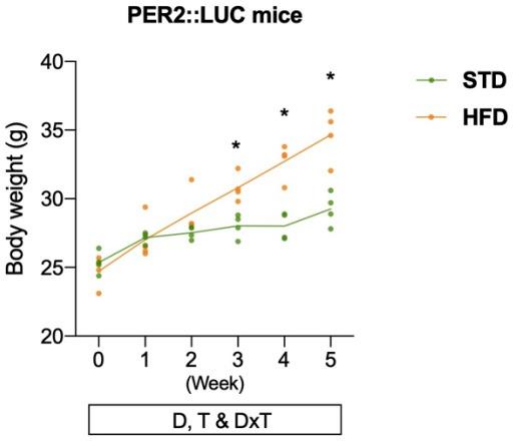

Figure S1. *Body weight development during 5 weeks of STD- or HFD in PER2::LUC mice. Two-way ANOVA followed by Bonferroni post-hoc test; D, diet effect; T, effect of time; DxT, interaction of diet and time.*

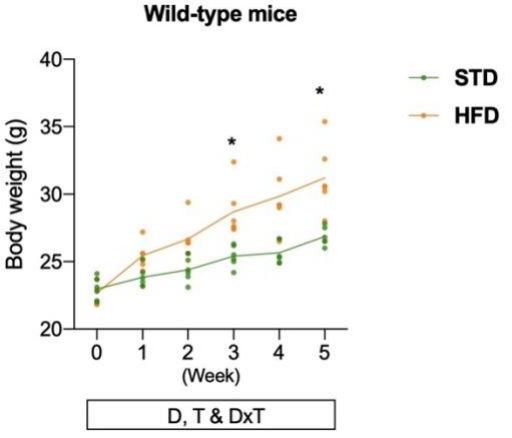

Figure S2. *Body weight during 5 weeks of STD or HFD in wildtype mice. Two-way ANOVA followed by Bonferroni post-hoc test; D, diet effect; T, effect of time; DxT, interaction of diet and time.*

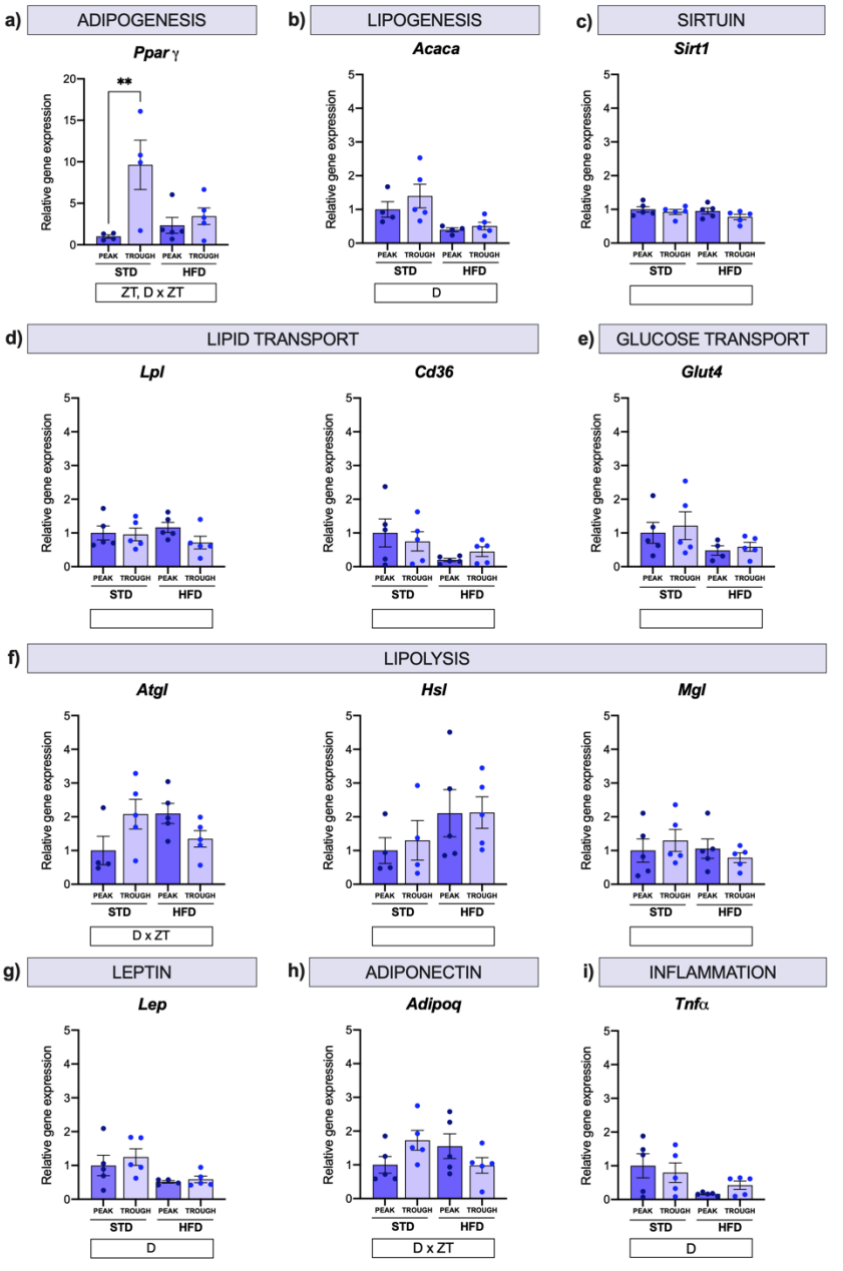

Figure S3. *Gene expression of STD and HFD iWAT explants which were prepared at two different times – peak or trough of PER2. Expression of genes related to adipogenesis (a), lipogenesis (b), sirtuin (c), lipid transport (d), glucose transport (e), lipolysis (f), leptin (g), adiponectin (h) and inflammation (i). Peak/non-treated explants with a partial medium changed at peak; trough/non-treated explants with a partial medium changed at trough. n = 4 - 5. Two-way ANOVA followed by Bonferroni post-hoc test; D, diet effect; DxZT, interaction of diet and time-of-day the experiment started.*

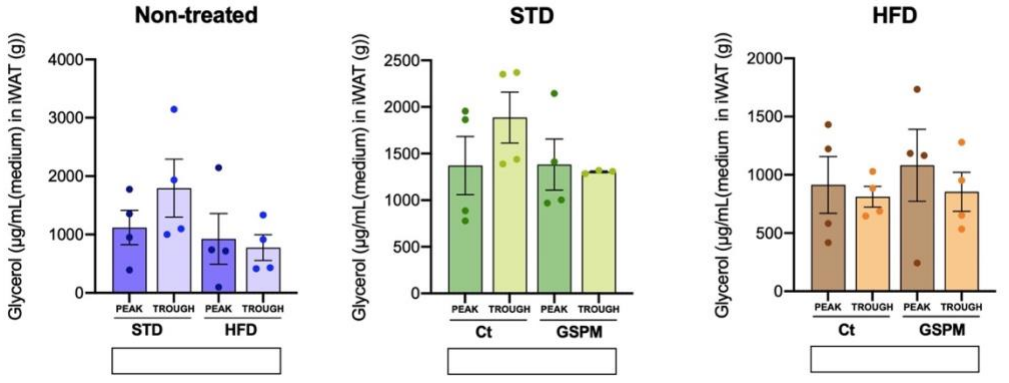

Figure S4. *Glycerol content in the medium of iWAT explants from STD- or HFD-fed wildtype mice prepared (for non-treated samples) or treated at peak or trough. STD, standard diet; HFD, high-fat diet; Ct, explants treated with serum metabolites from control; GSPM, explants treated with serum metabolites from GSPE. Two-way ANOVA was used; no significant effects were observed.*

Table S1. Summary of the qPCR data.

	DIET & ZT		STD T & ZT		HFD T & ZT	
	STD	HFD	+ Cont	GSPM	+ Cont	GSPM
Pparγ	-		TROUGH		TROUGH	
Acaca		↓		↑P	-	
Sirt1	-		-		PEAK	
Lpl	-		PEAK		PEAK ↑	
Cd36	-		-		-	
Glut4	-			↑	-	
Atgl	↑T x ↑P			↑P		↑
Hsl	-			↑	-	
Mgl	-			↑	-	
Lep		↓		↑P	PEAK	
Adipoq	↑T x ↑P		-		-	
Tnfα		↓	-		-	
	STD	HFD	+ Cont	GSPE	+ Cont	GSPE

Gene expression analyses after 10 hours GSPM treatment at peak or trough of PER2 of STD and HFD-fed iWAT explants. Diet: standard (STD) or high-fat (HFD); treatment: serum control (Ct) or serum GSPM (GSPM); time-of-day treatment (ZT): peak or trough. Arrows indicate upregulation or downregulation of the corresponding gene and the letter next to the arrows indicates significant differences ($p < 0.05$) with Bonferroni's post-hoc test at peak (P) or trough (T).

Manuscript 4

Bioactive multi-ingredient consumption influences white adipose tissue metabolism in a time-of-day-dependent manner in obese rats

Marina Colom-Pellicer[1], Romina M Rodríguez[1], Èlia Navarro-Masip[1], Marta Aguado[1], Begoña Muguerza[1], Miquel Mulero[1], and Gerard Aragonès[1]✉

[1] Universitat Rovira i Virgili, Department of Biochemistry and Biotechnology, Nutrigenomics Research Group, Tarragona, Spain.

Ready to be submitted to the
International Journal of Molecular Science
2022

Abstract: Bioactive compounds induce beneficial effects on white adipose tissue (WAT) metabolism. However, the co-administration of a bioactive multi-ingredient (MIX) based on grape-seed proanthocyanidins extract (25 mg/kg), berry anthocyanins (100 mg/kg), conjugated linoleic acid (100 mg/kg) and protein hydrolysate from chicken feet (55 mg/kg) could present greater effects compared to individual-compound consumption. The biology of adipose tissue in mammals is synchronized by circadian rhythms, and consequently, time-of-day MIX consumption could influence its metabolic effect on WAT. Therefore, the aim of this study was to determine the impact of time-of-day MIX administration on the metabolism and expandability of inguinal WAT (iWAT) and epididymal WAT (eWAT) in cafeteria diet-fed rats. Male Wistar rats (n=32) fed a cafeteria diet for 9 weeks were orally supplemented the last 4 weeks with MIX or vehicle when the lights turned on (ZT0) or turned off (ZT12). Interestingly, the supplementation of MIX at ZT0 increased adiponectin serum concentration and *Adipoq* mRNA expression in eWAT. In contrast, the supplementation of MIX at ZT12 tended to decrease body weight gain, significantly reduced proinflammatory markers in serum and iWAT, adipocyte size and lipolytic gene expression in iWAT. Therefore, MIX affects in a tissue-specific manner according to time-of-day administration.

Keywords: adiponectin; circadian clock; expandability; inflammation; lipolysis; polyphenols

1. Introduction

Obesity is characterized by an imbalance between caloric intake and energy expenditure which leads to excessive or abnormal fat accumulation. White adipose tissue (WAT) dysfunction is the principal contributor to many metabolic diseases associated with obesity including insulin resistance and inflammation [1]. In fact, non-healthy WAT is characterised to present high levels of proinflammatory cytokines, such as monocyte chemoattractant protein 1 (MCP-1) and interleukin 6 (IL-6), and low levels of adiponectin which are related with larger adipocytes (hypertrophic WAT) [2]. In contrast, an elevated number of smaller adipocytes are observed in healthy WAT, which is associated with low inflammatory activity and high insulin sensibility (hyperplasic WAT) [1].

In this context, because pharmacologic approaches to restore WAT expandability and metabolism have not yet been found, the use of bioactive food compounds such as as polyphenols, fatty acids and bioactive peptides have largely been investigated in the last years for their ability to improve the metabolic health of WAT [3]. In this sense, grape-seed proanthocyanidins extract (GSPE) has demonstrated to modulate adipose tissue expandability leading to an increment of adipocyte number and a reduction of adipocyte size [4]. In addition, it has been aslo reported that anthocyanins are able to reduce adipose tissue weight in obese mice [5]. Alternatively, conjugated linoleic acid (CLA) has been also largely investigated for the management of body weight. In fact, obese mice supplemented with CLA increased energy expenditure, fat oxidation and browning in subcutaneous WAT [6]. Finally, bioactive peptides from chicken feet hydrolysate such as Hpp11 has been described to be a potential anti-hypertensive component due to the capability to inhibit angiotensin-converting enzyme [7]. Although Hpp11 has not been reported to improve the metabolism of WAT, other angiotensin-converting enzyme inhibitors demonstrated to reduce adiposity and

body weight, improve insulin sensitivity and increase adiponectin plasma concentrations [8].

However, the use of a single family of bioactive compounds seems to not be sufficient to prevent WAT abnormalities and its associated pathologies under obesogenic conditions. Thus, the simultaenously co-administration of different bioactive compounds could exert higher clinical significant effects compared to its individual administration. In this context, a bioactive mulit-ingredient (MIX), composed of CLA, the flavonoids proanthocyanidins and anthocyanidins, and the antihypertensive hydrolysate Hpp11, has recently demonstrated to be useful in the management of metabolic syndrome, reducing fat accumulation and increasing energy expenditure and fat oxidation in cafeteria obese rats [9].

The main metabolic processes in mammals are influenced by the circadian clock, which is a complex biological timing system localized in the suprachiasmatic nuclei that regulates the daily metabolic oscillations of peripheral tissues such as WAT [10]. The principal molecular components of mammalian circadian clock are the heterodimer *Brain and Muscle ARNT-Like 1* (BMAL1) and *Clock Circadian Regulator* (CLOCK) which activate *Period Circadian Regulator* (PER) and *Cryptochrome Circadian Regulator* (CRY) proteins that induce a negative feedback loop to BMAL1 and CLOCK in a cycle of aproximately 24 hours [11]. Although, light is the principal synchronizer of molecular clock, dietary and lifestyle interventions also modulate the circadian rhythmicity [12]. In fact, it is plausible to speculate that the effectiveness of bioactive compounds in the prevention of WAT abnormalities could potentially differ according to the time-of-day in which they are consumed. Nevertheless, there is lack of research on studying the impact of diurnal rhythm on the beneficial effects of bioactive compounds. Therefore, the aim of the present study was to investigate whether the functionality and expandability of WAT in response to MIX consumption was

significantly influenced by the time-of-day of its consumption in diet-induced obese rats.

2. Results

2.1. MIX administration at ZT12 decreased body weight gain in CAF diet-fed rats

As shown in Table 1, no differences were found among groups in final body weight or body weight gain in response to MIX administration. However, when a Student's t test was applied, body weight gain tended to decrease only when MIX was supplemented at ZT12 when the lights turned off (P=0.09), but no changes were observed when MIX was supplemented at ZT0. In contrast, accumulated energy intake was not significantly affected by MIX consumption and only animals supplemented with VH or MIX at ZT0 showed higher energy intake values than animals supplemented at ZT12 (Two-way ANOVA, ZT effect; P=0.01). A similar pattern was observed on energy expenditure during light (resting) phase (Figure S1-A). Additionally, animals treated at ZT12 presented significant lower activity during the light phase compared to the animals treated at ZT0 (Figure S1-B). Interestingly, MIX administration caused a significant reduction of the locomotor activity during the resting phase in both ZT treatments compared to corresponding vehicle groups (Two-way ANOVA, T effect; P=0.0001). No changes were observed in respiratory quotient values (Figure S1-C).

Table 1. Final body weight, body fat content, relative weights of adipose tissues, fat gained and accumulated food intake of rats fed a CAF diet and supplemented for 4 weeks with MIX or vehicle at ZT0 or ZT12.

	VH-ZT0	MIX-ZT0	VH-ZT12	MIX-ZT12	Two-way ANOVA
Final body weight (g)	484.88 ± 9.3	475.63 ± 16.9	483.81 ± 21.4	471.88 ± 13.1	ns
Body fat content[1] (%)	17.78 ± 1.26	20.70 ± 1.51	21.93 ± 0.79	20.25 ± 1.51	ns
Body weight gain (g)	55.26 ± 2.6	49.13 ± 8.9	54.56 ± 4.0	41.06 ± 6.5 #	ns
iWAT (%)	2.20 ± 0.2	2.07 ± 0.2	2.40 ± 0.3	2.21 ± 0.2	ns
eWAT (%)	3.53 ± 0.2	3.89 ± 0.3	3.69 ± 0.2	3.23 ± 0.3	ns
Fat gained (%)	3.67 ± 0.29	4.23 ± 0.91	3.84 ± 0.57	4.02 ± 0.45	ns
Energy intake[2] (kJ/day)	2099.98 ± 172.8	1877.63 ± 26.9	1746.69 ± 85.1	1707.46 ± 51.1	ZT

Data represent mean ± s.e.m. (n=6-8).
 # denotes tendency (p= 0.05 - 0.1) using t-Student test between MIX supplementation and its corresponding VH group; ZT, effect of time-of-day supplementation; ns, no significant differences using two-way ANOVA (p > 0.05).
[1]Body fat content was assessed by quantitative magnetic resonance one week prior to sacrifice.
[2]Accumulated energy intake was calculated as the difference between food intake at week 9 and week 6.
***Abbreviations:** CAF, cafeteria; MIX; bioactive multi-compound; VH, vehicle; IWAT, inguinal white adipose tissue; EWAT, epididymal white adipose tissue.*

2.2. MIX administration at ZT0 increased adiponectin serum concentrations and gene expression in eWAT

Table 2 shows serum concentrations of main metabolic variables measured at the end of the experiment. Glucose, insulin, HOMA-IR, leptin, triacylglicerides, total cholesterol and NEFA values did not show significant differences between MIX and vehicle. Interestingly, animals supplemented with MIX at ZT0 presented significantly higher levels of serum adiponectin concentrations (34.05 ± 2.1 μg/mL) compared to its vehicle group (26.89 ±2.4 μg/mL). However, the supplementation of MIX at ZT12 did not present an increment on adiponectin serum concentration. Adiponectin plays a role in the improvement of metabolic flexibility facilitating the ability to adapt to an altered nutritional environment. As it is secreted mainly by the adipose tissue, we also analysed *Adipoq* mRNA relative expression in both

fat pads. In iWAT, we did not observe significant differences on *Adipoq* gene expression levels (Figure 2A). However, in eWAT, *Adipoq* mRNA relative concentration was lower in animals supplemented at ZT0 with respect to animals supplemented at ZT12. Nevertheless, MIX supplementation at ZT0 over-stimulated *Adipoq* in eWAT almost reaching the same levels as animals treated at ZT12 (Figure 2B).

Therefore, only when MIX was supplemented at ZT0 *Adipoq* expression levels increased in eWAT. Hence, the higher adiponectin levels found in serum of animals supplemented with MIX at ZT0 could be caused by the upregulation of its gene in eWAT and not in iWAT.

Table 2. Biochemical serum concentrations.

	VH-ZT0	MIX-ZT0	VH-ZT12	MIX-ZT12	Two-way ANOVA
Glucose (mM)	8.16 ± 0.3	7.99 ± 0.4	7.32 ± 0.2	7.80 ± 0.2	ns
Insulin (ng/mL)	8.60 ± 1.1	6.26 ± 1.1	7.44 ± 0.7	8.11 ± 1.2	ns
HOMA-IR	76.13 ± 11.8	55.76 ± 11.4	54.10 ± 4.9	73.12 ± 11.1	ns
Adiponectin (μg/mL)	26.89 ± 2.4	34.05 ± 2.1*	29.49 ± 2.8	31.21 ± 3.1	ns
Leptin (ng/mL)	35.80 ± 4.7	45.44 ± 4.7	35.86 ± 3.4	42.89 ± 5.4	ns
Triglycerides (mg/dL)	200.18 ± 10.5	212.9 ± 29.5	174.94 ± 11.4	201.6 ± 13.4	ns
Total cholesterol (mg/dL)	150.64 ± 9.2	145.62 ± 4.9	135.80 ± 4.6	144.58 ± 3.2	ns
NEFA (mg/dL)	31.78 ± 4.3	26.17 ± 2.3	22.95 ± 2.6	23.77 ± 0.68	ns
MCP-1 (pg/mL)	343.72 ± 33.4	338.33 ± 39.8	375.25 ± 20.4	284.25 ± 26.5 *	ns

Data represent mean ± s.e.m. (n=6-8).

** denotes significant differences (P < 0.05) using t-Student test between MIX supplementation and its corresponding VH group; ns, no significant differences using two-way ANOVA (p > 0.05).*

Abbreviations: *CAF, cafeteria; MIX; bioactive multi-compound; VH, vehicle; IWAT, inguinal white adipose tissue; EWAT, epididymal white adipose tissue.*

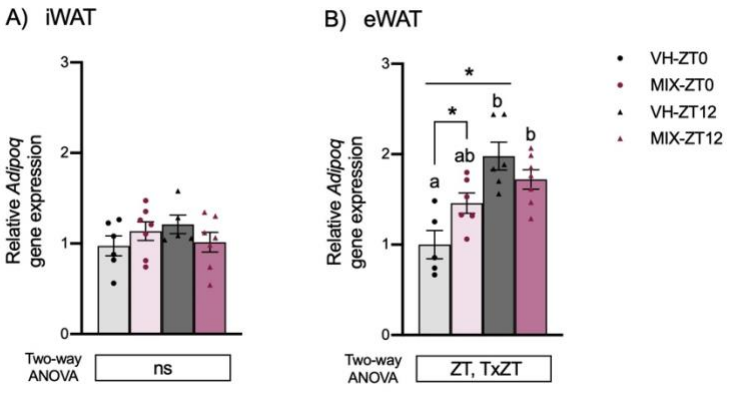

Figure 2. *MIX supplementation at ZT0 upregulates adiponectin gene expression in eWAT but not in iWAT. Relative adiponectin gene expression in iWAT (A) and eWAT (B) of rats fed a CAF diet supplemented with MIX or vehicle (VH) when the lights turned on (ZT0) or when the lights turned off (ZT12). Data represent mean ± s.e.m. (n=5-7). * significant differences ($p < 0.05$) using t-Student test between MIX supplementation and its corresponding VH group and between VH groups; ns, no significant differences; ZT, effect of time-of-day treatment; TxZT, interaction between treatment effect and time-of-day treatment using two-way ANOVA ($p < 0.05$) and ^{a,b} denotes significant differences between groups using Bonferroni post hoc test.*

Adiponectin plays a role on adipocyte differentiation. Therefore, we analysed important genes related to adipogenesis and lipogenesis on WAT depots. In iWAT (Figure 3A), MIX downregulated the mRNA expression of *Fasn* independently of time-of-day supplementation. However, in eWAT (Figure 3B), we first observed an effect of time-of-day vehicle administration shown by an upregulation of *C/ebpα*, *Fasn* and *Gpat* in animals treated with vehicle at ZT0 compared to animals treated with vehicle at ZT12. Moreover, animals treated with MIX at ZT0, which showed higher adiponectin levels, presented an unexpected reduction of the adipogenic gene *Pparγ*. On the other hand, the group supplemented with MIX at ZT12 presented an upregulation of the adipogenic gene *C/ebpα* and the lipogenic gene *Gpat*. The mRNA expression of these three genes presented an interaction between time-of-day treatment and MIX supplementation using two-way ANOVA; demonstrating the downregulation of *Pparγ* only when MIX was supplemented at ZT0, and an upregulation of *C/ebpα* and *Gpat* when MIX was supplemented at ZT12.

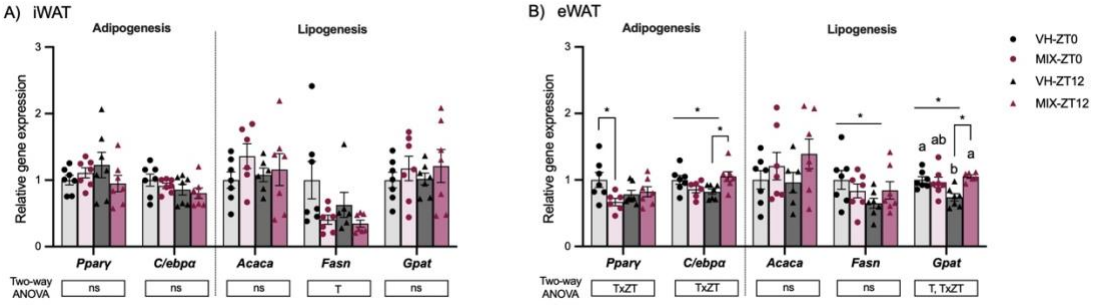

Figure 3. *MIX supplementation affects the expression of genes related to adipogenesis and lipogenesis in iWAT and eWAT in a timing-dependent manner. iWAT (A) and eWAT (B) gene expression was evaluated by qPCR on rats fed a CAF diet supplemented with MIX or vehicle (VH) when the lights turned on (ZT0) or when the lights turned off (ZT12). Data represent mean ± s.e.m. (n=5-7). * significant differences ($p < 0.05$) using t-Student test between MIX supplementation and its corresponding VH group and between VH groups; ns, no significant differences; T, treatment effect; ZT, effect of time-of-day treatment; TxZT, interaction between treatment effect and time-of-day treatment using two-way ANOVA ($p > 0.05$) and ^{a,b} denotes significant differences between groups using Bonferroni post hoc test. PPARγ, peroxisome proliferator-activated receptor γ; C/ebpα, CCAAT/enhancer-binding protein alpha; Acaca, acetyl-CoA carboxylase alpha; Fasn, Fatty acid synthase; Gpat, Glycerol-3-phosphate acyltransferase.*

2.3. MIX supplementation at ZT12 reduced MCP-1 serum concentration and downregulated the expression of pro-inflammatory genes in iWAT

The serum concentrations of MCP-1, a chemokine that regulates migration and infiltration of monocytes/macrophages in response to inflammation, were significantly reduced in the animals supplemented with MIX at ZT12 compared to the animals that received the vehicle at the same ZT. However, no differences on MCP-1 levels were found when MIX was administered at ZT0 (Table 2). In addition, the gene expression of inflammatory related genes in both iWAT (Figure 4A) and eWAT (Figure 4B) was further analyzed. *Tnfα* gene expression was downregulated in iWAT in response to MIX supplementation. This effect was more noticeable when MIX was administered at ZT12 (47.25% lower compared to corresponding vehicle group) than at ZT0 (25.42%). However, in eWAT, *Tnfα* gene expression was downregulated only when MIX was administrated at ZT0. Finally, *IL6* gene expression was downregulated in response to MIX supplementation in

both WAT depots, although when MIX was supplemented at ZT0 the downregulation was more evident in eWAT.

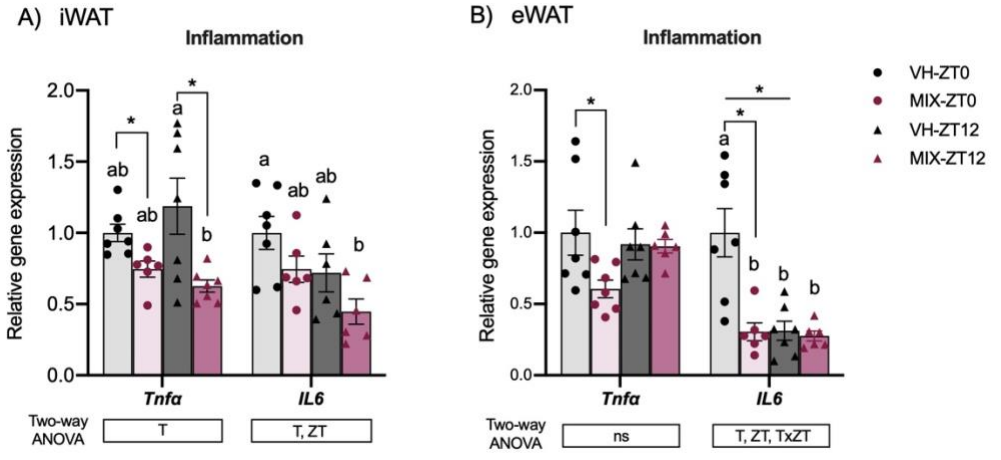

Figure 4. *Gene expression of proinflammatory factors in iWAT and eWAT. iWAT (A) and eWAT (B) gene expression was evaluated by qPCR on rats fed a CAF diet supplemented with MIX or vehicle (VH) when the lights turned on (ZT0) or when the lights turned off (ZT12). Data represent mean ± s.e.m. (n=5-7). * significant differences ($p < 0.05$) using t-Student test between MIX supplementation and its corresponding VH group and between VH groups; T, treatment effect; ZT, effect of time-of-day treatment; ns, no significant differences; TxZT, interaction between treatment effect and time-of-day treatment using two-way ANOVA ($p > 0.05$) and ^{a,b} denotes significant differences between groups using Bonferroni post hoc test. Tnfα, tumor necrosis factor alpha; Il6, interleukin 6.*

2.4. *MIX administration at ZT12, but not at ZT0, reduced adipocyte size and increased adipocyte number in iWAT*

As adiponectin and inflammation are closely related to WAT functionality, the next goal was to analyse the histological parameters of both fat depots. Interestingly, a significant reduction in adipocyte area as well as an increment in adipocyte number in iWAT was observed only when MIX was administered at ZT12 compared to the corresponding control (Figure 5A). Hence, the group supplemented with MIX at ZT12 presented a healthier iWAT expansion by hyperplasia without presenting a reduction of fat mass. Although animals supplemented with MIX at ZT0 did not present significant differences on

adipocyte size, an increment on adipocyte number was also detected, as the two-way ANOVA showed an effect of MIX independently of time-of-day treatment. In contrast, visceral eWAT histological analysis did not show significant differences between any group of animals (Figure 5B). A representative histological image of both fat depots, iWAT and eWAT, for each group of animals is present at Figure S2.

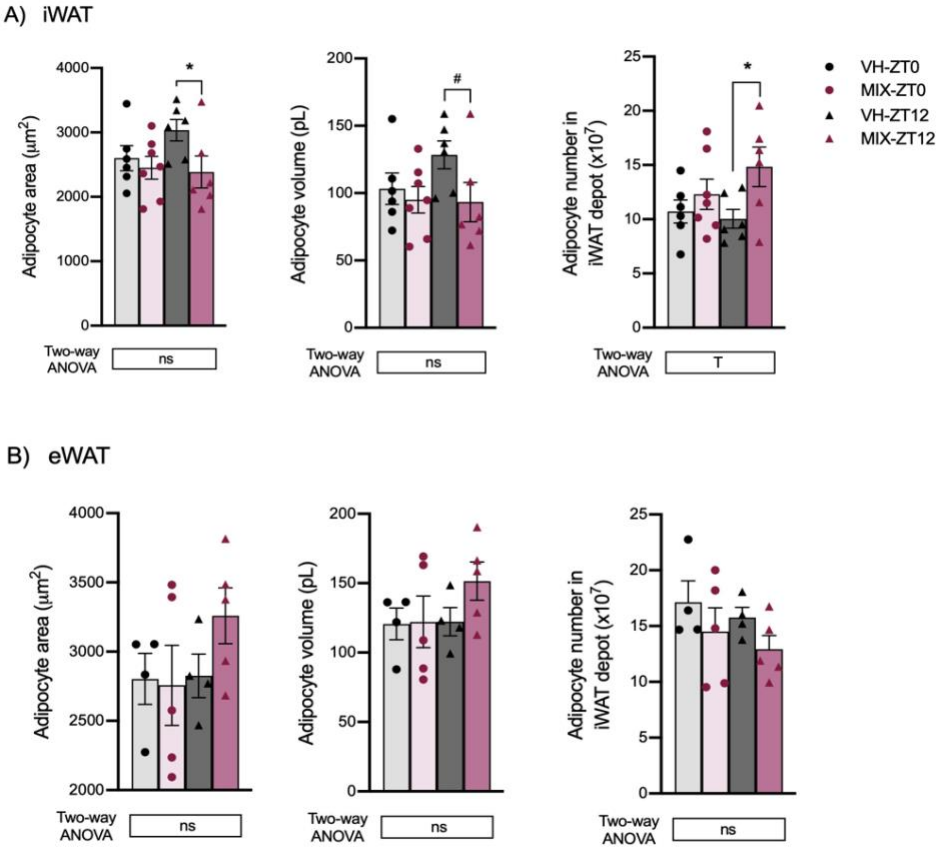

Figure 5. *Histology of iWAT and eWAT. Data represent mean ± s.e.m. (n=4-6). *significant differences ($p < 0.05$); # denotes tendency ($p = 0.05 - 0.1$) using t-Student test between MIX supplementation and its corresponding VH group; ns, no significant differences; T, treatment effect using two-way ANOVA ($p > 0.05$).*

2.5. *MIX supplementation at ZT12 downregulated the expression of genes involved in lipolysis and lipid transport in iWAT*

Next, we focused on the expression of genes related to lipid metabolism. Interestingly, the consumption of MIX produced a different pattern of gene expression in iWAT depending on the ZT in which MIX was administrated (Figure 6A). In fact, MIX consumption at ZT12 downregulated the expression of genes related to lipolysis (*Hsl*, *Mgl and Cpt1b*) and lipid transport (*Cd36* and *Fabp4*) in this tissue. In contrast, MIX consumption at ZT0 upregulated *Mgl* and *Cd36* gene expression compared to its vehicle group. In visceral eWAT (Figure 6B), consumption of MIX significantly affected the relative gene expression of *Fabp4* and *Atgl* at both ZT0 and ZT12.

2.6. *Clock gene expression was affected depending on the time-of-day of MIX supplementation*

It is known that circadian clock modulates the expression of key genes regulating certain metabolic pathways such as lipid metabolism and inflammation. Since we have observed changes on lipid metabolism and inflammation upon MIX supplementation according to time-of-day treatment, we also studied whether the consumption of MIX affected the expression of circadian clock genes in iWAT and eWAT. For this purpose, we analysed the expression pattern of *Bmal1*, *Per2, Cry1* and *Rev-erb-α* in response to MIX supplementation.

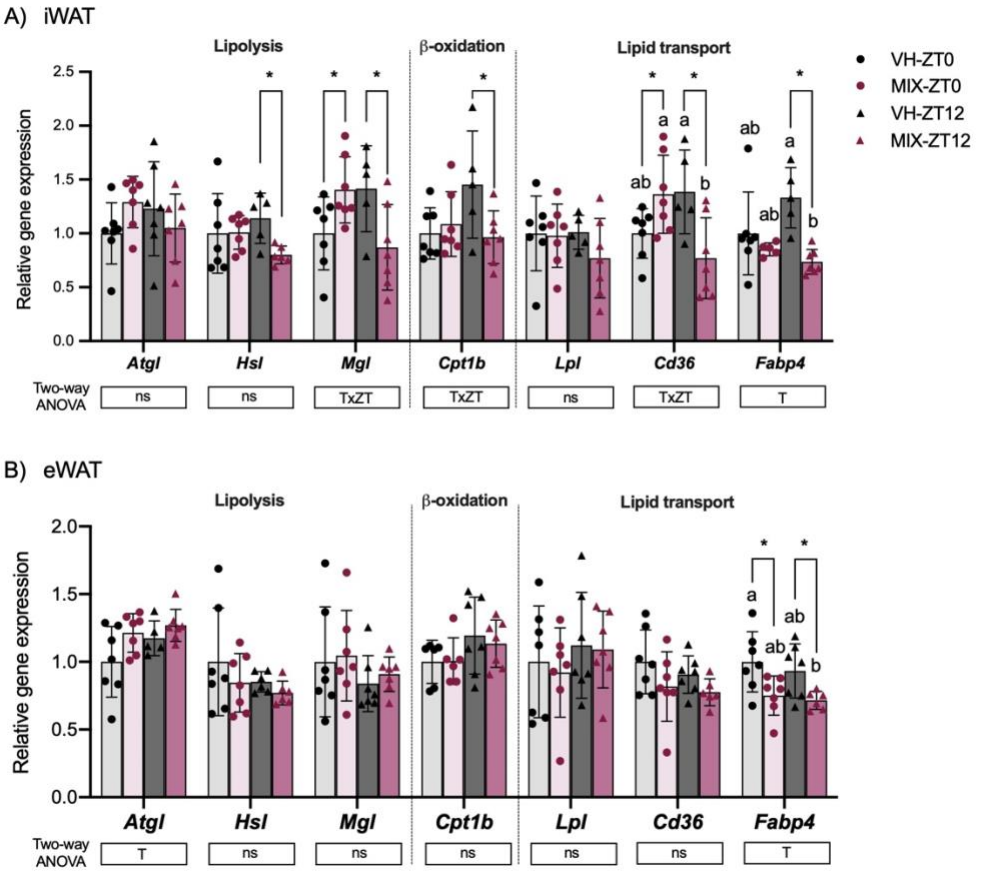

Figure 6. *Expresion of genes involved in lipid metabolism . iWAT (A) and eWAT (B) gene expression was evaluated by qPCR on rats fed a CAF diet supplemented with MIX or vehicle (VH) when the lights turned on (ZT0) or when the lights turned off (ZT12). Data represent mean ± s.e.m. (n=5-7). * significant differences ($p < 0.05$) using t-Student test between MIX supplementation and its corresponding VH group; ns, no significant differences; TxZT, interaction between treatment effect and time-of-day treatment; T, treatment effect using two-way ANOVA ($p > 0.05$) and ^{a,b} denotes significant differences between groups using Bonferroni post hoc test. Atgl, Adipose triglyceride lipase; Hsl, Hormone-sensitive lipase; Mgl, Monoacylglycerol lipase; Cpt1b, Carnitine Palmitoyltransferase 1B; Lpl, Lipoprotein Lipase; Cd36, cluster of differentiation 36; Fabp4, Fatty Acid Binding Protein 4.*

In iWAT (Figure 7A), in response to MIX consumption, animals presented a downregulation of *Bmal1*, *Per2* and *Rev-erb-α*. However, *Bmal1* downregulation was more evident when MIX was supplemented at ZT12, and for *Rev-erb-α* when MIX was supplemented at ZT0. Interestingly, in this tissue, the consumption of MIX produced a different pattern of *Cry1* gene expression. This interaction between

MIX consumption and ZT observed on *Cry1* gene expression was also observed in eWAT (Figure 7B) but, in this tissue, the downregulation of *Cry1* gene expresion was only detected at ZT0.

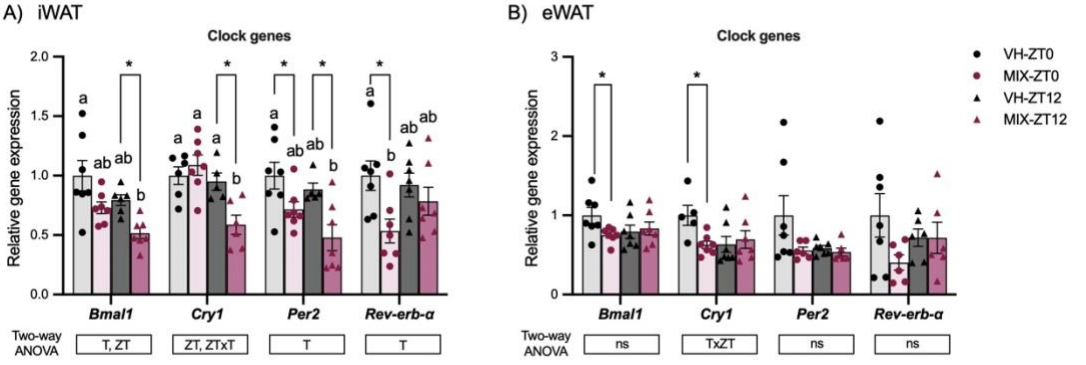

Figure 7. *MIX supplementation and different time-of-day treatment affects the expression of clock genes in iWAT and eWAT. iWAT (a) and eWAT (b) gene expression was evaluated by qPCR on rats fed a CAF diet supplemented with MIX or vehicle (VH) when the lights turned on (ZT0) or when the lights turned off (ZT12). Data represent mean ± s.e.m. (n=5-7). * significant differences ($p < 0.05$) using t-Student test between MIX supplementation and its corresponding VH group; T, treatment effect; ZT, effect of time-of-day treatment; TxZT, interaction between treatment effect and time-of-day treatment; ns, no significant differences using two-way ANOVA ($p > 0.05$) and ^{a,b} denotes significant differences between groups using Bonferroni post hoc test. Bmal1, Brain and Muscle ARNT-Like 1 (aryl hydrocarbon receptor nuclear translocator-like); Cry1, Cryptochrome Circadian Regulator 1; Per2, Period Circadian Regulator 2; Rev-erb-α, nuclear receptor subfamily 1, group D, member 1 (Nr1d1).*

In general, we observed a stronger effect in iWAT when MIX was supplemented at ZT12. However, when MIX was supplemented at ZT0, eWAT presented a higher affectation. This is also shown in the heatmaps representing the gene expression at supplemental Figure S3. Therefore, mRNA modulation by MIX consumption was dependent on fat pad and time-of-day consumption.

3. Discussion

Investigations for the management of obesity-related comorbidities through dietary bioactive compounds have risen in the past few years. However, individual administration of bioactive compounds at physiological doses is not

sufficient to ameliorate the metabolic alterations related to obesity. Therefore, we designed a bioactive multi-compound (MIX) to determine its capability to manage the metabolism and functionality of adipose tissue. MIX was composed of proanthocyanidins extracted from grape seeds (GSPE), anthocyanins from berries, conjugated linoleic acid (CLA) and protein hydrolysate from chicken feet (Hpp11). Further, as mammals are synchronized by circadian rhythms, the time-of-day administration could be crucial for the effectiveness of the bioactive compounds. Therefore, in the present study we demonstrated the effects of MIX consumption on the expandability, metabolism and functionality of iWAT and eWAT according to time-of-day consumption.

Cafeteria diet Wistar rats were used in this study because are considered a suitable model to develop and mimic human metabolic syndrome and obesity [13].

Our results demonstrated a tendency to decrease body weight gain during treatment period only in animals supplemented with MIX at ZT12, the beginning of the dark phase. However, no effect on body weight gain was observed in the animals supplemented with MIX at ZT0, the beginning of the light phase. No studies were performed analysing the effect of MIX treating at the beginning of the dark phase. Nevertheless, previous studies demonstrated a reduction in body weight and fat mass without causing any effect on lean body mass in Wistar rats fed a CAF diet for 11 weeks and the last 3 weeks supplemented with MIX at the beginning of the light phase, between 8a.m. and 9a.m. [14]. Only CLA supplementation (100 mg/kg of body weight) for 3 weeks ameliorated the increment of body weight gain [15]. Discrepancy exists regarding body weight modulation under MIX supplementation when comparing with other studies. This could be due to the duration of the experiments and the number of weeks of CAF diet before the starting day of MIX treatment.

It was shown that chronic MIX administration increased energy expenditure and fat utilization resulting in reduced energy balance [14]. Nevertheless, our findings did not demonstrate any effect on energy expenditure and respiratory quotient between the animals supplemented with MIX and the vehicle groups. We observed differences on time-of-day supplementation independently of treatment; MIX or vehicle, showing a reduction of accumulated food intake and energy expenditure and activity during light phase of animals treated at ZT12 against those treated at ZT0. Interestingly, MIX also caused a reduction of activity during the resting light phase, regardless of the time that MIX was supplemented, helping to rest at the proper time. This could suggest that our bioactive multi-compound exerted a positive action toward sleep quality. In fact, many bioactive metabolites, such as polyphenols, amino acids and proteins improved sleep disorders and other cognitive problems [16,17].

Plasma values of glucose, insulin, leptin, triacylglycerides, total cholesterol, NEFA and HOMA-IR did not show any differences between animals supplemented with MIX and animals supplemented with vehicle at any of the two time point treatments. However, other studies demonstrated a reduction of insulin and an amelioration of HOMA-IR after 3 weeks of MIX administration [14]. Insulin sensitivity is, in part, regulated by adiponectin. Indeed, adiponectin protects from insulin resistance increasing glucose uptake in adipose tissue [18]. Remarkably, in our study we demonstrated that the group treated with MIX at ZT0, when lights turned on, presented higher adiponectin levels in blood due to the stimulation of *Adipoq* mRNA expression in eWAT. However, mRNA expression of gens related to glucose metabolism did not demonstrate any statistical differences in eWAT of these animals (data not shown). Further, adiponectin plasma concentration and *Adipoq* expression levels in eWAT were not increased in the group treated with MIX at ZT12. This adipokine could be modulated by *Pparγ*, a nuclear receptor that

regulates the transcription of several genes. Polyunsaturated fatty acids, such as CLA present in MIX, could modulate adiponectin expression through *Pparγ* [19]. A study performed with Wistar rats fed a high-fat diet supplemented with CLA showed an increment on the expression of *Pparγ* and adiponectin in WAT [20]. Nevertheless, there are controversial results on the effects of CLA on *Pparγ* expression. Further, Hpp11 could be also a possible candidate for the increment of plasma adiponectin through the stimulation of its mRNA in eWAT. It has been reported that ACE inhibitors, like Hpp11, activate adiponectin secretion into plasma upon *Pparγ* upregulation in adipocytes [21]. Nevertheless, in our study, mRNA expression levels of *Pparγ* in the group supplemented with MIX at ZT0 were downregulated despite of adiponectin increment. Adiponectin upregulation probably was not entirely modulated by *Pparγ* but by another mechanism still not clarified [19]. Furthermore, this downregulation of *Pparγ* was probably not crucial when the rats were sacrificed, as *Pparγ* possessess a circadian rhythm having the peak of expression at ZT16 in WAT of mice [22]. Nevertheless, clock gene *Bmal1* regulates adipose tissue metabolism stimulating the expression of key adipogenic genes such as *Pparγ* [23]. Indeed, *Bmal1* expression was downregulated in eWAT of animals supplemented with MIX at ZT0. Altogether, these results suggested that the time-of-day at which MIX was administrated was crucial for adiponectin expression in eWAT.

Moreover, adiponectin is an adipokine produced by WAT. This tissue regulates physiologic and pathologic processes such as inflammation, producing anti-inflammatory factors, such adiponectin, and proinflammatory factors, such TNFα, IL6 and MCP-1 [2]. Adiponectin reduces the production and activity of TNFα and IL6. However, TNFα might present the capability to downregulate adiponectin production [2]. In our study, inflammatory-related genes (*Tnfα* and *Il6*) were downregulated in animals supplemented with MIX at ZT0 in both WAT

depots, with a stronger effect in eWAT compared to iWAT, which correlates with *Adipoq* expression in eWAT and blood adiponectin levels of this animal group. On the other hand, animals supplemented with MIX at ZT12 presented a downregulation of *Tnfα* in iWAT. Although we did not find an upregulation of *Adipoq*, a decrement of proinflammatory chemokine MCP-1 levels in blood was detected, suggesting an amelioration of the inflammatory state in iWAT only when MIX was supplemented at ZT12. The effect of MIX supplemented at ZT0 downregulated both proinflammatory genes, *Tnfα* and *IL6*, in iWAT and eWAT. However, when MIX was supplemented at ZT12, it only presented an effect on iWAT. The clock gene *Rev-erb-α* controls inflammation, up-regulating IL6 [24]. *Rev-erb-α* expression was downregulated in iWAT in both groups supplemented with MIX independently of the time-of-day treatment, where *IL6* was also downregulated. However, the different gene expression of *IL6* found in eWAT was not correlated with the *Rev-erb-α* expression, as no statistical differences were observed. As the gene expression of *Tnfα* and *IL6* present circadian rhythm, the effect of MIX on their modulation probably depends on the time-of-day administration, which coincides with their highest gene expression. The highest expression of these proinflammatory genes is during the resting/light phase, while the lowest expression is during the active phase. Hence, MIX could have stronger effect when it was administrated at ZT0, the beginning of resting/light phase when their expression is maximum.

Furthermore, anti-inflammatory factors such as adiponectin and lower levels of pro-inflammatory factors promoted a healthy expansion of adipose tissue through hyperplasia and prevented ectopic fat accumulation in the liver [25,26]. Despite the high levels of adiponectin found in animals treated with MIX at ZT0, we did not observe statistical differences on histological analysis neither in iWAT nor in eWAT. However, the group supplemented with MIX at ZT12 presented a

reduction on adipocyte area and adipocyte volume, as well as an increment on adipocyte number in the subcutaneous iWAT. This expandability of WAT is known as hyperplasia, which holds beneficial effects on the functionality and metabolism of adipose tissue under the hallmarks of the pathophysiology of obesity [26]. Indeed, obese insulin sensitive individuals are characterized by smaller adipocytes and less fat accumulation in the liver, compared to metabolically unhealthy obese insulin resistant individuals [27–29]. Adipocytes with lower size are more insulin-sensitive, present lower inflammation and exhibit a lower rate of lipolysis, preventing ectopic fat accumulation [30]. Conversely, hypertrophic adipocytes are insulin-resistant, show a higher inflammatory state and an increased lipolytic rate, which increases the risk of fat accumulation in other tissues. They also cause an increment of unesterified fatty acids and cholesterol into circulation, which reaches ectopic sites such as muscles and liver [26,31]. Interestingly, animals treated with MIX at ZT12, which showed an expansion of iWAT through hyperplasia, presented a significant downregulation of genes related to lipolysis (*Hsl*, *Mgl* and *Cpt1b*) and lipid transport (*Cd36* and *Fabp4*). Hence, the modification of iWAT expandability was probably induced by the suppression of genes related to lipolysis and lipid transport with no alteration of fat mass. The reduction of adipocyte size in adipose tissue is a matter of lower lipid uptake rather than higher rates of lipid release through lipolysis. We previously reported that male Wistar rats fed a cafeteria diet and supplemented with GSPE at ZT12 also presented smaller adipocytes, and increased adipocyte number in iWAT, a downregulation of the mRNA expression of genes related to lipolysis and lipid transport and lower percentage of fat mass. Therefore, the effect of MIX on the expandability of iWAT via the repression of the expression of these genes could probably be attributed to the properties of GSPE when it was administrated at ZT12. Furthermore, our research group discarded the possibility

of MIX causing fat accumulation in the liver. The histopathological analyses performed in a previous study showed no signs of liver damage aggravation in rats supplemented with MIX [14].

Therefore, the consumption of MIX at ZT12, but not at ZT0, led to a healthy expandability through hyperplasia and a downregulation of lipolytic genes in iWAT. The clock gene *Per2* is in phase coherence with the lipolytic gene *Hsl* [32]. *Hsl* was downregulated in the iWAT of animals supplemented with MIX at ZT12, as well as *Per2*. However, we also observed a downregulation of *Per2* on animals supplemented with MIX at ZT0 in iWAT, in spite of not showing a downregulation of *Hsl*. Moreover, *Per2* interacts with *Cry1*, which has a critical role in adipose tissue metabolism. *Cry1/2*$^{-/-}$ mice, despite of their hypophagia, presented a higher fat pad weight and adipocyte hypertrophy, resulting from an increment of lipid uptake and a reduction of adipogenesis[33]. In our study, animals supplemented with MIX at ZT12 presented a downregulation of *Cry1* in iWAT, but they presented adipocyte hyperplasia. Animals supplemented with MIX at ZT0 presented a downregulation of *Cry1* in eWAT, and no changes in adipocyte size or in *Lpl* gene expression.

The gene expression analysis performed in iWAT and eWAT illustrated the differences on mRNA expression levels of genes related to lipid metabolism, inflammation and circadian clock between the group supplemented with MIX at ZT0 and the group supplemented with MIX at ZT12. The gene expression of circadian clock and metabolic genes varies during the day and depending on the tissue [34]. Therefore, the effect of MIX differed depending on time-of-day administration and the fat pad. Gene expression of all genes studied is represented in two heatmaps which demonstrated that; when MIX was supplemented at ZT0, it moderately affected eWAT. However, when MIX was supplemented at ZT12, it had a stronger effect in iWAT.

In summary, our results demonstrated that the consumption of MIX at ZT0 (when the lights turned on) increased adiponectin plasma concentration, probably through the stimulation of *Adipoq* mRNA in eWAT, due to CLA and/or Hpp11 effects. This effect was not observed when MIX was consumed at ZT12. In contrast, the consumption of MIX at ZT12 (when the lights turned off), tended to decrease body weight gain and proinflammatory markers in blood probably due to the amelioration of inflammation in iWAT, which is related to adipocyte hyperplasia and repressed expression of lipolytic and lipid transport genes in the same fat pad, probably through GSPE effects in cafeteria diet-fed rats.

Therefore, the effect of MIX on the metabolism and functionality of adipose tissue was tissue-specific and time-of-day consumption dependent. Further studies are needed to elucidate the effectiveness of MIX according to time-of-day consumption on the expandability, metabolism and functionality of adipose tissue of cafeteria diet-induced obese rats, and to reveal the importance of circadian rhythm on the consumption of bioactive compounds.

4. Materials and Methods

4.1. Bioactive multi-compound (MIX) information

Grape seed proanthocyanidins extract, GSPE, was kindly provided by Les Dérives Résiniques et Terpéniques (Dax, France), and its composition was previously characterized by *Margalef et al* [35]. Anthocyanin extract (MEDOX®) was provided by MedPalett AS (Sandnes, Norway) and contained purified anthocyanins isolated from bilberries (*Vaccinium myrtillus*) and blackcurrant (*Ribes nigrum*), composition described by *Qin et al* [36]. CLA (Tonalin® TG 80) was purchased from BASF Chemical Company (Düsseldorf, Germany) and consisted of a mix of glycerides, of which 80% were conjugated linoleic acids. According to the manufacturer, the product was composed of equal amounts of two CLA

isomers *c9,t11* and *t10,c12*. The composition and manufacturing method of the protein hydrolysate from chicken feet, Hpp11, was previously described [7,37].

4.2. Animal experimental procedure

Eight-week-old male Wistar rats (N=32) were purchased from Charles River Laboratories (Barcelona, Spain). Animals were housed in pairs under a light/dark cycle of 12 hours, at 22 °C and fed *ad libitum* with standard chow diet-fed (STD, Panlab A04, Panlab, Barcelona, Spain) and tap water. After one week of adaptation, all animals were fed a CAF diet, which is highly palatable and induces voluntary hyperphagia. CAF diet consists of biscuits with pate, biscuits with cheese, ensaïmada (sweetened pastry), bacon, carrots and sweetened milk (20% sucrose w/v) in addition to standard diet (STD Panlab A04, Panlab, Barcelona, Spain). The composition of the cafeteria diet was 10% protein, 31.9% fat and 58.1% carbohydrates. This diet was provided fresh *ad libitum* every day to the animals for 9 weeks. During the last 4 weeks of the experiment, animals were randomly divided into four new groups (n=8) and were orally supplemented with vehicle or MIX at the beginning of the light period; at zeitgeber time 0 (ZT0), or at the beginning of the dark period; at zeitgeber time 12 (ZT12). Both vehicle groups received an oral dose of water and sweetened milk when the lights turned on (VH-ZT0) or when the lights turned off (VH-ZT12). The other two groups received the MIX diluted in water and sweetened milk when the lights turned on (MIX-ZT0) or when the lights turned off (MIX-ZT12). The MIX was composed of GSPE (25 mg/kg), anthocyanins (100mg/kg), CLA (100mg/kg) and Hpp11 (55mg/kg). Before supplementation, all rats were trained to voluntarily lick the milk, and vehicle groups were administered the same volume of condensed milk for four weeks. One week prior to sacrifice, fat mass was analysed by quantitative magnetic resonance using an EchoMRI-700 (Echo Medical Systems, LLC., TX, USA) without

anaesthesia. At the end of the experiment, the animals were fasted for 3h after ZT0 and then sacrificed by live decapitation. Total blood was collected from the neck and then was centrifuged (1500 x g, 15 min, 4ºC) to obtain serum. In addition, iWAT, eWAT and mesenteric WAT (mWAT) fat pads were excised, weighted and immediately frozen in liquid nitrogen. Serum and tissues were stored at −80°C until further use.

The Animal Ethics Committee of Universitat Rovira i Virgili approved all of the procedures (reference number 9495 by Generalitat de Catalunya). All the above-mentioned experiments were performed as authorized (European Directive 86/609/CEE and Royal Decree 223/1988 of the Spanish Ministry of Agriculture, Fisheries and Food, Madrid, Spain).

4.3. Serum analysis

Serum levels of insulin, leptin, adiponectin and monocyte chemoattractant protein-1 (MCP-1) were measured using an immunometric sandwich enzyme-linked immunosorbent assay (ELISA) using a *rat/mouse insulin ELISA kit* (EZRMI-13K), *rat leptin ELISA kit* (EZRL-83K), *rat adiponectin ELISA kit* (EZRADP-62K) and *rat anti-monocyte chemotactic protein-1 antibody ELISA kit* (AB1834P) purchased from Millipore Ibérica (Madrid, Spain). Serum samples were diluted and immunoassays were performed in duplicate according to the manufacturer's protocols. Serum glucose, triglycerides and total cholesterol were measured with enzymatic colorimetric kits (QCA, Barcelona, Spain). Serum non-esterified fatty acids (NEFA, or free fatty acids) were analysed with the enzymatic colorimetric *HR NEFA series kit* (Wako, CA, USA). Homeostasis model assessment-estimated insulin resistance (HOMA-IR) index was calculated from insulin and glucose serum levels.

4.4. Histology of adipose tissues

Frozen iWAT and eWAT samples were thawed and fixed in 4% formaldehyde. Tissues underwent successive dehydration and paraffin infiltration immersion (Citadel 2000, HistoStar, Thermo Scientific, Madrid, Spain) and paraffin blocks were cut into 2-µm-thick sections using a microtome (Microm HM 355S, ThermoScientific). The sections were subjected to automated hematoxylin–eosin staining (Varistain Gemini, Shandom, Thermo Scientific). Sections were observed and acquired at ×10 magnification using AxioVision ZeissImaging software (Carl Zeiss Iberia, S.L., Madrid, Spain). The area of adipocytes was measured using the Adiposoft open-source software (CIMA, University of Navarra, Spain). Four fields per sample were measured and six samples per group were analysed. The adipocyte area was calculated from the average value of cell area in all measured fields for each sample. Total adipocyte volume was calculated using the formula

$$\left[\frac{\pi}{6}\right] \times [3\sigma^2 \times \bar{d} + \bar{d}^3] \qquad [38]$$

(where $\bar{d}$ is the mean diameter and σ is the standard deviation of the diameter). Then, fat cell density was applied (0.92 g/ml) to determinate fat cell weight. The total number of fat cells in each fat depot of all animals was determined by dividing the total weight of the fat depot by the mean cell weight of all captured fields. Finally, the frequency distribution of adipocyte sizes across the tissue was calculated by distributing all counted cells of each sample into two groups according to their area, <3000µm² or >3000µm²; then, the number of total counted adipocytes was used to calculate the percentage of adipocytes in both categories.

4.5. RNA extraction and quantification by real-time qRT-PCR

Total RNA from iWAT and eWAT was extracted using *TRIzol* Reagent (Thermo Fisher Scientific, Barcelona, Spain) following the manufacturer's protocol. RNA was quantified in *NanoDrop ND-1000* spectrophotometer (Thermo

Scientific, Wilmington, DE, USA). The integrity of RNA was evaluated by RNA integrity number (RIN) trough 2100 Bioanalyzer Instrument (Agilent Technologies). cDNA was synthesized using the *High Capacity cDNA Reverse Transcription Kit* (Applied Biosystems, Barcelona, Spain) in a Multigene ThermalCycler (Labnet, Madrid, Spain). The cDNA was subjected to a quantitative reverse transcriptase polymerase chain reaction amplification using iTaq™Universal SYBR Green Supermix (Bio-Rad, Madrid, Spain) in 7900HT Fast Real-Time PCR System (Applied Biosystems). The primers used for the different genes are described in supplementary Table S1 and were obtained from *Biomers.net* (Ulm, Germany). The relative expression of each gene was calculated according to *Cyclophilin peptidylprolyl isomerase A* (Ppia) mRNA levels and normalized to the levels measured in the corresponding control group. The ΔΔCt method was used and corrected for primer efficiency[39].

4.6. Statistical analysis

Data are expressed as the mean ± S.E.M. (n=6-8). Grubbs' test was used to detect outliers, which were discarded before subsequent analyses. The data were analysed using two-way analysis of variance (ANOVA) followed by Bonferroni post hoc test, comparing simultaneously the effect of MIX at each ZT studied (ZT0 and ZT12). Additionally, Student's t-test was also applied comparing MIX-treated and vehicle groups at each ZT and between vehicle groups. All statistical tests were performed using XL-Stat 2017 software (Addinsoft, Paris, France) and graphics were prepared using GraphPad Prism 9 (GraphPad Software, San Diego, CA, USA). A P value ≤0.05 was considered statistically significant.

Supplementary Materials: Figure S1: The supplementation with MIX or vehicle (VH) at ZT12 reduces accumulated food intake, and during the light phase reduces energy expenditure and activity. MIX supplementation promotes the reduction of activity at the light phase independently of time-of-day treatment, Figure S2: Hematoxylin and eosin (H&E) staining of iWAT (A) and eWAT (B) of rats treated with MIX or vehicle when the lights turned on (ZT0) or when the lights turned off (ZT12), Figure S3: Heatmap illustrating the differential gene expression in iWAT (A) and eWAT (B) of rats treated with MIX or vehicle when the lights turned on (ZT0) or when the lights turned off (ZT12), Table S1: Primers for the Q-PCR analysis.

Author Contributions: Conceptualization, B.M., M.M. and G.A.; methodology, M.C-P, R.M.R.; formal analysis, M.C-P. and M.A.; investigation, M.C-P and G.A.; data curation, M.C-P.; writing—original draft preparation, M.C-P.; writing—review and editing, M.C-P., E.N-M, G.A.; supervision, G.A. All authors have read and agreed to the published version of the manuscript.

Funding: This research was funded by Spanish government, grant number AGL2013-40707-R and AGL2016-77105-R. M.C-P received a pre-doctoral fellowship from the government of Catalonia (2021 FI_B2 00105). R.M.R. and E.N-M. received a grant for Ph.D. students from the Universitat Rovira i Virgili. G.A. and M.M. are Serra-Húnter fellows at the Universitat Rovira i Virgili.

Institutional Review Board Statement: The study was conducted according to the guidelines of European Directive 86/609/CEE and Royal Decree 223/1988 of the Spanish Ministry of Agriculture, Fisheries and Food, Madrid, Spain, and approved by The Animal Ethics Committee of Universitat Rovira i Virgili (reference number 9495 by Generalitat de Catalunya).

Acknowledgments: We gratefully acknowledge the aid of laboratory technicians Niurka Dariela Llópiz and Rosa Pastor.

Conflicts of Interest: The authors declare no conflict of interest.

References

[1] M. Longo *et al.*, "Adipose tissue dysfunction as determinant of obesity-associated metabolic complications," *Int. J. Mol. Sci.*, vol. 20, no. 9, 2019, doi: 10.3390/ijms20092358.

[2] G. Fantuzzi, "Adipose tissue, adipokines, and inflammation," *J. Allergy Clin. Immunol.*, vol. 115, no. 5, pp. 911–919, 2005, doi: 10.1016/j.jaci.2005.02.023.

[3] L. Brown, H. Poudyal, and S. K. Panchal, "Functional foods as potential therapeutic options for metabolic syndrome," *Obes. Rev.*, vol. 16, no. 11, pp. 914–941, 2015, doi: 10.1111/obr.12313.

[4] A. Pascual-Serrano *et al.*, "Grape seed proanthocyanidin supplementation reduces adipocyte

size and increases adipocyte number in obese rats," *Int. J. Obes.*, vol. 41, no. 8, pp. 1246–1255, Aug. 2017, doi: 10.1038/ijo.2017.90.

[5] T. Wu, Z. Jiang, J. Yin, H. Long, and X. Zheng, "Anti-obesity effects of artificial planting blueberry (Vaccinium ashei) anthocyanin in high-fat diet-treated mice," *Int. J. Food Sci. Nutr.*, vol. 67, no. 3, 2016, doi: 10.3109/09637486.2016.1146235.

[6] L. J. Den Hartigh *et al.*, "Metabolically distinct weight loss by 10,12 CLA and caloric restriction highlight the importance of subcutaneous white adipose tissue for glucose homeostasis in mice," *PLoS One*, vol. 12, no. 2, pp. 1–25, 2017, doi: 10.1371/journal.pone.0172912.

[7] F. I. Bravo, A. Mas-Capdevila, M. Margalef, A. Arola-Arnal, and B. Muguerza, "Novel Antihypertensive Peptides Derived from Chicken Foot Proteins," *Mol. Nutr. Food Res.*, vol. 63, no. 12, 2019, doi: 10.1002/mnfr.201801176.

[8] R. S. Weisinger, T. K. Stanley, D. P. Begg, H. S. Weisinger, K. J. Spark, and M. Jois, "Angiotensin converting enzyme inhibition lowers body weight and improves glucose tolerance in C57BL/6J mice maintained on a high fat diet," *Physiol. Behav.*, vol. 98, no. 1–2, pp. 192–197, 2009, doi: 10.1016/j.physbeh.2009.05.009.

[9] A. Gibert-Ramos, M. Z. Martín-González, A. Crescenti, and M. Josepa Salvadó, "A mix of natural bioactive compounds reduces fat accumulation and modulates gene expression in the adipose tissue of obese rats fed a cafeteria diet," *Nutrients*, vol. 12, no. 11, pp. 1–17, 2020, doi: 10.3390/nu12113251.

[10] J. S. Menet, S. Pescatore, and M. Rosbash, "CLOCK:BMAL1 is a pioneer-like transcription factor.," *Genes Dev.*, vol. 28, no. 1, pp. 8–13, Jan. 2014, doi: 10.1101/gad.228536.113.

[11] D. Lekkas and G. K. Paschos, "The circadian clock control of adipose tissue physiology and metabolism," 2019, doi: 10.1016/j.autneu.2019.05.001.

[12] A. Engin, "Circadian Rhythms in Diet-Induced Obesity," Springer, Cham, 2017, pp. 19–52.

[13] B. P. Sampey *et al.*, "Cafeteria diet is a robust model of human metabolic syndrome with liver and adipose inflammation: Comparison to high-fat diet," *Obesity*, vol. 19, no. 6, pp. 1109–1117, 2011, doi: 10.1038/oby.2011.18.

[14] M. Z. Martín-González *et al.*, "A novel dietary multifunctional ingredient reduces body weight and improves leptin sensitivity in cafeteria diet-fed rats," *J. Funct. Foods*, vol. 73, no. July, p. 104141, 2020, doi: 10.1016/j.jff.2020.104141.

[15] M. Z. Martín-González, H. Palacios, M. A. Rodríguez, L. Arola, G. Aragonès, and B. Muguerza, "Beneficial effects of a low-dose of conjugated linoleic acid on body weight gain and other cardiometabolic risk factors in cafeteria diet-fed rats," *Nutrients*, vol. 12, no. 2, 2020, doi: 10.3390/nu12020408.

[16] J. Godos *et al.*, "Diet and mental health: Review of the recent updates on molecular mechanisms," *Antioxidants*, vol. 9, no. 4, pp. 1–13, 2020, doi: 10.3390/antiox9040346.

[17] F. Gomez-Pinilla and T. T. J. Nguyen, "Natural mood foods: The actions of polyphenols against psychiatric and cognitive disorders," *Nutr. Neurosci.*, vol. 15, no. 3, pp. 127–133, 2012, doi: 10.1179/1476830511Y.0000000035.

[18] J. H. Stern, J. M. Rutkowski, and P. E. Scherer, "Adiponectin, Leptin, and Fatty Acids in the Maintenance of Metabolic Homeostasis through Adipose Tissue Crosstalk.," *Cell Metab.*, vol. 23, no. 5, pp. 770–84, May 2016, doi: 10.1016/j.cmet.2016.04.011.

[19] J. M. Tishinsky, D. W. L. Ma, and L. E. Robinson, "Eicosapentaenoic acid and rosiglitazone increase adiponectin in an additive and PPARγ-dependent manner in human adipocytes," *Obesity*, vol. 19, no. 2, 2011, doi: 10.1038/oby.2010.186.

[20] X. R. Zhou, C. H. Sun, J. R. Liu, and D. Zhao, "Dietary conjugated linoleic acid increases PPARγ gene expression in adipose tissue of obese rat, and improves insulin resistance," *Growth Horm. IGF Res.*, vol. 18, no. 5, pp. 361–368, 2008, doi: 10.1016/j.ghir.2008.01.001.

[21] K. Kohlstedt, C. Gershome, C. Trouvain, W. K. Hofmann, S. Fichtlscherer, and I. Fleming, "Angiotensin-converting enzyme (ACE) inhibitors modulate cellular retinol-binding protein 1 and adiponectin expression in adipocytes via the ACE-dependent signaling cascade," *Mol. Pharmacol.*, vol. 75, no. 3, 2009, doi: 10.1124/mol.108.051631.

[22] X. Yang *et al.*, "Nuclear Receptor Expression Links the Circadian Clock to Metabolism," *Cell*, vol. 126, no. 4, pp. 801–810, 2006, doi: 10.1016/j.cell.2006.06.050.

[23] S. Shimba *et al.*, "Brain and muscle Arnt-like protein-1 (BMAL1), a component of the molecular clock, regulates adipogenesis," *Proc. Natl. Acad. Sci. U. S. A.*, vol. 102, no. 34, pp. 12071–12076, 2005, doi: 10.1073/pnas.0502383102.

[24] H. Migita, J. Morser, and K. Kawai, "Rev-erbα upregulates NF-κB-responsive genes in vascular smooth muscle cells," *FEBS Lett.*, vol. 561, no. 1–3, pp. 69–74, 2004, doi: 10.1016/S0014-5793(04)00118-8.

[25] R. Ye and P. E. Scherer, "Adiponectin, driver or passenger on the road to insulin sensitivity?," *Mol. Metab.*, vol. 2, no. 3, pp. 133–41, Apr. 2013, doi: 10.1016/j.molmet.2013.04.001.

[26] F. Haczeyni, K. S. Bell-Anderson, and G. C. Farrell, "Causes and mechanisms of adipocyte enlargement and adipose expansion," *Obes. Rev.*, vol. 19, no. 3, pp. 406–420, Mar. 2018, doi: 10.1111/obr.12646.

[27] V. Primeau *et al.*, "Characterizing the profile of obese patients who are metabolically healthy," *International Journal of Obesity*, vol. 35, no. 7. 2011, doi: 10.1038/ijo.2010.216.

[28] N. Klöting *et al.*, "Insulin-sensitive obesity," *Am. J. Physiol. - Endocrinol. Metab.*, vol. 299, no. 3, 2010, doi: 10.1152/ajpendo.00586.2009.

[29] N. Stefan, H. U. Häring, F. B. Hu, and M. B. Schulze, "Metabolically healthy obesity: Epidemiology, mechanisms, and clinical implications," *The Lancet Diabetes and Endocrinology*, vol. 1, no. 2. 2013, doi: 10.1016/S2213-8587(13)70062-7.

[30] U. Smith and B. B. Kahn, "Adipose tissue regulates insulin sensitivity: role of adipogenesis, de novo lipogenesis and novel lipids," *J. Intern. Med.*, vol. 280, no. 5, pp. 465–475, 2016, doi: 10.1111/joim.12540.

[31] Y. D. Tchoukalova, C. Koutsari, M. V. Karpyak, S. B. Votruba, E. Wendland, and M. D. Jensen, "Subcutaneous adipocyte size and body fat distribution," *Am. J. Clin. Nutr.*, vol. 87, no. 1, pp. 56–63, 2008, doi: 10.1093/ajcn/87.1.56.

[32] A. Shostak, J. Meyer-Kovac, and H. Oster, "Circadian regulation of lipid mobilization in white adipose tissues," *Diabetes*, vol. 62, no. 7, pp. 2195–2203, 2013, doi: 10.2337/db12-1449.

[33] J. L. Barclay *et al.*, "High-fat diet-induced hyperinsulinemia and tissue-specific insulin resistance in Cry-deficient mice," *Am. J. Physiol. - Endocrinol. Metab.*, vol. 304, no. 10, pp. 1053–1063, 2013, doi: 10.1152/ajpendo.00512.2012.

[34] A. Korenčič, R. Košir, G. Bordyugov, R. Lehmann, D. Rozman, and H. Herzel, "Timing of circadian genes in mammalian tissues," *Sci. Rep.*, vol. 4, pp. 1–9, 2014, doi: 10.1038/srep05782.

[35] M. Margalef, Z. Pons, L. Iglesias-Carres, F. I. Bravo, B. Muguerza, and A. Arola-Arnal, "Lack of tissue accumulation of grape seed flavanols after daily long-term administration in healthy and cafeteria-diet obese rats.," *J. Agric. Food Chem.*, vol. 63, no. 45, pp. 9996–10003, Nov. 2015, doi: 10.1021/acs.jafc.5b03856.

[36] Y. Qin *et al.*, "Anthocyanin supplementation improves serum LDL- and HDL-cholesterol concentrations associated with the inhibition of cholesteryl ester transfer protein in dyslipidemic subjects," *Am. J. Clin. Nutr.*, vol. 90, no. 3, 2009, doi: 10.3945/ajcn.2009.27814.

[37] F. I. Bravo, L. Arola, and B. Muguerza, "Method for obtaining a chicken feet hydrolysate with antihypertensive activity, the hydrolysate that is obtained and the peptides it contains," *World Intellect. Prop. Organ. PCT*, no. 12, 2017.

[38] D. Eriksson-Hogling *et al.*, "Adipose tissue morphology predicts improved insulin sensitivity following moderate or pronounced weight loss," *Int. J. Obes.*, vol. 39, pp. 893–898, 2015, doi: 10.1038/ijo.2015.18.

[39] M. W. Pfaffl, "Relative quantification," *Real-time PCR*, pp. 64–82, 2007.

GRAPHICAL ABSTRACT

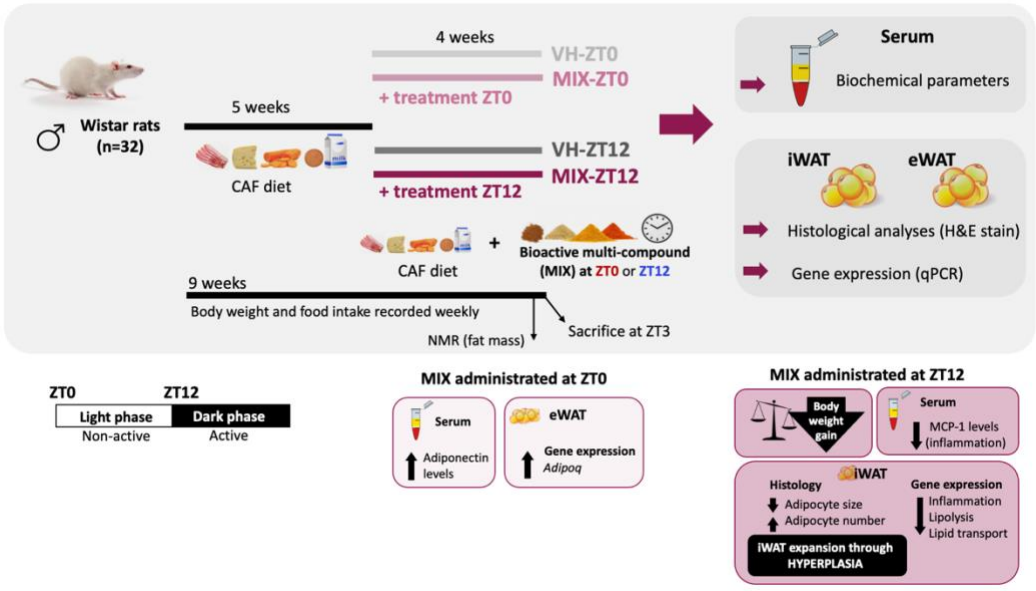

SUPPLEMENTARY MATERIAL

Table S1. Primers for the Q-PCR analysis.

	Forward (5'...3')	**Reverse (5'...3')**
Acacα	GCGGCTCTGGAGGTATATGT	TCTGTTTAGCGTGGGGATGT
Adipoq	GTTCCAGGACTCAGGATGCT	CGTCTCCCTTCTCTCCCTTC
Atgl	GAAGACCCTGCCTGCTGATT	CACATAGCGCACCCCTTGAA
Bmal1	GTAGATCAGAGGGCGACGGCTA	CTTGTCTGTAAAACTTGCCTGTGAC
C/ebpα	TGTACTGTATGTCGCCAGCC	TGGTTTAGCATAGACGCGCA
Cd36	CAGTGCAGAAACAGTGGTTGTCT	TGACATTTGCAGGTCCATCTATG
Cpt1b	GCAAACTGGACCGAGAAGAG	CCTTGAAGAAGCGACCTTTG
Cry1	TGGAAGGTATGCGTGTCCTC	TCCAGGAGAACCTCCTCACG
Fabp4	GAAAGAAGTGGGAGTTGGCT	TACTCTCTGACCGGATGACG
Fasn	TAAGCGGTCTGGAAAGCTGA	CACCAGTGTTTGTTCCTCGG
Gpat	GAATACAGCCTTGGCCGATG	GAGGCGTGCATGAATAGCAA
Hsl	AGTTCCCTCTTTACGGGTGG	GCTTGGGGTCAGAGGTTAGT
IL6	GCTTCCCTCAGGATGCTTGT	ATTAACTGGGGTGCCTGCTC
Lpl	GGCCCAGCAACATTATCCAG	ACTCAAAGTTAGGCCCAGCT
Mgl	ATCATCCCCGAGTCAGGACA	TGACTCCCCTAGACCACGAG
Per2	CGGACCTGGCTTCAGTTCAT	AGGATCCAAGAACGGCACAG
Pparγ	AGGGCGATCTTGACAGGAAA	CGAAACTGGCACCCTTGAAA
Ppia	CTTCGAGCTGTTTGCAGACAA	AAGTCACCACCCTGGCACATG
Rev-erb-α	CTGCTCGGTGCCTAGAATCC	GTCTTCACCAGCTGGAAAGCG
Tnfα	GCTGCACTTTGGAGTGATCG	GTGTGCCAGACACCCTATCT

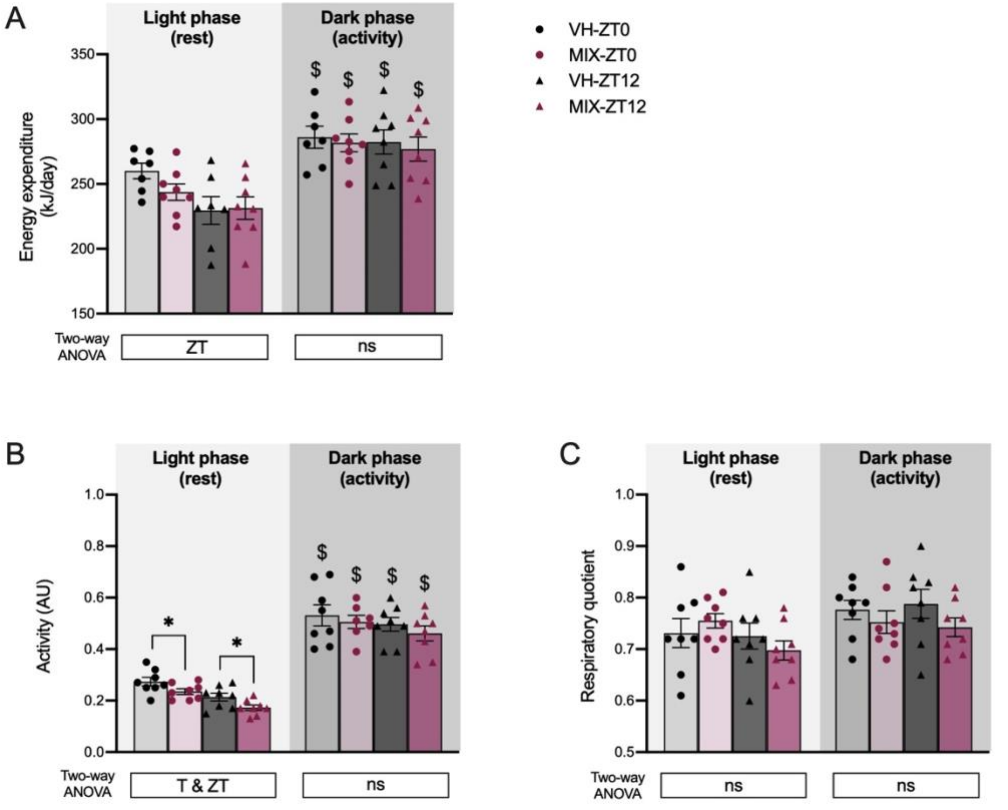

Figure 1S. The supplementation with MIX or vehicle (VH) at ZT12 reduces energy expenditure and activity during the light phase. MIX supplementation promotes the reduction of the activity at the light phase independently of time-of-day treatment. *A) energy expenditure, B) activity and C) respiratory quotient during light and dark phase of rats fed a CAF diet supplemented with MIX or VH when the lights turned on (ZT0) or when the lights turned off (ZT12). Data represent mean ± s.e.m. (n=7-8). * and $, significant differences ($p < 0.05$) using t-Student test between vehicle and treated group and between the same group at the light phase vs dark phase, respectively; ns, no significant differences; ZT, effect of time-of-day treatment; T, the effect of treatment using two-way ANOVA ($p < 0.05$).*

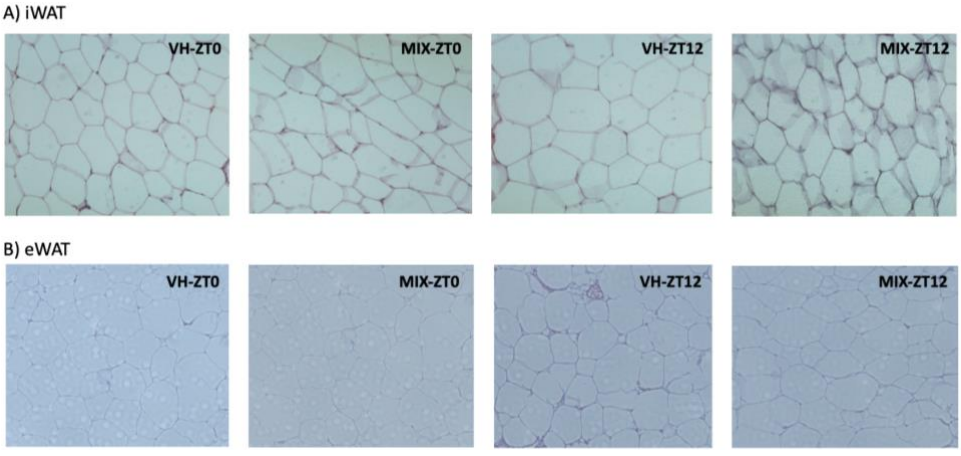

Figure S2. *Hematoxylin and eosin (H&E) staining of iWAT (A) and eWAT (B) of rats treated with MIX or vehicle when the lights turned on (ZT0) or when the lights turned off (ZT12). H&E magnification x10.*

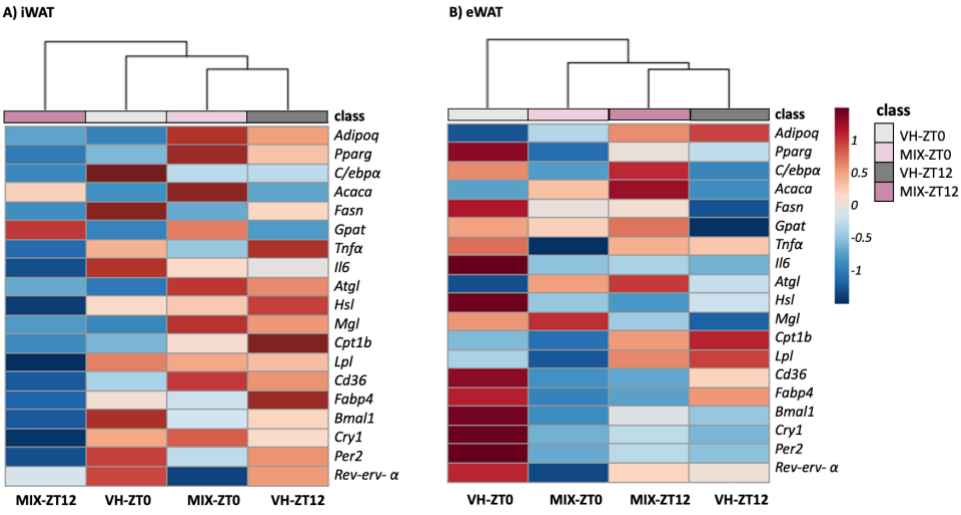

Figure S3. *Heatmap illustrating the differential gene expression in iWAT (A) and eWAT (B) of rats treated with MIX or vehicle when the lights turned on (ZT0) or when the lights turned off (ZT12).*

General discussion

The high prevalence of obesity lead to classified it as an epidemic [1]. When energy intake is higher than energy expenditure, WAT stores the excess of energy in form of fat inducing obesity. However, obesity is not mere an excess of fat, but it is a risk factor for many metabolic disorders including type 2 diabetes, cardiovascular diseases, inflammation, and cancer [2]. Natural bioactive compounds are a good strategy to prevent and ameliorate these obesity-related disorders. Previous research demonstrated that the consumption of proanthocyanidins from grape seed present anti-obesity properties and concomitantly modulate the molecular clock system in adipose tissue and other metabolic tissues [3,4]. The clock system allows the anticipation of environmental changes and adaptation to the time of day and food availability through the generation of circadian rhythms, which are intimately related to metabolic regulation. This important function can be altered and disrupted under certain situations, as in obesity, thereby compromising health [5]. However, since many metabolic pathways present circadian rhythm, the effects of proanthocyanidins on WAT metabolism and circadian rhythm might differ depending on the time-of-day administration. For this reason, the main objective of the present Doctoral Thesis was to determine whether GSPE consumption showed different effects on WAT metabolism depending on the time-of-day in which it was administrated.

The experimental animal model used in this Doctoral Thesis was mainly cafeteria diet-fed rats, since this diet and species closely mimic the development of metabolic syndrome in humans, from the beginning by promoting hyperphagia to the development of all metabolic symptoms [6]. In fact, this similar development of metabolic syndrome between rats and humans is what has prompted us to work with this dietary model and species, despite of the laborious preparation and the biological variability. Our research group present a large experience in the detrimental effects of cafeteria diet in the metabolism of these animals. From a nutritional point of view,

cafeteria diet consisted in biscuits with cheese and paté, bacon, ensaïmada (sweetened pastry), carrots, and milk with sucrose, which makes it a highly palatable diet.

The first objective of the present Doctoral Thesis was to explore the differential effects of GSPE on subcutaneous and visceral WAT metabolism according to time-of-day administration in obese rats. Our results showed that GSPE effects were tissue-specific and depend on time-of-day consumption presenting antidiabetic and anti-inflammatory effects on eWAT when GSPE was consumed at the beginning of the light phase (ZT0) and hyperplastic effects on iWAT when it was consumed at the beginning of the dark phase (ZT12) (**Manuscript 1**).

Previous studies demonstrated a reduction of body weight by reducing food intake and activating β-oxidation in subcutaneous adipose tissue, however, GSPE doses were higher (200-500 mg / kg of body weight) or the treatment period was longer (more than 10 weeks) [7,8]. Nevertheless, these studies did not take into account the time-of-day GSPE administration. Our results showed that the consumption of GSPE (25 mg/kg of body weight) for four weeks exerted an effect reducing body weight gain and food intake in obese rats when it was consumed at the beginning of the dark phase (ZT12) but not at ZT0. Additionally, previous studies demonstrated that GSPE did not reduce body weight gain neither adiposity but improved visceral retroperitoneal WAT expansion by preventing hypertrophy and increasing hyperplasia in a dose-dependent manner (25, 100 or 200mg of proanthocyanidins/kg of body weight) in obese rats. When energy intake is higher than energy expenditure, WAT can expand through hyperplasia which is a healthy expansion of adipose tissue where preexisting adipocyte cell precursors from WAT become mature adipocytes, thus, increasing adipocytes number. The mechanism by which GSPE remodeled WAT expansion was hypothesized to be through the inhibition of Sirt1, which stops the repression of PPARγ [3]. Authors observed lower effects of GSPE in subcutaneous iWAT compared to retroperitoneal WAT where GSPE tended to reduce hypertrophy [9]. In this

Doctoral Thesis, obese rats showed a significant reduction of adipocyte hypertrophy and an increment of hyperplasia in iWAT when GSPE was consumed at ZT12 (**Manuscript 1**), without showing any effect on eWAT.

Hyperplasia of WAT is positively correlated with lower lipid uptake and lipolysis per adipocyte as it was observed in this Docotoral Thesis at ZT12 (**Manuscript 1**) [10,11]. It is well known that WAT expansion through hyperplasia protects against metabolic disorders including insulin resistance and inflammation, while hypertrophy increases the risk [11,12]. Moreover, subcutaneous fat accumulation causes less metabolic disturbances than visceral adiposity, which is strongly associated with metabolic syndrome. This could be related to metabolic differences between subcutaneous and visceral fat depots with respect to lipolysis, fatty acid storage, adipokine secretion and general gene expression profile. Therefore, the proper storage of energy excess in subcutaneous adipose tissue protects against visceral fat accumulation and tissue inflammation. The rationale for using inguinal adipose tissue as a model of subcutaneous fat depot in this Doctoral Thesis was because of its role in metabolic homeostasis. In fact, in rodent models, surgical removal of inguinal WAT can eventually lead to metabolic dysfunction and ectopic lipid accumulation [13]. Conversely, transplantation of inguinal WAT into the visceral cavity of mice leads to improved glucose homeostasis and body composition, which occurs alongside beneficial alterations in circulating adipokines [14]. With respect to visceral fad pads, epididymal adipose tissue is one of the most used because it makes up the largest portion of the total adipose tissue of abdominal cavity and allows more accurate weighing due to easy extraction. In this sense, our study also demonstrated that GSPE administrated at ZT0, but not at ZT12, downregulated the pro-inflammatory IL-6 in eWAT and reduced HOMA-IR suggesting an improvement of insulin sensitivity in this tissue (**Manuscript 1**) [15].

Although, some studies have shown beneficial effects of GSPE on reducing cholesterol and TAG circulating levels [15], our data did not demonstrate that GSPE prevented hyperlipidemia (**Manuscript 1 and 2**). However, the circadian rhythm of serum TAG concentration was significantly restored when GSPE was consumed at ZT12 (**Manuscript 2**). In this context, another objective of this Doctoral Thesis was to determine whether GSPE can restore the circadian rhythm lost in obesity in a time-dependent manner in iWAT. We continued studying iWAT, since GSPE modulated the expansion of iWAT through hyperplasia in a time-dependent manner, while this modification was not observed in eWAT. First, we analyzed the circadian rhythm of iWAT metabolites assessed by nuclear magnetic resonance spectrometry in both STD and CAF rats supplemented with vehicle or GSPE (25 mg/kg of body weight) at the beginning of the light phase (ZT0) of at the beginning of the dark phase (ZT12).

White adipocytes from subcutaneous WAT have the capacity to be converted into brown-like adipocytes and increase energy expenditure, being beneficial for obesity [16]. Brown adipose tissue present a dynamic metabolic role in maintaining body temperature across the day/night cycle where increases fatty acid oxidation and Krebs cycle activity to generate heat during the rest phase and fat storage during the active phase when rats feed [17]. Therefore, metabolites in this tissue present a diurnal rhythm because of its active metabolism. In this sense, WAT also is influenced by light/dark cycle inducing lipogenesis during feeding and lipolysis during fasting to supply energy for other tissues.

Interestingly, in our study some lipophilic metabolites including oleic acid, linoleic acid, monounsaturated fatty acid, total fatty acid, TAG, and certain hydrophilic metabolites involved in lipid metabolism presented diurnal rhythms in the iWAT of STD animals. The rhythmicity of these metabolites was lost under CAF diet, and it was restored in response to GSPE consumption at the beginning of the dark phase (ZT12), but not at ZT0. Indeed, STD animals presented 18 rhythmic metabolites, which 16 lost their rhythm under CAF diet, and interestingly, 12 metabolites restored the

rhythm only when GSPE was administrated at ZT12. These iWAT metabolites with diurnal rhythm in STD animals and CAF animals supplemented with GSPE at the beginning of the dark phase were involved in in alanine, aspartate, and glutamate metabolism. This suggests that iWAT is a metabolically active tissue in lean mice, which its functionality was lost in obesity, and it was recovered with GSPE consumption in a time-dependent manner (**Manuscript 2**).

In addition to the obvious role of WAT on lipid homeostasis, this tissue also plays an important role in systemic amino acid metabolism. Subcutaneous WAT is the primary tissue which uptakes BCAA (leucine, isoleucine and valine) from liver, after feeding, together with glutamate uptake and the release of asparagine, glutamine and alanine from adipocytes [18,19]. Glutamine and alanine are liberated from WAT as a mechanism to remove nitrogen and avoid nitrogen toxification in the tissue. Glutamine is taken up by kidneys and intestine where it enters in the Krebs cycle, while alanine is taken up by the liver where it might be a substrate for gluconeogenesis or urea cycle [20,21].

To further study the effects of GSPE on the circadian rhythm of obese iWAT, we evaluate the effects of GSPE-derived serum metabolites (GSPM) on the circadian rhythm of *PER2* bioluminescence in obese WAT explants according to time-of-day treatment. An important aspect of polyphenols is the biochemical changes that occur to these molecules after their metabolization by intestinal cells, microbiota and liver. Indeed, the molecular forms that reach the circulation and tissues are different from those that are present in food plants [22]. Therefore, the bioactive flavanols in serum and WAT differ considerably from the compounds that are present in GSPE. Thus, to evaluate *in vitro* the effects of GSPE on WAT explants, it is important to use the metabolites found in serum of GSPE-administered rodents. In this study the serum was obtain 2 hours after the administration of GSPE since the highest plasma peak concentrations of flavanols are around 2 hours after the ingestion of the extract [23–

25]. It was administrated 1 g/kg of body weight of GSPE to obtain enough concentrations of GSPM. A previous study from our group, also combined the *in vivo* and *in vitro* system and showed a decrease in the *de novo* lipid synthesis and excretion in hepatic human cells (HepG2 cells) incubated with GSPM [26].

It is known that high fat diets lead to a desynchrony of eating patterns and the disruption of the circadian rhythm [27,28]. In this sense, our results showed that the circadian rhythm of *PER2* presented longer period, a phase delay and lower amplitude in obese WAT explants (WAT from HFD-fed mice) compared to lean explants (WAT from STD-fed mice). Previous studies determined that GSPE was capable to modulate clock genes in WAT and other tissues [4]. Interestingly, our results showed that the incubation of GSPM with WAT explants restore *PER2* bioluminescence rhythmicity only when the explants were incubated with GSPM at the trough of *PER2* bioluminescence, inducing a phase advance and increasing period and amplitude. On the other hand, GSPM incubation exerted stronger effects on lipid metabolism upregulating the relative expression of genes related to lipid transport when obese explants were treated at peak of *PER2* bioluminescence (**Manuscript 3**). Although GSPM effects on *PER2* circadian parameters were observed when explants were treated at trough of *PER2* bioluminescence, lipid metabolism gene expression data reveled marked effects when explants were treated at peak of *PER2* bioluminescence. Nevertheless, it should be considered that bioluminescence data was obtained over a treatment period of 5 days, while gene expression data took place in a shorter treatment period of only 10 hours (**Manuscript 3**). Taken altogether, our studies demonstrated that GSPE presented beneficial effects on obese iWAT in a time-dependent manner regulating molecular clock and lipidic metabolic genes. Therefore, proanthocyanidins could be a good strategy for the management of obesity on the chrononutraceutical field, although further research through different experimental models is needed to find out the mechanisms of action by which GSPE modulates the diurnal rhythms of tissues.

To efficiently treat obesity and obesity-related disorders, the synergy of other bioactive compounds together with GSPE would be a more powerful strategy than the administration of an individual bioactive compounds. Therefore, a bioactive multi-compound (MIX) was designed to determine its ability to manage the functionality of WAT. MIX was based on proanthocyanidins from grape seeds (GSPE) together with anthocyanins from berries, conjugated linoleic acid (CLA) and protein hydrolysate from chicken feet (Hpp11). Each bioactive compound has individually demonstrated beneficial effects against metabolic disorders; CLA is capable to reduce fat mass, Hpp11 present antihypertensive properties, anthocyanidins are anti-diabetic and anti-inflammatory molecules, and the properties of proanthocyanidins from grape-seed have been already discussed [29–31]. Our results confirmed the potential effects on body weight gain reduction, which were showed in obese rats treated with MIX at ZT12. These animals also presented lower adipocyte size and higher number of smaller adipocytes in iWAT, and not in eWAT. In addition, these histological changes were associated with a lower expression of genes related to lipid transport and lipolysis (**Manuscript 4**). Our previous studies demonstrated that GSPE reduced body weight gain when it was consumed at ZT12 (**Manuscript 2**). Moreover, animals that consumed GSPE at ZT12 presented hyperplasia in iWAT and lower expression of genes related to lipid transport and lipolysis (**Manuscript 1**). Therefore, the reduction of body weight gain and the induction of hyperplasia in iWAT would be attributed to GSPE effects in a time-dependent manner. Surprisingly, animals supplemented with MIX at ZT12 concomitantly presented both lower concentrations of the proinflammatory molecule MCP-1 in serum and *Tnfα* gene expression in iWAT, although animals supplemented with MIX at ZT0 presented lower gene expression of proinflammatory cytokines in both WAT depots (**Manuscript 4**), while the supplementation of GSPE at ZT0 only presented the reduction of a proinflammatory genes in eWAT (**Manuscript 1**).

Interestingly, the same animals supplemented with MIX at ZT0 presented an upregulation of *Adipoq* in eWAT and higher circulating adiponectin levels (**Manuscript 4**). The upregulation of adiponectin could be attributed to CLA and Hpp11 through *PPARγ* upregulation, although no clear findings are exposed [32,33]. Even though adiponectin protects against insulin resistance [34], these animals did not show a reduction of HOMA-IR, as we observed in the animals supplemented with GSPE at ZT0 (**Manuscript 1**). Nevertheless, previous studies demonstrated beneficial properties of MIX against insulin resistance at ZT0 [35].

Therefore, the beneficial effects associated with the consumption of GSPE and MIX in diet-induced obese animals are related to the diurnal rhythmicity of WAT metabolism and are strongly influenced by the time-of-day in which it was consumed. Therefore, it is plausible to speculate that the consumption of bioactive food compounds at the most optimal time-of-day could properly potentiate the metabolism and function of tissues in a tissue-specific manner, affecting the whole-body energy metabolism and, consequently, contributing to the management of overweight and obesity.

References

[1] "World Health Organization (who.int), 2022.pdf."

[2] A. L. Ghaben and P. E. Scherer, "Adipogenesis and metabolic health" *Nat. Rev. Mol. Cell Biol.*, vol. 20, no. 4, pp. 242–258, 2019.

[3] A. Pascual-Serrano, C. Bladé, M. Suárez, and A. Arola-Arnal, "Grape Seed Proanthocyanidins Improve White Adipose Tissue Expansion during Diet-Induced Obesity Development in Rats" *Int. J. Mol. Sci.*, vol. 19, no. 9, p. 2632, 2018.

[4] A. Ribas-Latre *et al.*, "Chronic consumption of dietary proanthocyanidins modulates peripheral clocks in healthy and obese rats" *J. Nutr. Biochem.*, vol. 26, pp. 112–119, 2015.

[5] Y. Li *et al.*, "Circadian rhythms and obesity: Timekeeping governs lipid metabolism" *J. Pineal Res.*, vol. 69, no. 3, pp. 1–11, 2020.

[6] B. P. Sampey *et al.*, "Cafeteria diet is a robust model of human metabolic syndrome with liver and adipose inflammation: Comparison to high-fat diet" *Obesity*, vol. 19, no. 6, pp. 1109–1117, 2011.

[7] J. Serrano *et al.*, "A specific dose of grape seed-derived proanthocyanidins to inhibit body weight gain limits food intake and increases energy expenditure in rats" *Eur. J. Nutr.*, vol. 56, no. 4, pp. 1629–1636, 2017.

[8] Z. Pons, M. Margalef, F. I. Bravo, A. Arola-Arnal, and B. Muguerza, "Chronic administration of grape-seed polyphenols attenuates the development of hypertension and improves other cardiometabolic risk factors associated with the metabolic syndrome in cafeteria diet-fed rats" *Br. J. Nutr.*, vol. 117, no. 2, pp. 200–208, 2017.

[9] A. Pascual-Serrano *et al.*, "Grape seed proanthocyanidin supplementation reduces adipocyte size and increases adipocyte number in obese rats" *Int. J. Obes.*, vol. 41, no. 8, pp. 1246–1255, 2017.

[10] C. Farnier *et al.*, "Adipocyte functions are modulated by cell size change: Potential involvement of an integrin/ERK signalling pathway" *Int. J. Obes.*, vol. 27, no. 10, pp. 1178–1186, 2003.

[11] S. Laforest, J. Labrecque, A. Michaud, K. Cianflone, and A. Tchernof, "Adipocyte size as a determinant of metabolic disease and adipose tissue dysfunction" *Crit. Rev. Clin. Lab. Sci.*, vol. 52, no. 6, pp. 301–313, 2015.

[12] K. N. Manolopoulos, F. Karpe, and K. N. Frayn, "Gluteofemoral body fat as a determinant of metabolic health" *Int. J. Obes.*, vol. 34, no. 6, pp. 949–959, 2010.

[13] K. Cox-York, Y. Wei, D. Wang, M. J. Pagliassotti, and M. T. Foster, "Lower body adipose tissue removal decreases glucose tolerance and insulin sensitivity in mice with exposure to high fat diet" *Adipocyte*, vol. 4, no. 1, pp. 32–43, 2015.

[14] Thien T. Tran, Yuji Yamamoto, Stephane Gesta, "Beneficial Effects of Subcutaneous Fat Transplantation on Metabolism" *Cell Metab.*, vol. 7, no. 5, pp. 410–420, 2008

[15] N. Cermakian *et al.*, "Crosstalk between the circadian clock circuitry and the immune system" *Chronobiol. Int.*, vol. 30, no. 7, pp. 870–888, 2013.

[16] P. Seale *et al.*, "Prdm16 determines the thermogenic program of subcutaneous white adipose tissue in mice" *J. Clin. Invest.*, vol. 121, no. 1, pp. 96–105, 2011.

[17] C. Castro, W. Briggs, G. K. Paschos, G. A. Fitzgerald, and J. L. Griffin, "A metabolomic study of adipose tissue in mice with a disruption of the circadian system" *Mol. Biosyst.*, vol. 11, no. 7, pp. 1897–1906, 2015.

[18] S. Christou *et al.*, "Circadian regulation in human white adipose tissue revealed by transcriptome and metabolic network analysis" *Sci. Rep.*, vol. 9, no. 1, pp. 1–12, 2019.

[19] D. E. Lackey *et al.*, "Regulation of adipose branched-chain amino acid catabolism enzyme expression and cross-adipose amino acid flux in human obesity" *Am. J. Physiol. - Endocrinol. Metab.*, vol. 304, no. 11, pp. 1175–1187, 2013.

[20] T. J. Kowalski, W. U. Guoyao, and M. Watford, "Rat adipose tissue amino acid metabolism in vivo as assessed by microdialysis and arteriovenous techniques" *Am. J. Physiol.*, vol. 273, no. 3 PART 1, 1997.

[21] J. S. Burrill *et al.*, "Inflammation and ER stress regulate branched-chain amino acid uptake and metabolism in adipocytes" *Mol. Endocrinol.*, vol. 29, no. 3, pp. 411–420, 2015.

[22] P. A. Kroon *et al.*, "How should we assess the effects of exposure to dietary polyphenols in vitro?" *Am. J. Clin. Nutr.*, vol. 80, no. 1, pp. 15–21, 2004.

[23] M. Serafini, R. Bugianesi, G. Maiani, S. Valtuena, S. De Santis, and A. Crozier, "Plasma antioxidants from chocolate" *Nature*, vol. 424, no. 6952, p. 1013, 2003.

[24] D. Rein, S. Lotito, R. R. Holt, C. L. Keen, H. H. Schmitz, and C. G. Fraga, "Epicatechin in human plasma: In vivo determination and effect of chocolate consumption on plasma oxidation status"

J. Nutr., vol. 130, no. 8., pp. 2109–2114, 2000.

[25] A. Serra *et al.*, "Bioavailability of procyanidin dimers and trimers and matrix food effects in in vitro and in vivo models" *Br. J. Nutr.*, vol. 103, no. 7, pp. 944–952, 2010.

[26] L. Guerrero *et al.*, "Serum metabolites of proanthocyanidin-administered rats decrease lipid synthesis in HepG2 cells" *J. Nutr. Biochem.*, vol. 24, no. 12, pp. 2092–2099, 2013.

[27] A. Chaix, T. Lin, H. D. Le, M. W. Chang, and S. Panda, "Time-Restricted Feeding Prevents Obesity and Metabolic Syndrome in Mice Lacking a Circadian Clock" *Cell Metab.*, vol. 29, no. 2, pp. 303-319, 2019.

[28] K. L. Branecky, K. D. Niswender, and J. S. Pendergast, "Disruption of daily rhythms by high-fat diet is reversible" *PLoS One*, vol. 10, no. 9, pp. 1–12, 2015.

[29] M. W. Pariza, Y. Park, M.E. Cook, "The biologically active ismoers of conjugated linoleic acid" *Prog. Lip Res*., vol 40, 283-298, 2001.

[30] F. I. Bravo, A. Mas-Capdevila, M. Margalef, A. Arola-Arnal, and B. Muguerza, "Novel Antihypertensive Peptides Derived from Chicken Foot Proteins" *Mol. Nutr. Food Res.*, vol. 63, no. 12, 2019.

[31] T. Tsuda, "Recent progress in anti-obesity and anti-diabetes effect of berries" *Antioxidants*, vol. 5, no. 2, 2016.

[32] X. R. Zhou, C. H. Sun, J. R. Liu, and D. Zhao, "Dietary conjugated linoleic acid increases PPARγ gene expression in adipose tissue of obese rat, and improves insulin resistance" *Growth Horm. IGF Res.*, vol. 18, no. 5, pp. 361–368, 2008.

[33] K. Kohlstedt, C. Gershome, C. Trouvain, W. K. Hofmann, S. Fichtlscherer, and I. Fleming, "Angiotensin-converting enzyme (ACE) inhibitors modulate cellular retinol-binding protein 1 and adiponectin expression in adipocytes via the ACE-dependent signaling cascade" *Mol. Pharmacol.*, vol. 75, no. 3, 2009.

[34] J. H. Stern, J. M. Rutkowski, and P. E. Scherer, "Adiponectin, Leptin, and Fatty Acids in the Maintenance of Metabolic Homeostasis through Adipose Tissue Crosstalk." *Cell Metab.*, vol. 23, no. 5, pp. 770–84, May 2016.

[35] M. Z. Martín-González *et al.*, "A novel dietary multifunctional ingredient reduces body weight and improves leptin sensitivity in cafeteria diet-fed rats" *J. Funct. Foods*, vol. 73, no. July, p. 104141, 2020.

Conclusions

1. **The effects of a chronic consumption of GSPE depend on the time-of-day administration and the type of WAT depot in obese rats.** GSPE consumption at ZT0 exerted antidiabetic effects and downregulated the expression of proinflammatory genes in visceral WAT. While GSPE consumption at ZT12 induced subcutaneous WAT expansion through hyperplasia and downregulated the expression of genes related to lipid transport and lipolysis.

2. **GSPE has the ability to restore the diurnal rhythm of alanine, aspartate and glutamate metabolism pathway in subcutaneous WAT only when it is consumed at ZT12.** A total of 45 metabolites were detected, 19 of which presented diurnal rhythms in healthy animals. Most metabolites became arrhythmic in diet-induced obesity, however GSPE consumption at ZT12 - but not at ZT0 - restored the rhythmicity of 12 metabolites including compounds involved in alanine, aspartate and glutamate metabolism.

3. **GSPM have the capacity to restore *PER2* circadian rhythm on subcutaneous WAT only when they are treated at trough - not at peak - of *PER2* bioluminescence.** In obese subcutaneous WAT explants, GSPM induced a phase advance and increased the amplitude of *PER2* similar to healthy subcutaneous WAT explants.

4. **GSPM upregulate fatty acid uptake in obese subcutaneous WAT explants only when they are treated at peak – not at trough - of *PER2* bioluminescence.** GSPM upregulated *Lpl* expression, suggesting a higher rate of fatty acid uptake into adipocytes, in a time-dependent manner in obesity.

5. **The effects of a chronic consumption of MIX (based on GSPE) depend on the time-of-day administration and type of WAT depot in obese rats.** The consumption of MIX at ZT0 increased adiponectin serum concentration due to the stimulation of *Adipoq* mRNA expression in visceral WAT. While the consumption of MIX at ZT12 tended to decrease body weight gain, and significantly reduced proinflammatory markers in serum and subcutaneous WAT, lipolytic gene expression and adipocyte size in subcutaneous WAT.

As a final conclusion, the present Doctoral Thesis demonstrated that the beneficial effects associated with the consumption of GSPE in diet-induced obese animals are related to the diurnal rhythmicity of WAT metabolism and are strongly influenced by the time-of-day in which it was consumed. Therefore, it is plausible to speculate that the consumption of bioactive food compounds at the most optimal time-of-day could properly potentiate the metabolism and function of tissues in a tissue-specific manner, affecting the whole-body energy metabolism and, consequently, contributing to the management of overweight and obesity.

Annexes

♦ List of publications

1. Manuscripts included in the thesis

Colom-Pellicer M, Rodríguez R M, Navarro-Masip È, Bravo F I, Mulero M, Arola L and Aragonès G. Time-of-day dependent effect of proanthocyanidins on adipose tissue metabolism in rats with diet-induced obesity. *Int J Obes*. 2022, May 6. doi: 10.1038/s41366-022-01132-0.

Colom-Pellicer M, Rodríguez R M, Soliz-Rueda J R, de Assis L V M, Navarro-Masip È, Quesada-Vázquez S, Escoté X, Oster H, Mulero M and Aragonès G. Proanthocyanidins Restore the Metabolic Diurnal Rhythm of Subcutaneous White Adipose Tissue According to Time-Of-Day Consumption. *Nutrients.* 2022, 14(11), 2246. doi: 10.3390/nu14112246.

Colom-Pellicer M[*], de Assis L V M[*], Rodríguez R M, Mulero M, Arola-Arnal A, Oster H and Aragonès G. Proanthocyanidins modulate PER2 circadian rhythm and metabolic gene expression in mice adipose tissue explants in a time-dependent manner. Submitted to *Frontiers in Nutrition*. June 2022.

Colom-Pellicer M, Rodríguez R M, Aguado M, Navarro-Masip È, Mulero M and Aragonès G. Bioactive multi-ingredient consumption influences white adipose tissue metabolism in a time-of-day-dependent manner in obese rats. Ready to be submitted to the *International Journal of Molecular Science*.

2. Other manuscripts

Auguet T , Aragonès G, **Colom M**, Aguilar C, Martín-Paredero V, Canela N, Ruyra X and Richart C. Targeted metabolomic approach in men with carotid plaque. *PLoS One*. 2018 Jul 16;13(7):e0200547. doi: 10.1371/journal.pone.0200547.

Colom M, Aragonès G and Auguet T. Insights in Gut Microbiota and Non-Alcoholic Fatty Liver Disease. *Adv Res Gastroentero Hepatol*. 2018 Mar 9(3). doi: 10.19080/ARGH.2018.09.555761

Aragonès G, **Colom-Pellicer M**, Aguilar C, Guiu-Jurado E, Martínez S, Sabench F, Porras J A, Riesco D, Del Castillo D, Richart C and Auguet T. Circulating microbiota-derived metabolites: a "liquid biopsy?. *Int J Obes*. 2020 Apr;44(4):875-885. doi: 10.1038/s41366-019-0430-0

Quesada-Vázquez S, **Colom-Pellicer M**, Navarro-Masip È, Aragonès G, Del Bas J M, Caimari A and Escoté X. Supplementation with a Specific Combination of Metabolic Cofactors Ameliorates Non-Alcoholic Fatty Liver Disease, Hepatic Fibrosis, and Insulin Resistance in Mice. *Nutrients*. 2021 Oct 9;13(10):3532. doi: 10.3390/nu13103532

Rodríguez R M, Cortés-Espinar A J, Soliz-Rueda J R, Feillet-Coudray C, Casas F, **Colom-Pellicer M**, Aragonès G, Avila-Román J, Muguerza B, Mulero M and Salvadó M J. Time-of-Day Circadian Modulation of Grape-Seed Procyanidin Extract (GSPE) in Hepatic Mitochondrial Dynamics in Cafeteria-Diet-Induced Obese Rats. *Nutrients*. 2022, Feb 12;14(4):774. doi: 10.3390/nu14040774.

Rodríguez R M, **Colom-Pellicer M**, Blanco J, Calvo E, Aragonès G and Mulero M. Grape-Seed Procyanidin Extract (GSPE) Seasonal-Dependent Modulation of Glucose and Lipid Metabolism in the Liver of Healthy F344 Rats. *Biomolecules*. 2022, Jun, 12, 839. https://doi.org/10.3390/biom12060839.

♦ List of conferences

Colom-Pellicer M, Aguado M, Cruz-Carrión Á, Arola-Arnal A, Suárez M, Aragonès G. Time-of-day dependent effects of bioactive compounds: a preliminary study of white adipose tissue function and expandability in obese rats. 2019. Alimentómica. XI Seminario sobre Alimentación y estilos de vida saludables. 23-24 de julio de 2019, Barcelona.

Rojas-Criollo M, Cruz-Carrión Á, **Colom-Pellicer M**, Iglesias-Carres L, Aragonès G, Arola-Arnal A, Suárez M. La biodisponibilidad de los compuestos fenólicos de extracto de proantocianidinas de semilla de uva se ve afectada por los ritmos circadianos. 2019. Alimentómica. XI Seminario sobre Alimentación y estilos de vida saludables. 23-24 de julio de 2019, Barcelona.

Colom-Pellicer M, Aguado M, Cruz-Carrión Á, Arola-Arnal A, Suárez M, Aragonès G. Time-of-day dependent effect of bioactive compounds on white adipose tissue metabolism and expandability in obese rats. NuGO - NuGOweek 2019, 16ht edition. From foodomics to nutrigenomics – Trnaslating food composition data into healthy diets. 9-12 September 2019, Agroscope, Bern, Switzerland.

Colom-Pellicer M, Aguado M, Cruz-Carrión Á, Arola-Arnal A, Suárez M, Aragonès G. Time-of-day dependent effect of grape-seed procyanidins on white adipose tissue function in diet-induced obese rats. ICPH2019 KOBE. The 9th International Conference on Polyphenol and Health. November 28 – December 1, 2019. Kobe International Conference Center, Kobe, Japan.

Rodríguez R M, **Colom-Pellicer M**, Blanco J, Aragonès G and Mulero M. (2022). Seasonal dependent effects of Grape Seed Proanthocyanidin Extract (GSPE) on hepatic metabolism of healthy F344 rats. The 10th International Conference on Polyphenols and Health. April 20-23, 2022. London, UK.

Colom-Pellicer M, Rodríguez R M, Soliz-Rueda J R, Mulero M, Muguerza B and Aragonès G. Las proantocianidinas reestablecen el ritmo circadiano del tejido adiposo blanco dependiendo del momento del día en que se consumen. I Jornadas sobre Nutracéutica: Compuestos bioactivos y Nutracéuticos. March 3-4, 2022. Tarragona, Spain.

Rodríguez R M, Soliz-Rueda J R, **Colom-Pellicer M**, Muguerza B, Aragonès G and Mulero M. (2022). Impacto del consumo del extracto de procianidina de semilla de uva (GSPE) sobre el reloj circadiano hepático en ratas obesas. I Jornadas sobre Nutracéutica: Compuestos bioactivos y Nutracéuticos. March 3-4, 2022. Tarragona, Spain.

In obesity,
the dysfunction of adipose tissue is
associated with the risk to suffer metabolic disorders.
Circadian rhythm, governed by light/dark cycle and fasting/
feeding cycle, synchronize many metabolic processes, therefore its
disruption has been also related to the development of metabolic disorders.
The increasing prevalence of obesity remarks the importance of its prevention
and treatment. In this context, proanthocyanidins from grape seed (GSPE) have
been demonstrated to modulate the biology and molecular clock components of
white adipose tissue (WAT). Nevertheless, it has not been studied yet whether GSPE
could affect WAT chronobiology depending on time-of-day consumption. Therefore, the
aim of this thesis was to determine whether GSPE and a bioactive multi-compound
based on these proanthocyanidins have different effects on the metabolism and
circadian rhythm of WAT in obese animals depending on time-of-day
administration. High calorie intake disrupted molecular clock genes and
the metabolism of WAT. Interestingly, the consumption of GSPE restored
the metabolism and molecular rhythmicity of WAT in a time-dependent
and tissue-specific manner. The combination of different bioactive
compounds is also an interesting strategy for the
management of obesity depending on the
time-of-day administration.

UNIVERSITAT
ROVIRA i VIRGILI